HEAT POWERED CYCLES 2018
Book of Abstracts

Heat Powered Cycles Conference

University of Bayreuth, Germany
16th -19th September 2018

Published by Heat Powered Cycles

This Book of Abstracts was prepared with the extended abstracts that were accepted by the Organizing Committee of the Eight Heat Powered Cycles Conference. This material aims to assist authors and presenters to easily access the presentations and have a brief explanation regarding the subject of each accepted work, including Keynote Lectures and regular Oral Presentations.
Art Work and information related to the Conference, Organizing Committee, Executive Committee and Advisory Board were taken from the conference's web site.

Edited by:
Prof. Dr. Roger R. Riehl – National Institute for Space Research – INPE/DMC - Brazil

Reviewed by:
Prof. (FH) Dr.-Ing. Markus Preißinger - Energy Research Center, University of Applied Sciences Vorarlberg, Austria

Prof. Dr. Ian W. Eames, University of Nottingham, UK

Dr. Mike Tierney, University of Bristol, UK

HEAT POWERED CYCLES 2018
Book of Abstracts

ISBN 978-0-9563329-7-4

Welcome to the Eight Heat Powered Cycles Conference

This is the eighth Heat Powered Cycles Conference. The first was held at Nottingham in 1997. This time the event is being co-organised by the *University of Bayreuth*, (Germany), *The University of Applied Sciences, Vorarlberg*, (Austria), *The National Institute for Space Research*, (Brazil) and *The University of Bristol*, (UK). The conference is to be held at the University of Bayreuth and hosted by the Centre for Energy Technology at the University of Bayreuth by *Prof. Dieter Brüggemann*, as director of the Center, and *Prof, Markus Preißinger*, former executive manager of the Centre. In addition to formal presentations of technical papers, including invited Keynote papers, the event will include poster sessions and workshops. There will also be a full social programme for both delegates and accompanying partners. The conference is concerned with scientific and technological innovations relating to the efficient and economic use of heat, derived from all its sources, for the production of cooling, heating and mechanical power either independently or co-generatively.

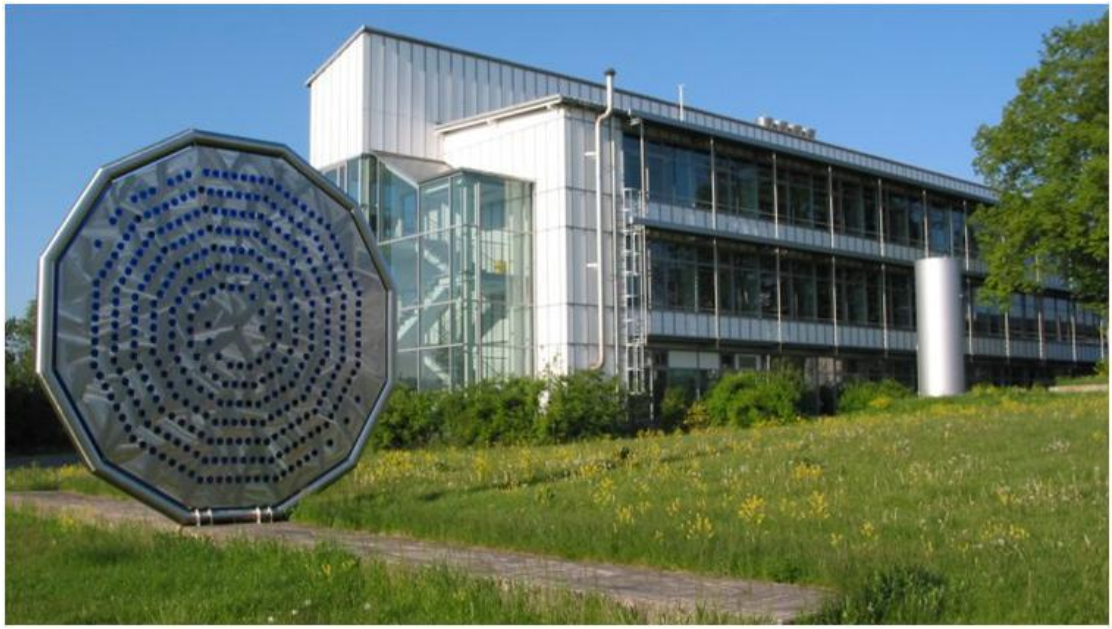

Center of Energy Technology at the Faculty of Engineering Science, University of Bayreuth

Subject areas of particular interest include; hybrid cycles, ORCs, Stirling cycle machines, thermo-acoustic engines and coolers, sorption cycle refrigerators and heat pumps, jet-pump (ejector) machines, temperature amplifiers (heat transformers), chemical heat pumps, new working fluids, mass and heat transfer phenomena, desalination of brackish water and seawater, compact heat exchanger research (including foams and other micro-channel research), thermo-economics, process optimisation and modelling, process and cycle thermodynamics.

History

2016: Nottingham

The seventh Heat Powered Cycles conference was co-organised by the Universities of Nottingham and Bristol. The conference was held at the University of Nottingham and was hosted by the HVASCR & Heat Transfer Group.

2012: Alkmaar

The sixth Heat Powered Cycles conference was hosted by Energy research Center of the Netherlands (ECN) in the Golden Tulip Hotel in Alkmaar.

2009: Berlin

The fifth Heat Powered Cycles conference was hosted by the Technical University of Berlin.

2006: Newcastle

The fourth Heat Powered Cycles conference was hosted by University upon Tyne Newcastle.

Three special Issues after HPC 2018

The Organizing Committee of the Heat Powered Cycles Conference will select some presented manuscripts, after the conference is finished, to be invited for publication in a special issue of *Applied Thermal Engineering* (Elsevier), *Energy* (Elsevier) and *Energies* (MDPI). The selection of the manuscripts will be based on their quality and presentation. The selected manuscripts will undergo a the normal review process for those journals.

Organizing Committee

Conference Chair

Prof. Dr.-Ing. Dieter Brüggemann
Center of Energy Technology, University of Bayreuth, Germany

Conference Co-Chair

Prof. (FH) Dr.-Ing. Markus Preißinger
illwerke vkw Endowed Professor for Energy Efficiency, Energy Research Center, University of Applied Sciences Vorarlberg, Austria

Review Chair

Prof. Dr. Roger R. Riehl
Faculty of Thermal/Fluid Sciences and Thermal Control Specialist, National Institute for Space Research - INPE/DMC - Brazil

Executive Committee

Prof. Dr. Ian W. Eames, University of Nottingham, UK
Dr. Mike Tierney, University of Bristol, UK

Scientific Advisory Panel

Adriano Milazzo, University of Florence, Italy
Angelo Freni , CNR-ITAE, Italy
Bob Critoph, University of Warwick, UK
Brian Agnew , University of Newcastle, UK
Christian Schweiger, Munich University of Applied Sciences, Germany
Christos Markides, Imperial College, London UK
David A. Reay, David Reay & Associates, UK
David Hann, Nottingham University,UK
Francis Meunier, CANAM, Paris, France
Giovanni Restuccia, CNR-ITAE, Italy
Giulio Santori, University of Edinburgh, UK
Guangming Chen, Zhejiang University, China
Hisham Sabir, QNRF, Qatar
Ian Eames, University of Nottingham, UK
Joan Carlos Bruno ,Universitat Rovira i Virgili, Spain
Larisa Gordeeva , Boreskov Institute of Catalysis
Markus Preißinger, Vorarlberg University of Applied Sciences, Austria
Michel van der Pal, ECN, Alkmar, Netherlands
Mike Tierney, University of Bristol, UK
Philip Davies, Aston University, UK
Phillipe Blanc-Benon, École Centrale de Lyon , France
Pierre Neveu, University of Perpignan, France
Rayah Al-Dadah, University of Birmingham, UK
Robert Keolian, Penn State University, USA
Roger R. Riehl , National Institute for Space Research – INPE/DMC, Brazil
Ruzhu Wang, SJTU, Shanghai, China
Steven Garrett, Penn State University, USA
Yann Bartosiewicz , University Catholique de Louvain UCL, Belgium
Yukitaka Kato, Tokyo Institute of Technology, Japan
Yuri Aristov, Boreskov Institute of Catalysis, Russia
Zacharie Tamainot-Telto , University of Warwick, UK

Summary

Keynote Lectures

Extended Abstracts

Keynote Lectures

A Fission-Powered Thermoacoustic In-Core Sensor

Steven L. Garrett

151 Sycamore Drive, State College, PA 16801

sxg185@psu.edu

Abstract

Motivated by the Fukushima nuclear reactor disaster in March 2011, a thermoacoustic engine was designed to have dimensions that are identical to a fuel rod to exploit the energy-rich conditions in the core of a nuclear reactor to acoustically measure and telemeter core condition information to reactor operators without a need for external electrical power. The standing-wave thermoacoustic heat engine is self-powered and can wirelessly transmit the temperature (encoded as a frequency) and reactor power level (proportional to sound amplitude) by generation of a pure tone that can be detected outside the reactor.

Keywords: Thermoacoustic engines, Wireless telemetry, Nuclear reactor sensing

Introduction/Background

The generation of sound by heat has been documented as an "acoustical curiosity" since 1568 when a Buddhist monk reported the loud tone generated by a ceremonial rice-cooker in his diary [1]. In 1850, Karl Friedrich Julius Sondhauss investigated an observation made by glassblowers who noticed that when a hot glass bulb was attached to a cooler glass tubular stem, the stem tip sometimes emitted a pure tone [2]. The Sondhauss tube [3] is the earliest thermoacoustic engine that is a direct antecedent of this fission-powered in-core sensor.

The first qualitative explanation of the Sondhauss effect was provided by Lord Rayleigh: "If heat be given to the air at the moment of greatest condensation or be taken from it at the moment of greatest rarefaction, the vibration is encouraged" [4]. This new thermoacoustic sensor automatically does both. The standing sound wave transfers heat from a solid substrate to the gas (in our case a mixture of 75% helium and 25% argon rather than air) at the phase of the acoustic cycle during which the condensation (*i.e.*, density and pressure) is maximum and removes heat from the gas and deposits it on a solid substrate (at a different location) at the phase of the cycle when the condensation is a minimum [5].

In our case, the solid substrate, called the "stack" [2], is visible in Fig. 1 (Lower right). It consists of an extruded cordierite ceramic material with straight pores of square cross-section that has commercial application as a substrate in automotive catalytic converters [6] A previous publication provides a (qualitative) Lagrangian description of the cyclic heat transfer resulting in the production and maintenance of an acoustic standing-wave resonance [7].

It is worthwhile to point out that our thermoacoustic sensor is an extremely simple heat engine when compared to an automobile engine that requires pistons, valves, cams, rocker-arms, flywheel, etc. to ensure that the compressions and expansions are synchronized with the heat input and exhaust at the proper phases in the cycle. By contrast, this standing-wave thermoacoustic process is phased by thermal diffusion and requires no moving parts other than the oscillatory motion of the gas. The irreversibility of the diffusion process reduces efficiency from that achievable using a traveling-wave thermoacoustic-Stirling cycle [8], but in the energy-rich core of a nuclear reactor, efficiency is less important than simplicity.

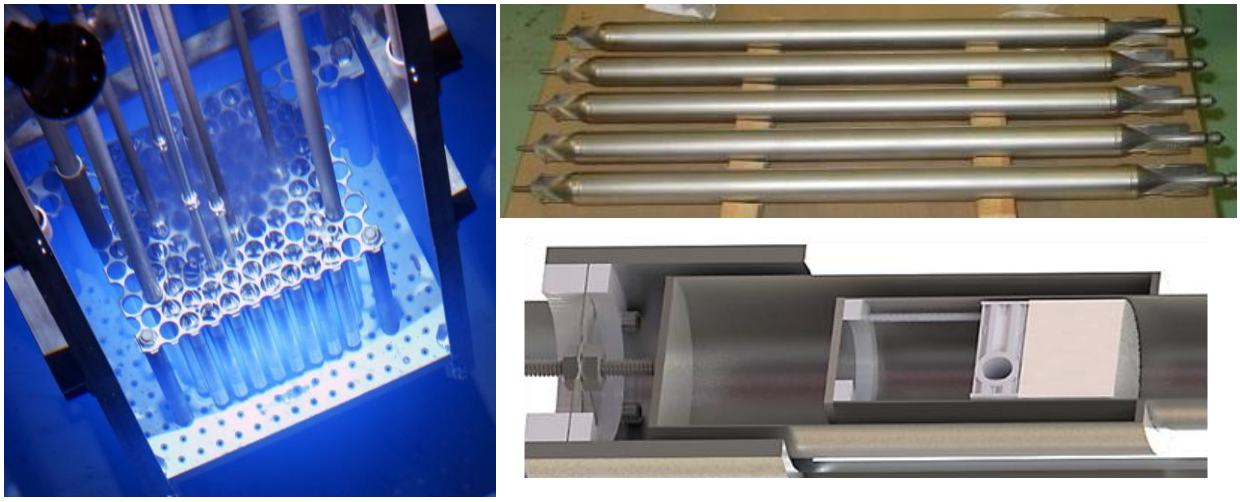

Figure 1. Fuel rods used in the Breazeale Nuclear Reactor. (Left) Photograph of the reactor's core. (Upper right) Several fuel rods. (Lower right) Cross-sectional rendering of the hot end of the thermoacoustic resonator showing one of two suspension springs that attach the resonator to the "slotted tube," the insulation space surrounding the hot end (SiO_2 insulation floss not shown), and the hot heat exchanger that is in physical contact with the Celcor® ceramic stack that had 170 cells/cm^2.

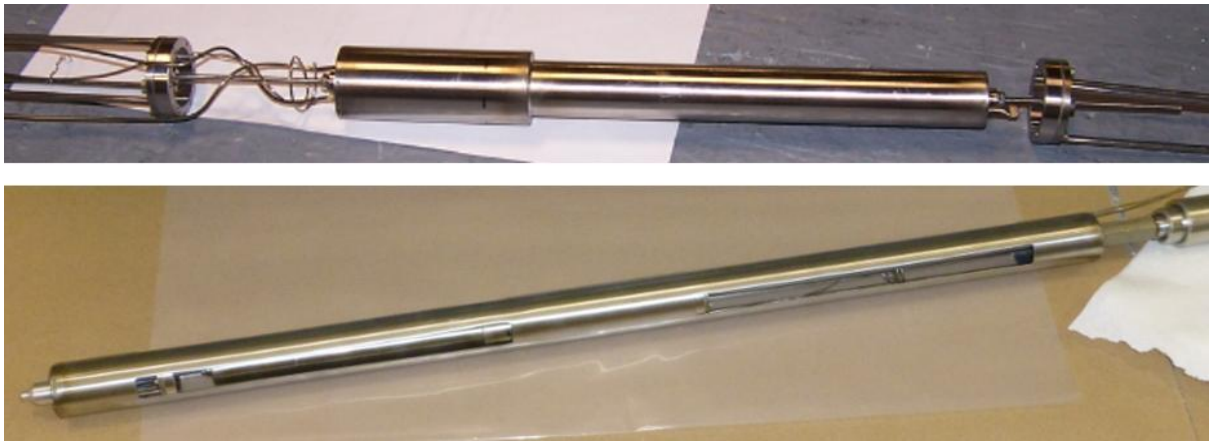

Figure 2. "Fuel rod" thermoacoustic sensor. (Above) The thermoacoustic resonator is shown at the center of the photograph. The resonator tube has an inside diameter of 2.2 cm and is 22 cm long. The insulated hot section of the resonator holds the hot heat exchanger that contains two enriched ^{235}U fuel pellets that are each approximately 5 mm in diameter and 10 mm long, as well as the extruded ceramic "stack" shown in Fig. 1. The resonator tube contains the 2.0 MPa He/Ar gas mixture. The empty portion of the resonator, to the right of the insulated section, is in good thermal contact with the reactor's coolant. Two 4-40 threaded rods extend from either end of the resonator. The rods are attached to two circular stainless steel disks (200 μm thick) that have six spokes acting as cantilever springs to allow the resonator to vibrate axially but constrain the resonator to remain coaxial within the surrounding "slotted tube." One of the thermocouples is silver-soldered (brazed) to the thin-walled section of the resonator next to the heat exchanger and the other is silver-soldered to the hot end of the resonator. Both thermocouples are located within the insulation space. (Below) The resonator and springs are contained within a "slotted tube" that has the same outer diameter as the fuel rods. The slots allow the reactor's coolant to remove the heat of fission from the thermoacoustic sensor and facilitated testing of the resonator's axial mobility before insertion in the reactor's core.

Discussion and Results

This thermoacoustic sensor converts the heat released by ^{235}U fission to create a standing sound wave. It was designed to have a size and shape that is identical to the fuel rods in the Breazeale Nuclear Reactor on Penn State's University Park campus, shown in Fig. 1. Those fuel rods have a maximum external diameter of 3.7 cm and an overall length of 72 cm. The acoustic resonator and the "slotted tube" that contains the resonator are shown in Fig. 2. A cut-away representation of the stack, heat exchanger, suspension spring, and insulation space is provided in Fig. 1. Based on our measurements of the vibro-acoustic spectra of the pump-dominated background noise in the coolant pool [9], a 2.0 MPa mixture of 75% helium and 25% argon was selected as the engine's "working fluid" to place the resonance frequency at approximately 1,350 Hz, above most of that background noise, which was below 1.0 kHz. That inert gas mixture provides the largest possible polytropic coefficient (*i.e.*, ratio of specific heats) while also lowering the Prandtl number [10], thus improving the thermoacoustic energy conversion process [11].

The high-amplitude acoustic standing wave that is generated thermoacoustically causes the gas in the "empty" section of the resonator to be pumped by non-zero time-averaged nonlinear acoustic forces that create streaming cells [12]. This acoustically-induced flow forcibly convects heat from the ambient-temperature end of the stack to the walls of the resonator that are bathed in the reactor's cooling water. Previous measurements in a similar electrically-heated "fuel rod resonator" have shown that this acoustically-driven streaming flow increases the thermal contact between the gas in the ambient-temperature end of the stack and the coolant by a factor-of-three [13]. This acoustically-enhanced heat transfer makes our thermoacoustic sensor even simpler than previous standing-wave thermoacoustic engines [14], since no separate cold heat exchanger is required.

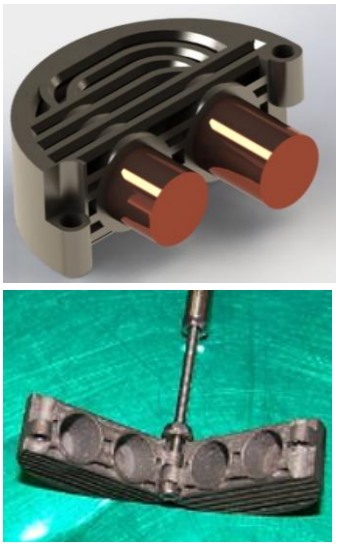

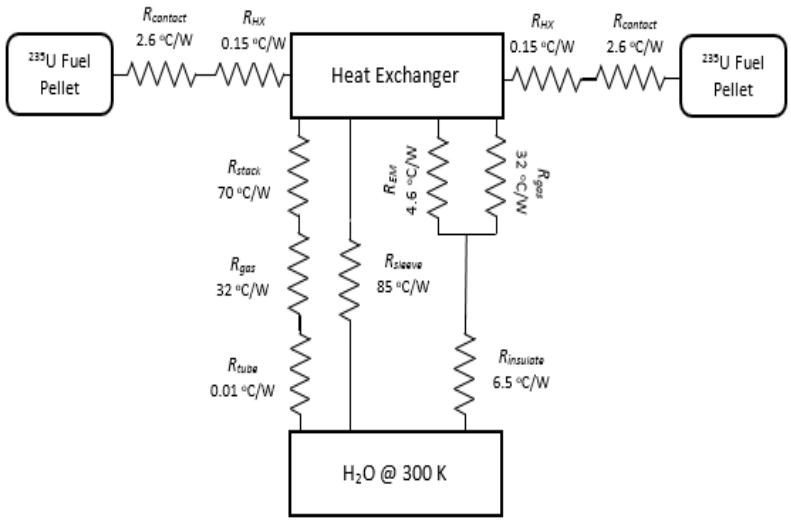

Figure 3. Hot heat exchanger. (Left) SolidWorks® rendering of one-half of the hot heat exchanger containing both enriched ^{235}U pellets. The exchanger was fabricated by additive manufacturing in two halves that were joined by two 0-80 machine screws as shown in the photo below the rendering. (Right) The lumped-element static thermal conduction model includes the contact resistance from each pellet to the heat exchanger, $R_{contact}$, as well as the resistance of the stainless steel exchanger, R_{HX}. Heat from the pellets can reach the coolant along the resonator wall, R_{sleeve}, or can leak through the insulation's thermal resistance, $R_{insulate}$, after either conduction through the gas or by electromagnetic radiation, R_{EM}. The heat that passes through the stack will generate the thermoacoustic oscillations once the system reaches onset. Prior to onset, the heat diffuses through the ceramic stack material and

the gas within the stack's pores, R_{stack}, then reaches the water through the static gas's thermal resistance, R_{gas}.

The hot heat exchanger is responsible for the transfer of the heat produced by the irradiated ^{235}U pellets to the gas within the resonator. The left side of Fig. 3 shows the SolidWorks® model used to produce the two halves of the 3-D printed stainless steel heat exchanger that contained both pellets. The right side of Fig. 3 shows the static conduction model used to determine the temperature of the hot heat exchanger prior to thermoacoustic onset. Such a model is necessary to assure that no part of the stainless steel resonator reaches a temperature that would cause the material to weaken and possibly release either the compressed gas mixture or the enriched uranium prior to onset of the oscillations, which enhance the heat transfer and limit the temperature.

The detectability of the sound radiated by the thermoacoustic sensor depends upon the acoustics of the coolant pool and the vibroacoustic background noise level that was dominated by the pumps used to circulate the coolant. In the Breazeale Nuclear Reactor's coolant pool, the dominant noise was created by a diffusor pump that is used to circulate coolant (deionized light water) over the reactor core to prevent aggregation of short-lived radioactive ^{16}N into bubbles that would rise before decaying, thus triggering radiation alarms.

The reactor pool is a reverberant acoustical environment. The standing-wave modal structure of the pool and the acoustic reverberation times were measured. The reactor's 70,000 gallon (265 m^3) coolant pool has equivalent rectangular dimensions that are 8.65 m long, 4.27 m wide, and 7.32 m deep. The lowest standing-wave modal frequency occurs at about 51 Hz. In a 3-dimensional enclosure, the number of modes below a given frequency increases with the cube of that frequency [15]. At some frequency, there will be three modes with resonance frequencies which overlap within the half-power bandwidth of the central mode. That "overlap" frequency is known within the architectural acoustics community as the Schroeder frequency, f_S [16]. Above that frequency, the sound field can be treated as being diffuse (*i.e.*, uniform energy density approximately independent of the location of the source and the sensors), so the sound field can be approximated as a "phonon gas" and the sound pressure can be estimated using statistical energy analysis. Based on our measurements of the reverberation time (T_{60} = 120 ± 20 ms), $f_S \cong$ 230 Hz << $f \cong$ 1,350 Hz. The sound pressure created by the fuel-rod thermoacoustic sensor will then be fairly homogeneous and isotropic at measurement distances from the source greater than the critical radius, $r_d = c_{H_2O} / 5 f_S \cong 1.3\, m$ [15]. The speed of sound in water is $c_{H_2O} \cong 1,500$ m/s .

Our thermoacoustic sensor was tested during eight irradiation runs in the Breazeale Nuclear Reactor. Provisions of the reactor's license limit the accumulation of radioactive iodine isotopes produced by the fuel pellets to less than a total of 1.5 Ci. As a consequence, the sensor's irradiation dose restricted operations to a reactor time-integrated-power of approximately seven MW-minutes. Following each run, the experiment was idled while the unstable iodine isotopes were allowed to decay [5].

Figure 4 is a time record made during the 5th irradiation. It shows the temperature of the thermocouple that was brazed to the hot-end of the thermoacoustic resonator, contained within the insulation space, as well as the output of two hydrophones that were located far from the core in the reactor's coolant pool. Short Time Fast (essentially sliding-average) Fourier transforms of ten-second time records were produced every two seconds and the frequency of only the largest-amplitude spectral component is plotted in Fig. 4 for both hydrophones. The thermoacoustic sensor achieved onset at about t = 810 s, which is the time the largest amplitude spectral components for both hydrophones coalesced to the same frequency. It is also possible

to detect a subtle indication of the onset of thermoacoustic oscillations suggested by the slight increase of the slope of the thermocouple's temperature *vs.* time after onset. This increased heating rate indicated a hydrodynamically-enhanced increase in the uniformity of the distribution of the heat from the hot heat exchanger to all other locations within the resonator.

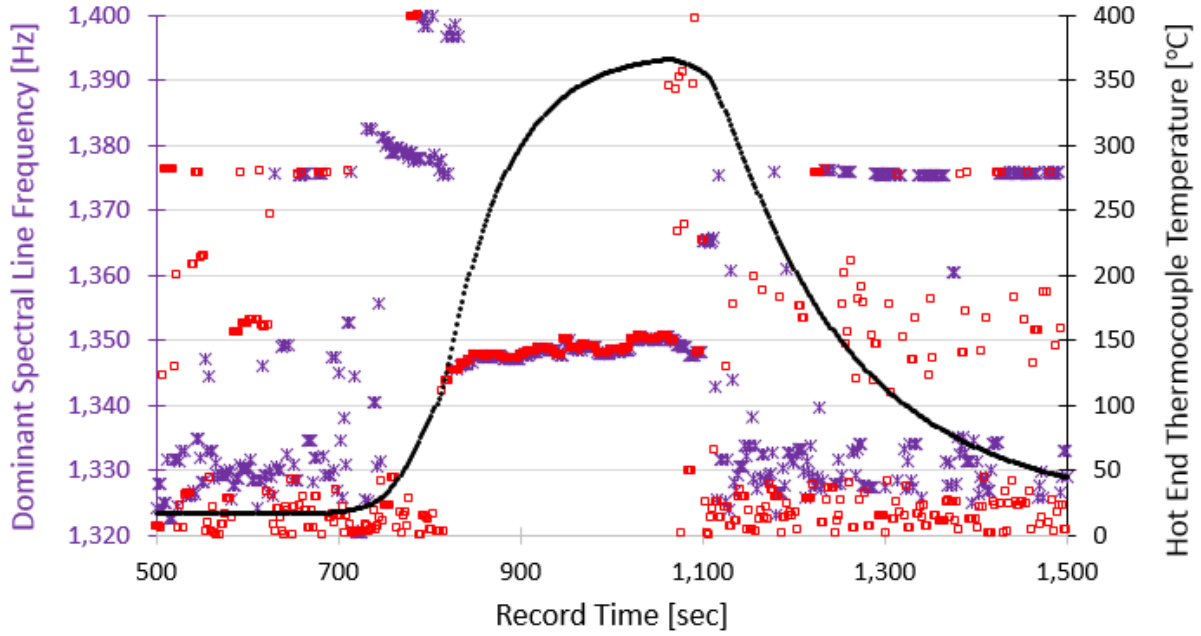

Figure 4. Time record of the temperature and the frequency of the largest spectral component received by two hydrophones at different locations. The temperature of a Type-K thermocouple brazed to the hot-end of the thermoacoustic resonator is plotted as the black circles. Those temperatures should be read from the black right-hand axis. The star symbols "✳" and hollow square symbols "□" are the frequencies of the largest spectral component within the frequency range between 1,320 Hz ≤ f ≤ 1,400 Hz. Those frequencies should be read from the left-hand axis. All data points are plotted every two seconds. The time axis is labeled from the start of the recording. The reactor reached full power (1.0 MW) at $t \cong 800$ s. The reactor power was reduced to 800 kW at $t \cong 1{,}060$ s, then the reactor was shut down at $t \cong 1{,}100$ s, since fission had produced the maximum allowable amount of radioactive iodine.

Before onset of thermoacoustic oscillations ($t < 810$ s) and after their cessation ($t > 1{,}100$ s), the frequencies of the dominant spectral components from both hydrophones' signals are fairly random and were different due to the proximity of the hydrophones to the sources of pump noises in those different locations. This is as would be expected when only the pump noises were received within the displayed bandwidth, $\Delta f = \pm 40$ Hz.

Figure 5 shows one of several accelerometers that were attached to structures external to the reactor's coolant pool. The sonogram is taken from a 16-bit, 44.1 kilosamples/second digital audio recording of one accelerometer's output and displays the frequency of the detected vibration as a function of time with the amplitude of the signal coded as color from blue to yellow. Because the characteristic impedance of the water is close to the impedance of the solid structures that penetrate the reactor pool, the sound produced by the sensor couples well to those structures.

As demonstrated in Fig. 6, the frequency of the thermoacoustically generated sound provides an accurate determination of the reactor's coolant temperature. We were able to reduce the reactor coolant temperature by running the reactor's heat exchanger overnight.

The speed of sound in an ideal gas or gas mixture, c, is related to the acoustically-averaged absolute (Kelvin) temperature [7], T, the mean molecular mass of the gas mixture, M, the mixture's polytropic coefficient, $\gamma \equiv c_P/c_V = 5/3$, and the Universal Gas Constant, $\Re$: $c = (\gamma \Re T / M)^{1/2}$.

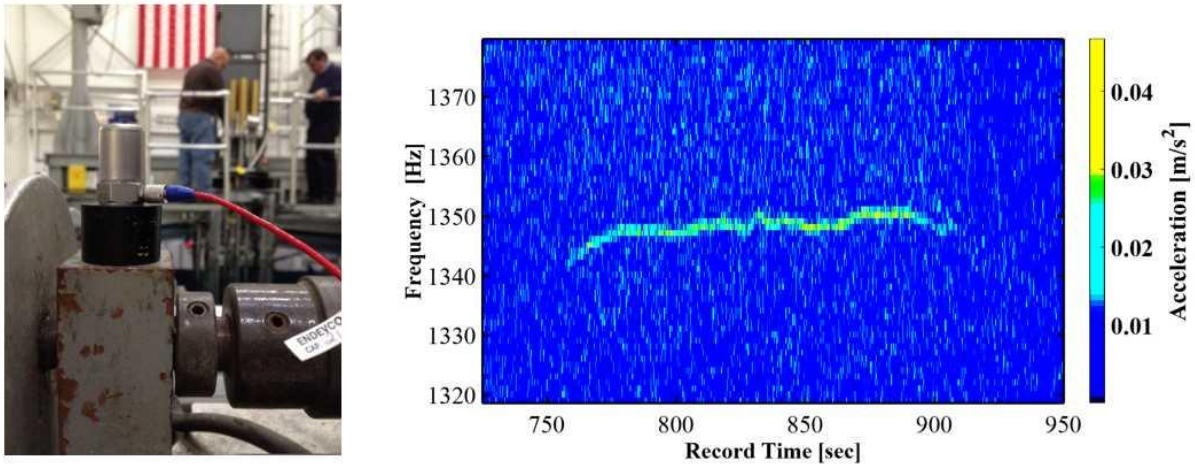

Figure 5. Time record (spectrogram) of the vibration signal received by an accelerometer mounted on a structure outside the reactor pool. (Left) Accelerometer with a magnetic base attached to the motor mount of an instrumentation tower that extends into the reactor pool. (Right) Spectrogram showing the accelerometer's output frequency on the vertical axis as a function of time represented by the horizontal axis.

Ignoring the small localized changes in the resonator's otherwise uniform cross-sectional area caused by the porous heat exchanger and the stack, the fundamental resonance frequency of the thermoacoustic sensor occurs when the wavelength of the sound in the gas mixture, $\lambda = c/f$, is approximately twice the resonator's length, $L \cong \lambda/2$: $f^2 = (c^2/4L^2) = (\gamma \Re T / 4 M L^2) \propto T$.

The temperature of the gas mixture within the thermoacoustic resonator varies significantly from the high temperatures at the hot end (containing the heat exchanger) to about the temperature of the reactor coolant in the longest portion of the resonator between the ambient-temperature end of the stack and the ambient-temperature end of the resonator. A simple lumped-element model of the resonator as a "gas mass" at the center of the resonator surrounded by two "gas springs" suggests that the frequency is determined largely by the density of the lower temperature gas near the center of the resonator. The temperature of the central gas mass is controlled by the temperature of the reactor's coolant. A more detailed model, treating the resonator as the concatenation of 31 lumped-elements, is able to provide a better estimate of the relationship between resonance frequency and coolant temperature [7].

As is apparent from Fig. 6, just forming the ratio of the square of the measured resonance frequency, f^2, to the absolute (Kelvin) temperature of the reactor's coolant, T, produces values of f^2/T that vary by only ±0.12%, while the temperature changes by 3.4% [17].

Summary/Conclusions

We have demonstrated the ability to acoustically telemeter temperature and power information beyond the core of a nuclear reactor without requiring external electrical power or wiring. Such a sensor might have provided useful information in a reactor accident like the one which destroyed the Fukushima complex in March 2011. In a commercial reactor, the flux of gamma radiation could provide sufficient heating that tungsten or stainless steel could be used instead of fissionable fuel. This would avoid degradation in the sensor's sensitivity with time due to fuel

depletion and remove the regulatory controls required for handling of enriched uranium. Multiple sensors in various core locations could also be used to optimize power distribution and improve a commercial reactor's operational efficiency.

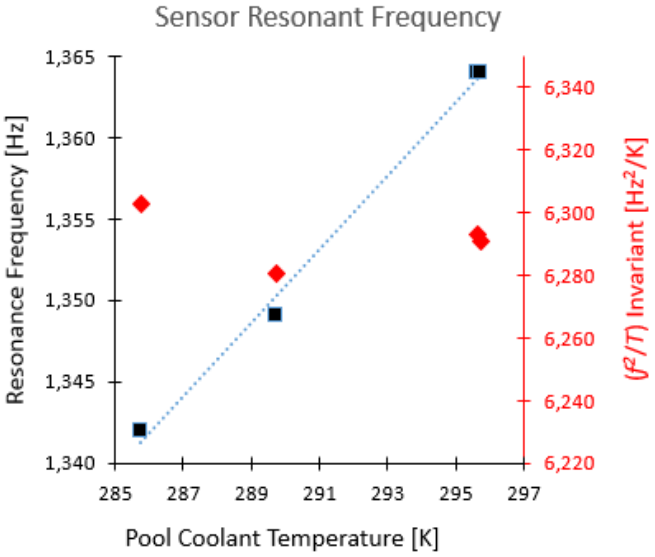

Figure. 6. Resonance frequency of the thermoacoustic sensor's standing-wave for different coolant temperatures. The sensor's resonance frequencies were measured at four different water temperatures between 12.6 °C and 22.6 °C in the reactor's pool. Frequencies corresponding to those temperatures are plotted as the black squares and their values are given by the left-hand axis that spans ±1.7%. The right-hand axis has the same relative span, but the value of the f^2/T invariant, plotted as red diamonds, has a standard deviation of only ±0.12% [17].

While this report has focused on in-pile nuclear reactor sensing, the thermoacoustic sensor is an utilitarian device that could be effectively adapted to other applications that involve large temperature gradients, hostile or corrosive environments, and hard to "wire" locations. Effective sensor adaptations can be configured to monitor melting glass or metal, hydrocarbon crackers, smoke stacks, and other processes or systems in which high temperatures are used that are difficult to measure. [18] Multiple sensors can be frequency multiplexed wirelessly using only a single detector (*e.g.*, microphone, hydrophone, or accelerometer). The sensors can be configured to be temperature sensors by monitoring the frequency of the acoustic standing wave, which depends upon the effective temperature of the gas in the resonant chamber. The thermoacoustic sensor can also be used to monitor the molecular mass of the gas mixture within the resonant chamber [19], thus the thermoacoustic sensor can also be used to monitor the progress of chemical reactions.

Acknowledgements

The design and optimization of this sensor relied upon the Design Environment for Low-Amplitude Thermoacoustic Energy Conversion (DELTAEC), a software package developed and supported for over twenty-five years by G. W. Swift and W. W. Ward at the Los Alamos National Laboratory. The author is grateful for the support of Larry Bodendorf, Iain Wilson, James Lynch, and Brandon Rieck of IST Mirion for fabrication of the resonator and for its fueling. Support provided by Penn State's Radiation Science & Engineering Center for ensuring that the experiment could be operated safely and in full compliance with all NRC regulatory limits is appreciated. James A. Smith, James Lee, Vivek Agarwal, and Keith Jewell, from Idaho National Laboratory, assembled and tested the data acquisition system and also provided assistance with the data analysis. The participation of Randall Ali, Joshua Hrisko, and Andrew Bascom, three of the author's graduate students, each contributed to the success of these experiments. This research was supported by the U.S. Department of Energy's Idaho National Laboratory and by the Westinghouse Global Technology Development Department of the Westinghouse Electric Company.

References:

[1] Noda, D. and Ueda, Y., "A thermoacoustic oscillator powered by vaporized water and ethanol," Am J. Phys. **81**(2), 124-126 (2013).

[2] Swift, G. W., "Thermoacoustic engines," J. Acoust. Soc. Am. **84**(4), 1145-1180 (1988).

[3] Sondhauss, K. F. J., Über die Schallschwingungen der Luft in erhitzten Glasröhren und in geteckten Pfeifen von ungleicher Weite," Ann. Phys. (Leipzig) **79**, 1 (1850).

[4] Strutt, J. W. (Lord Rayleigh), "The explanation of certain acoustical phenomena," *Nature* **18**, 319-321 (1878).

[5] Garrett, S. L., Smith, J. A., Smith, R W. M., B. J. Heidrich, and M. D. Heibel, "Using the sound of nuclear energy," Nuclear Technology **195**(3), 353-362 (2016).

[6] Liu, J., Garrett, S., Long, G., and Sen, A., "Separation of thermoviscous losses in Celcor™ ceramic," J. Acoust. Soc. Am. **119**(2), 857-862 (2006).

[7] Ali, R. A., Garrett, S. L., Smith, J. A., and Kotter, D. K., "Thermoacoustic thermometry for nuclear reactor monitoring," IEEE J. Instrumentation & Measurement **16**(3), 18-25 (2013).

[8] Backhaus, S. and Swift, G. W., "A thermoacoustic-Stirling engine," Nature **399**, 335-338 (1999).

[9] Hrisko, J., Garrett, S. L., Smith, R. W. M., Smith, J. A. and Agarwal, V., "The vibroacoustical environment in two nuclear reactors," J. Acoust. Soc. Am. **137** (2), 2198 (2015).

[10] Giacobbe, F. W., "Estimation of Prandtl numbers in binary mixtures of helium and other nobel gases," J. Acoust. Soc. Am. **96**(6), 3538-3580 (1994).

[11] Swift, G. W., *Thermoacoustics: A unifying perspective for some engines and refrigerators*, 2nd ed., Springer-ASA Press 2017; ISBN 978-3-319-66932-8. See §8.1.

[12] Strutt, J. W. (Lord Rayleigh), "On the circulation of air observed in Kundt's tubes, and on some allied acoustical problems," Phil. Trans. Royal Soc. London **175**, 1-21 (1883); *Scientific Papers*, Dover, 1964, Art. 108, Vol. II, pp. 239-257.

[13] Ali, R. A. and Garrett, S. L., "Heat transfer enhancement through thermoacoustically-driven streaming," Proc. of Meetings on Acoustics (POMA) **19**, 030001 (2013); DOI: 10.1121/1.4799202.

[14] Swift, G. W. "Analysis and performance of a large thermoacoustic engine," J. Acoust. Soc. Am. **92**(3), 1551-1563 (1992).

[15] Garrett, S. L., *Understanding Acoustics: An experimentalist's view of sound and vibration*, Springer-ASA Press, 2017; ISBN 978-3-319-49976-5. See Ch. 13.

[16] Schroeder, M. R., "The 'Schroeder frequency' revisited," J. Acoust. Soc. Am. **99**(5), 3240-3241 (1996).

[17] Garrett, S. L., Smith, J. A., Smith, R W. M., Heidrich, B. J. and Heibel, M. D., "Fission-powered in-core thermoacoustic sensor," Appl. Phys. Lett. **108**, 144102 (2016).

[18] Garrett, S. L., Smith, J. A. and Kotter, D. K., "Thermoacoustic enhancements for nuclear fuel rods and other high temperature applications," US Pat. No. 9,646,723 (May 9, 2017).

[19] Polturak, E., Garrett, S. L. and Lipson, S. G., "Precision acoustic gas analyzer for binary mixtures," Rev. Sci. Inst. **57**, 2837-2841 (1986).

Honey, I Shrunk the Sorption Lab
- Model-based Scale-up of Adsorption Systems -

S. Graf, A. Gibelhaus, U. Bau, F. Lanzerath, A. Bardow*

Institute of Technical Thermodynamics, RWTH Aachen University, Schinkelstraße 8, 52062 Aachen, Germany

*Corresponding author: andre.bardow@ltt.rwth-aachen.de

Abstract

Performance assessment and development of adsorption chillers typically requires large-scale experiments of whole adsorption chiller setups. In this work, we present a model-based approach to drastically reduce the required lab space and time. A workflow is illustrated that starts with a simple kinetic experiment with a small adsorbent sample to determine heat and mass transfer coefficients of a packed-bed adsorbent. These coefficients are used in a dynamic model to predict the SCP and COP of a full-size adsorption chiller. We show that the resulting model is able to predict the performance close to the measurement accuracy. With our approach, we thus can scale-up adsorption systems from milligram adsorbent samples to real machines with kilograms of adsorbent material. The underlying models for performance evaluation and development of adsorption machines are based on our freely available Modelica library SorpLib. The SorpLib library provides opportunities for the broad model-based development and optimization of adsorption systems and their control.

Introduction

Dynamic models of adsorption chillers are widely used to study the influence of input conditions, component designs, cycle designs or control on performance. With the availability of object-oriented modeling languages such as Modelica, dynamic models are increasingly easy to setup. However, they not necessarily lead to a reliable prediction of the specific cooling power SCP and the coefficient of performance COP compared to experimental results [1].

For reliable performance prediction, the models need to be calibrated. In previous studies, high accuracies required experimental data from full-scale adsorption chiller setups [2, 3].

In this work, we exploit the predictive power of physical models to simplify the required experiments to the Infrared-Large-Temperature-Jump (IR-LTJ) experiment that uses only a small adsorbent sample (< 1 g). A dynamic model is used to calibrate the heat and mass transfer coefficients. With the heat and mass transfer coefficients, we parametrize an adsorption chiller model. We show that the model is able to predict the SCP and COP of a complete adsorption chiller with high accuracy allowing for model-based optimization and control.

Discussion and Results

To illustrate the suggested approach, we first determine heat and mass transfer coefficients for a packed bed of silica gel 123 with a mean particle size of 0.9 mm. For this purpose, we place 1 to 3 layers of adsorbent (< 1 g) on a planar adsorbent carrier and conduct an IR-LTJ experiment [4]. The experimental data is used in a dynamic model for the adsorbent and the vapor phase . By fitting the measured pressure and temperature, we determine the heat and mass transfer coefficients α, λ, and D_{eff}, cf. table 1.

Table 1: Heat and mass transfer coefficients for packed bed of SG 123 from IR-LTJ-experiments.

	Adsorption	Desorption
α_{eff} in W/m²K	331	406
λ_{eff} in W/mK	0.15	0.2
D_{eff} in m/s²	1.17×10^{-9}	6.33×10^{-10}

Second, we use the coefficients to parametrize a full-scale model of an adsorption chiller. The adsorber consists of aluminum tubes with an outer fin structure, which also holds the adsorbent. To account for the adsorber geometry, we discretize in 3 dimensions. The adsorber model is connected to models for the evaporator and condenser. We predict the heat flows of the adsorption chiller for the cycle temperatures 10/35/90°C, times for adsorption and desorption of 900s and compare them with measurements of a whole adsorption chiller setup (Figure 1).

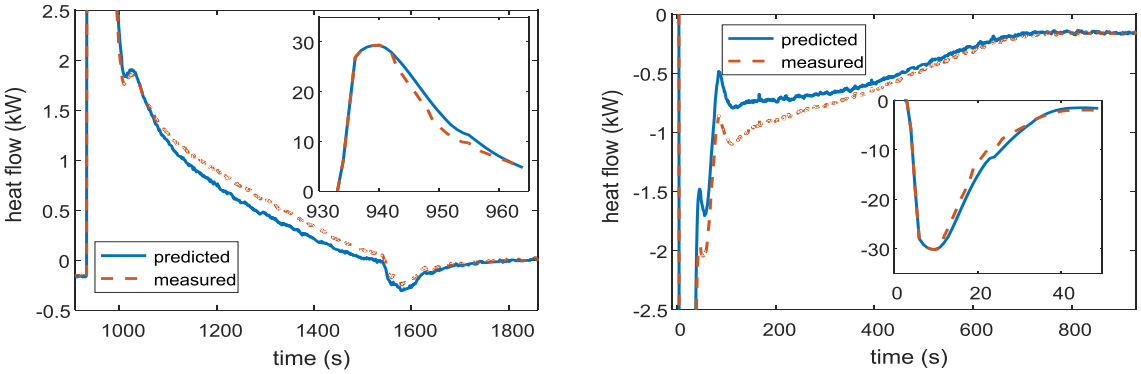

Figure 1: Predicted and measured heat flows in the adsorber for adsorption (left) and desorption (right).

From the predicted heat flows, the SCP and COP are determined to 81W/kg and 0.35. These values differ by 8.7% and 5.4% from the measured SCP of 88.7W/kg and COP of 0.37. Even the measured heat flows are well captured. Thus, the prediction has the same high accuracy as directly calibrated models in literature.

Summary

For reliable adsorption chiller models, calibration with experimental data is necessary. Instead of conducting experiments with a full-size adsorption chiller, we require only a simple IR-LTJ experiment with a small adsorbent sample (<1g) to determine heat and mass transfer coefficients. With the coefficients, we parameterize a complex adsorption chiller model. The model predicts the SCP and the COP in the whole adsorption chiller with deviations of less than 9% compared to experiments. Thus, the accuracy is in the same range as for models calibrated to full-size adsorption chillers. Our approach allows for an easy and reliable performance prediction of full-scale adsorption chillers based on small-scale IR-LTJ experiments. The underlying models are freely available in our Modelica library SorpLib [5] and can be used for scaling up small-sized experiments and to develop and optimize adsorption systems.

Acknowledgement

This work has been carried out within the project “TailorSorb – Tailored adsorbents for stationary adsorption thermal energy transformation” (03SF0515A). The project is funded by the German Federal Ministry of Education and Research (BMBF) within the funding priority “Materialforschung für die Energiewende”.

References

[1] Pesaran, A., Lee, H., Hwang, Y., Radermacher, R., Chun, H.-H., „Review article: Numerical simulation of adsorption heat pumps“, Energy, 2016, doi:10.1016/j.energy.2016.01.103

[2] Schicktanz, M., Núñez, T., „Modelling of an adsorption chiller for dynamic system simulation“, International Journal of Refrigeration, 2009, doi:10.1016/j.ijrefrig.2009.02.011

[3] Lanzerath, F., Bau, U., Seiler, J. Bardow, A., Optimal design of adsorption chillers based on a validated dynamic object-oriented model”, Science and Technology for the Built Environment, 2015, doi:10.1080/10789669.2014.990337

[4] Graf, S., Lanzerath, F., Bardow, A., “The IR-Large-Temperature-Jump method: Determining heat and mass transfer coefficients for adsorptive heat transformers”, Applied Thermal Engineering, 2017, doi:10.1016/j.applthermaleng.2017.06.054
[5] Bau, U., Lanzerath, F., Gräber, M., Schreiber, H., Thielen, N., Bardow, A., Adsorption energy systems library - Modeling adsorption based chillers, heat pumps, thermal storages and desiccant systems. In: H. Tummescheit und K.-E. Årzén, Hg. Proceedings of the 10th International Modelica Conference. Linköping: Modelica Association, 2014, S. 875-883. ISBN 9789175193809. http://www.ep.liu.se/ecp/096/091/ecp14096091.pdf

Mining and Upgrading Low-Grade Heat: From Infinite Potential to Practical Reality

Srinivas Garimella[1]

[1]George W. Woodruff School of Mechanical Engineering, Georgia Institute of Technology, Atlanta, GA 30332 USA

[*]Corresponding author: sgarimella@gatech.edu

Abstract

Much is made of the abundance of waste heat and its potential to offset primary energy needs. However, waste heat is waste heat for a reason! It is hard to eke out useful output from waste heat without potentially crippling capital costs, and without parasitic loads. Realistic opportunities, challenges, and innovations in the implementation of low-grade heat powered cycles are discussed. An overall framework for assessing the potential for waste heat without detailed design exercises, and the matching of different kinds of waste heat to a variety of applications are presented. In addition, examples of compact thermal systems that harvest low-grade heat and upgrade it to produce power, cooling, and other end uses are presented.

Keywords: Waste heat; sorption; work recovery; cooling; heat transformation.

Introduction/Background

A Nobel prize-winning physicist interested in energy for the masses asks, "What is the Carnot limit for this technology?" and "Why are we not there?" The responsible engineer should respond, "It does not matter," and "Irrelevant question." Carnot limits are good expressions of the limits of achievability; however, they also need infinite heat transfer capabilities, infinite thermal capacities, and other "infinites and infinitesimals" to be converted to reality. Unfortunately, these infinites translate to infinite $, and when addressing the issue of waste heat, one must recognize that to begin with, it is waste heat for some very good reasons. To achieve or even approach a small fraction of Carnot limits requires investments in capital cost that cannot be justified, especially in this mission, which is by definition, a scavenging task.

Waste Heat Availability and Constraints

Waste heat is ubiquitous: at the national and global levels, as much as 2/3 of the primary energy utilization is rejected as waste heat [1]. Depending on the location and exergy of the available waste heat, applications such as power generation, residential air-conditioning, process heating, water heating, industrial and commercial and residential space heating can be found. However, this requires an appropriate distributed generation infrastructure, temporal and spatial matching between sources and applications, and/or thermal, chemical, mechanical or electrical storage, all of which need significant capital investment. Practical considerations such as working fluids with appropriate vapor-liquid-equilibrium characteristics, thermodynamic and transport properties, and compatibility with heat exchanger materials also present challenges.

Avenues for Utilization, Realistic Performance Expectations

Options for outputs from a waste heat recovery system include recuperation and reuse, power generation, cooling, temperature boosting, and storage. An overall framework for assessing the potential for waste heat without detailed design exercises, and the matching of different

kinds of waste heat to a variety of applications can be developed [2]. Source and sink temperatures, waste heat availability and coupling to gas or liquid streams, and heat source scale (W – MW) are factors in choosing an appropriate cycle and output. For a representative gas source stream at 120°C with T_{sink} = 35°C, a maximum efficiency of power production through an organic Rankine cycle would be ~0.11. While this low efficiency limits the applications in which it may be implemented, an even bigger challenge is the heat transfer surface requirement: this efficiency means that for every 11 W generated, ~100 W must be supplied across typically high gas-phase thermal resistances, and ~89 W must be rejected across similarly high thermal resistances, leading to large capital investment requirements. If on the other hand, the source was a hot liquid stream and heat rejection was also to a liquid, even with T_{source} = 60°C and T_{sink} = 20°C (representing an indoor condition), an efficiency of 0.08 can be achieved, with heat exchangers an order of magnitude smaller than those needed for gas-phase sources and sinks due to the high density, specific heat, and thermal conductivity of liquids. Even greater utility can be achieved if the end use is cooling instead of work or electricity production. Organic Rankine vapor compression cycles can provide cooling at 5°C with COPs of ~0.41 for the abovementioned gas-source case, and 0.68 for the liquid coupling case due to the heat pumping accomplished in a cooling scenario. Absorption heat pumps would yield even better results for these cases, COPs of ~0.70-0.80, respectively. For the very low grade heat sources, e.g., data-center waste heat at ~60°C, instead of cooling or work output, temperature boosting up to ~120°C can be achieved at a COP of ~0.47, providing upgraded heat as a commodity. Thus, useful outcomes are possible in these temperature constrained low-grade heat recovery applications, but only with proper selection of end uses, cycles, and protection of temperature lift against the penalties of caloric ΔT of the source and sink, and driving ΔT due to thermal resistances. Adsorption cycles provide more passive operation, and ejector-based refrigeration cycles offer lower complexity at the cost of efficiency.

Representative Cases and Conclusions

Enhancement of phase-change heat and mass transfer in microchannels can also be exploited to enhance the performance potential and/or compactness of such waste heat recovery cycles. Applications range from systems that use waste heat to deliver 300 W [3] of cooling in modular, monolithic absorption heat pumps the size of a textbook, all the way up to MW of cooling [4] in cascaded cycles for aircraft carriers. Such systems have also been developed for thermally driven residential cooling and water heating systems, and systems that use exhaust heat from diesel engines to provide cooling at military bases at $T_{ambient}$ ~52°C [5]. It is emphasized, however, that implementation of real-world waste heat recovery systems presents challenges ignored in conceptual analyses, such as auxiliary high-grade electric loads of recirculation pumps and fans. Despite the potential of innovative cycles, these constraints determine the bounds for the utility and economic viability of waste heat.

References

1. A. S. Rattner and S. Garimella (2011), “Energy Harvesting, Reuse and Upgrade to Reduce Primary Energy Usage in the USA,” *Energy*, Oct 2011, Vol. 36, Issue 10, pp. 6172-6183.
2. A. B. Little and S. Garimella (2011), "Comparative Assessment of Alternative Cycles for Waste Heat Recovery and Upgrade," *Energy*, Vol. 36, pp. 4492-4504.
3. M. D. Determan and S. Garimella (2012), Design, Fabrication, and Experimental Demonstration of a Microscale Monolithic Modular Absorption Heat Pump, *Applied Thermal Engineering*, vol. 47, p. 119-125.

4. S. Garimella, A. M. Brown and A. K. Nagavarapu (2011), "Waste Heat Driven Absorption/Vapor Compression Cascade Refrigeration System for Megawatt Scale, High-Flux, Low Temperature Cooling," *Int. J. Refrig.*, Vol. 34, Issue 8, pp. 1776-1785.
5. M. J. Ponkala, A. Goyal, M. A. Staedter, S. Garimella, "A packaged waste-heat driven ammonia-water absorption chiller for severe ambient operation," *Int. Sorption Heat Pump Conf.* 2017, Aug. 7-10, Tokyo, Japan.

From cycle efficiency to physical properties - Comprehensive analyses of ORC working fluids by theoretical and experimental methods

F. Heberle*, T. Weith and D. Brüggemann

Chair of Engineering Thermodynamics and Transport Processes (LTTT),
Center of Energy Technology (ZET), University of Bayreuth
Universitätsstraße 30, 95447 Bayreuth, Germany
*Corresponding author: florian.heberle@uni-bayreuth.de

Abstract

The selection of a suitable working fluid is one of the key decisions regarding the design of an organic Rankine cycle (ORC) power system. The determination of the ORC fluid is crucial for the cycle efficiency, component design and costs. Depending on the characteristics of the heat source and the heat sink, different groups of substances like refrigerants, hydrocarbons or siloxanes are potential candidates. In case of applications for waste heat recovery within a temperature range of 250 °C and 500 °C, first and second law analysis show that hexamethyldisiloxane (MM) is a promising working fluid. The applied simulation models are validated by experimental data from an ORC test rig with a nominal electrical power output of 15 kW. In addition, extensive experimental investigations are conducted for MM in order to improve the existing heat transfer prediction methods and reduce uncertainties regarding fluid properties. Consequently, a more reliable heat exchanger sizing and an increase in cost efficiency can be realized.

Keywords: Organic Rankine Cycle, working fluid, fluid properties, heat transfer

Introduction/Background

In general, organic Rankine cycle (ORC) power systems are applied for heat source temperatures in the range of 100 °C up to 500 °C. In this context, waste heat recovery from industrial processes as well as stationary or mobile combustion engines has high energy-saving potential. The wide range of heat source temperatures for these applications lead in principal to a large number of candidates for the ORC working fluid. A preselection can be achieved by considering non-thermodynamic aspects like toxicity, safety issues or climate relevance. However, a first reliable technical and energetic evaluation is realized by a thermodynamic analysis based on steady state or dynamic simulation models. In order to validate these models on cycle or component level, a 15 kW test rig is set up in operation at the Center of Energy Technology (University of Bayreuth). Figure 1 shows the experimental setup in the test hall. A special focus is led on the analysis of the turbine-generator-unit, in particular the turbine efficiency at part load condition is investigated. In addition, flow boiling measurements are conducted for pure siloxanes and their mixtures. A scheme of the corresponding test rig is presented in Figure 2. The experimental data lead to a fundamental understanding of the heat transfer process, pressure losses and evolving flow patterns. In this context, heat flux density, mass flux density and saturation pressure are systematically varied during measurements. Finally, the characteristic fluid properties like density, surface tension and dynamic viscosity of MM are measured in the temperature range from 283.15 K and 343.15 K using the IMETER®. The experimental data are compared to common prediction methods for fluid properties like Peng-Robinson equation-of-state or the REFPROP database in order to quantify the uncertainties of the applied models.

Figure 1: ORC test rig at the Center of Energy Technology with an electrical power of up to 15 kW

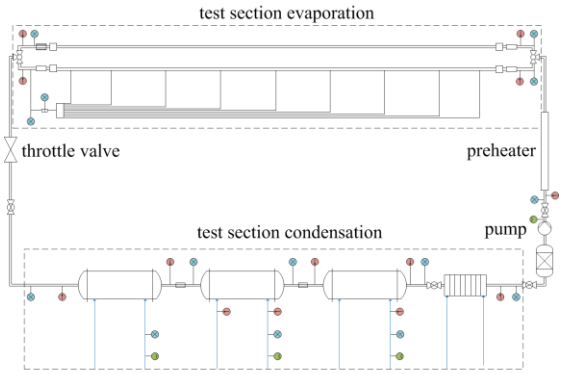

Figure 2: Scheme of test rig for the measurement of flow boiling heat transfer coefficients

Discussion and Results

First and second law analyses of ORC systems for waste heat recovery show that MM is a promising working fluid for temperatures between 250 °C and 500 °C. A case study is conducted for a stationary biogas-engine as heat source [1]. For the ORC module, MM is considered as working fluid. In the case of a pure electricity generation, the determined second law efficiency of 26.2 % is significantly higher compared to the use of octamethyltrisiloxane (MDM) as working fluid. In general, the heat transfer measurements show that especially at constant saturation temperature, the present flow pattern has a considerable effect on the heat transfer characteristics. The observed effects at varying operational parameters are in accordance to literature. Exemplarily, high pressure and heat flux density lead to an increase in the heat transfer coefficient in the nucleate boiling dominated region. The model of Wojtan et al. and the correlation of Kandlikar can be recommended for the prediction of flow pattern and heat transfer coefficients. A further adaption of these models leads to a reduction of the mean deviation. Concerning the fluid properties of MM, a comparison between experimental data and predicted values lead to a maximum relative error below 7 %. This accuracy is sufficient for the experimental determination of heat transfer coefficients as well as for their theoretical prediction.

Summary/Conclusions

Based on a comprehensive investigation consisting of thermodynamic modelling and experimental setups, a reliable ORC design procedure can be established for an ORC working fluid and its class of substance. In particular, the uncertainties of the simulation models and design methods can be significantly reduced by the fluid-specific adaption of existing approaches.

Acknowledgments

The authors acknowledge the support of the co-workers and students of the research group “Energy Systems and Technologies”, which were involved in the ORC related research activities in the last decade. In particular, we would like to thank at this point Tim Eller, Markus Görl, Ivanka Milcheva, Markus Preißinger, Sebastian Kuboth, Sebastian Kutzner and Matthias Welzl.

References:

[1] T. Weith, F. Heberle, M. Preißinger, D. Brüggemann, *Performance of Siloxane Mixtures in a High-Temperature Organic Rankine Cycle Considering the Heat Transfer Characteristics during Evaporation*, Energies 2014, vol. 7, Issue 9, pp. 5548-5565, doi:10.3390/en7095548

Metal Organic Framework Materials for Adsorption Heat Pumps

R.K. AL-Dadah[1], Saad Mahmoud[1], Eman Hussein[1], Peter Youssef[1], Fadhel Al-Mousawi[1]

[1] School of Engineering, University of Birmingham, Birmingham, B15 2TT United Kingdom

[*] r.k.al-dadah@bham.ac.uk

Abstract

There are huge amounts of low grade heat sources with temperatures below 150^0C like solar thermal energy, geothermal and many industrial processes which are currently not exploited. Adsorption heat pumps offer a huge potential in a number of vital applications like energy storage, cooling and heating, and water desalination which can be driven by these low grade heat sources leading to significant reduction on fuel consumption and CO_2 emissions. The adsorbent material is the key element in adsorption heat pump systems which determine the performance, size and cost of such technology. Metal Organic Framework Materials (MOFs) are new class of adsorbent materials with superior water uptake, high pore volume and surface area. This abstract presents research work at the University of Birmingham, United Kingdom on the development of adsorption heat pumps using MOFs for various applications including heat storage, cooling, power generation and water desalination.

Keywords: Adsorption heat pumps, Metal Organic Framework materials (MOFs), Heat storage, Cooling, Water desalination, Power generation.

Introduction/Background

Thermally-driven adsorption heat pumps and chillers have clear advantages over traditional heating/cooling and vapour compression heat pump systems due to their low environmental impact and their ability to efficiently use low grade heat sources, such as solar energy, industrial or automotive waste heat and geothermal resources. Adsorption systems utilise the affinity of a porous material to a certain working fluid such as water to generate the heat pumping mechanism. **Erro! Fonte de referência não encontrada.**Figure 7 and Figure 8 illustrate schematically the operation of two bed adsorption system and the Duhring thermodynamic cycle diagram respectively. Using water as a refrigerant, the adsorption system can be used for water desalination where sea water is evaporated in the evaporator due to the adsorption effect. Thus water based adsorption systems can be applied for cooling and heating (heat pump) [1-3], energy storage [4] and water desalination [5-6].

Currently available adsorption heat pump systems utilise silica gel/ water, zeolite/water and activated carbon/ammonia working pairs which suffer from low water uptake or hazardous fluid in the case of ammonia. Metal Organic Frameworks (MOFs) are new micro-porous materials with exceptional high porosity, well-defined molecular adsorption sites and large surface area (up to 5500m^2/g). The author and her co-workers have synthesised and tested a wide range of MOF materials that have shown superior water adsorption performance compared to that of the existing conventional porous materials like silica gel and zeolites. This abstract describes research work carried out at the School of Engineering, University of Birmingham, United Kingdom on MOF/water adsorption systems in terms of (i) MOF materials water adsorption characteristics and thermal properties; (ii) enhancement of MOF material thermal properties using Graphene Oxide and Calcium Chloride; (iii) experimentally testing MOF materials in single bed adsorption system for energy storage application and (iv) experimentally testing MOFs in two-bed adsorption system for water desalination and cooling.

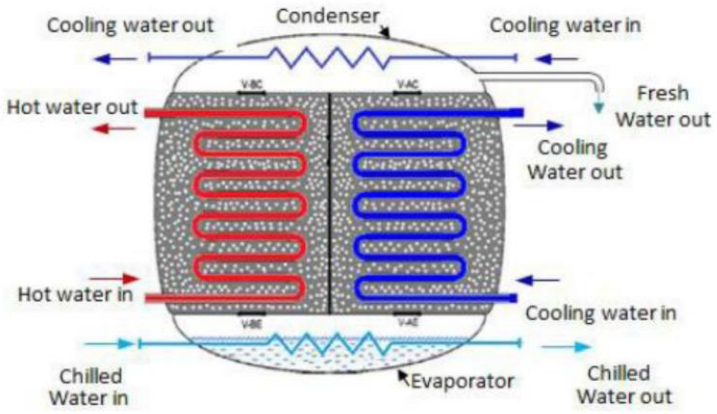

Figure 7, Schematic diagram of the 2-bed system [5]

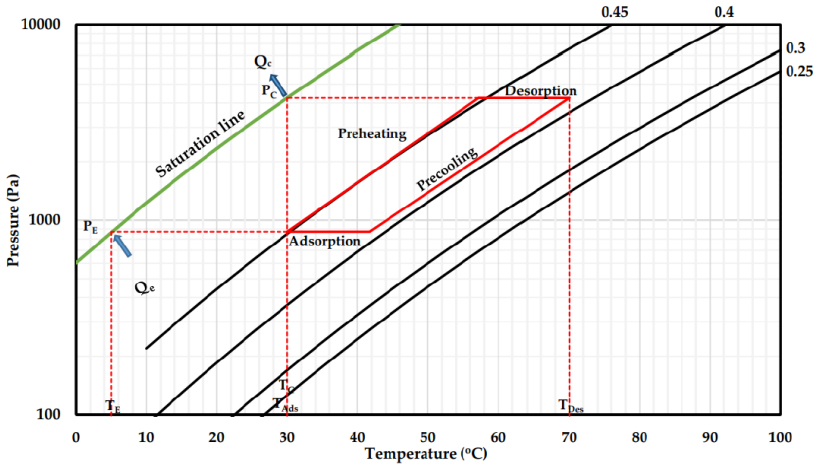

Figure 8, P-T-X diagram of Adsorption Cycle [2]

Discussion and Results

MOF Materials

Figure 9 shows the water adsorption isotherms of the MOF materials synthesised and characterised by the author's research group. It can be seen that MIL-101(Cr) shows the highest equilibrium water uptake followed by MIL-100(Fe), Aluminium Fumarate and CPO-27(Ni). However, MIL101(Cr) and MIL100(Fe) show isotherm shape of type IV with the adsorption of water occurring at high relative pressure of (0.5 and 0.3 respectively). Aluminium Fumarate shows the same isotherm type IV but the steep increase occurs at a partial pressure of 0.2. On the other hand, CPO-27(Ni) shows water adsorption isotherm of type I. Figure 10 shows the adsorption kinetics of the four MOF materials mentioned above. It can be seen that CPO-27(Ni) has the fastest adsorption kinetics followed by MIL-101(Cr) and MIL-100(Fe) then aluminium fumarate.

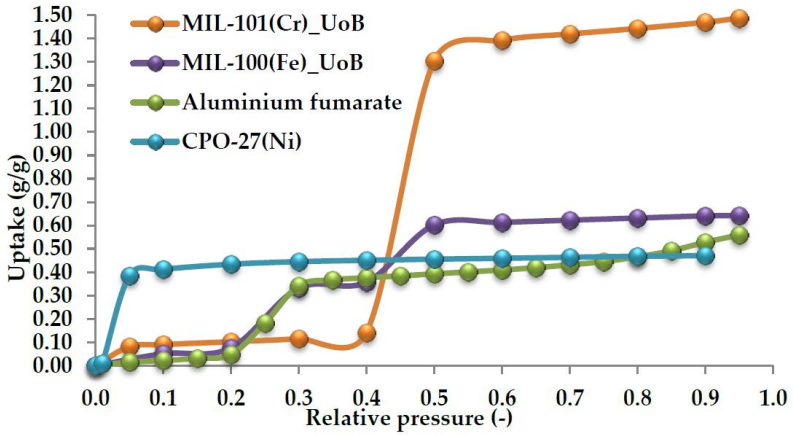

Figure 9, Water adsorption isotherm of metal-organic framework materials and silica gel at 25°C.

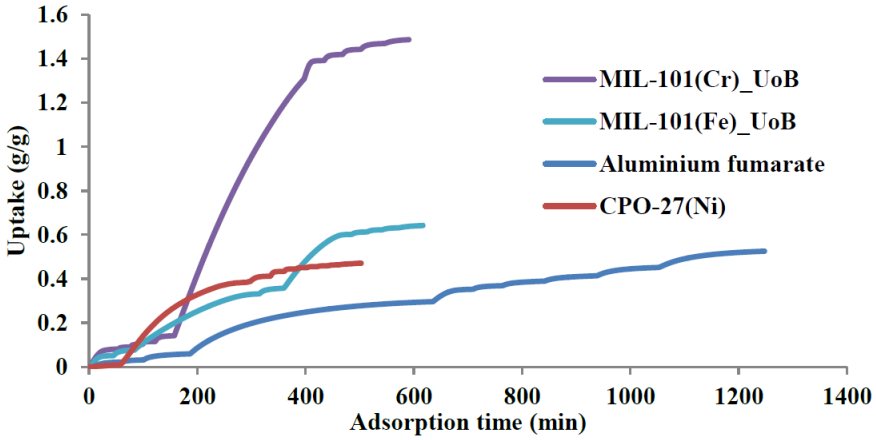

Figure 10, Water adsorption rate of metal-organic framework materials and silica gel at 25°C.

Figure 11 (a) and (b) show the effect of using Graphene Oxide and Calcium Chloride on the water adsorption isotherms of MIL101(Cr) respectively. It can be seen that introducing GrO and $CaCl_2$ improved the water uptake on both the high and low relative pressure range.

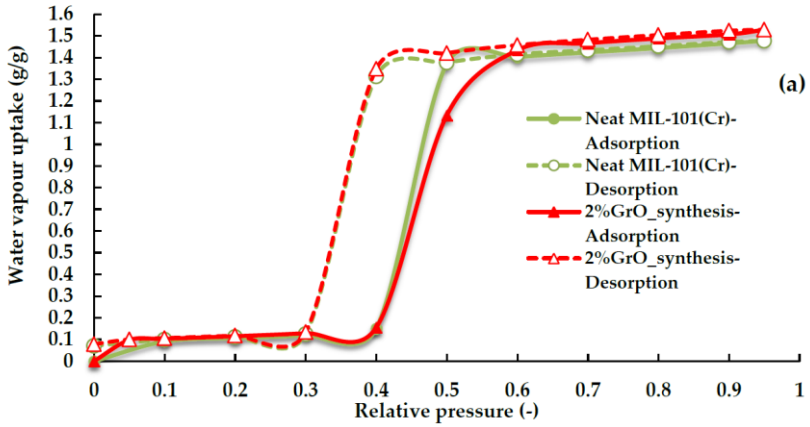

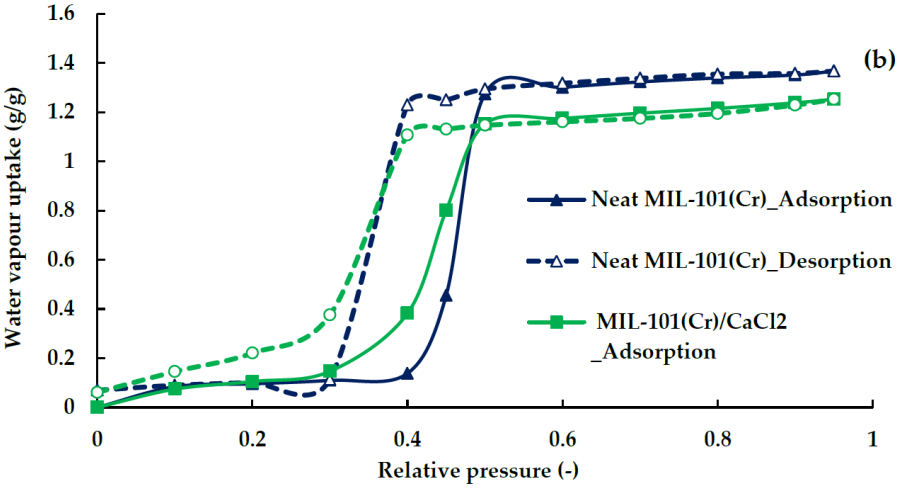

Figure 11, Water adsorption isotherm of

(a) MIL-101(Cr)/GrO and (b) MIL-101(Cr)/$CaCl_2$ at 25^oC.

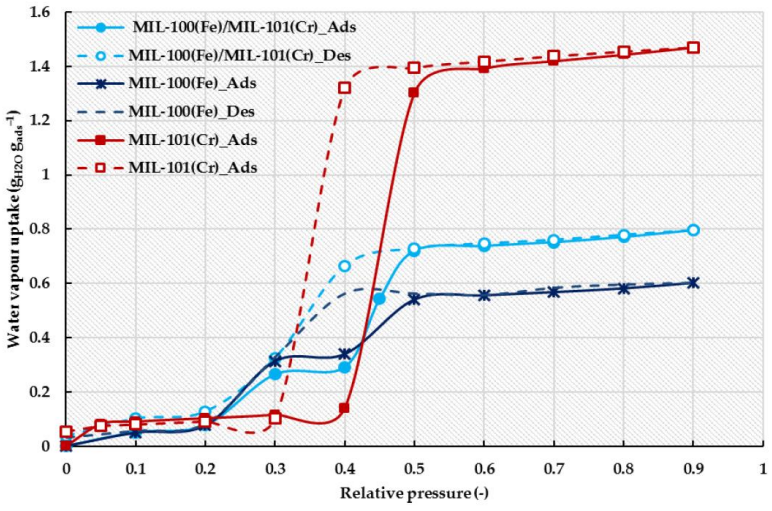

Also,

Figure 12 shows the effect of incorporating MIL-100(Fe) with MIL-101(Cr) on the water adsorption isotherms of MIL100(Fe). It can be seen that it improved the water vapour capacity in the high relative pressure range.

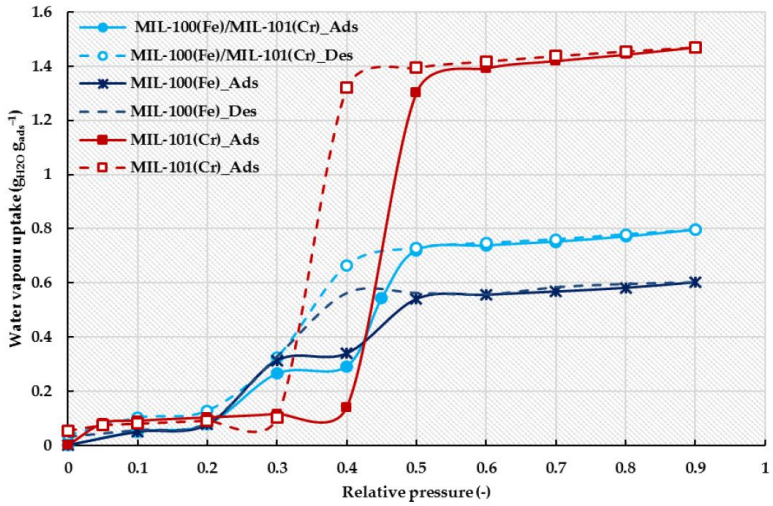

Figure 12, Water adsorption isotherms of MIL-100(Fe)/ MIL-101(Cr) composite at 25°C.

MOF/Water Adsorption Systems

Thermodynamic simulation of these MOF materials in an industrial adsorption system manufactured by Weatherite Air Conditioning Ltd for water desalination and cooling illustrated the potential of such material. Figure 13 and Figure 14 show the specific daily water production and specific cooling of CPO-27Ni that can be obtained at 95 °C heat source temperature at a range of condenser cooling temperature of 5 to 30°C and evaporator temperatures of 10 to 40°C. It is clear that increasing the condenser water inlet temperature has the same effect as decreasing the evaporator inlet water temperature resulting in less water production and cooling. The reason for that is the difference between the system's two partial pressure ratios, which depend on the condenser and evaporator operating temperatures. It is found that by decreasing the evaporator temperature from 40 to 10°C, water production decreases by 202% from 20.6 to 6.8 m^3.tonne adsorbent^{-1}.day^{-1} at condenser water inlet temperature of 10°C. Similarly, increasing the condenser water temperature from 5 to 30°C, decreases SDWP by 135% from 7.5 to 3.2 m^3.tonne adsorbent^{-1}.day^{-1} at evaporator water inlet temperature of 10°C. The cooling effect produced by the cycle can be used for different applications depending on the evaporation temperature. For air conditioning applications where evaporation temperature of 10-20°C is required, the adsorption-desalination system can provide specific cooling capacity of 225 W.kg^{-1}. For process cooling where evaporation temperature of 40°C can be used, the adsorption desalination system can provide specific cooling power of 750 W.kg^{-1}.

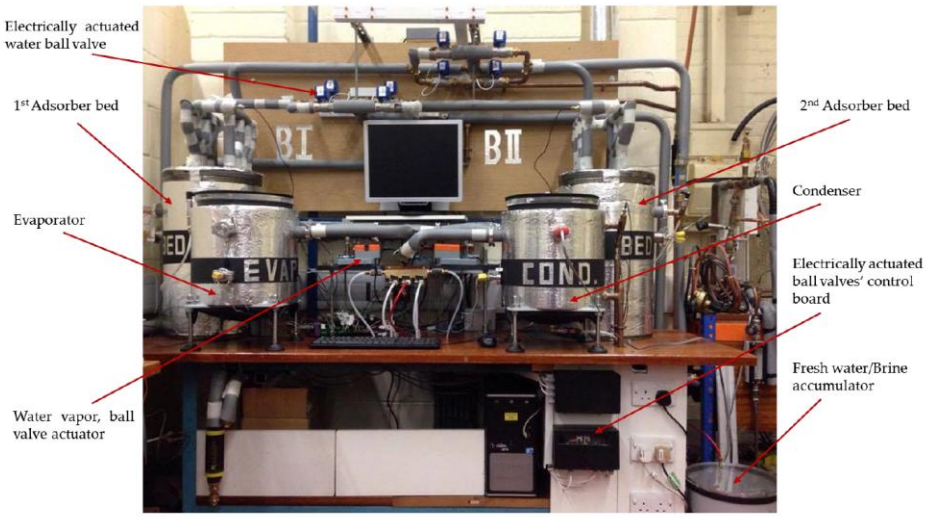

Figure 15 shows the two-bed adsorption experimental facility developed to evaluate the performance of MOF materials for water desalination & cooling applications. Two commercially available MOF materials were used in these test facilities namely CPO-27(Ni) manufactured by Johnson Matthey Plc and Aluminium Fumarate manufactured by MOF Technology Ltd. Figure 16 and Figure 17 show the specific daily water production and specific cooling obtained at heat source temperature range of 65 to 95^{o}C, condenser cooling temperature of 30^{o}C and various evaporator temperatures. It can be seen that evaporator water inlet temperature significantly affects cycle outputs where SDWP increased by 366% from 5.4 to 25.2 $m^3.tonne^{-1}.day^{-1}$ and SCP increased by 464% from 140 to 790 W/kg when evaporator inlet water temperature increased from 10 to 40^{o}C. On the other hand, desorption temperature has a minimal effect on cycle outputs specially at low evaporator temperatures less than 20^{o}C where water and cooling production rise by 17% and 13% respectively when desorption temperature increases from 65 to 95^{o}C. This behaviour is attributed to the shape of Aluminium Fumarate isotherm type IV where the uptake value is almost constant at all pressure ratios <0.2, therefore changing desorption temperature (i.e. the lower pressure ratio) does not affect the system uptake and hence the system performance. It is found that 95^{o}C desorption temperature and 40^{o}C evaporator water inlet temperature achieve maximum SDWP and SCP of 25.3 $m^3.tonne^{-1}.day^{-1}$ and 789.4 W/kg, respectively.

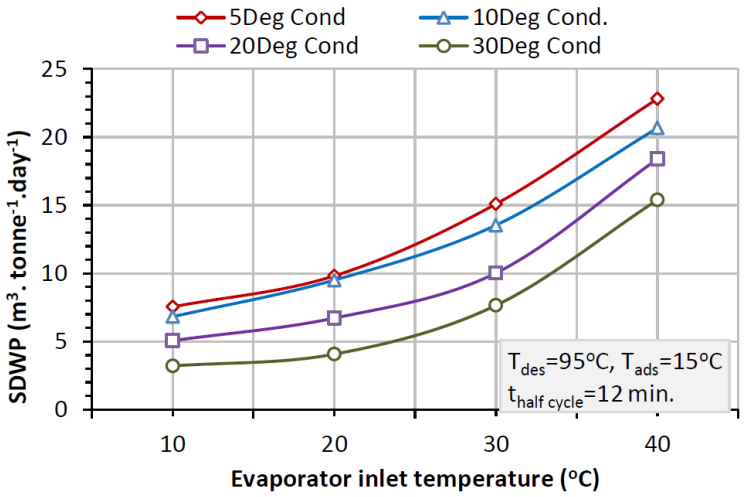

Figure 13, Specific daily water production at various evaporator and condenser water inlet temperatures using CPO-27Ni [6]

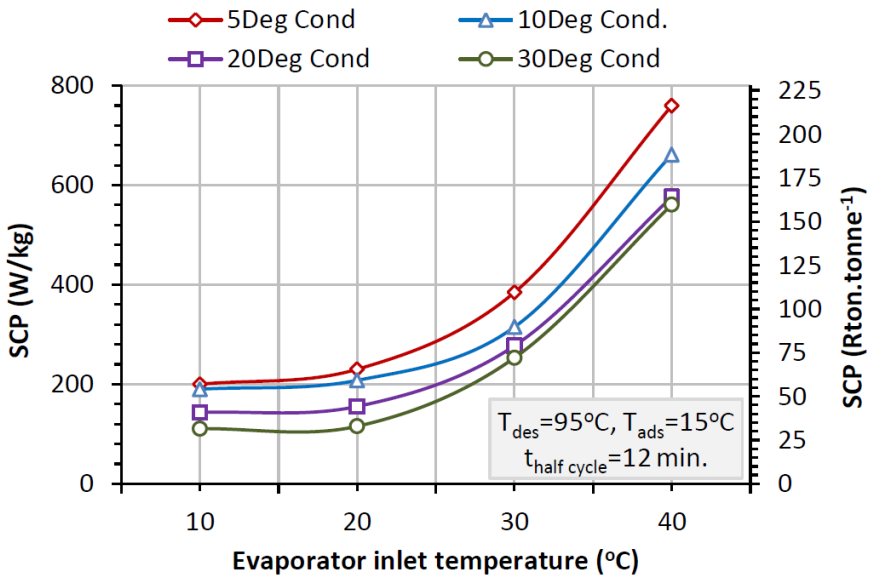

Figure 14, Specific cooling power for various evaporator and condenser water inlet temperatures using CPO-27Ni [6]

Figure 15, Testing facility of the double-bed adsorption system

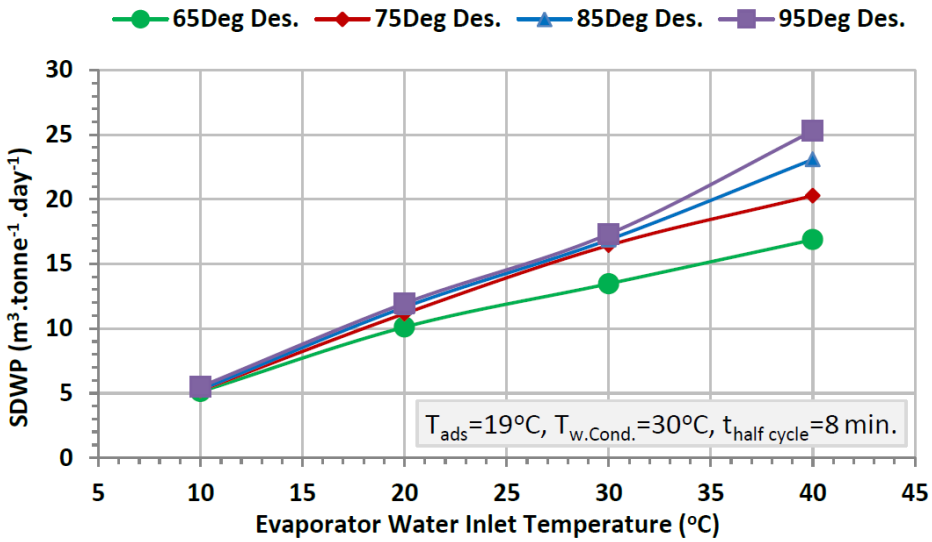

Figure 16, Specific daily water production at various desorption and evaporator water inlet temperatures using (Al-Fumarate)

For energy storage, a single bed adsorption was used to investigate the energy storage performance of CPO-27(Ni) as shown in Figure 18 where energy is stored during the desorption process and recovered during the adsorption process. Figure 19 shows the water uptake of the adsorbent material using various energy storage time of one day, 3 days and one week. It can be seen that the uptake of the adsorbent material was not affected by the length of storage time highlighting the potential of MOFs for both short and long term energy storage. The energy density achieved was found to be 166kW.hr.m^{-3}.

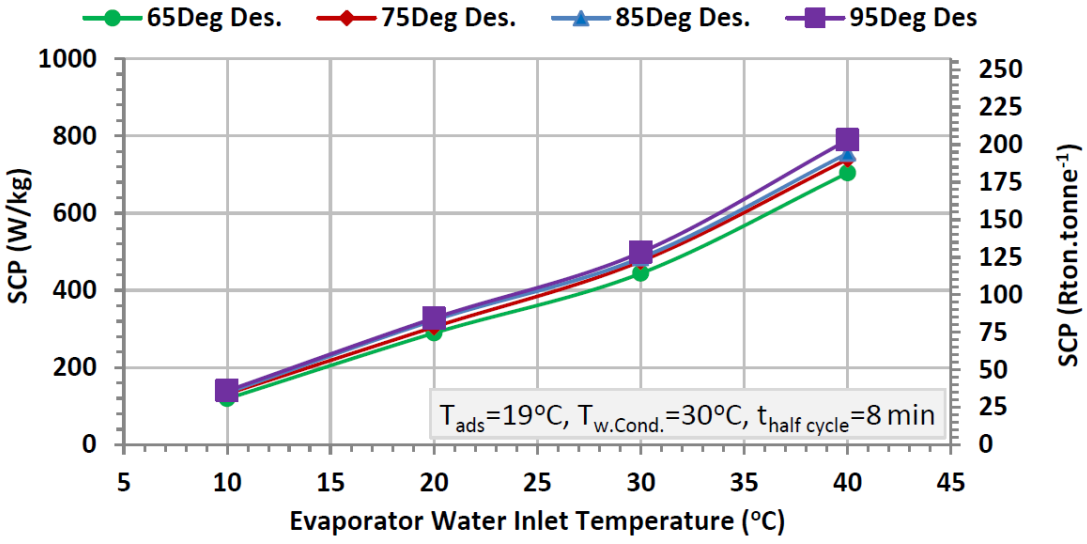

Figure 17, Specific cooling power at various desorption and evaporator water inlet temperatures using (Al-Fumarate)

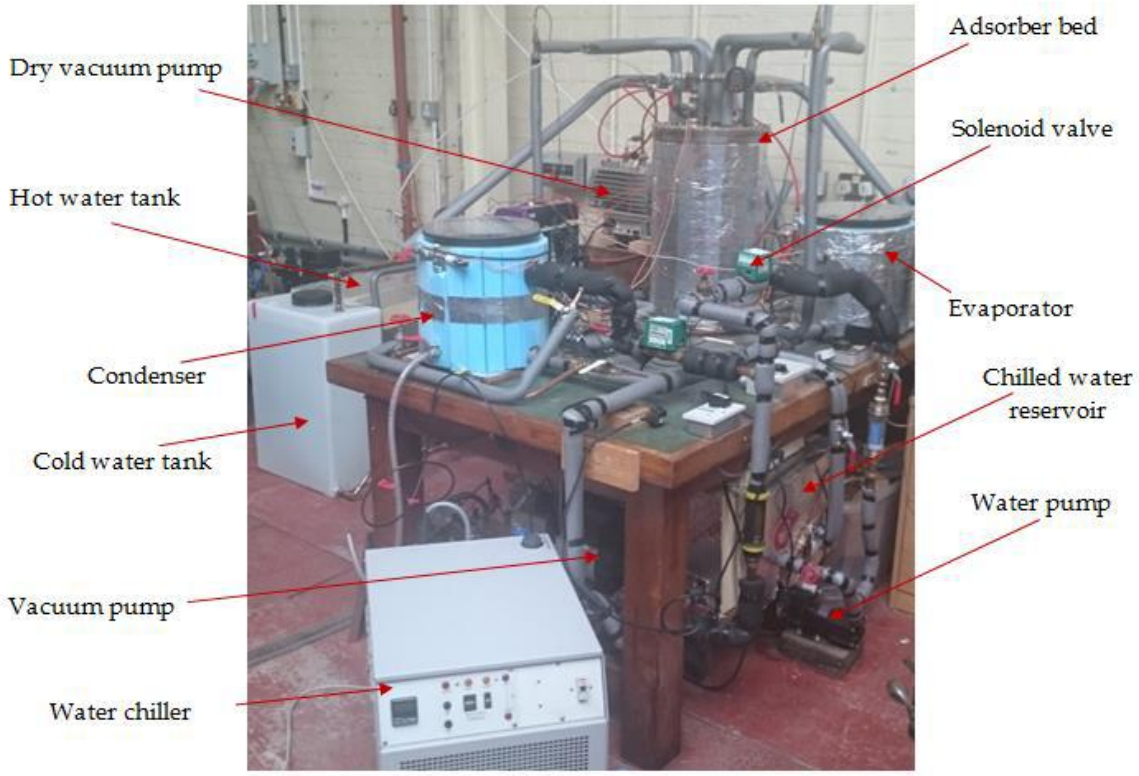

Figure 18, Pictorial view of the single bed test facility [6]

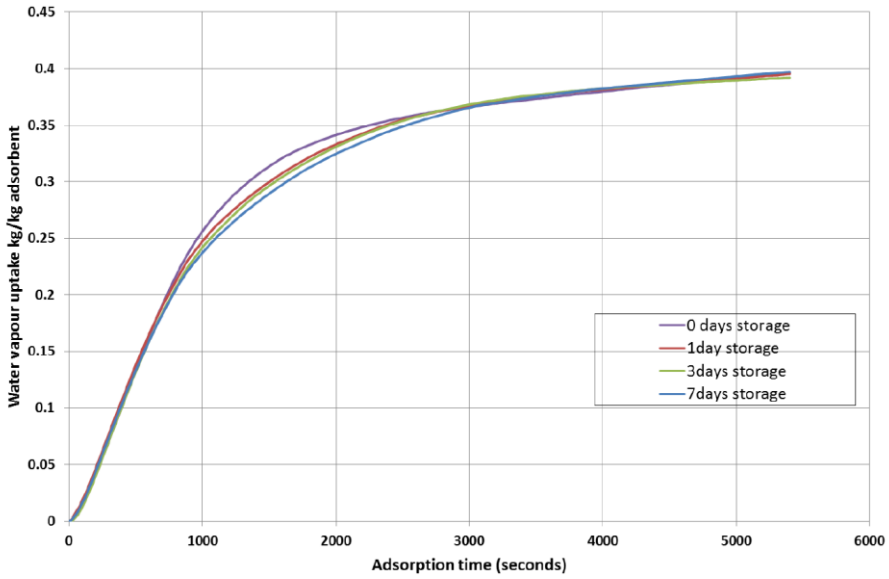

Figure 19, Water uptake of CPO-27(Ni) at various storage times.

Finally research work to investigate theoretically the potential of producing power in addition to cooling was carried out by integrating a turbine between the desorber bed and the condenser or by integrating the adsorption system with Organic Rankine Cycle as shown in Figure 21 which shows the modified adsorption system for cooling and electricity ASCE (to the right) and the basic adsorption cooling system BACS (to the left) or by integrating the adsorption system with Organic Rankine Cycle IAOSCE as shown in Figure 21. Figure 22

shows the effective Coefficient of Performance of the systems shown in Figure 20 and Figure 21 where IAOSCE shows the highest COPe. Experimentally, the two bed adsorption system was integrated with Organic Rankine Cycle consisting of evaporator, condenser pump and radial inflow turbine with R245fa as the refrigerant. Two operating scenarios were investigated where in scenario 1, the ORC was driven by the cooling fluid leaving the adsorber bed to recover the adsorption energy, scenario 2, the ORC was driven by the heating fluid after passing through the desorber bed. Figure 23 shows the experimental COP/COPe values IAOSCE (scenario 1) utilising CPO-27(Ni) and R245fa.

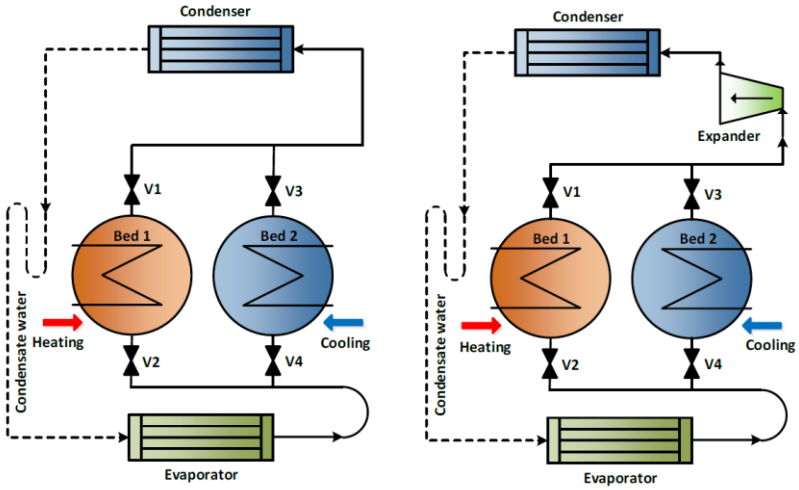

Figure 20, Schematic diagram of basic adsorption cooling system BACS (left), and adsorption system for cooling and electricity ASCE (right)

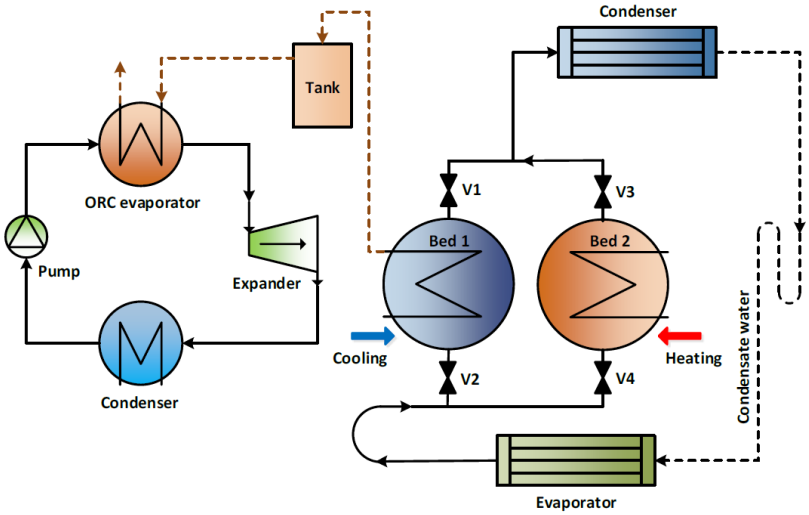

Figure 21, Schematic diagram of integrated adsorption-ORC system for cooling and electricity IAOSCE

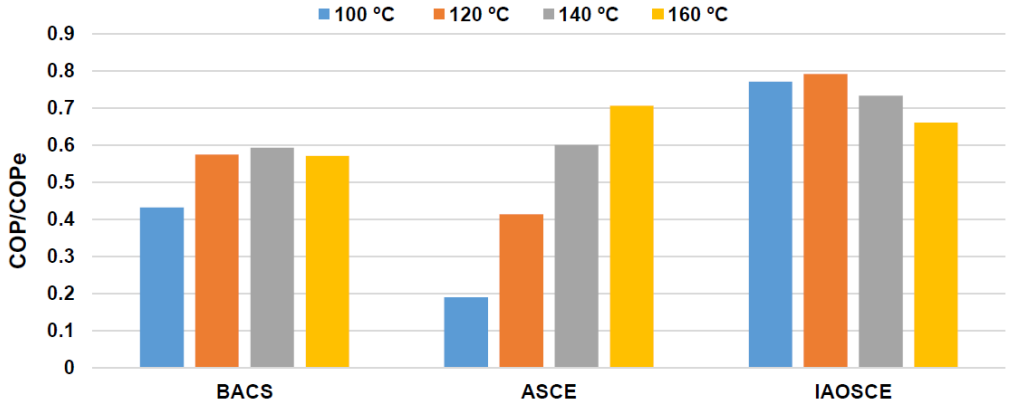

Figure 22, COP/COPe of different adsorption configurations used to generate cooling and electricity compared to that of BACS utilising CPO-27(Ni) with a range of heat source temperature

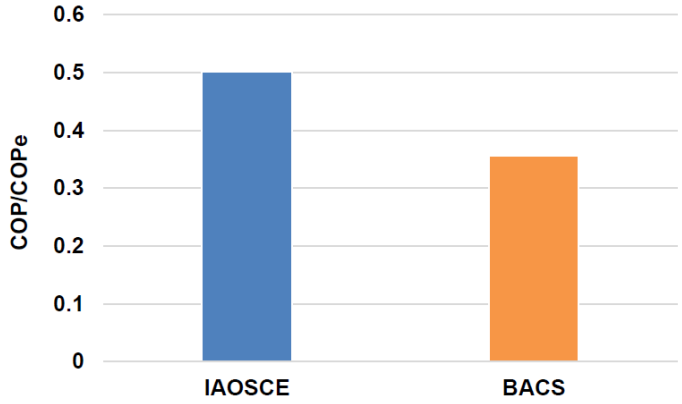

Figure 23, Experimental COP/COPe values for the integrated adsorption-ORC system for cooling and electricity IAOSCE (scenario 1) utilising CPO-27(Ni) and R245fa utilising heat source temperature of 95 °C

Summary/Conclusions

MOF/Water adsorption heat pumps offer significant potential in various applications including energy storage, water desalination & cooling and power generation. For water desalination, Al-Fumarate can work at low desorption temperatures as low as 65^{o}C while at 95^{o}C maximum SDWP of 25.3 m^3.$tonne^{-1}$.day^{-1} and SCP of 789.4 W/kg were obtained while according to literature, the maximum experimentally obtained specific daily water production (SDWP) using "Silica-gel" is 13.5 m^3per tonne of adsorbent per day. For energy storage, CPO27(Ni) MOF material showed energy density of 166 kW.hr.m^{-3} more than 3 times that of hot water tanks. For power generation, including a turbine in the adsorption system can produce power output and increase the effective Coefficient of Performance of the adsorption cooling system by 22%. Integrating the adsorption cooling system with Organic Rankine Cycle can produce an effective Coefficient of performance of 0.8.

References:

[1] Shi, B., Al-Dadah, R., Mahmoud, S., Elsayed, A, Elsayed, E., *CPO-27(Ni) metal–organic framework based adsorption system for automotive air conditioning*. Applied Thermal Engineering, 2016 https://doi.org/10.1016/j.applthermaleng.2016.05.109

[2] Elsayed, E., Al-Dadah, R., Mahmoud, S., Elsayed, A., & Anderson, P. A. Aluminium fumarate and CPO-27(Ni) MOFs: *Characterization and Thermodynamic Analysis for Adsorption Heat Pump Applications*. Applied Thermal Engineering, 2016. doi: 10.1016/j.applthermaleng.2016.01.129

[3] Elsayed, E., Wang, H., Anderson, P., Al-Dadah, R., Mahmoud, S., Navaro, H., Ding, Y., Bowen, J., *Development of MIL-101(Cr)/GrO composites for adsorption heat pump applications*, Microporous and Mesoporous Materials, 2017. https://doi.org/10.1016/j.micromeso.2017.02.020

[4] Elsayed, A., Elsayed, E., Al-Dadah, R., Mahmoud, S., Elshaer, A., & Kaialy, W. *Thermal energy storage using metal–organic framework materials*. Applied Energy, 2016 http://dx.doi.org/10.1016/j.apenergy.2016.03.113

[5] Youssef, P. G., Al-Dadah, R. K., Mahmoud, S. M., Dakkama, H. J., & Elsayed, A., *Effect of Evaporator and Condenser Temperatures on the Performance of Adsorption Desalination Cooling Cycle*. Energy Procedia, 2015, doi: 10.1016/j.egypro.2015.07.263

[6] Youssef, P. G., Dakkama, H., Mahmoud, S. M., & Al-Dadah, R. K., *Experimental investigation of adsorption water desalination/cooling system using CPO-27Ni MOF*. Desalination, 2017, doi: http://dx.doi.org/10.1016/j.desal.2016.11.008

Accepted Extended Abstracts

Bubble Columns in Humidification Dehumidification Technology: From a Demonstration Unit to Fundamental Research in Optical Accessible Laboratory Bubble Columns

M.Preißinger[1]

[1]illwerke vkw Professorship for Energy Efficiency, University of Applied Sciences Vorarlberg, 6850 Dornbirn, Austria, www.fhv.at/en/research/energy

[*]Corresponding author: markus.preissinger@fhv.at

Abstract

For many countries, water is the foundation for a liveable world in the future. Desalination is a crucial application in this context; however, also treatment technologies for brackish water and industrial wastewater are necessary. Hence, we present a demonstration unit based on humidification dehumidification technology, which is able to use low-grade heat. In the first part, the demonstration unit and the gained experimental results are analysed. In the second part, we report about the design of two new test-rigs, in which we are able to analyse the humidification of air in a bubble column in more detail. Hopefully, this will help the research community to increase the efficiency of HDH technology in the future.

Keywords: Humidification Dehumidification Technology. HDH, Desalination, Waste Water Treatment, Bubble Columns

Introduction

Secure, affordable and resource efficient water supply systems will be as significant for future societies as the energy system, and both undergo similar changes. Thermal water treatment systems are advantageous within this topic as they offer the chance to use solar and industrial (waste) heat on low exergy level. Humidification Dehumidification (HDH) technology is a promising process which can be applied for solar desalination as well as for thermal treatment of industrial wastewater. However, the process is energetically not yet competitive compared to conventional technologies, as contemporary technical design criteria for the process are scarce. This study is a first step towards a thorough understanding of the most crucial point: the humidification of air in a bubble column.

Discussion and Results

A demonstration unit for bilge water treatment was set-up at the former institute of the author, the Center of Energy Technology at the University of Bayreuth [1]. Bilge water is a mixture of oil, water and salt and it is treated in large centrifuges in harbours all around the world. As the centrifuges are just able to concentrate the oil phase in the mixture to about 50 %, it cannot be used as recycling oil but is burned in the cement industry. Our work aimed to concentrate the oil phase to get a water content of less than 2 %. Therefore, a rectangular bubble column with an area of 1m² and a height of 1 m was constructed including five nozzles for air entry at different heights. Although the contact time between air bubbles and bilge water is about 2-3 times higher for nozzle A1 than for nozzle A5, Figure 1 shows an almost constant productivity. A possible explanation would be a fully saturated air bubble even for the shortest contact time (nozzle A1). However, if this would be the case, spraying further medium from the top would not result in the higher productivity of Figure 1. Hence, the results are not in accordance with ideal thermodynamics and some unexpected effects occur.

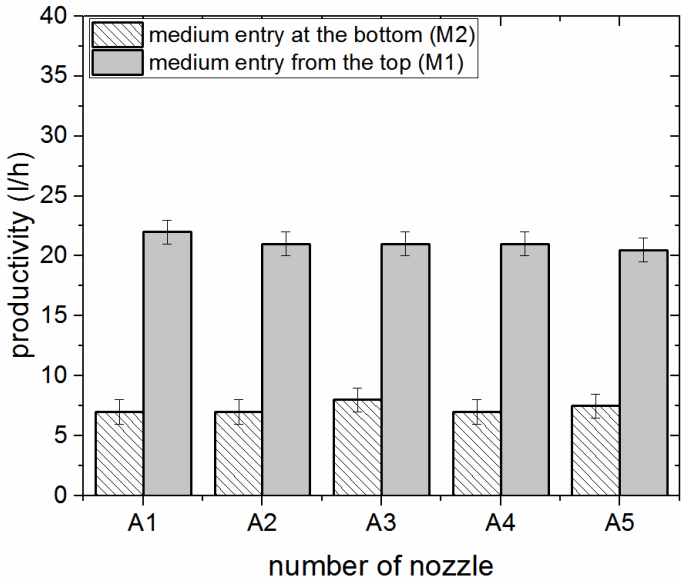

Figure 24: Productivity of bubble column humidifier for bilge water treatment (nozzles A1 to A5 are at different heights of the bubble column, hence, giving different contact times between air bubble and bilge water)

Obviously, it is necessary to intensify research work towards a clear understanding on the mechanisms and parameters that influence humidification of air in a bubble column. Therefore, in the second part of this publication a two newly designed optical accessible laboratory humidifiers including fast camera systems are presented. Based on the new set-up, we intend to deduce semi-empirical correlations, which link humidification rate with thermodynamic and geometric boundary conditions as well as with physical-chemical properties of the liquid phase.

Conclusion

Humidification Dehumidification technology is a promising way for desalination and wastewater treatment based on solar energy or industrial waste heat. A demonstration unit for salt water as well as for bilge water serves as prove of concept. However, we identified several necessary steps to optimize the process energetically with a special focus on a clear understanding of the applied bubble column humidifier. The semi-empirical correlations for the humidification of air in a bubble column, which we intend to deduce from the two test-rigs, will help to replace commonly applied assumptions with experimentally validated equations. This is necessary to reduce uncertainties during simulation and technology design, and to increase the efficiency of thermal water treatment systems based on HDH technology.

Acknowledgment

The work is partly financed by the German Federal Ministry of Economic Affairs and Energy within the Central Innovation Programme for SMEs due to an enactment of the German Bundestag. The work is also partly financed by the Austrian Science Fund (FWF): Project number P31103. The authors want to thank the company “Hopf GmbH” in Bayreuth, Germany, for the construction of the demonstration unit.

References:

[1] Preissinger, M., *Experimental Analysis of a Demonstration Plant for Bilge Water Treatment and Desalination Based on Humidification Dehumidification Technology*. 15th International Conference on Environmental Science and Technology. Rhodes, Greece, 31 August to 2 September 2017.

Iron(III) Trimesate (MIL-100(Fe)) in Adsorption Desalination

Eman Elsayed[1,2*], Raya AL-Dadah[1], Saad Mahmoud[1], Paul Anderson[2], Ashraf Hassan[3]

[1]School of Mechanical Engineering, University of Birmingham, Birmingham, B15 2TT, UK.

[2]School of Chemistry, University of Birmingham, Birmingham, B15 2TT, UK.

[3]Qatar Environment and Energy Research Institute (QEERI), Qatar Foundation, P.O. Box, 5825, Doha, Qatar.

[*]Corresponding author: EXH496@student.bham.ac.uk

Abstract

Metal-organic framework (MOF) materials has been one of the most growing and explored class of porous materials over the last two decades [1]. As the name suggests, metal organic frameworks consist of inorganic nodes (metal ions) and organic linkers (organic ligands). Due to the exceptional properties of the high surface areas, their structure functionality and their tunable pore size, these materials can be used in numerous applications [2]. Applications may vary from catalysis, gas separations and storage, sensors to heat pumps and very recently adsorption desalination [3].

Iron(III) trimesate is a MOF material (Fig.1) that has a high-water vapour capacity of 0.6 $g_{H2O}.g_{ads}^{-1}$ and high cyclic stability hence has the potential to be used in adsorption applications. One of the adsorption applications that have not been fully explored is adsorption desalination. Adsorption desalination has been identified with many advantages such as environmentally friendly, driven by low-grade heat sources, low capital cost, low evaporation temperature and hence reduced fouling (formation of scales causing the damage of the evaporation units) effect [4]. This study investigates the potential of MIL-100(Fe) (Materials Institute Lavoisier) in adsorption desalination application. The synthesized material is characterized in terms of their water adsorption uptake, pore size distribution, surface area and X-Ray diffraction. The water adsorption isotherm (Fig.2) showed a unique two step S shape isotherm which gave this material the advantage to work at a wider range of relative pressure compared to other materials such as aluminium fumarate and MIL-101(Cr) can work at.

The P-T-x diagrams were developed based on the equilibrium water adsorption characteristics to show the potential of MOF material in the adsorption desalination application. The P-T-x diagrams were also used to choose the most suitable operating condition to ensure the highest cycle efficiency. Results showed that, at an evaporation temperature of 10°C, a condenser and adsorber temperatures of 30°C and a desorption temperature of 90°C, the material gave a net water loading difference of 0.26 l.kg-1 and a COP of the whole cycle of 0.7. When increasing the evaporation temperature to 20°C, the water loading difference increased to 0.57 $l.kg^{-1}$ and gave a COP of the whole cycle of 0.833. This shows that based on the equilibrium data and at the same operating conditions, the MIL-100(Fe) can perform other MOF materials such aluminium fumarate and CPO-27(Ni). A previous study showed that at an evaporation temperature of 20°C the aluminium fumarate gave water loading difference of 0.46 and a COP of 0.7 while CPO-27(Ni) gave water loading difference of 0.18 and a COP of 0.63 [3]. This shows the advantage of the high performance of the investigated material at the adsorption desalination application even at a low desorption temperature of 90°C.

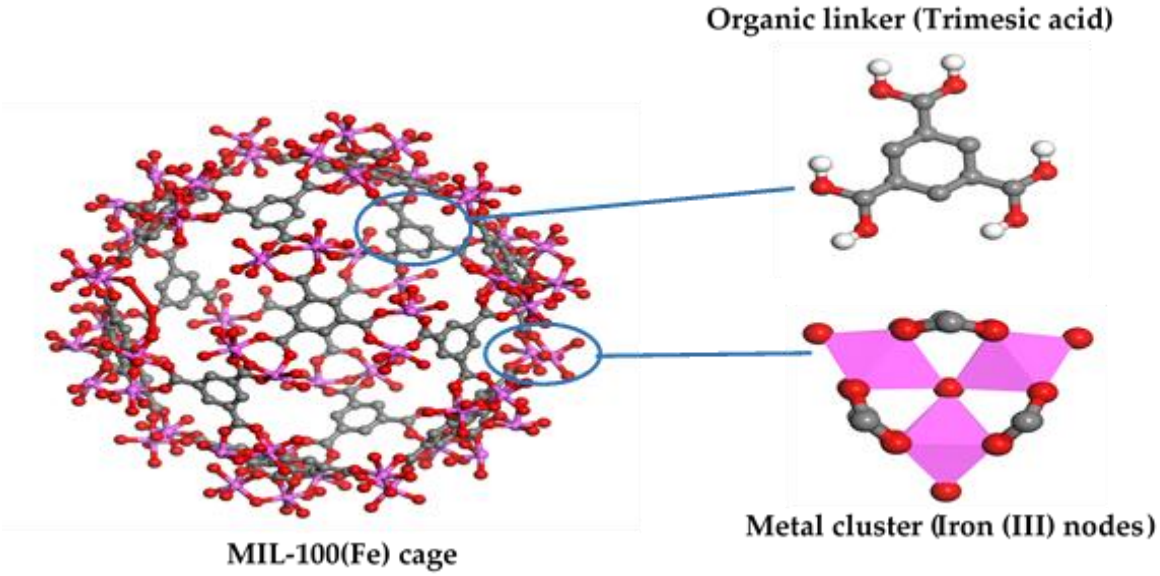

Fig.1 Crystal structure of MIL-100(Fe)

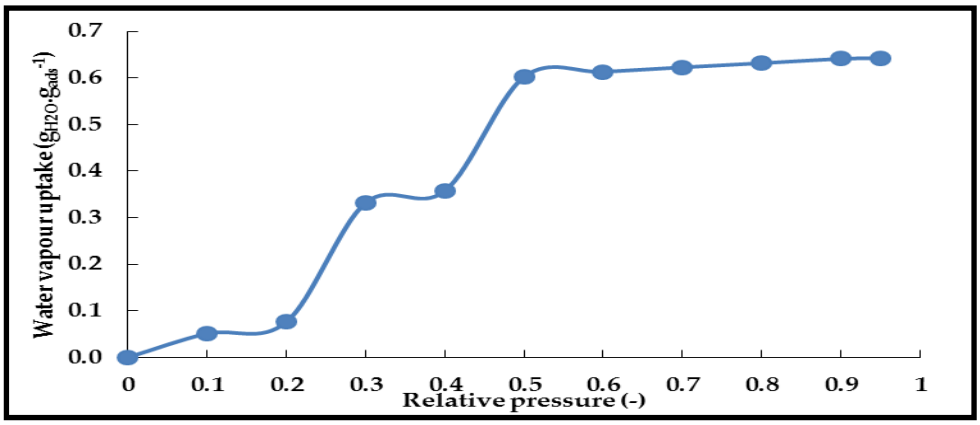

Fig.2 Water adsorption isotherm of MIL-100(Fe) at 25°C.

References

1. Li, L., et al., *Facile Fabrication of Ultrathin Metal–Organic Framework-Coated Monolayer Colloidal Crystals for Highly Efficient Vapor Sensing.* Chemistry of Materials, 2015. **27**(22): p. 7601-7609.
2. Meek, S.T., J.A. Greathouse, and M.D. Allendorf, *Metal-organic frameworks: A rapidly growing class of versatile nanoporous materials.* Advanced Materials, 2011. **23**(2): p. 249-267.
3. Elsayed, E., et al., *Aluminium fumarate and CPO-27 (Ni) MOFs: characterization and thermodynamic analysis for adsorption heat pump applications.* Applied Thermal Engineering, 2016. **99**: p. 802-812.
4. Elsayed, E., et al., *CPO-27 (Ni), aluminium fumarate and MIL-101 (Cr) MOF materials for adsorption water desalination.* Desalination, 2017. **406**: p. 25-36.

The effects of graphite flake on specific cooling power of sorption chillers: An experimental study

H. Bahrehmand, M. Khajehpour, W. Huttema, C. McCague and M. Bahrami*

Laboratory for Alternative Energy Conversion (LAEC), School of Mechatronic Systems Engineering, Simon Fraser University, Surrey, British Columbia, Canada

*Corresponding Author: mbahrami@sfu.ca

Abstract

Adding natural graphite flakes to sorbents of sorption cooling systems can enhance the total thermal diffusivity, while reducing the active material and increasing mass transfer resistance. To find the best compromise between these counteracting trends, the specific cooling power (SCP) of CaCl2-silica gel composite sorbents with 0-20 wt% graphite flake content was tested with a custom-built gravimetric large pressure jump (G-LPJ) test bed. It was observed that when the sorption rate is high, i.e. the first 20 min of sorption, graphite flake additive increases the SCP and COP due to the higher sorbent thermal diffusivity. Nevertheless, as the sorption rate reduces with time, the need for heat transfer enhancement, i.e. graphite flake additive, decreases. Furthermore, adding 20 wt.% graphite flakes to the composite sorbent has led to a 67% increase in SCP0.8.

Keywords: Sorption cooling system, graphite flakes, heat transfer enhancement, specific cooling power, thermal diffusivity

Introduction

Conventional vapor compression refrigeration systems consume approximately 15% of global electrical energy and use environmentally harmful refrigerants [1]. An alternative clean technology is sorption cooling systems. However, commercialization of sorption cooling systems faces fundamental challenges, including low SCP due to poor heat transfer between sorber bed heat exchanger (HEX) [2]–[4] and the sorbent. Sorber beds need to be cooled down/heated up during sorption/desorption processes. These oscillatory cool down/heat up processes are performed with the heat transfer fluid flowing through the sorber bed HEX. As such, the thermal diffusivity of the sorbent coating and HEX are crucially important in determining its performance. Thermal diffusivity of $CaCl_2$-silica gel composite sorbents can be enhanced by adding highly conductive additives such as natural graphite flakes and consolidating the mixture with a binder, which accelerates the oscillatory heat transfer in sorber beds; thus increasing the SCP [5]. In this paper, $CaCl_2$-silica gel composite sorbents with 0-20 wt% graphite flake contents are prepared and tested in a custom-built gravimetric large pressure jump (G-LPJ) test bed to study the counteracting effect of graphite additive on the transient heat and mass transfer performance and SCP of sorption cooling systems.

Experimental Details

Sorbent materials consisting of $CaCl_2$, silica gel B150, PVP-40, and 0-20 wt% graphite flakes was coated on graphite sheets and tested in a custom-built gravimetric large pressure jump (G-LPJ) test bed. A schematic diagram and a picture of the G-LPJ test bed is shown in Figure 1. To simulate the operation of a sorption chiller the pressure is stepped from 0.65 kPa to 2.33 kPa while the sample temperature is maintained at 40 °C.

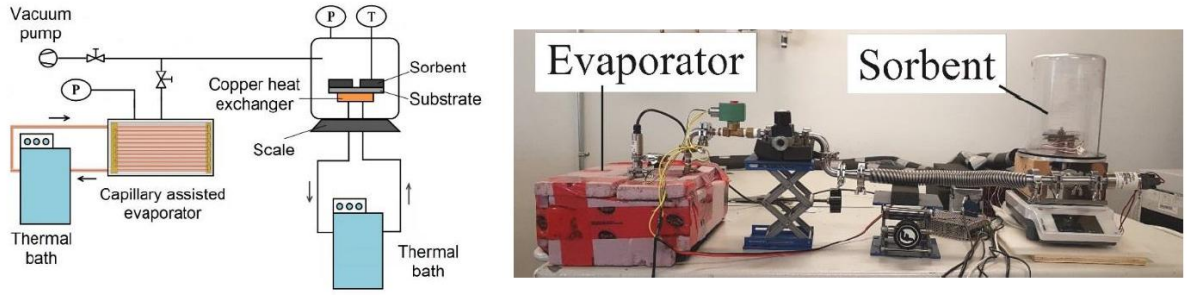

Figure 1. Schematic diagram and picture of the GLAP test bed

Discussion and Results

Figure 2 shows the variation of SCP and COP with sorption time for different graphite flake contents. As shown, adding graphite flakes to the sorbent material, over the targeted range, increases the SCP and COP as the sorbent thermal diffusivity increases.

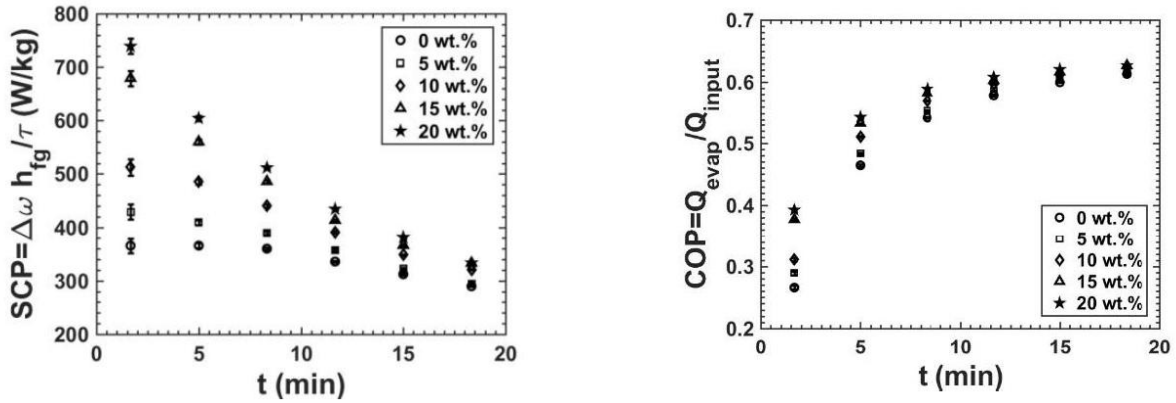

Figure 2. Variation of SCP with sorption time for various graphite flake contents

Conclusions

The effect of adding graphite flakes on the SCP and COP of sorption cooling systems was studied using a custom-built G-LPJ testbed. It was found that for high sorption rates, the sorber bed performance enhances by adding graphite flake due to the higher sorbent thermal diffusivity.

References

[1] "Building Energy Data Book", U.S. Dep. Energy, 2012.
[2] Wu, W., Zhang, H., Sun, D., "Mathematical simulation and experimental study of a modified zeolite 13X–water adsorption refrigeration module," Appl. Therm. Eng., vol. 29, pp. 645–651, 2009.
[3] Zhao, Y., Hu, E., Blazewicz, A., "Dynamic modelling of an activated carbon–methanol adsorption refrigeration tube with considerations of interfacial convection and transient pressure process," Appl. Energy, vol. 95, pp. 276–284, 2012.
[4] Sharafian, A., McCague, C., Bahrami, M., "Impact of fin spacing on temperature distribution in adsorption cooling system for vehicle A/C applications," Int. J. Refrig., vol. 51, pp. 135–143, 2015.
[5] Fayazmanesh, K., "Consolidated composite adsorbent containing graphite flake for sorption cooling systems", PhD thesis, Simon Fraser University, Summer 2017.

The Influence of Heat Input Ratio on Electrical Power Output of a Dual-Core Travelling-Wave Thermoacoustic Engine

Wigdan Kisha[1*], David Hann[2] and Paul H.Riley[3]

[1, 2] Faculty of Engineering, University of Nottingham, UK

[3] School of Mathematics, Computer Science & Engineering. City, University of London, UK

Corresponding author: *Email address: wigdan.kisha@nottingham.ac.uk

Abstract

This paper presents an analytical and experimental investigation of an electricity generator that employs a two-stage looped tube travelling-wave thermoacoustic prime-mover to deliver acoustic power from heat energy, a loudspeaker to extract electricity from sound energy and a tuning stub to compensate the changes in the acoustic field within the engine to enable close to travelling wave operation at the loudspeaker. Furthermore, the paper explains how to enhance the output power utilizing different heat input ratios through the engine cores. A well-known thermoacoustic design tool called DeltaEC is used to simulate the wave propagation through the different parts of the system. The electrical power predicted from the low-cost prototype was 44 W, while it was 22W from the tested rig. This confirms the potential for developing low cost thermoacoustic electricity generator for heat recovery from low-grade heat sources.

Keywords: Regenerator, thermoacoustic, acoustic power, loudspeaker as generator, DeltaEC

Background

Thermoacoustics is a new promising technique that uses heat to produce sound energy and in turn can produce electricity. A thermoacoustic engine (TAE) eliminates the mechanical moving parts by its simple construction [1]. An early travelling-wave thermoacoustic engine was designed for space application using a flexure-bearing linear alternator, the electrical power produced from this engine was 39 W with 18% thermal-to-electrical efficiency [2]

Test Set-up

The engine comprises a two-stage TAE operating in mainly travelling wave mode, tuning stub and a loudspeaker as in **Figure 1**. Each stage comprises an ambient heat exchanger, regenerator, hot heat exchanger, thermal buffer tube and a secondary ambient heat exchanger.

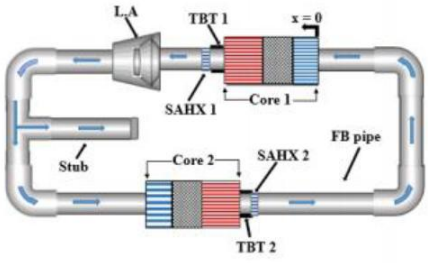

Figure 1: Functional Diagram of the twin regenerator travelling wave thermoacoustic system

Results and discussion

The distribution of the acoustic power along the loop was analysed for three different heat input ratios as illustrated in **Figure 2**. For all the cases, the change in the acoustic power along x direction has the same trend and is increased with the heat input as in **Figure 3**. However, it can be noticed that a 10 W increase in the acoustic power was achieved when the two cores had different heat inputs; 60% in the first core and 40% in the second. This can be justified by the location of the loudspeaker which is immediately after the TBT of the first engine. For this case,

the calculated electrical power is 44.7 W with thermal-to-acoustic efficiency of 4.1%, thermal-to-electric efficiency of 1.8% and an acoustic-to-electric efficiency of 52 %.

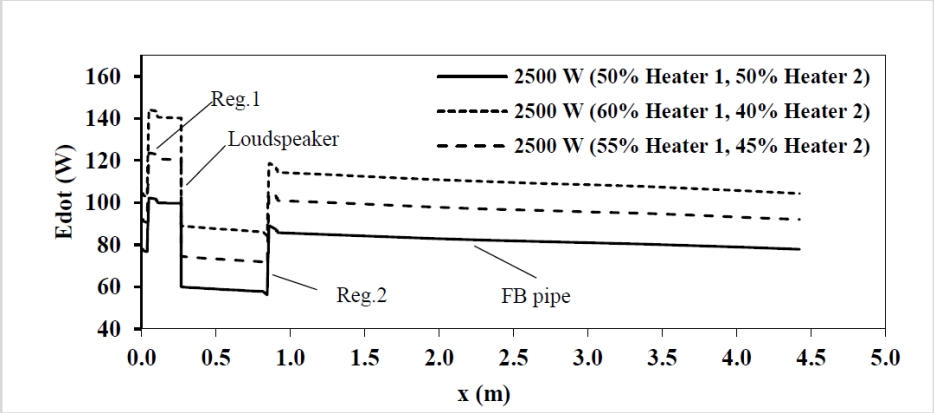

Figure 2: Acoustic power distribution along the engine loop

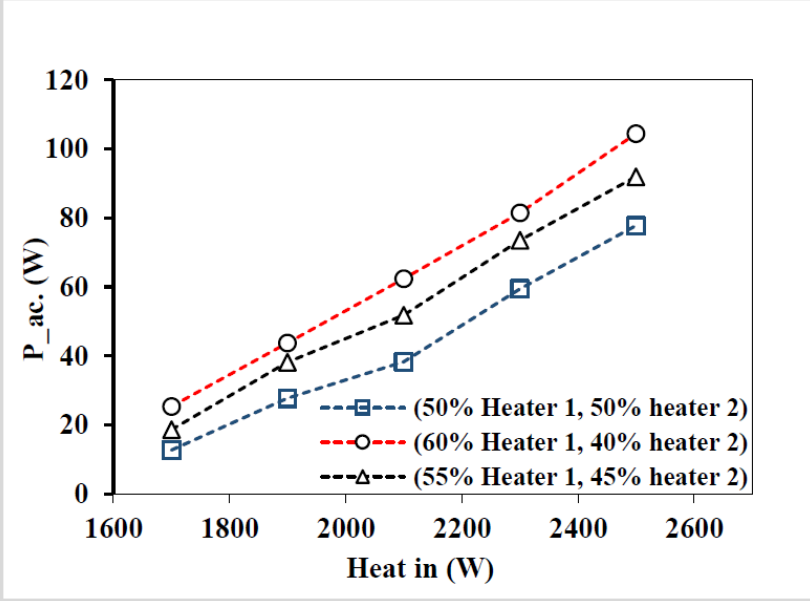

Figure 3: Loop acoustic power relation to the total heat input through the engine cores for three input ratios

Summary

In this paper, the influence of the heat input ratio into a looped-tube thermoacoustic engine was discussed. The engine converts acoustic power to electrical energy using a commercially available low-cost loudspeaker. DeltaEC is used to simulate the acoustic field within the system. DeltaEC results reflect that the electrical power output from the system equals 44 W from 2.5 kW heat input. An extra 10 W of electricity could be obtained by applying 60% of the heat into the first hot heat exchanger.

References:

[1] Backhaus, S. and G.W. Swift, *A thermoacoustic-Stirling heat engine: Detailed study.* The Journal of the Acoustical Society of America, 2000. **107**(6): p. 3148-3166.

[2] Petach, M., E. Tward, and S. Backhaus. *Design and testing of a thermal to electric power converter based on thermoacoustic technology*. in *2nd International energy conversion engineering conference. The American Institute of Aeronautics and Astronautics, Providence, Rhode Island*. 2004.

Experimental and Numerical Study of the Thermal Performance of Water-Stainless Steel Heat Pipes Operating in Mid- Level Temperature

Silva. Débora de O.[1], Riehl. Roger R.[2*]

[1]PhD Student, Space Mechanics and Control Division - DMC

[2]Senior Research Engineer and Faculty, Space Mechanics and Control Division – DMC

National Institute for Space Research, São José dos Campos, 12227-010 SP Brazil,

[*]E-mail: roger.riehl@inpe.br

Abstract

Thermal performance of water-stainless steel screen mesh wick heat pipes was investigated in this study. Three screen mesh wick heat pipes were fabricated and tested all different inclinations, and their thermal conductance in different modes were compared (experimental, calculated and numerical). The different mesh numbers can bring different meanings in terms of both liquid flow resistance and capillary pumping. The aim was to analyze the thermal behavior in the permanent and transient regime for each power when operated with the power step and power cycles in mid-level temperature, for use in several industrial and aerospace applications when those levels of temperature are required. The calculated thermal conductances based on the thermal resistance analysis were used to be compared with the obtained experimental thermal conductances. An adjustment factor was calculated with the objective of being used in the results of the calculated thermal conductances to bring them closer to the actual results that were obtained experimentally with the water-stainless heat pipes. The numerical approaches undertaken in analysing the transient thermal performance was used the multifluid model where two different fluid zone were created to represent vapour flow in the middle and liquid flow in the porous wick. The predicted surface temperatures with varying heat inputs (25 W - 125 W) from the numerical model and experimental tests were used for thermal conductance (numerical and experimental) were compared with calculated thermal conductance.

Keywords: heat pipe, experimental heat pipe, simulation, thermal performance.

Introduction

Heat pipes are passive heat transfer devices that can successfully transfer large amounts of heat. The robust and simple tubular structure with no moving parts makes the heat pipe a perfect choice for different applications such as industrial or aerospace. Heat pipe technology for industrial applications has been widely used on heat recovery system, with an increasing development for thermal control of electronic equipment and heat exchangers performance augmentation [1-4]. The heat was applied to the evaporator by a controlled electric heater, being used the testing power step, the heat source was applied to each heat pipe to observe, at first, the start-up effect. Once the temperatures for the start-up power have reached stability, power was changed according to the testing profile, following the sequence to temperature stabilization.

Discussion and Results

With the tests performed for the power cycles of 25, 50, 75, 100 and 125 W it was possible to verify the temperatures along the heat pipes to obtain the temperature profile for operating at 0° (Figure 1a). The experimental results may raise possible variations, which came from heat

pipe manufacturing standpoint and it affects heat pipe operation. Considering that the heat pipes were manually manufactured, an adjustment factor was taken into consideration for the thermal conductance results in such a way that it could result in a more accurate analysis in a way to put into consideration these possible variations. The adjustment factor is defined as follows

$$Factor = \frac{G_E}{G_{global}} \tag{1}$$

$$G_{global} = \alpha \frac{Q}{T_e - T_a} \qquad \text{where } 0.8 \leq \alpha \leq 3.0 \tag{2}$$

The calculated thermal conductance used in this study for each power applied to the heat pipe can be defined as

$$G_C = \frac{1}{R_T} * Factor \tag{3}$$

Figure 1b presents the results of the thermal conductance obtained from Eq. (3) for a better analysis of the heat pipes thermal operation.

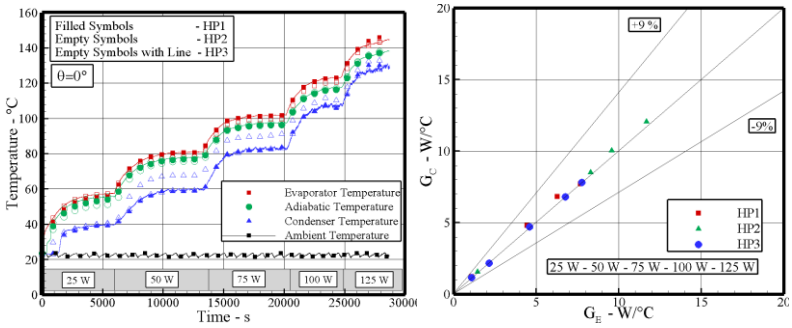

Figure 1. (a) Temperature profiles, (b) Thermal Conductance for HP1, HP2 and HP3

Conclusions

The results show a good correlation between the experimental, calculated and numerical results. The proposed calculated thermal conductance and thermal conductance numerical, correctly predicted the increase in thermal conductance with the increase in the heat input and the same has been validated experimentally. The highest experimental thermal conductance was obtained by HP2 of 12 W/°C The heat pipe HP2 showed better thermal performance due to smaller pore size, lower porosity and permeability and higher capillary pressure. The theoretical thermal conductance presented results of approximately 9,6 W/°C for the HP1, 15.5 W/°C for the HP2 and 23 W/°C for the HP3.

References

[1] Faghri, A., *Heat Pipe Science and Technology*, Taylor and Francis, 1995.

[2] Peterson, G. P., *An Introduction to Heat Pipes Modeling, Testing, and Applications*, John Wiley & Sons, INC, 1994.

[3] Chi, S.W., *Heat Pipe Theory and Practice*, Hemisphere Publishing Corporation, 1976.

[4] Reay, D. A., Kew, P. A., *Heat Pipes-Theory, Design and Applications*, 5th Ed., Elsevier's Science & Technology, 2006.

CO selective methanation for PEMFC applications

P. Garbis, C. Kern and A. Jess

Chair of Chemical Engineering, University of Bayreuth, Universitätsstraße 40, 95440 Bayreuth
Center of Energy Technology (ZET), Universitätsstraße 30, 95447 Bayreuth

panagiota.garbis@uni-bayreuth.de

Abstract

The world's shift to alternative forms of energy production leads to the housing constructions which are independent from electricity prices and reduce CO_2 emission. In the recent years, the interest in the development of proton exchange membrane fuel cells (PEMFC) in stationary application is increased. PEMFCs could supply households with electrical power using natural gas or, as a perspective, biogas. As is well known, the compound CO is undesirable in the PEMFC operating gas, as CO degrades the PEMFC by poisoning the hydrogen oxidation reaction catalyst [1, 2]. One of options to reduce the CO content to a value lower than 10 ppm is the selective methanation of CO [2, 3]. For this purpose, supported noble metal catalysts were prepared by impregnation of γ-Al_2O_3 spheres and screened for the selective CO methanation. A manufactured Ru/Al_2O_3 catalyst was selected for further investigation. The CO methanation with and without the presence of water is examined and a kinetic approach based on a Langmuir-Hinshelwood expression is suggested.

Keywords: selective methanation, ruthenium, Fuel Cell, carbon monoxide

Introduction

CO methanation can be considered an attractive technique to reduce the carbon monoxide content to guarantee the long life of PEMFCs. Conventionally, in the course of carbon monoxide methanation of a reformate gas, three main reactions can take place. viz.: CO methanation itself (Eq. (1)), CO_2 methanation (Eq. (2)) and the Reverse-Water-Gas-Shift (RWGS) reaction (Eq. (3)) where CO is produced again.

$$CO + 3\,H_2 \leftrightarrow CH_4 + H_2O \qquad \Delta H^0_{298} = -206\ \text{kJ mol}^{-1} \qquad (1)$$

$$CO_2 + 4\,H_2 \leftrightarrow CH_4 + 2\,H_2O \qquad \Delta H^0_{298} = -165\ \text{kJ mol}^{-1} \qquad (2)$$

$$CO_2 + H_2 \leftrightarrow CO + H_2O \qquad \Delta H^0_{298} = 41\ \text{kJ mol}^{-1} \qquad (3)$$

For these purposes, different catalysts have been prepared to select the most appropriate one. The suitable catalyst should promote the CO methanation and at the same time suppress both the CO_2 methanation and the RWGS reaction.

Discussion and Results

Catalysts are prepared and screened in order to find a suitable one for the selective CO methanation. In comparison with the other catalysts, the Ru based catalysts indicate higher activity and selectivity. Although a catalyst loaded with 2 wt% Ru and 1.3 wt% Cl showed the highest selectivity, the catalyst is unsuitable for further applications. Since chloride is discharged from the catalyst bed during the run. Not only does not it guarantee the selectivity of the reaction, but could also affect the PEMFC. Therefore, the catalyst with 2 wt% Ru/Al_2O_3 is more preferable and was used for further investigations.

The reformate gas, which is the feed for the PEMFC, consists in particular of CO, H_2, H_2O and CO_2. For this reason, it is important to evaluate the impact of each component on CO methanation. Firstly, the CO methanation was examined without CO_2 in the feed gas. A kinetic approach based on a Langmuir-Hinshelwood approach is suggested. The approach was evaluated for a variety of CO, H_2O and H_2 concentrations.

Since CO_2 has to be a content of the feed gas, the influence of CO_2 in the CO methanation was examined. It turned out that CO_2 had a small inhibiting effect on the CO conversion which could be neglected. Furthermore, no CO_2 conversion was noticed for temperatures lower than 220 °C.

Summary/Conclusions

In comparison with the other catalysts, the Ru based catalysts indicate higher activity and selectivity. Therefore, the catalyst with 2 wt% Ru/Al_2O_3 is more preferable for further investigations. Furthermore, a kinetic model, based on a Langmuir-Hinshelwood approach, is suggested for the CO methanation taking into consideration H_2O in the feed gas. The influence of CO_2 in the CO methanation is also investigated. Upcoming is a kinetic approach for the CO_2 methanation in order to fully describe the selective CO methanation.

References:

[1] Baschuk, J. J. and Li, X., Carbon monoxide poisoning of proton exchange membrane fuel cells, Int. J. Energy Res., 2001, DOI: 10.1002/er.713.

[2] Djinović, P., Galletti, C., Specchia, S., and Specchia, V., Ru-based catalysts for CO selective methanation reaction in H2-rich gases, Catalysis Today, 2011, DOI: 10.1016/j.cattod.2010.11.007.

[3] Eckle, S., Denkwitz, Y., and Behm, R. J., Activity, selectivity, and adsorbed reaction intermediates/reaction side products in the selective methanation of CO in reformate gases on supported Ru catalysts, Journal of Catalysis, 2010, DOI: 10.1016/j.jcat.2009.10.025.

On the Thermal Cyclic Precipitation of Aqueous Solutions for Heat Powered Cycles.

Francisco J Arias[1*], Salvador de las Heras[1]

[1]Department of Fluid Mechanics, Universitat Politècnica de Catalunya (UPC),

ESEIAAT C/ Colom 11, 08222 Barcelona, Spain

*Corresponding author: francisco.javier.arias@upc.edu

Abstract

Consideration is given to a novel process for heat transport, mass transport, thermal storage and mechanical transformation of heat based in the cyclic precipitation of aqueous solutions when an input of heat is applied or extracted from the solution. If in an initial aqueous solution heat is applied (by heating) or extracted (by cooling), -depending on the specific behaviour of the given aqueous solution, it ca be promoted the physical separation of the initial aqueous solution into two streams with different salinities, namely, one enriched in solute and the other depleted in solute. If the initial thermal state is restored (by releasing the heat absorbed or absorbing the heat extracted) the solubility is recovered and both streams could be mixed restoring the solution to its initial state and then ready to repeat indefinitely the cycle. However, if during the stage of mixing between the two streams with different salinities a semipermeable membrane is used it is possible to harness the increase of entropy by extracting osmotic energy from the system. This osmotic energy, can be transformed directly into mechanical energy to run the cycle, generation of electricity, promote convection or storing the thermal energy indefinitely which only sill be released when the two streams are mixed. The process could operate cyclically and indefinitely driven by an external thermal input because no degradation of the solubility on aqueous solutions with thermal cycles have been reported at the present. Utilizing a simplified physical model, it is shown that by the proper choice of the initial concentration of a given aqueous solution a heat powered cycle is possible. A quantification of the maximum extractable/stored energy was reckoned by calculating the spontaneous change in the Gibbs free energy during the mixing.

Keywords: Solubility, Aqueous Solution, Convection, Osmotic pressure.

Introduction/Background

The object of this work was to analyse the possibility for a novel process for heat and mass transport as well as storage and mechanical transformation of heat based in the physical property of aqueous solutions to precipitate when an input of heat is applied or extracted and the conversion of heat into osmotic energy.

Discussion and Results

Let us consider the thermal cycle depicted in Fig. 1. Let us fix a solution with an initial temperature $_1T$ and concentration $_oS$ -which is below of its saturation at that temperature (i.e., below of $_1S$) as depicted in Fig. 1., i.e, the solution is *undersaturated*. Now, if this solution change its temperature from $_1T$ to $_2T$ (e.g., by an input of external heat), and if the initial solubility $_oS$ is now higher than the saturation solubility $_2S$ at $_2T$, then the initial unsaturated solution is now *supersaturated* and precipitation occurs. Therefore, one requirement for aqueous-solution thermo-osmotic cycle, is that the initial concentration of the aqueous solution be supersaturated at its initial temperature and supersaturated at the final temperature, i.e., satisfying

$$S_1 > S_o > S_2 \qquad (1)$$

Suffice is to say that because the solubility can increase or decrease with temperature, then this kind of thermo-osmotic process is possible with $T_1 > T_2$ or $T_1 < T_2$. Now, once supersaturation occurs, the excess of particles of solute precipitate and can be separated by using a proper filter.

At this point, we have on one hand a solution which has been depleted of solute with a new concentration $_2S$ equal to its saturation at temperature $_2T$ and the precipitated solute.

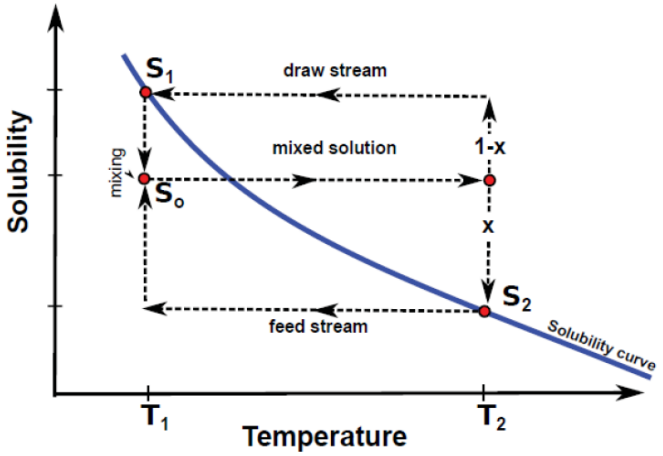

Fig.1. Aqueous solution-thermo-osmosis for heat powered cycles.

Referring to Fig. 1, let us separate the supersaturated solution into a volume fraction of the depleted solution, say, (x) and the rest of volume. i.e., a fraction (1-x) containing the precipitated. After this, the solutions are recovering its initial temperature $_1T$ and as a result, their solubility increase. This makes that the solute in the fraction (1-x) is totally dissolved forming a homogenous solution. If the proper fraction x was chosen, then it is possible that the dissolved fraction (1-x) get a solution with the maximum solubility at T_1 , i.e., S_1 . In summary, from an initial solution with concentration S_o at T_1 , and after a change in temperature to T_2 , we are forming a low-salinity solution S_2 and a high-salinity solution S_1 . Finally, if both solutions are brought together by using a permeate membrane, it is possible harnessing the osmotic pressure generated to propel the fluid. Fig. 2 shows a sketch what a thermo-osmotic heat powered cycle using aqueous solution separation-mixing would look using as heat external source the Sun isolation. The heat in this case is harnessed as sensible heat (heating domestic water) as well as osmotic energy transformed into mechanical and then into electricity.

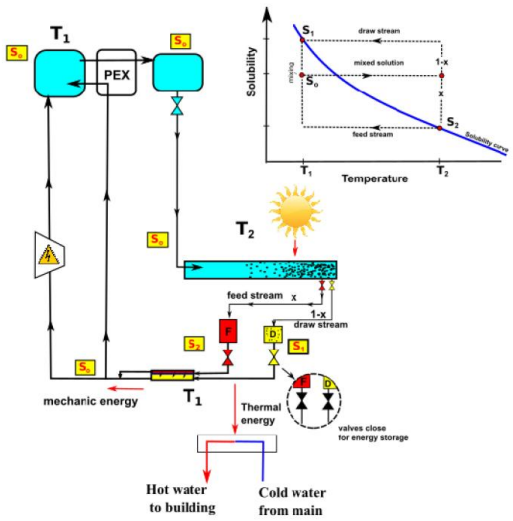

Fig. 2. Heat powered cycle using continuous aqueous solution-thermo-osmosis separation. In this case, the sensible heat used to precipitate the solution is solar. Part of the sensible heat is recovered by heating domestic water and part is transformed into osmotic pressure during the mixing which can be used to run a small turbine and thus generating electricity.

The obtainable energy by using the separation-mixing process of the aqueous solutions could be evaluated by calculating the increase in entropy when the mixing occurs. In this paper, the conditions required for a closed-cycle as well as the attainable energy will be theoretically evaluated and discussed

Summary/Conclusions

a) It is possible to promote a heat powered cycle by the use of aqueous solutions and the cyclic precipitation-mixing of the solution by extracting the osmotic energy during the mixing stage.
b**)** The energy obtained, besides the sensible heat, is the osmotic energy which can be transformed directly into mechanical energy.
c) This mechanic energy can be used to propel the fluid inside the system (convection) and generation of electricity.
d) The process allows the store of thermal energy indefinitely eliminating expensive isolators systems owing that the energy is stored as potential osmotic energy which only is released when the two different salinities stream are mixed.

Acknowledgements

This research was supported by the Spanish Ministry of Economy and Competitiveness under fellowship grant Ramon y Cajal: RYC-2013-13459.\\

References

[1] Yip Y.N., Elimelech M. 2012. Thermodynamic and Energy Efficiency Analysis of Power Generation from Natural Salinity Gradients by Pressure Retarded Osmosis. Environ. Sci. Technol., 2012, 46, 9. pp. 5230-5239

Deliberate Salinization of Domestic Wastewater in Housing Estates for Energy

Francisco J Arias[1*], Salvador de las Heras[1]

[1]Department of Fluid Mechanics, Universitat Politècnica de Catalunya (UPC),

ESEIAAT C/ Colom 11, 08222 Barcelona, Spain

[*] Corresponding author: francisco.javier.arias@upc.edu

Abstract

In previous work, it was investigated the possibility for deliberate salinization of seawater for desalination of seawater by using a pressure retarded osmosis (PRO) process. In that work, it was found that considering the price of the salt in comparison with the price of the electricity from the grid, the method is starting to become attractive in some countries like Germany and in others like USA, the break-even point is not far from the near future if the current trend in the cost of salt and grid electricity is maintained. In this paper, we will assess the method but for domestic self-supply of communal electricity in housing states.
The two different concentration solutions needed to run a pressure ratarded osmosis and then Obtaining energy when both are mixed, are obtained from the deliberate salinization of domestic wastewaters before being drained to the sewer. It will be shown that the proposed process could be potentially able for self-supply the communal electricity in typical housing estates.
Keywords: Solubility, Natural convection, Thermal gradient, Osmotic pressure.

Introduction/Background

In a recent work, [1] it was proposed the deliberate salinization of seawater and its mixing with seawater in order to obtain energy from the mixing of the two solutions driven by the osmosis pressure which generally is named as pressure retarded osmosis (PRO) process. The overall conclusion of that work was that the idea is already economically attractive in some countries (as Germany) and in others will be soon if the current trend in cost (of salt and grid electricity) increases is maintained.

Discussion and Results

In this work we want to explore the same idea but in application to domestic wastewaters and with reference in application of housing states. The idea pursued here is schematically depicted in Fig. 1.

According with this scheme we have: Initially, domestic wastewater from a housing state **(1)** is conducted to a pressure retarded osmosis chamber (PRO chamber) where is mixing with a stream with high salinization **(3).** From this mixing, PRO energy is extracted in the PRO chamber for the self-supply of communal electricity of the housing state, and then some fraction of this mixture is drained to the sewer **(4)** and other fraction is recirculated to the salinization chamber **(3)** where is again salinized by the use of salt-tablets and then obtaining again the regenerated stream **(3)**. Preliminary results show that the process could be economically attractive. For example, in countries as Germany where the price of the electricity from the grid is high,[2], in comparison with the price of the salt required to run the salination, and, in countries as USA, where the current price of the electricity is around 10 kWh per dollar and considering the strong increase of the cost of electricity in

comparison with the almost steadily cost of salt, the break-even is expected to occur at the end of 2020 or thereabouts.

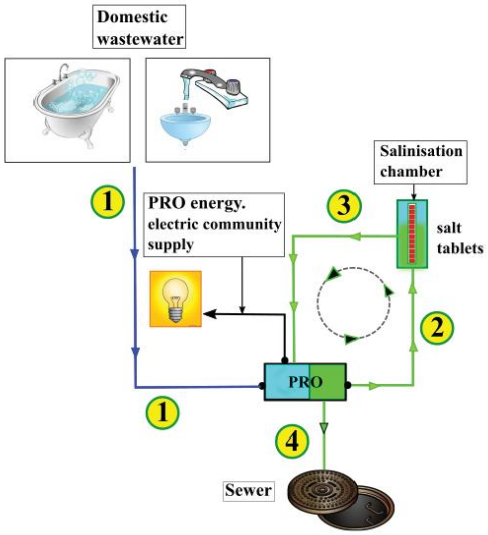

Fig. 1. Sketch of the idea. Here domestic wastewater is being treated before being drained to the sewer. Deliberate salinization required could be performed in salinization tanks by using salt-tablets which can be periodically replaced.

Summary/Conclusions

a) Deliberate salinization of domestic wastewater in housing estates could be an attractive option for self-supply of energy in housing estates.

b) Some countries with high cost of grid electricity, as Germany, the idea is already attractive and economically competitive, in others, as USA, because the comparative trend of the cost of salt and electricity from the grid, the break-even point is not far from the near future.

Acknowledgements

This research was supported by the Spanish Ministry of Economy and Competitiveness under fellowship grant Ramon y Cajal: RYC-2013-13459.

References

[1] Arias F.J., 2017, Deliberate Salinization of Seawater for Desalination of Seawater. Journal of Energy Resources Technology.

[2] Electricity price statics. Eurostat. Statics Explained. Data extracted in November 2016.

A novel hybrid dew point cooling system for mobile applications

Mark. Worall[1*], Adam. Dicken[2], Mahmoud. Shatat[1], Sam. Gledhill[2], Saffa. Riffat[1]

[1]Buildings, Energy and Environment Research Group, Faculty of Engineering, The University of Nottingham, University Park, Nottingham, NG7 2RD, UK

[2] Environmental Process Systems, Unit 32 Mere View Industrial Estate, Yaxley, PE3 7HS, UK

*Corresponding author: mark.worall@nottingham.ac.uk

Abstract

A novel dew point cooling system for truck cabin cooling has been designed and tested, which shows excellent performance in environments of low to medium relative humidity. Experimental results showed that cooling capacity of over 1kW could be achieved with up to 12K of sensible cooling of the supply air and a COP of up to 7. The DPC unit can provide comfort cooling to a vehicle using a rooftop unit whose DPC core is no larger than 0.5m x 0.5m x 0.25m.

Keywords: indirect evaporative cooler, dew point cooler, mobile air conditioning, natural refrigerants

Introduction/Background

This paper reports on a novel vehicle cooling system that uses natural refrigerants to provide cooling for a truck cabin. A compact and lightweight dew point cooling system is being developed that will either reduce the need for conventional vapour compression systems or replace them altogether.

Dew point cooler

Figure 1 is a diagram of a dew point cooler (DPC), showing the cooling process involved. The DPC is a heat and mass exchanger constructed of a series of paired channels. Air flows into the DPC through the product channel, also known as the dry channel. Openings along the channel allow some of the air to pass to the working channel, also known as the wet channel. Water is supplied to the wet channel and as air flows across the wetted surface, evaporative cooling occurs, cooling the air in the dry channel by direct contact across the wall. The interaction continues until the air leaves the DPC as cool air without a gain in moisture. The working air leaves warm and with an increase in moisture. A single DPC core was obtained, 450 mm (L): 505 mm (W): 250 mm (H), and a design was developed for use as a truck roof-top cooling unit. Figure 2 shows an image of the DPC rooftop unit developed. Air

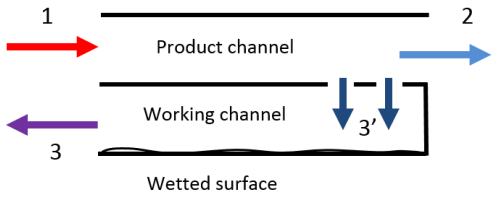

Fig 1. Schematic diagram of DPC

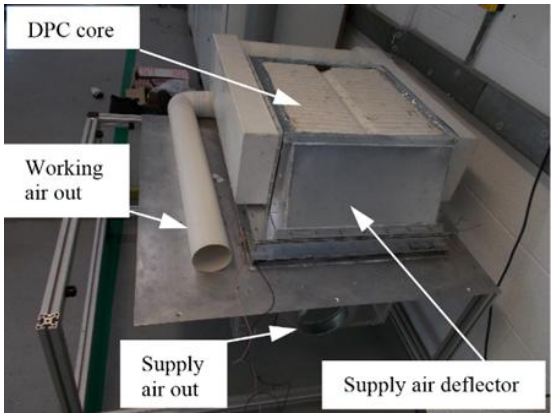

Fig 2. DPC cabin cooler prototype

is drawn in from the underside connected to the truck cabin and directed to the rear of the DPC core, where it is deflected toward the entrance to the core. The air flows and splits in the DPC, with the supply air leaving at the front and deflected down toward the inlet to the truck cabin. The working air is collected on both sides and leaves in a single duct. Water is delivered to the central channel by a 12V DC peristaltic pump and the air is circulated by two 24V DC compact blowers. The unit was tested under controlled conditions in an environmental chamber over a range of RH from 40 to 80% and temperatures from 25 to 45°C. The working air to supply air flow ratio (*AR*) was approximately 0.35.

Discussion and Results

Figure 3a shows that the maximum cooling capacity (*Q*) was just over 1100W at an inlet temperature of 45°C and an RH of 40%, and the minimum was just over 130W at an inlet temperature of 25°C and an RH of 80%. These results show that substantial cooling can be achieved together with a decent sensible cooling effect. The high temperature, low RH environment gives maximum performance because of the large driving mechanism, but it is applicable in only a few locations around the world, such as arid and dry regions. The largest potential market for such a system would be temperate, but hot climates around North America and the Mediterranean. These climates experience moderate and high cooling

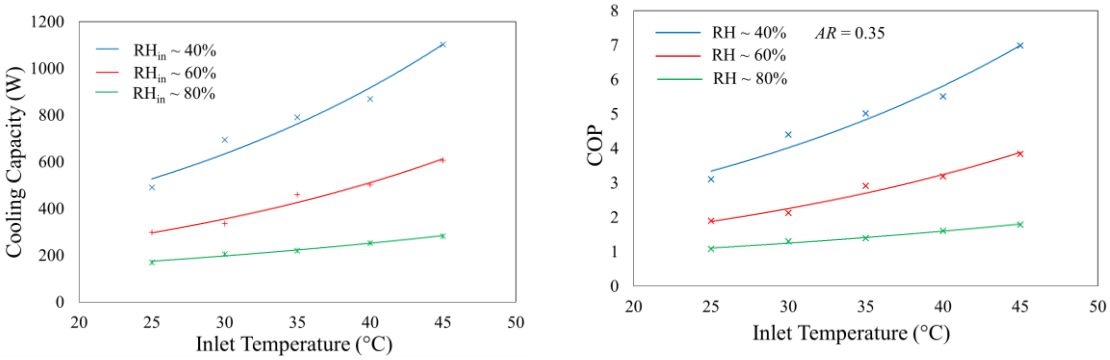

Fig 3. Variation in a) cooling capacity, b) COP with inlet temperature at constant RH

demands at temperatures ranging from 25°C to 35°C and RH ranging from 40% to 60%. At 25°C, *Q* increases from 300W to 500W as RH decreases from 60% to 40%. At 35°C, *Q* increases from 400W to 800W as RH decreases from 60% to 40%. Figure 3b shows how COP varies with inlet temperature and relative humidity. At 40%RH, COP increases from 3.28 at 25°C to 6.85 at 45°C. As RH increases, COP decreases. At 60%RH, COP increases from 1.87 at 25°C to 3.78 at 45°C and at 80%RH, COP increases from 0.84 at 25°C to just under 2 at 45°C. At low to medium conditions the system provides cooling with a COP ranging from approximately 2 to 5, and can achieve a COP up to 7.

Conclusions

Experimental results showed that cooling capacity of over 1kW could be achieved with up to 12K of sensible cooling of the supply air and a COP of up to 7. The DPC unit can provide comfort cooling to a vehicle using a rooftop unit whose DPC core is no larger than 0.5m x 0.5m x 0.25m.

Porous copper coated low pressure condenser/evaporator for sorption chillers

P. Cheppudira Thimmaiah[1], A. Fradin[1], W. Huttema[1] and M. Bahrami[1*]

[1]Simon Fraser University, Laboratory for Alternative Energy Conversion (LAEC), School of Mechatronic Systems Engineering, Surrey, British Columbia, Canada

[*]Corresponding author: mbahrami@sfu.ca

Abstract

In sorption chillers, a vapor passage constriction between the evaporator or condenser and the sorber beds can significantly reduce the specific cooling power. Therefore, developing an efficient low pressure (LP) integrated evaporator/condenser unit (ECU) is key for enhancing the performance, reducing footprint, and costs. At low pressure (~1 kPa), the performance of a flooded evaporator is negatively affected by the hydrostatic pressure of the water column. To overcome this issue, it is necessary to exploit thin-film evaporation. However, for efficient condensation, dropwise condensation corresponds to a high heat transfer coefficient. Therefore, an integrated ECU should perform as both evaporator and condenser. In this study, we built a porous copper coated evaporator/condenser unit (ECU) and performed comprehensive experiments to investigate its performance. The primary objective of this study was to examine the performance of the coated ECU during condensation mode. Therefore, the performance of the coated ECU was compared with the performance of a commercial condenser (coil-in-shell coil, see Fig.1). The results showed that for the same chilled water inlet temperature, the condensing power of the ECU was, on average, 40% higher than the commercial condenser.

Keywords: Low-pressure, Heat Exchangers, Adsorption chillers, Integrated evaporator/condenser unit.

Introduction/Background

The automotive industry is coming to widespread agreement on the need to reduce emissions, and it is evident that in an internal combustion engine of a light-duty vehicle 65-70% of the total fuel energy released is dissipated as waste heat[1]. This stimulated interest in waste-heat-driven sorption chillers. However, there are some technical limitations, including the need to maintain a high vacuum, and the low specific cooling power (SCP) and coefficient of performance (COP) of the incumbent systems. Furthermore, a vapor passage constriction between the evaporator or condenser and the sorber beds can significantly reduce the SCP. These limitations lead to a large and heavy system compared to a conventional vapor compression refrigeration system. Designing an efficient ECU plays a significant role in reducing the mass and size of a sorption chiller. In a low pressure evaporator, the operating pressure of the refrigerant (water) is quite low (~1 kPa), and the cooling power generation in a flooded evaporator is negatively affected by the saturation pressure difference along the height of the water column. To resolve this issue, we designed a new capillary assisted low pressure evaporator (CALPE) and performed comprehensive experimental studies to investigate the performance of our CALPE. The results showed that the external thermal resistance on the outside of the evaporator tubes accounts for up to 60%

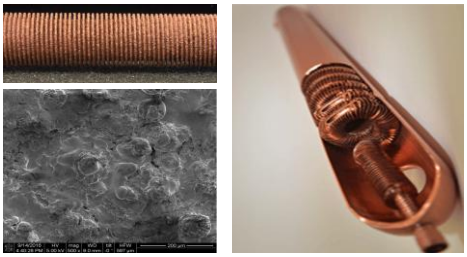

Figure 1: Left: Coated ECU; Right: commercial condenser coil

of the overall thermal resistance in the LP evaporator. To reduce the external thermal resistance, the outside surface of the evaporator tubes was coated with highly-porous open-cell copper metal foam. The overall heat transfer coefficient of the coated CALPE increased by 1.4 times, and the cooling power by two times [2]. In the present study, we tested the coated CALPE as a condenser and assessed its performance during condensation. This study will help to analyze the impacts of geometry and porous coatings on the condensation performance.

Discussion and Results

The experimental setup, as shown in Fig. 2, consisted of two vacuum chambers which are evacuated before the measurement by using a vacuum pump. The condenser to be tested is mounted inside the measurement chamber (MG) while the secondary chamber (SG) contains a permanently installed large evaporator which is partially flooded by water and serves as a vapor generator (VG). The condenser and the vapor generator are connected to temperature control systems (TCS) to provide a constant temperature thermal fluid (chilled water) at different mass flow rates. Experiments began with the VG tubes submerged in a pool of water and continued as continuous evaporation decreased the height of the water and the water vapor was condensed on the surface of the coated tubes in the MG. The experiment ended when the secondary chamber was dry. The condensing power of the ECU and commercial condenser (CC) are compared in Fig. 3. By increasing the chilled water inlet temperature difference (ΔT) between VG and ECU from 5°C to 15°C, the condensing power ($\dot{Q}$) of the ECU increases from 260 to 1000 W. The $\dot{Q}$ of our coated ECU is 40% higher than that of the CC.

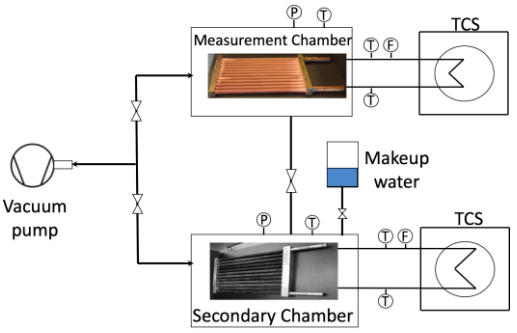

Figure 2: Schematic of the test setup

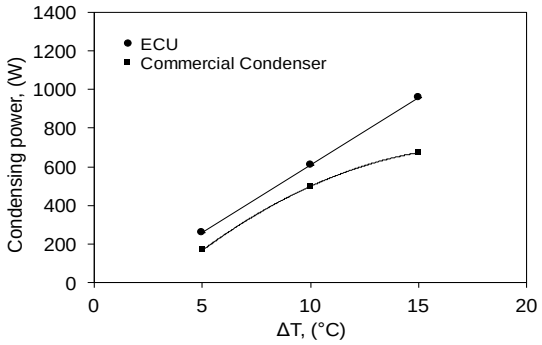

Figure 3: Comparison between ECU and CC

Conclusions

Suitability of a porous copper coated evaporator/condenser unit (ECU) was tested for adsorption chillers with applications in vehicle air conditioning. The primary objective was to examine the performance of the coated ECU during condensation mode and compare with a commercial condenser. The test results were promising and showed that the condensing power of the ECU is 40% higher than that of the commercial condenser.

References:

[1] Suzuki, M., *Application of adsorption cooling systems to automobiles*, Heat Recover Syst CHP,13:335–40.

[2] Poovanna, C.T., *Impact of Porous Copper Coating on Capillary-Assisted Low Pressure Evaporator for an Adsorption Chiller,* International Sorption Heat Pumps Conference, 2017.

LiCl/vermiculite – the new material for adsorption cycle "HeCol" for upgrading the ambient heat: equilibrium and dynamics of methanol sorption

A.D. Grekova[1, 2], L.G. Gordeeva[1, 2*] and Yu.I. Aristov[1, 2]

[1]Boreskov Institute of Catalysis, Ac. Lavrentiev av. 5, Novosibirsk 630090, Russia

[2]Novosibirsk State University, Pirogova st. 2, Novosibirsk 630090, Russia

[*]Corresponding author: gordeeva@catalysis.ru

Abstract

Adsorption heat transformation is an environment and energy saving technology for effective utilization of low-temperature heat sources. Recently, a novel adsorption cycle, so-called "Heat from Cold" (HeCol), has been suggested for upgrading the temperature of the ambient heat in cold regions up to higher level suitable for heating. This paper addresses the new composite sorbent of methanol LiCl/Verm, based on LiCl inside expanded vermiculite pores, specialized for the HeCol. The equilibrium and dynamics of methanol sorption on the LiCl/Verm was studied under conditions of the HeCol cycle, and its potential for utilization in HeCol cycle was evaluated in term of the heating capacity. The main findings are as follows: 1) the amount of methanol cycled at the HeCol cycles reaches 1.0-1.6 g/g that far exceeds that for other adsorbents; 2) the heating capacity of the LiCl/Verm varies from 1.3 to 2.0 kJ/g under conditions of different HeCol cycles that is of high practical interest.

Keywords: Adsorption heat amplification, Composite sorbent LiCl/vermiculite, Methanol, Equilibrium, Dynamics.

Introduction

Adsorptive heat transformation is an emerging technology for cooling/heating driven by low-temperature thermal energy. Recently, a novel adsorption cycle, the so called "Heat from Cold" (HeCol), has been suggested for amplification of the ambient heat [1]. It uses two natural heat reservoirs, both being at low temperature (about zero and below), to produce the heat at higher temperature. The ambient air at low temperature T_L is the heat sink, while a natural non-freezing basin (ocean, sea, river, lake, underground water, etc.) at medium temperature T_M is the heat source. In cold countries during winter time, the temperature difference between them can reach 30^{o}C and more, thus having a potential to produce a work, which then can be used for upgrading the temperature of the heat source up to a higher level T_H sufficient for heating. The isothermal HeCol cycle consists of two isosters and two isotherms. The useful heat Q_{ad} is produced and transferred to a consumer at temperature T_H during the isothermal adsorption. The heat for evaporation Q_{ev} is consumed from the water basin at T_M. The regeneration of the adsorbent is carried out by drop of the methanol pressure over the adsorbent. The desorption heat Q_{des} is consumed from the water basin at temperature T_M; the condensation heat Q_{con} is dissipated to the ambient air at T_L. Thus, the heat of natural source, which is available for free, is transferred to the useful heat, having commercial value.
The adsorbent is a key component of the HeCol unit. Here we present the novel methanol adsorbent, based on LiCl confined to expanded vermiculite pores, specialized for the HeCol cycle. The methanol adsorption equilibrium and dynamics is studied under conditions of the HeCol cycle; the potential of LiCl/Verm composite for the cycles is evaluated.

Results and Discussion

The characteristic curve of methanol sorption, presented as function of the adsorption potential ΔF is a step-wise curve (Fig. 1), which are profitable for the HeCol cycles because allows the adsorbent regeneration at "milder conditions" means at higher temperature $T_{L,}$ or lower T_M [2]. At ΔF=4.3-4.4 kJ/mol LiCl reacts with methanol vapour forming a solvate $LiCl{\cdot}3CH_3OH$ [3] that results in a step on the methanol uptake n from 1 to 3 mole/mole. At further decrease in ΔF, the $LiCl{\cdot}3CH_3OH$ liquefies forming a LiCl-methanol solution inside the pores, which further absorbs methanol vapour; the uptake rises gradually. The methanol sorption capacity of the LiCl/Verm composite reaches 1.5 g/g (Fig. 1). The isosteric heat of methanol sorption ΔH_{ads} is calculated as 42±1 kJ/mol at n=0.1–5 mole/mole.

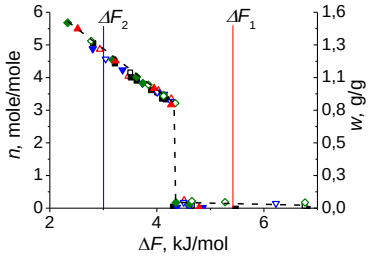

Figure 1. Characteristic curve of methanol sorption (solid symbols) and desorption (open symbols) on the LiCl/Verm composite**.**

Table 1. The heating capacity of the LiCl/Verm at the HeCol cycles.

$T_L/T_M/T_H$, °C	Δw, g/g	Q_{use}, kJ/g
-30/3/30	1.0	1.3
-20/10/35	1.1	1.4
-20/10/30	1.4	1.8
-20/20/50	1.0	1.3
-20/20/35	1.5	2.0

The amount Δw of methanol exchanged under conditions of the HeCol cycle is evaluated as $\Delta w = w(\Delta F_2) - w(\Delta F_1)$, where ΔF_2 and ΔF_1 are the values of adsorption potential, corresponding to adsorption and regeneration stages, respectively. Under different operating conditions Δw reaches 1.0-1.5 g/g (Table 1) that exceeds the appropriate values for other adsorbents. The heating capacity of the LiCl/Verm estimated as $Q_{use}=\Delta H_{ads}\Delta w\text{-}C\text{p}(T_H\text{-}T_M)$, where *C*p is the specific heat of the composite, varies from 1.3 to 2.0 kJ/g (Table 1) for different HeCol cycles. The methanol adsorption dynamics on loose grains of the adsorbent LiCl/Verm will be studied under conditions of the HeCol cycle, and the specific heat reachable in the HeCol cycle employing the LiCl/Verm sorbent will be evaluated further.

Summary/Conclusions

The novel composite sorbent LiCl/Verm is intently prepared for the adsorption cycle HeCol for upgrading the ambient heat temperature. The equilibrium and dynamics of methanol sorption on the LiCl/Verm are studied under conditions of the HeCol cycles. It is shown that the amount of methanol exchanged on the LiCl/Verm reaches 1.0-1.6 g/g under different operating conditions of the cycles; the heating capacity of the LiCl/Verm varies from 1.3 to 2.0 kJ/g. The results demonstrate the high potential of the LiCl/Verm sorbent for utilization in the HeCol cycle.

Acknowledgements

This work is supported by the Russian Science Foundation (grant 16-19-10259).

References:

[1] Aristov, Yu. I., "Adsorptive transformation of ambient heat: a new cycle", Applied Thermal Engineering, 2017, doi:10.1016/j.applthermaleng.2017.06.051

[2] Tokarev, M. M., Gordeeva, L. G., Shkatulov, A. I., Aristov., Yu. I., "Testing the lab-scale "Heat from Cold" prototype with the "LiCl/silica – methanol" working pair", Energy Conversion and Management (submitted).

[3] Gordeeva, L., Freni, A., Krieger, T., Restuccia, G., Aristov, Yu., "Composites "Lithium Halides in Silica Gel Pores": Methanol Sorption Equilibrium", Microporous Mesoporous Materials, 2008, doi:10.1016/j.micromeso.2007.09.040

Get your tubes wet: capillary-assisted thin-film evaporation of water for adsorption chillers

J. Seiler[1], F. Lanzerath[1], C. Jansen[2] and A. Bardow[1*]

[1]Institute of Technical Thermodynamics, RWTH Aachen University, Schinkelstraße 8, 52062 Aachen

[2]Pallas Oberflächentechnik GmbH & Co. KG, Adenauerstraße 17, 52146 Würselen

[*]Corresponding author: Andre.Bardow@ltt.rwth-aachen.de

Abstract

The power density of adsorption chillers can be increased by evaporating of water in thin films. Efficient evaporators rely on capillary action to create a thin film. We experimentally show the impact of surface properties on thin-film creation: high porosity, surface extension and roughness promote the creation a thin film on the tube and increase the heat transfer *UA*-value of the investigated tubes up to a factor of 10.

Keywords: capillary action, copper coating, overall heat transfer coefficient, tube.

Introduction/Background

Adsorption chillers use low-grade heat to supply environmentally friendly heat and cold. However, their power densities still need to be improved: next to the adsorber, increasing the power density of the evaporator is of high interest as efficient heat transfer for evaporation at low pressures is difficult.

Often, water is used as refrigerant in adsorption processes as it is environmentally absolutely safe and offers high enthalpy of vaporization. However, evaporation of water at the low pressures of adsorption processes is challenging: the hydrostatic pressure imposed by a liquid head increases the saturation temperature at the heat exchanger strongly. Thus, nucleate boiling requires high wall superheats [1] and can therefore usually not be used. To still achieve large heat transfer coefficients, alternative evaporator designs are investigated [2-4].

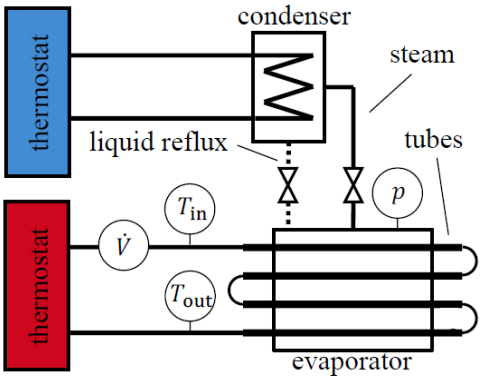

$$UA = \frac{\dot{Q}}{\Delta T_{ln}} \quad (1)$$

$$\dot{Q} = \dot{V}\,\rho_{in}\left(h_{in}(T_{in}) - h_{out}(T_{out})\right) \quad (2)$$

$$\Delta T_{ln} = \frac{T_{in} - T_{out}}{\ln\left(\frac{T_{in} - T_{sat}(p)}{T_{out} - T_{sat}(p)}\right)} \quad (3)$$

Fig. 1: Experimental setup for measuring overall *UA*-value of investigated tubes. Four identical tubes (total outer surface area 0.094 m²) are serially connected and placed in a horizontal plane (top view on evaporator). Condenser sets the saturating pressure. Data reduction to evaluate the *UA*-value (overall heat transfer coefficient multiplied times the area of heat transfer) is conducted according to equations (1) to (3), where QQ is the heat flow through the tubes, $\rho\rho$ the density and h is the specific enthalpy of the liquid water, ΔTT_{ln} the logarithmic driving temperature difference and $TT_{sat}(pp)$ the saturation pressure of water at pressure pp. Other measured variables (volume flow VV and temperature at in-/outlet TT_{in} and TT_{out}) are in the flow sheet.

Efficient sub-atmospheric evaporation of water with small superheats is possible by reducing the static head of the liquid through thin-film evaporation [2]. Thin-film evaporation is common in state-of-the-art evaporators, e.g., falling film evaporators. However, falling film evaporators require electric energy for pumps.

In this work, we exploit capillary action to create a thin film on the heat exchanger [4]. The capillary action is provided by special coatings on the tubes. We used the experimental setup shown in fig.1 to examine the ability of different coatings to efficiently evaporate water at low-pressure condition. We correlate the evaporation performance to surface properties (roughness, surface extension, porosity and layer thickness) of the coatings.

Discussion and Results

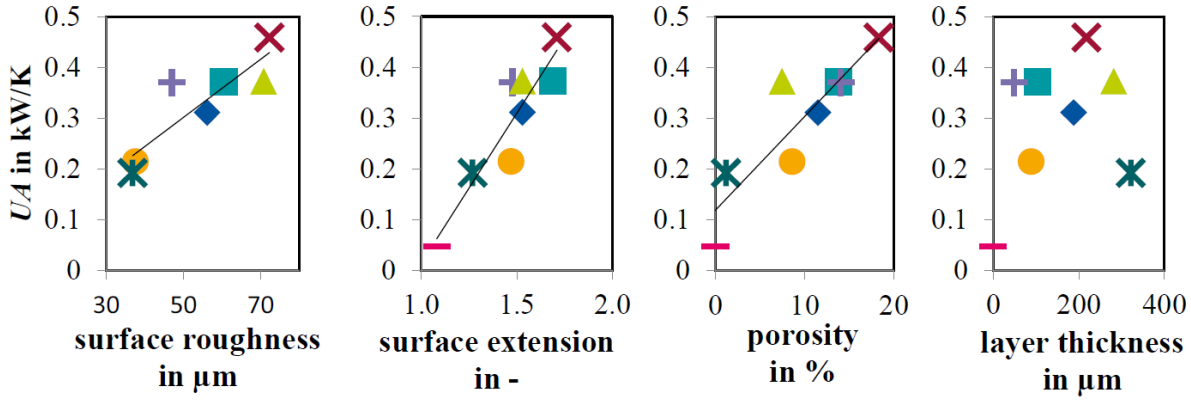

The experimental results in fig. 2 show that there is a strong correlation between the *UA*-value and surface roughness, extension and porosity. The layer thickness does not seem to be correlated to the *UA*-value. The highest UA-value occurs at the highest value of all three correlated properties. Higher surface roughness can amplify capillary forces, which enhance the *UA*-value. Extending the surface area consequently also increases the *UA*-value. Higher porosity might increase capillarity and enhance mass transfer through the coating, which also leads to higher *UA*-values. Since the *UA*-value seems to be independent of the layer thickness, thin coatings are favourable due to lower material use and costs. The increase in *UA*-value (up to factor 10) from the uncoated tube (—) to the coated tubes is caused by the creation of a thin water film on the coated tubes. Suitable surface properties ensure that the coated tubes stay wetted leading to high potential of thin film evaporation of water in low-pressure conditions.

Summary/Conclusions

Thin-film evaporation can improve heat transfer coefficients up to a factor of 10. Experimental results show that coatings for exploiting thin-film evaporation should have a high roughness, surface extension and porosity whereas the layer thickness can be thin. These findings can be exploited in the design of future evaporators for adsorption chillers with high power density.

References:

[1] Giraud, F., Rullière, R., Toublanc, C., Clausse, M., Bonjour, J., “Experimental evidence of a new regime for boiling of water at subatmospheric pressure”, Exp. Therm Fluid Sci., 2015, doi:10.1016/j.expthermflusci.2014.07.011
[2] Wang, R.Z., Xia, Z.Z., Wang, L.W., Lu, Z.S., Li, S.L., Li, T.X., Wu, J.Y., He, S., “Heat transfer design in adsorption refrigeration systems for efficient use of low-grade thermal energy”, 2011, Energy, doi:10.1016/j.energy.2011.07.008
[3] Schnabel, L., Witte, K., Kowol, J., Schossig, P. “Evaluation of different evaporator concepts for thermally driven Sorption Heat Pumps and Chillers”, ISHPC Proceedings, 2011.
[4] Lanzerath, F., Seiler, J., Erdogan, M., Schreiber, H., Steinhilber, M., Bardow, A., “The impact of filling level resolved: Capillary-assisted evaporation of water for adsorption heat pumps”, Appl. Therm. Eng., 2016, doi:10.1016/j.applthermaleng.2016.03.052

Analytical Investigation of Zeolite-NaY-Water for Thermochemical Heat and Cold Storage Utilizing High Temperature Heat

K. Geilfuß[1] and B. Dawoud[2*]

[1]OTH Regensburg Technical University of Applied Sciences, Faculty of Engineering, Galgenberg Str. 30, 93053 Regensburg, Germany, Tel.: +49-941-943-9418 (Laboratory for sorption processes), Email: kristina.geilfuss@st.oth-regensburg.de

[2] OTH Regensburg Technical University of Applied Sciences, Faculty of Engineering, Galgenberg Str. 30, 93053 Regensburg, Germany, Tel.: +49-941-943-9892, Email: belal.dawoud@oth-regensburg.de
Corresponding author: email address (belal.dawoud@oth-regensburg.de)

Introduction / Abstract

The energy sector, including the generation of heat, cold and electricity, contribute significantly to the global warming and consequently to the climate change. More efficient and environmentally friendly technologies are, therefore, inevitable. Over the last decades, the interest in storage principles has been increasing in order to compensate the discrepancy between periods of surplus energy and peak times. Sorption processes offer a very promising alternative for heat and cold storage. One of the main advantages encountered herewith, is that most of the working pairs are entirely environmentally friendly, have zero ODP and zero GWP. In the last decades, sorption technologies have been considered mainly for solar cooling or heat pumping [1]. Research in adsorption technologies in particular is still focussing on decreasing the unit cost and increasing both durability and efficiency in order to increase the market penetration rates [2-4]. First storage prototypes are being tested or designed with different or innovative storage materials and new reactor concepts [3, 5]. Yet, there has been almost no research dedicated to applications combining the use of heat and cold, especially if high temperature heat is available for storage. This work is dedicated, therefore, to analytically investigate the potential of applying NaY-Water/Zeolite as a working pair in both heat and cold storage applications upon utilizing high temperature process heat. It turned out that both the heat capacity of the adsorber heat exchanger and the heat losses between charge and discharge phases shall be minimized, in order to maximize the stored heat utilization efficiency in heat and cold.

Keywords: sorption, storage, heat, cold, zeolite NaY-Water

Methodology

Zeolite NaY is one of the most stable zeolites against hydrothermal cycling [6] and its application becomes more promising at temperatures above 150°C. This work introduces an analytical study to investigate the effect of the most important design and operating conditions on the performance of high temperature process heat (≥ 200 °C) storage for day/night heat and cold storage applications. The mass-specific useful heat "q_h" is defined as the sum of adsorption heat and sensible heat during the adsorption phase as well as heat of condensation, while mass-specific cooling effect "q_c" equals the heat of evaporation of the differential water uptake. Following the procedure of Freni et al. [6], the coefficient of performance "*COP*" for both heat and cold storage, defined as the ratio between "q_h+q_c" and the heat of desorption is represented by a set of dimensionless parameters. Among other dimensionless parameters, the one related to the adsorber heat exchanger "K_{AdHX}" represents the ratio between the heat capacity of the adsorber heat exchanger including its heat transfer medium holdup and the heat capacity of the adsorbent.

Results and Discussion

Figure 1 depicts the influence of the dimensionless parameter K_{AdHX} on q_h, q_c and COP of the high temperature thermochemical heat storage at an operating temperature of 20°C for the evaporator, 80°C for the condenser and the adsorber as well as of 250°C for regeneration. A temperature gradient of 5K has been taken into account for heat transfer inside all components. In order to account for the heat losses between charging and discharging phases, a temperature difference (ΔT_3) has been

introduced and shall be understood as the temperature reduction of the adsorber heat exchanger between both storage operation phases. ΔT_3 of zero for an ideal (loss free) storage as well as 30K and 60K for real storages have been investigated. The influence of the dimensionless parameter K_{AdHX}, zero for the ideal storage (neglecting the heat capacity of the adsorber heat exchanger and its heat transfer medium content), up to 7 for the real storage has been investigated as well.

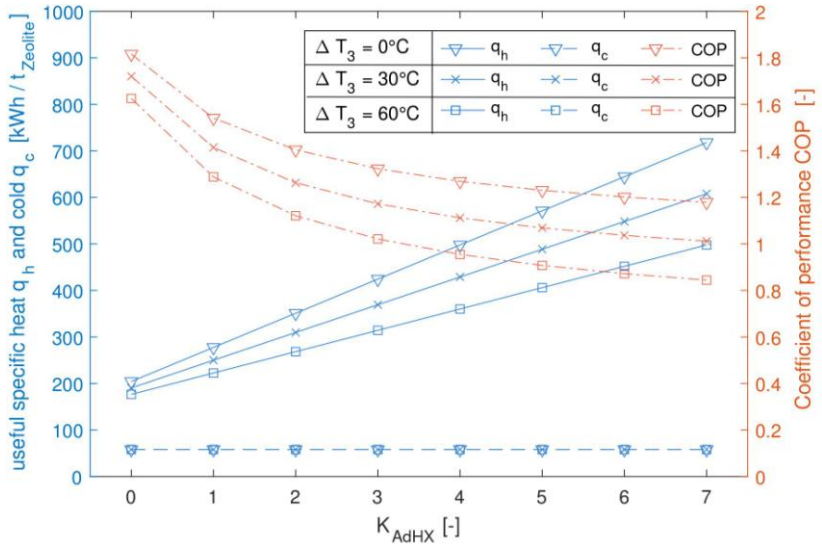

Fig. 1. Influence of the dimensionless parameter K_{AdHX} and ΔT_3 on the useful specific heat q_h and useful specific cold q_c as well as COP with a temperature gradient of 5K for heat transfer inside all components at $T_{evaporator}$ = 20°C, $T_{condenser}$ = $T_{adsorber}$ = 80°C and $T_{desorption}$ = 250°C.

The ideal process (ΔT_3 = 0, K_{AdHX} = 0) shows a *COP* of 1.8. Temperature drops ΔT_3 of 30 and 60K reduce the *COP* of the ideal storage by 1.7 %. For a real storage with (K_{AdHX} = 7) ΔT_3 of 30 and 60K result in reducing COP by 5.2% and 10.5%, respectively. This is mainly attributed to the loss of sensible heat. The specific cooling effect stored q_c is dependent only on the differential water uptake, which is not altered by ΔT_3 = 0 or K_{AdHX}, the reason why it remains constant at the level of 58 kWh/$t_{zeolite}$. Increasing K_{AdHX} from 0 to 7 result in enhancing q_h from 204 up to 720kWh/$t_{zeolite}$ for the ideal storage ((ΔT_3 = 0). Typical values of K_{AdHX} for the so far realized adsorber heat exchangers in the literature lies between 4 and 7. This is good for enhancing the stored heat q_h but it clearly result in decreasing COP of the stored heat utilization in heat and cold. An adsorber heat exchanger having K_{AdHX} of 5 is accompanied with a reduction of COP of 32.3% compared to the ideal COP (K_{AdHX} =0). Heat losses between charging and discharging phases, leading to ΔT_3 of 30 and 60K, result in further diminishing COP by 13.9 and 24.4, respectively.

It can be concluded that adsorber heat exchangers of K_{AdHX} <4 are quite necessary to enhance the heat utilization efficiency (COP) of the investigated thermochemical heat and cold storage. Constructive measures to reduce the thermal losses deem also of same importance to enhance the COP and the dischargeable heat of thermochemical heat storage systems.

References

[1] Yu, N., Wang, R. & Wang, L., *Sorption thermal storage for solar energy*, Progress in Energy and Combustion Science 39 (5), 489–514, 2013.

[2] Bataineh, K. & Taamneh, Y., *Review and recent improvements of solar sorption cooling systems*, Energy and Buildings 128, 22–37, 2016.

[3] Cabeza, L. F., Solé, A. & Barreneche, C., *Review on sorption materials and technologies for heat pumps and thermal energy storage*, Renewable Energy 110, 3–39, 2017.

[4] Chidambaram, L., Ramana, A., Kamaraj, G. & Velraj, R., *Review of solar cooling methods and thermal storage options*, Renewable and Sustainable Energy Reviews 15 ,(6), 3220–3228, 2011.

[5] Li, T. X., Wang, R. Z. & Yan, T., *Solid-gas thermochemical sorption thermal battery for solar cooling and heating energy storage and heat transformer*, Energy 84, 745–758, 2015.

[6] Freni, A., Dawoud, B., Bonaccorsi, L., Chmielewski, S., Frazzica, A., Calabrese, L. & Restuccia, G., *Characterization of Zeolite-Based Coatings for Adsorption Heat Pumps*, Springer International Publishing, 2015.

Effect of Conductive Additives on Performance of $CaCl_2$-Silica Gel Sorbent Materials

M. Khajehpour, C. McCague, S. Shokoya and M. Bahrami*

Laboratory for Alternative Energy Conversion (LAEC), School of Mechatronic Systems Engineering, Simon Fraser University, BC, V3T 0A3 Canada

*Corresponding author: mbahrami@sfu.ca

Abstract

Adsorption cooling systems (ACS), in which low-grade waste heat or renewable energy sources are used, are environmentally benign systems that are being considered as viable alternatives to compression refrigeration systems [1-3]. The performance of ACS systems significantly relies on the properties and effectiveness of working pairs. In this study, we analyzed the amendments in thermal conductivity, thermal diffusivity, and water uptake of consolidated $CaCl_2$-silica gel sorbent material by addition of graphite flake (GF) and carbon nanotube (CNT) as thermal conductive additives. Different structural effects and varying optimum loading amounts were observed for GF and CNT.

Keywords: Sorbent material, Adsorption, Silica gel, Graphite flakes, Carbon nanotube

Introduction

Adsorption cooling systems (ACS) are emerging as promising alternatives to electrical compression heating/cooling systems in which low-grade waste heat or renewable energy sources are used [1]. However, there are significant challenges and operational complexities facing widespread application of ACSs. The limitations originate from low thermal transport and uptake capacity of active sorbent materials in the operating conditions [3-5]. To overcome the limitations of current sorbents, synthesis of new composites - featuring additives to improve heat transfer properties, operational cycles and/or overall power densities – have received great attention [2, 3]. To this end, the present study investigates the effect of additives on thermal conductivity/diffusivity of sorption composite materials. Moreover, the uptake capacity is evaluated through water adsorption/desorption isotherms for two sets of composites. The objective is to establish an optimum composition of the considered composite sorbent material that can provide the best specific cooling power in an ACS.

Experimental Results and Discussion

In this study, the consolidated composites consist of 1:1 weight ratio of silica gel B150 and $CaCl_2$, 10 wt.% polyvinylpyrrolidone (PVP) binder, and varying concentrations between 0 to 20 wt.% of graphite flakes (GF) and carbon nanotubes (CNT). To compare the performances of the targeted additives, thermal transport and uptake characteristics are measured for the composites. The composites with 5 wt.% concentration of CNT and GF were chosen as representatives of the composites to study the effect of different additives on pore volume, surface area, and the morphology of the composites. Then, composites with various amount of conductive additives are considered in the next section to evaluate the thermal transport properties.

According to the porosity characterization results (Table 1), both surface area and pore volume were slightly higher for the CNT sample compared to that of the GF sample. This could be attributed to the geometry and size of the additive particles and their interaction with

the host matrix. The combination of higher surface area and smaller particle size of CNTs, (0.01-0.03) x (5-20) µm versus (50-800) x (≥150) µm for GFs, leads to more available surface and less pore-plugging with CNTs compared to GFs. SEM images (Figure 1) indicate notable changes in morphology and binder structure as a result of GF and CNT addition. It seems that CNTs are more engaged with the polymer binder and are more concentrated within the polymer, while GFs are most likely exist as stacks and are distributed throughout the composite. Based on the differences in interactions and morphologies of the components, different thermal transport properties are expected for the composites with the mentioned additives.

Table 1- Surface area and pore volume of composites

Sample	Composition (wt.%)					S_{BET} (m^2/g)	Total pore volume (cc/g) at P/P_0= 0.98
	PVP	Silica Gel	$CaCl_2$	Graphite flakes	CNT		
PVP-SG-$CaCl_2$-GF 5%	10	42.5	42.5	5	0	60.000	0.2049
PVP-SG-$CaCl_2$-CNT 5%	10	42.5	42.5	0	5	65.909	0.2251
PVP-SG-$CaCl_2$	10	45	45	0	0	269.692	1.1300
Silica Gel (B150)	0	100	0	0	0	112.324	0.4771

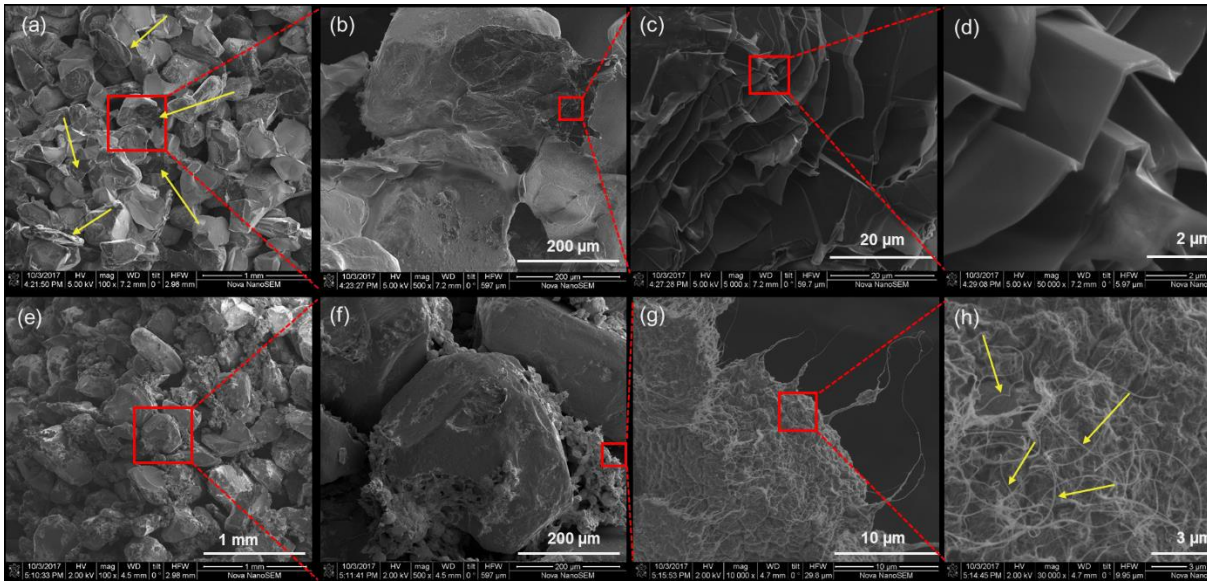

Fig 1. SEM images (a), (b), (c), and (d) PVP-SG-$CaCl_2$-5 wt.% GF, (e), (f), (g), and (h) PVP-SG-$CaCl_2$-5 wt.% CNT. Arrows point at (a) graphite flakes and (h) CNTs dispersed in the composites

Thermal conductivity and diffusivity results (Figure 2a) reveal that addition of conductive additives improves thermal transport; e.g. up to 376% higher conductivity and 483% higher diffusivity for sample with 20 wt.% of GF, and up to 90% higher conductivity and 95% higher diffusivity with 15 wt.% of CNT. Results show that both thermal conductivity and thermal diffusivity change linearly with the GF content. However, there is not such a linear trend for increasing thermal diffusivity and conductivity by CNT addition at concentrations above 5 wt.%. The reason is that CNTs are more likely agglomerate in the binder matrix, as shown in SEM images (Figure 1h). Therefore, extra CNTs within the same amount of binder wouldn't have enough space to form a network to conduct heat in the composite. Consequently, the excessive amount of CNTs might interfere with the network formation and negatively impact the heat conduction.

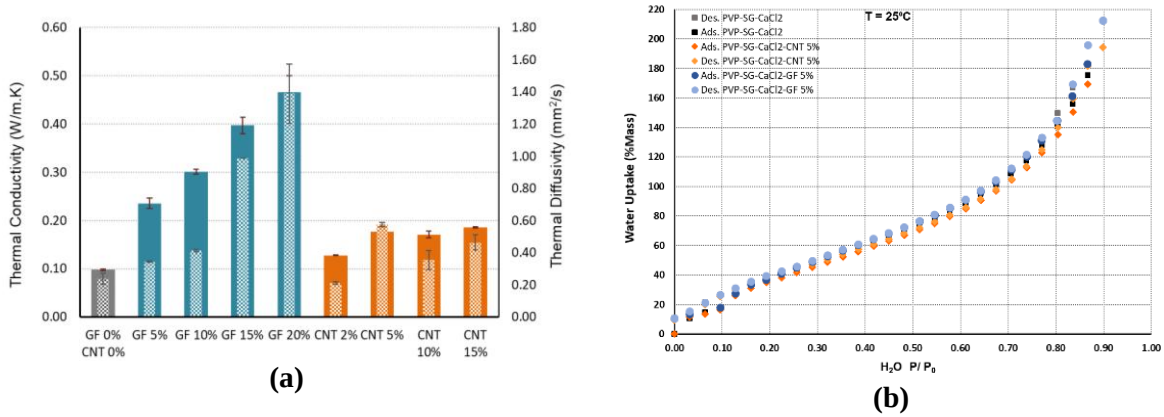

Fig 2. (a) Thermal conductivity (solid columns) and thermal diffusivity (hatched columns) of composites with various wt.% of GF and CNT. (b) Water uptake isotherms

Water uptake isotherms (Figure 2b) show that there is no significant change in the uptake capacity of the composites at 5 wt.% concentration of either GF or CNT in comparison with the sample without conductive additives. This can be used to develop new composites with increased thermal conductivity and thermal diffusivity with negligible impact on uptake capacity. However, the composites with larger amount of conductive additives would have less water uptake due to less active sorbent material content, as expected. Therefore, optimal compromise for water sorption capacity and thermal transport properties should be found according to the specific operation conditions.

Summary

Two set of consolidated composites with different loadings of GF and CNT were prepared to evaluate the effect of conductive additives on the performances of sorbent materials. Results confirm that there are differences in the effect of CNT and GF on the structure, thermal transport and uptake characteristics of the composites due to their different geometry, morphology, and interaction within the composites.

References

[1] Gordeeva, L., Frazzica, A., Sapienza, A., Aristove, Y., Freni, A., *Adsorption cooling utilizing the "LiBr/silica-ethanol" working pair: Dynamic optimization of the adsorber/heat exchanger unit*, Energy, 2014.

[2] Graf, S., Lanzerath, F., Sapienza, A., Frazzica, A., Freni, A., Bardow, A., *Prediction of SCP and COP for adsorption heat pumps and chillers by combining the large-temperature-jump method and dynamic modeling*, Applied Thermal Engineering, 2016.

[3] Sharafian, A., NematiMehr, M., Huttema, W., Bahrami, M., *Effects of different adsorber bed designs on in-situ water uptake rate measurements of AQSOA FAM-Z02 for vehicle air conditioning applications*, Applied Thermal Engineering, 2016.

[4] Narayanan, S., Kim, H., Umans, A., Yang, S., Li, X., Schiffres S. N., Rao S. R., McKay, I. S., Perez, C. A. R., Hidrovo, C. H., Wang, E. N., *A thermophysical battery for storage-based climate control*, Applied Energy, 2017.

[5] Rieth, A. J., Yang, S., Wang, E. N., Dinca, M., *Record Atmospheric Fresh Water Capture and Heat Transfer with a Material Operating at the Water Uptake Reversibility Limit*, ACS Central Science, 2017.

An innovative solid-gas chemisorption heat transformer system with a large temperature lift for high-efficiency energy upgrade

S. Wu[1], T.X. Li[*1], T. Yan[2], R.Z. Wang[1]

[1] Institute of Refrigeration and Cryogenics, Shanghai Jiao Tong University, Shanghai 200240, China

[2] College of Energy and Mechanical Engineering, Shanghai University of Electric Power, Shanghai 200090, China

[*]Corresponding author: Litx@sjtu.edu.cn

Abstract

Heat transformer can reutilize the low-grade heat by upgrading its temperature to meet the energy demand. Conventional heat transformers based on sorption process suffer from the common drawback of low temperature-lift capacity. In this paper, we propose an innovative four-component solid-gas chemisorption heat transformer system based on the pressure-reducing desorption and temperature-lifting adsorption techniques for the energy upgrade of low-grade heat with a high temperature lift and high energy efficiency. The sorption working pairs of $MnCl_2$-$SrCl_2$-NH_3 were employed to analyse its working performance. The system can upgrade low-grade heat from 60~100^oC to 180~220 ^oC at ambient temperature of -10~30^oC, and the energy efficiency can reach about 0.3. Two main impact factors of energy efficiency including global conversion of reactive salts and mass ratio of metallic reactor to reactive salt were analysed and discussed.

Keywords: heat transformer, chemisorption, energy upgrade, large temperature lift.

Introduction

There exists an enormous amount of low-grade energy resources such as the solar thermal, industrial waste heat, and exhaust gases from engines. Most of them are wasted due to the limitation of their relatively low temperature. Thermal-driven heat transformer/heat pump can make low-grade heats become useful energy resources by upgrading their working temperature [1].

In this paper, on the basis of our previous research [2,3], we propose an innovative solid-gas chemisorption heat transformer system with four components based on the pressure-reducing desorption and temperature-lifting adsorption techniques for energy upgrade of low-grade heat with a high temperature lift and high energy efficiency. The related performance parameters including temperature lift and energy efficiency would be investigated and their impact factors would be analysed.

Discussion and Results

Fig.1 shows the theoretical Clapeyron diagram of the innovative solid-gas chemisorption heat transformation cycle using a group of sorption working pairs $MnCl_2$-$SrCl_2$-NH_3. The equilibrium lines marked with NH_3(*l/g*), $SrCl_2$(8/2), and $MnCl_2$(6/2) correspond to the reversible chemisorption reaction equations (1), (2) and (3), respectively. The dot lines represent the synthesis lines, and solid lines are the decomposition lines.

$$NH_3(gas) \underset{evaporation}{\overset{condensation}{\rightleftharpoons}} NH_3(liq) + \Delta H \quad (1)$$

$$SrCl_2 \cdot 2NH_3 + 6NH_3(gas) \underset{decomposition}{\overset{synthesis}{\rightleftharpoons}} SrCl_2 \cdot 8NH_3 + \Delta H_{SRS} \quad (2)$$

$$MnCl_2 \cdot 2NH_3 + 4NH_3(gas) \underset{decomposition}{\overset{synthesis}{\rightleftharpoons}} MnCl_2 \cdot 6NH_3 + \Delta H_{PRS} \quad (3)$$

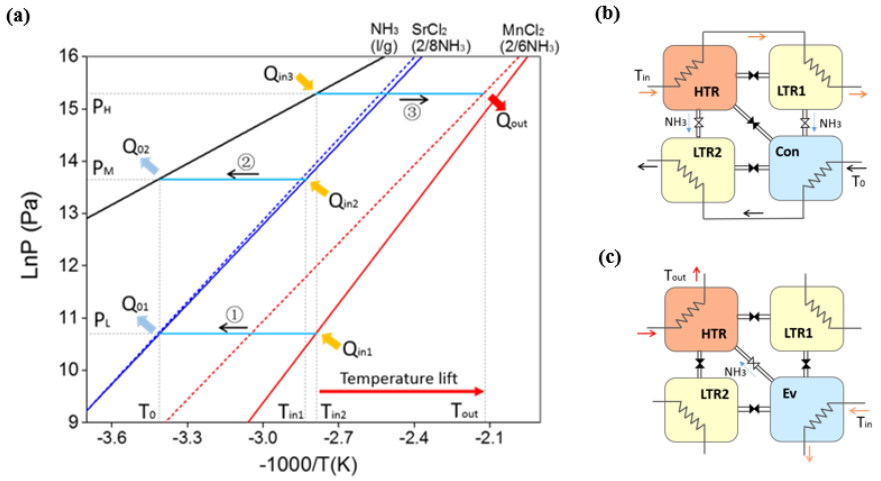

Fig. 1. (a) Clapeyron diagram of the chemisorption heat transformation cycle using $MnCl_2$-$SrCl_2$-NH_3 working pairs. (b) Schematic diagram of four-component system corresponding to process ① and ② in Fig.1a. (c) Corresponding to process ③ in Fig.1a. HTR is filled with $MnCl_2$, LTR1 and LTR2 are filled with $SrCl_2$, and Con/Ev is used to store liquid ammonia.

Due to the monovariant characteristic of chemisorption between ammonia and metal halides, the minimum heat source temperature and maximum output temperature would be a determined value once the ambient temperature is determined. In theory, the system can upgrade low-grade heat from 60~100^{o}C to 180~220 ^{o}C at ambient temperature of -10~30^{o}C. The temperature lift range is further larger than that of the conventional single-salt sorption and double-salt resorption cycle [4]. Based on the novel large temperature lift heat transformation cycle, an innovative four-component system is constructed with shorter cycle time compared to the previous one owing to the simultaneous regeneration of high temperature reactive salt and low temperature reactive salt. The global conversion of reactive salts and mass ratio of metallic reactor and reactive salt are two key factors to impact the energy efficiency of system. The energy efficiency can reach about 0.3.

Summary/Conclusions

We propose an innovative four-component solid-gas chemisorption heat transformer system based on the pressure-reducing desorption and temperature-lifting adsorption techniques for energy upgrade of low-grade heat with a high temperature lift and high energy efficiency. The system can upgrade low-grade heat from 60~100^{o}C to 180~220 ^{o}C at ambient temperature of -10~30^{o}C with energy efficiency about 0.3.

References:

[1] Cabeza, L.F., Solé, A., Barreneche, C., “Review on sorption materials and technologies for heat pumps and thermal energy storage”, Renew. Energ., 2016, doi:10.1016/j.renene.2016.09.059.
[2] Wu, S., Li, T.X., Yan, T., Wang, R.Z., “Experimental investigation on a novel solid-gas thermochemical sorption heat transformer for energy upgrade with a large temperature lift”, Energy Conversion and Management, 2017, doi:10.1016/j.enconman.2017.05.041.
[3] Li, T.X., Wang, R.Z., Kiplagat, J.K., “A target-oriented solid-gas thermochemical sorption heat transformer for integrated energy storage and energy upgrade”, AIChE Journal ,2013, doi:10.1002/aic.13899.
[4] Haije, W.G., Veldhuis, J.B.J., Smeding, S.F., Grisel, R.J.H., “Solid/vapour sorption heat transformer: Design and performance”, Applied Thermal Engineering, 2007, doi:10.1016/j.applthermaleng.2006.10.022.

Comparison of Storage Density and Efficiency for Cascading Adsorption Heat Storage and Sorption assisted Water Storage

Matthias S. Treier[1*], Aditya Desai[1] and Ferdinand P. Schmidt[1]

[1]Karlsruhe Institute of Technology, Institute of Fluid Machinery, Karlsruhe, Germany

[*]Corresponding author: Matthias.Treier@kit.edu

Keywords: Sorption, Cascading Adsorption, Heat Storage

Introduction/Background

The increasing contribution of renewable energy sources in recent times often leads to a time disparity in the demand and supply of energy. Energy storage is necessary to compensate for this mismatch [1]. For heat storage systems, the storage density and efficiency are the main figures of merit. These two figures have to be defined for each use case in adsorption based systems, since desorption and adsorption phase involve a heat transformation step with an additional heat source or sink [2;3]. The assumptions made about system boundaries and operating conditions (like minimal usable temperature lift during discharge) influence achievable energy densities and efficiencies. Initial work on standardizing the evaluation of thermochemical heat storages has been performed in the framework of a joint IEA task / Annex [4]. Within this contribution, a cascading adsorption heat storage and a sorption assisted water storage (SAWS) are discussed and compared.

Calculation of Storage Density and Storage Efficiency

The volumetric energy density of both the storages is the ratio of the usable heat that can be extracted from the storage during discharge to its volume. Here, the system boundary for the determination of the storage volume is chosen such as to include the required auxiliary components for each type of storage. The same system boundary is employed to determine the usable heat delivered by the storage system, which means that a heat pumping effect brought about by the storage may increase its effective volumetric energy density.
Storage efficiency is a ratio of two amounts of heat, the useful heat divided by the heat that is needed to desorb the storage. The condensation heat that is released during the desorption half cycle is not considered as useful heat with respect to storage efficiency.
During the storage time, sensible heat losses can occur and have to be taken into account for both storage types. These losses affect the sorption and sensible storage components differently.

System description

Both of the storage systems considered here, the adsorption storage systems and the SAWS system aim to increase the storage density and the storage efficiency.
The idea of an adsorption storage is to store heat by desorbing the storage. When the heat is needed, the adsorption half cycle is started and the adsorption heat can be extracted from the storage. Thus, the heat is released at different temperature levels. The heat at a very high temperature level, can be used to drive a sorption heat pump cycle (Figure 25). Once the temperature is too low to drive the sorption heat pump, the adsorption heat is used directly. Possible materials are classical hydrophilic zeolites of the faujasite and LTA types [1].

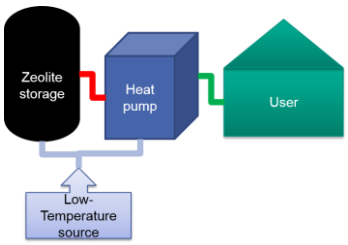

Figure 25: Configuration for Cascading

The other storage system considered here is a SAWS. Here, a stratified water tank is used to store heat. Hot water from the upper regions of the tank is used to drive an adsorption heat pump (AHP), while cold water from its lower regions can be used as heat source for the evaporator of the AHP. The stratified storage can also be used for internal heat recovery between the half-cycles of the AHP [5]. When the highest temperature in the tank is insufficient for desorbing the AHP, the heat can be used directly.

Discussion and Results

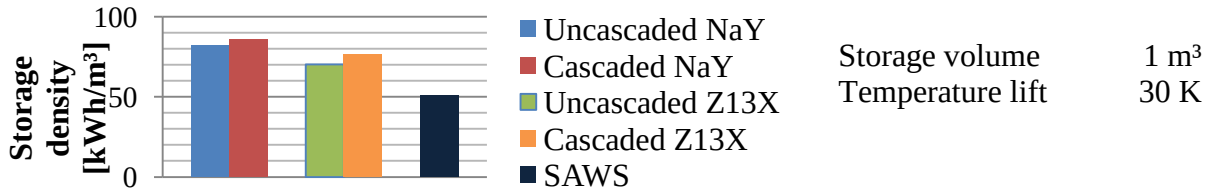

Figure 2: Storage densities and boundary conditions for considered systems

Storage densities for different systems and materials are shown in Figure 2, taking into account the volumes for auxiliary components and insulation. The values for the cascading system increase in comparison to the uncascaded system. The best value for the SAWS in this study is 51 kWh/m³.

Summary/Conclusion

Simulations showed, that through for the cascading system both the storage density and the storage efficiency can be increased, but the considered boundaries have a great impact. The values of the SAWS show, that there are more simulations with better fitting boundary conditions necessary to use the advantages of the system.

Acknowledgement

Funding by the German Federal Ministry of Education and Research (BMBF) through the cooperative project MAKSORE (grant no. 03SF0441A) is gratefully acknowledged.

References

[1] Yu, N., Wang, R. Z. & Wang, L., *Sorption thermal storage for solar energy*, Progress in Energy and Combustion Science, 489-514, 2013

[2] Hauer, A., *Thermal Energy Storage with Zeolite for Heating and Cooling*, Proceedings of the 7th International Sorption Heat Pump Conference ISHPC, 385-390, 2002.

[3] N'Tsoukpoe, K.E., Liu H, Le Pierres, N. & Luo, L., *A review on long-term sorption solar energy storage*, Renewable and Sustainable Energy Reviews 13, 2385-2396, 2009.

[4] Rommel M., Hauer A., van Helden, W., *IEA SHC Task 42 / ECES Annex 29 Compact Thermal Energy Storage*, Proceedings of the 4th International Conference on Solar Heating and Cooling for Buildings and Industry, 226-230, 2015

[5] Schwamberger, V., Schmidt, F. P., *Smart use of a stratified hot water storage through the coupling to an adsorption heat pump cycle*, Proceedings of 8th International Renewable Energy Storage Conference and Exhibition (IRES), 2013

Design and control of adsorption cooling systems based on dynamic optimization

A. Gibelhaus, T. Tangkrachang, U. Bau, F. Lanzerath and A. Bardow*

RWTH Aachen University, Chair of Technical Thermodynamics, Aachen, Germany

*Corresponding author: andre.bardow@ltt.rwth-aachen.de

Abstract

Thermally driven adsorption chillers offer a sustainable alternative to compression chillers. However, the sustainability of adsorption chillers often suffers from a high electrical energy consumption of the peripheral devices due to poor control and system design. To overcome this problem, we propose simultaneous optimization of control and design. For this purpose, first, we set up a holistic system model of a thermally-driven adsorption cooling system, including peripheral devices. Then, we use efficient dynamic optimization to simultaneously optimize control and system design aiming at minimum electrical energy consumption. By simultaneous optimization, we assure that both control and design optimally fit to the application requirements, which improves competitiveness of thermally driven chillers.

Keywords: thermal cooling, adsorption chiller, system simulation, electrical efficiency

Introduction

Thermally driven adsorption chillers allow for an efficient use of solar or waste heat to meet cooling demands and, thus, offer an alternative to conventional compression chillers [1]. However, also thermally-driven adsorption chillers may suffer from low electrical efficiency due to peripheral devices, such as circulating pumps and heat rejection fan. In many cases, the electrical efficiency of adsorption cooling systems is only marginally higher than that of conventional compression cooling systems [2], due to two main reasons: (1) poor control and (2) poor system design. By poor control, we mean the non-optimal choice of control parameters, such as adsorption chiller phase times, pump speeds, or fan speeds. By poor system design, we mean the under- or oversizing of components, such as dry cooler or solar collector, leading to an unbalanced system design with bottlenecks. Whereas the effect of control on electrical efficiency is tackled in current research studies [3], the influence of system design on the electrical efficiency has not been investigated yet. However, control and system design influence each other and have to be optimized simultaneously to achieve maximum electrical efficiency.

In this study, we simultaneously optimize control and system design of a solar-driven adsorption cooling system. For this purpose, we set up a holistic dynamic model consisting of adsorption chiller and peripheral devices (circulating pumps, dry cooler and solar collector). Then, we simultaneously optimize control and system design, using the efficient multiple-shooting optimization algorithm MUSCOD-II [4]. The optimization results show a significant potential regarding the electrical efficiency of thermally-driven adsorption cooling systems.

Methods and Results

We model the thermally-driven adsorption cooling system **Figure 26** (left) in the object-oriented language Modelica, using the LTT adsorption energy systems library developed at RWTH Aachen University. The system model consists of: 1) an experimentally validated 2-bed adsorption chiller model with the working pair silica gel / water [5], 2) a dynamic solar collector model, parameterized with manufacturer data, 3) a dry cooler model based on the

NTU method [6], parameterized with manufacturer data and 4) efficiency based thermodynamic models for all circulating pumps.
The system has five control parameters, which are the cycle time of the adsorption chiller, the pump speed of the three circulating pumps and the fan speed of the dry cooler. These five control parameters have a great influence on the electrical efficiency of the system, defined by the Energy Efficiency Ratio EER $= \dot{Q}_{\text{cool}} / P_{\text{el,tot}}$, where $\dot{Q}_{\text{cool}}$ is the cooling capacity of adsorption chiller and $P_{\text{el,tot}}$ is the total electrical energy consumption of peripheral devices. A deviation from the optimal fan speed by 50 % leads to an EER decrease of about 50 %. Furthermore, the control parameters also influence each other, e.g. a higher fan speed can compensate a lower pump speed in the dry cooler circuit and vice versa. Thus, all control parameters have to be optimized simultaneously to achieve maximum EER. We perform this control optimization by an efficient multiple-shooting algorithm MUSCOD-II [4] for typical ambient conditions (irradiation and temperature).
In the next step, we investigate the effect of system design (sizing of solar collector and dry cooler) on the EER. For this purpose, we calculate the EER at optimal control for different system designs, see **Figure 26** (right). The results show that the system design has a great influence on the efficiency, since there is up to a factor six in EER dependant on design. Note that each system design is evaluated at optimal control and the variation of optimal control parameters dependant on system design is significant (not shown). Thus, a simultaneous optimization of control and periphery is important to achieve a high electrical efficiency.

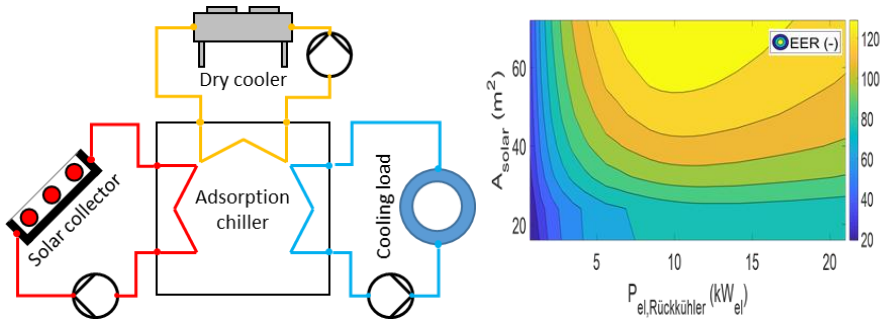

Figure 26: Solar-thermally driven adsorption cooling system (left) and energy efficiency ratio (EER) of the system dependent on the area of solar collector (A_{solar}) and the nominal size of the dry cooler ($P_{el,dry}$).

Conclusions

Control and system design of thermally driven cooling systems is important to achieve high electrical efficiency (EER) and to compete with conventional compression cooling systems. In this study, we propose simultaneous optimization of control and system design. The results show that the EER can be increased by about factor six, which highlights the importance of simultaneous optimization.

References

[1] Choudhury, B., Saha, B. B., Chatterjee, P. K. and Sarkar, J. P., "*An overview of developments in adsorption refrigeration systems towards a sustainable way of cooling*", Applied Energy, 2013

[2] Weber, C., Mehling, F., Fregin, A., Daßler, I. and Schossig, P., "*On Standardizing Solar Cooling – Field Test in the Small Capacity Range*", Energy Procedia, 2014

[3] Nienborg, B., Dalibard, A., Schnabel, L. and Eicker, U., "*Approaches for the optimized control of solar thermally driven cooling systems*", Applied Energy, 2017

[4] Leineweber, D. B., Bauer, I., Bock, H. G. and Schlöder, J. P., "*An efficient multiple shooting based reduced SQP strategy for large-scale dynamic process optimization. (Parts I and II)*", Computers & Chemical Engineering, 2003

[5] Lanzerath, F., Bau, U., Seiler, J. and Bardow, A., "*Optimal design of adsorption chillers based on a validated dynamic object-oriented model*", Science and Technology for the Built Environment, 2015

[6] Dalibard, A., "*TRNSYS Type 821 - Closed wet cooling tower model for TRNSYS, Model Description*", Research Center for Sustainable Energy Technology (zafh.net), Stuttgart, 2013.

Early Design of a Magnetic Mover for Adsorbents

M. J. Tierney[1], J. Yon[1]

[1]Department of Mechanical Engineering, University of Bristol, BS8 1TR, UK

[2]Affiliation and full institutional address

[*]Corresponding author: mike.tierney@bristol.ac.uk

Abstract

The use of magnetic fields to move adsorbent within an adsorption heat pump (AHP) is proposed and the design is analysed. The tentative electrical coefficient of performance (COP, ratio of cooling power to electrical power) is in the region from 33 to 49 and the cooling power for a 3-mm diameter guide tube is 47-to-115 watts. The "magnetic mover" is intended to improve thermal COP and to smooth the load on the evaporator.

Keywords: Adsorption, heat pump (AHP), magnetic field

Introduction

AHPs exploit low grade heat for cooling and/ or heat amplification and (compared to absorption machines) offer straightforward mechanical design and the use of low cost materials. However, the necessary thermal cycling of containment walls and extended surfaces creates dynamic heat losses and an uneven load on the evaporator. Circulating the adsorbent then becomes attractive. The proposed AHP (Figure 1) would comprise sequences of holding chambers, adsorption chamber and desorption chamber (items 1 to 4) plus a "magnetic mover" (item 5). Adsorbent pellets would be impregnated with iron; item #5 is therefore a modified "coil gun" [1]. The magnetic field (H) was calculated by finite element code or (along the axis) analytically. A particle of pure iron is subject to an acceleration $\mathbf{a_m} = \mu_o \chi_v \, \mathbf{H} \nabla \mathbf{H} / \rho_{Fe}$, modified for the payload masses, gravity and friction.

Discussion and Results

We considered a single 50.8-mm long coil, raising single particles 1 metre and sufficient turns (N) to give an exit velocity of 0.5 m/s. A "cut-off" was defined as fractional position of the particles within the coil at which the current had been disengaged and the magnetic field decayed to zero. This led to the ohmic dissipation of energy in the coil ($I^2R\ t_{cut}$) and for given particle moisture loading (and thus refrigeration effect) the electrical coefficient of performance (COPe). We plot the impact of cut-off on COPe, required number of turns N, and cooling power (Figure 2). Table 1 shows the thermal COP for different mass ratio (mass of metal divided by mass of adsorbent), assuming the adsorbent achieves loading close to its equilibrium value (data from [2]. The lower ratio of 0.25 characterises "magnetic moving", whereas 6 might be more representative of a basic cycle. The corresponding specific cooling power was 53 W/ kg (adsorbent) (based on characteristic times defined in [2]).

Summary/Conclusions

The pleasing indicative COPe for a magnetic moving system warrant further investigation.
(The full paper discusses optimisation of the single coil, finite element analysis, more advanced coil strategies, and early experiments with the magnetic mover.)

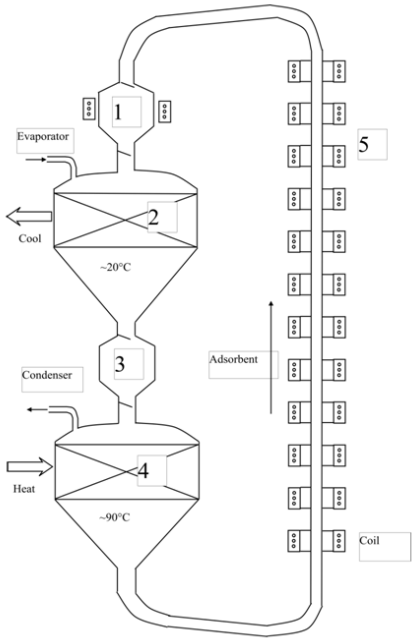

Figure 1 AHP with Magnetic Mover (1, 3 - air locks, 2 absorber, 4 generator, 5 magnetic mover)

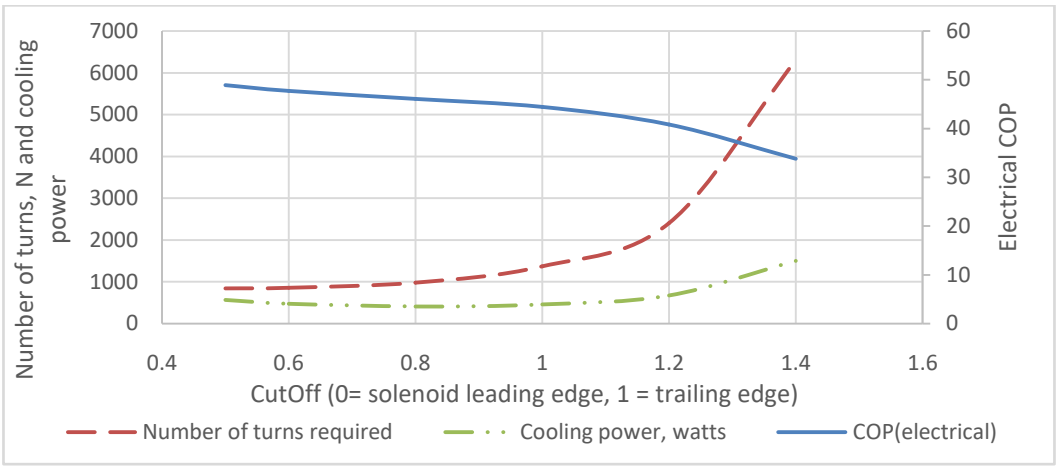

Figure 2 Influence of coil design and machine performance to cut-off

Table 1 Mass Ratio versus Thermal Coefficient of Performance (Condenser and adsorber at 20°C, evaporator at 5°C, desorber at 90°C. Silica gel characteristics in [2]

Mass Ratio	0.25	1	3	6
COP (thermal)	0.771	0.732	0.646	0.550

References:

[1] Cole A. A.., "*Electric gun.*" U.S. Patent 2,235,201, issued March 18, 1941.

[2] Ahamat, M.A. and Tierney, M.J., 2012. *Calorimetric assessment of adsorbents bonded to metal surfaces*: Application to type A silica gel bonded to aluminium". Applied Thermal Engineering, 40, 2012, doi.org/10.1016/j.applthermaleng.2012.02.021.

Squaring the circle in drying high-humidity air by a novel composite sorbent with high uptake and low pressure-drop

Meltem Erdogan[1], Claire McCague[2], Stefan Graf[1], Majid Bahrami[2], and André Bardow[1*]

[1] Institute of Technical Thermodynamics, RWTH Aachen University, Schinkelstraße 8, 52062 Aachen, Germany,
[2]Laboratory for Alternative Energy Conversion, Simon Fraser University, Surrey, BC, Canada V3T 0A3

[*]Corresponding author: andre.bardow@ltt.rwth-aachen.de

Abstract

For drying of air with relative humidity higher than 60%, a novel sponge-structured composite sorbent of $CaCl_2$ was prepared in a mesoporous silica gel host matrix consolidated with poly(vinyl alcohol binder). The sorbent is hydrothermally stable. The uptake capacity was determined by thermogravimetric vapor sorption analysis and tested in an open sorption test bed which also allowed to determine the pressure drop. The composite sorbent had ~2.4 times higher uptake and 8-10 times lower pressure drop than a benchmark microporous silica gel for drying applications. The higher uptake and lower pressure drop across the bed enable the proposed novel composite sorbent to reduce packaging and fan power in adsorption drying.

Keywords: composite sorbent, adsorptive drying, calcium chloride, silica gel

Introduction

The key to efficient adsorption drying are sorbents with high moisture removal capacity [1]. High water uptake has been reported for composite sorbents of hygroscopic salts in mesoporous host matrices [2-4]. However, these sorbents are used in packed beds leading to large pressure drops [5]. In this study, we therefore present such a promising composite sorbent that is also easy to produce as sponge structure to reduce pressure drop. We show that the novel composite is highly suitable for drying high humidity air (>60% RH).

Synthesis and experimental Setups

The composite sorbent was prepared in batches of 400 g with a ratio of 55 wt.% silica gel (SiliaFlash® B150, Silicycle Inc.), 30 wt.% $CaCl_2$ and 15 wt.% poly(vinyl alcohol) (PVA) (MW 85,000-124,000, 99+% hydrolyzed, Sigma Aldrich). PVA binder was combined with anhydrous calcium chloride (ACP Chemicals) and dissolved in 600 mL of DI water. The solution was combined with a mesoporous silica gel (250-500 µm irregular grains) to create a slurry. The composite was oven dried at 80°C and cured at 150°C creating 3-5 mm thick pieces. The material was further baked at 250°C for 24 h, turning dark due to charring of the binder. The composite sorbent was compared to microporous silica gel in 3.2 mm diameter beads (Sylobead® B 125, Grace Materials Technologies). A thermogravimetric analyzer (IGA-002, Hiden Isochema) was used to collect vapor sorption isotherms at 25°C and run 150 pressure swing cycles to assess the uptake capacity and durability of the composite sorbent. The practical performance of the sorbents was then evaluated in a fixed packed bed for 40°C air flow with 60, 70 and 80% RH, and regeneration temperatures of 100°C and 150°C. Cylindrical tubes with a diameter of 100 mm and a length of 50 mm were used as fixed volumes of sorbent (0.393 L). The sorbent was exposed to ambient air conditioned with a heater and steam humidifier. Temperature and relative humidity were measured before and after the packed bed. The volumetric flow after the fan and the pressure drop across the bed were measured. The mass of the sorbent was measured when each equilibrium was reached (T_{in}-T_{out} < 1°C).

Discussion and Results

Water sorption isotherms for the composite sorbent and the silica gel are shown in Fig. 1. The uptake of the composite sorbent is more than twice as high as for the silica gel.

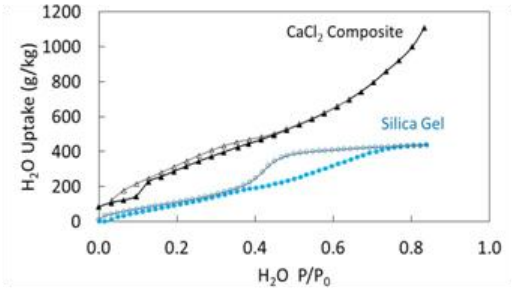

Figure 1: Water vapour sorption isotherms at 25°C.

For high humidity air (>80% RH), the composite sorbent reaches a maximum uptake of more than 1 kg/kg. Results from the test-bed experiments are shown in Fig. 2 for 60-80% RH and desorption at 100°C and 150°C. The composite sorbent had a maximum uptake of about 0.8 kg/kg and absorbed significantly more than silica gel. The composite sorbent had a 8-10 times lower pressure drop than the silica gel (Figure 2b). The silica gel bed was packed with spherical beads of ~2 mm, while the composite sorbent bed was melted to an open porous sponge structure inside the adsorber during the oven treatment. Such a sponge structure is easy to implement in existing facilities without the need for any major construction work.

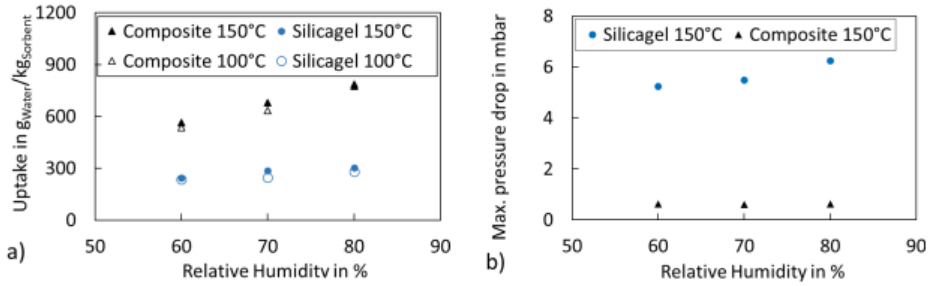

Figure 27: a) Uptake during open cycle tests of composite and silica gel dried at 100°C (open symbols) and 150°C (filled symbols) in the open sorption test bed. b) Pressure drop across the sorbent beds for composite and silica gel at 60-80%RH.

Summary/Conclusions

We prepared composite sorbent in an easy way and examined its suitability for drying high humidity air by experimental investigations in a custom test bed and a thermogravimetric analyzer. Due to its high uptake and low pressure drop, the composite sorbent allows small packaging and requires low fan power. Its sponge structure makes it easy to integrate in existing facilities.

References:

[1] Yadav, L., Yadav, A., Dabra, V., and Yadav, A. 2014. Effect of desiccant isotherm on the design parameters of desiccant wheel. *Heat Mass Transfer* 50, 1, 1–12.

[2] Aristov, Y. 2003. Selective water sorbents – New family of materials. Minsk International Seminar "Heat Pipes, Heat Pumps, Refrigerators", Minsk.

[3] Liu, H., Nagano, K., and Togawa, J. 2015. A composite material made of mesoporous siliceous shale impregnated with lithium chloride for an open sorption thermal energy storage system. *Sol Energy* 111, 186–200.

[4] Wu, H., Wang, S., and Zhu, D. 2007. Effects of impregnating variables on dynamic sorption characteristics and storage properties of composite sorbent for solar heat storage. *Sol Energy* 81, 7, 864–871.

[5] Tretiak, C.S., and Ben Abdallah, N. 2009. Sorption and desorption characteristics of a packed bed of clay-$CaCl_2$ desiccant particles. *Sol Energy* 83, 1861–1870.

Lab-scale sorption chiller comparison of FAM-Z02 coating and pellets

C. McCague, W. Huttema, A. Fradin, and M. Bahrami*

Laboratory for Alternative Energy Conversion (LAEC), School of Mechatronic Systems Engineering, Simon Fraser University, 250-13450 102 Avenue, Surrey, BC, Canada, V3T 0A3
*Corresponding author: mbahrami@sfu.ca

Abstract

Water adsorbent AQSOA FAM-Z02 (Z02) coatings and pellets were evaluated in our custom-built lab-scale sorption chiller with two adsorber beds. Two finned-tube heat exchangers (HEx) (3.835 dm^3) were coated with Z02 by Mitsubishi Plastics and compared with two equivalent HEx packed with Z02 pellets. When tested for a 15 °C, 30 °C and 90 °C cooling cycle and 5 to 30 min cycle times, the sorption chiller had a peak volumetric specific cooling power of 90 ± 5 W/m^3 with Z02 coated HEx compared to 59 ± 2 W/m^3 for HEx packed with Z02 pellets. The specific cooling power (SCP) and coefficient of performance (COP) were determined for a range of operating conditions and were greater for Z02 coatings compared to pellets.

Keywords: Sorption chiller, ASQOA FAM-Z02, specific cooling power, coefficient of performance.

Introduction

Water sorbent Z02 is used in desiccant wheels and adsorption chillers operating with low regeneration temperatures [1-4]. System performance during initial tests with Z02 pellet sorbent was limited by piping between the evaporator and the sorber beds in our testbed [5]. Here, an improved sorption chiller is used to compare the performance of Z02 pellets and coatings.

Experimental

The lab-scale sorption chiller is shown in Fig. 1. The two sorber beds (Fig. 2) were connected to two heating/cooling (H/C) circulators using two four way valves for automated cycling from adsorption to desorption temperatures. The sorber bed specifications and operating conditions are given in Table 1. Two additional H/C circulators controlled the temperature of the condenser and custom-built capillary-assisted low-pressure evaporator (CALPE) [6]. Vapor flow was controlled by a check valve (cracking pressure < 0.25 kPa) between each sorber and the condenser, and two 50 mm gate valves between the sorber beds and the evaporator. Three flowmeters, four pressure sensors, and twelve thermocouples were used for detailed monitoring of the cycle. Isotherms and isobars of Z02 powder, spherical pellets with dia.=1.8 mm, and coating were collected using a thermogravimetric sorption analyser (TGA).

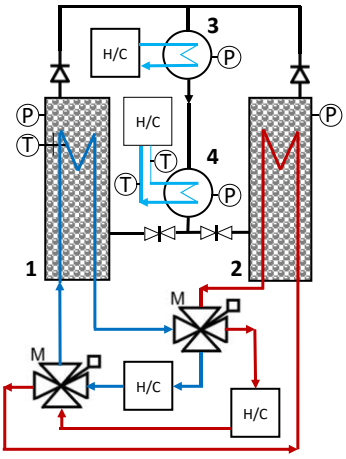

Fig. 28. Schematic of lab-scale sorption chiller with two sorber beds (1,2), condenser and CALPE evaporator.

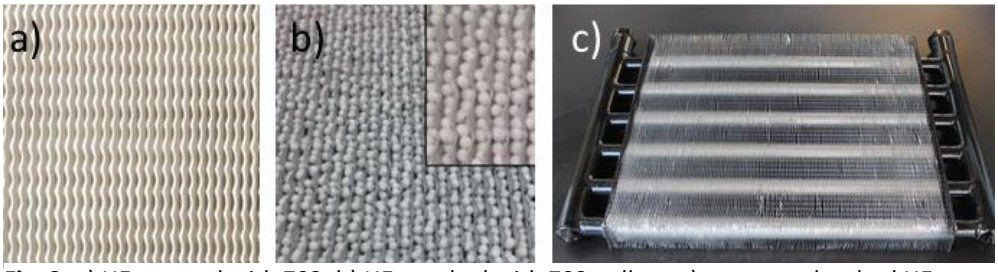

Fig. 2. a) HEx coated with Z02, b) HEx packed with Z02 pellets, c) empty sorber bed HEx

Results and Discussion

TGA measurements on Z02 samples showed 9% and 13% decreases in equilibrium water uptake for the pellets and coating, respectively, relative to Z02 powder (Fig. 3). As shown in Fig. 4, in lab-scale sorption chiller tests the Z02 coated HEx had greater volumetric and mass specific cooling powers than the Z02 pellet filled HEx. This was in part due to the thermal contact resistance between the pellets and the HEx, which impedes heat transfer. For 10 min cycles, an SCP of 456 W/kg (90 kW/m^3) and a COP 0.27 was achieved with the Z02 coated HEx. Sorption chiller tests on a small coated HEx (0.08 kg sorbent) by Freni et al. achieved 93 kW/m^3 and 675 W/kg [3]. Dawoud reported a sorption rate of 0.06 g/100 g·s for small samples of 0.3 mm Z02 coatings, and much slower uptake rates for HEx coated with 1.5 kg of sorbent (57% uptake capacity in 10 min) [4]. For 30 min cycles with our Z02 coated HEx, the uptake rate was 0.04-0.05 g/100 g·s during with first 4 min of sorption and 96% of sorption capacity was achieved in 10 min.

Conclusion

The performance of the lab-scale sorption chiller was comparable to the expected potential of Z02 coatings based on previous kinetic studies of small samples and small coated heat exchangers.

Table 1. Adsorber bed specifications, operating conditions, and equations

HEx (L,W,H)	35×3.8×30.5 cm^3
Fin spacing	2.54 mm
Cycle times	5, 10, 20, 30 min
$T_{desorption}$	75, 80, 90 °C
T_{ads}, T_{cond}	20, 30, 40 °C
$T_{evaporator}$	5, 10, 15 °C
HEx weight	2.51 ± 0.03 kg
Z02 coating	0.80 kg per HEx
Z02 pellets	1.97 kg per HEx
COP=Q_{evap}/Q_{heat}	SCP=$Q_{evap}/(m_{ads}\cdot\tau)$
Q_{evap} (J)=$\int_0^\tau \dot{m}c_p(T_{in}-T_{out})dt$ with cold water $\dot{m}$ = 2.5 L/min and c_p = 4.18 kJ/kg	

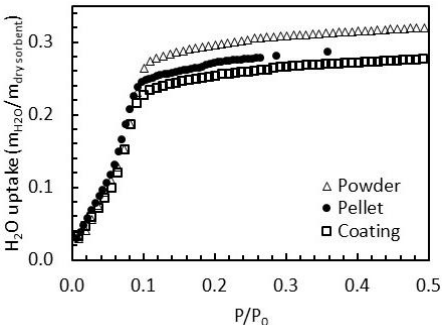

Fig. 3. Water sorption isobars for Z02 powder, pellets, and coating.

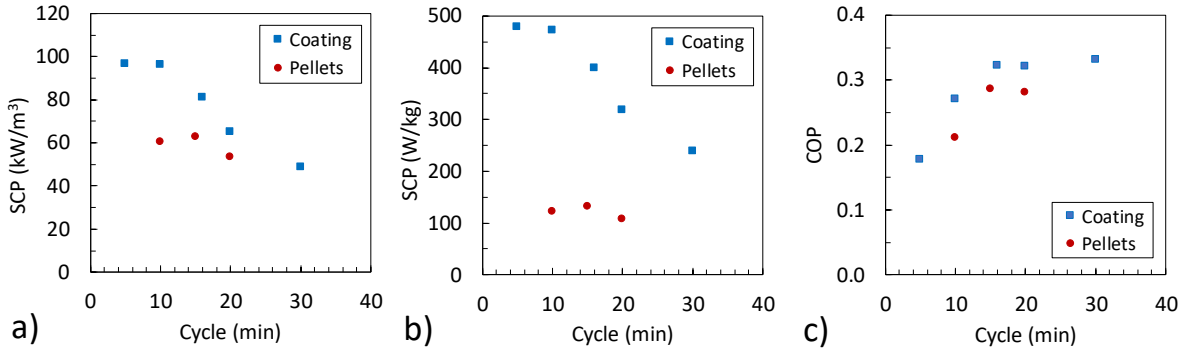

Fig. 4. Performance of sorption chiller for Z02 coating and pellet; a) SCP by HEx volume, b) SCP by sorbent weight, and c) COP. Operating conditions: T_{evap}= 15 °C, T_{cond}=T_{ads}= 30 °C, and T_{des}= 90 °C,

References

[1] A. Freni, G. Maggio, A. Sapienza, A. Frazzica, G. Restuccia, S. Vasta, *Applied Thermal Engineering* 104 (2016) 85–95
[2] Ilya S. Girnik, Yuri I. Aristov, *Energy* 114 (2016) 767-773.
[3] A. Freni, L. Bonaccorsi, L. Calabrese, A. Caprì, A. Frazzica, A. Sapienza, *Applied Thermal Engineering* 82 (2015) 1-7
[4] B. Dawoud, *Applied Thermal Engineering*, 50 (2013) 1645-1651.
[5] A. Sharafian, S. M. Nemati Mehr, P. Thimmaiah, W. Huttema, M. Bahrami, *Energy* 112 (2016) 481-493.
[6] P. C. Thimmaiah, A. Sharafian, M. Rouhani, W. Huttema, and M. Bahrami, *Energy*, 122 (2017) 144-158.

A new generation of hybrid adsorption washer dryers

J. Cranston[1], A. Askalany[1.2*], G. Santori[1]

[1]The University of Edinburgh, School of Engineering, Institute for Materials and Processes, Mayfield Road, The King's Buildings, EH9 3JL, Edinburgh, UK

[2]Mechanical Engineering Department, Faculty of Industrial Education, Sohag University, Sohag, 82524, Egypt

[*]Corresponding author: ahmed_askalany3@yahoo.com

Abstract

Domestic appliances consumes at least 30% of the total energy consumption at the UK where wet appliances comes as the second most energy intensive class of household devices. Thanks to the widespread of these technologies, increased energy savings have potential for global emission reduction. In this research, the benefits of using adsorption technology in the drying process of a washer-dryer has been investigated. A hybrid heat pump-adsorption washer dryer has been experimentally and theoretically investigated by using commercial silica gel.

Keywords: Drying, Energy saving, Adsorption.

Introduction/Background

Drying applications specially in house appliances such as dishwasher and washer dryer consumes a huge amount of produced energy to the extent that in 2013 the Department of Energy & Climate Change categorised wet appliances as the second most energy intensive class of household devices (1.3 mtoe) in the UK [1, 2]. In 2001, 91.7 million units have been produced worldwide which consume an energy of 48143 GWh producing 24.1 megatons of CO_2. Adsorption drying could be driven thermally and it could be employed in decreasing the electricity dependence. From this point of view, this research presents an investigation of the potential benefits of employing the adsorption technology in the drying process of the washing machine.

Discussion and Results

An adsorption bed has been posted in a heat pump tumble dryer. The working principle of this drying machine considers cycling humid air from the drying drum through an evaporator and a condenser returning it back to the drum. A dehumidification process occurs on the evaporator by cooling the air down as low as the dew point temperature then the cooled humid air is heated up through the condenser.

The installed adsorption bed has been located straight forward after the evaporator as shown in Fig.1. The bed is regenerated by using hot dry air from the condenser.

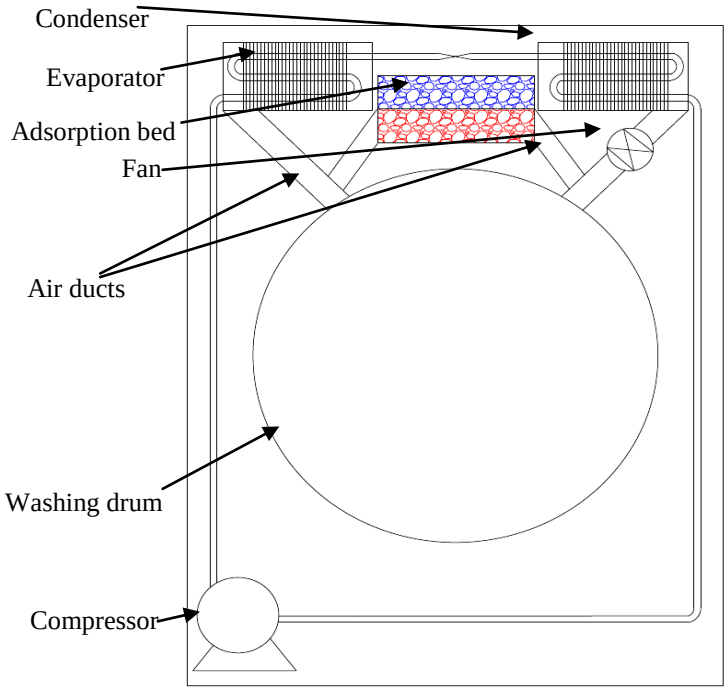

Fig.1. Layout of the adsorption heat pump washer dryer**.**

Summary/Conclusions

Benefit of employing the adsorption technology within the drying process of the heat pump washer dryer has been studied. A new arrangement for using an adsorption bed with the heat pump components has been presented and tested. An energy saving of 10% has been achieved comparing to the tumble dryer with heat pump considering the same amount of removed water.

Acknowledgements

This research is supported by EPSRC within the "Micro-scale energy storage for super-efficient wet appliances" project EP/P010954/1.

References:

[1] DECC The Carbon Plan: Delivering our low carbon future. (2011)

[2] DECC Energy Consumption in the UK, demostic data table 2014, Table 3.10

Formulation influence on the preparation of silica nanoparticle-based ionogels

Hongsheng Dong[1,2], Ahmed A. Askalany[2,3] and Giulio Santori[2*]

[1] Key Laboratory of Ocean Energy Utilization and Energy Conservation of Ministry of Education, School of Energy & Power Engineering, Dalian University of Technology, Dalian 116024, China

[2] The University of Edinburgh, School of Engineering, Institute for Materials and Processes, Sanderson Building, The King's Buildings, Mayfield Road, EH9 3BF Edinburgh, Scotland, UK

[3]Mechanical Engineering Department, Faculty of Industrial Education, Sohag University, Sohag, 82524, Egypt

[*]Corresponding author: G.Santori@ed.ac.uk

Abstract

This research presents an experimental investigation of adsorption isotherms of water vapour onto impregnated silica gel in ionic liquid solutions. Adsorption/desorption isotherms silica gel (Syloid)/water vapour without any additions has been measured. Then the adsorption isotherms have been detected for impregnated Syloid with ionic liquid (1-ethyl-3-methylimidazolium methanesulfonate) at different concentrations (10%, 20 and 50%) at 25ºC. Ionic liquid shows a significant improvement in the adsorption capacity of water vapour onto Syloid however, the adsorption type has been changed from I to III. The maximum adsorption capacity at 25ºC has been increased from 0.3 kg/kg to 0.7 kg/kg.

Keywords: Adsorption, water, silica gel, ionic liquid.

Introduction/Background

Adsorption technology has been employed recently in different applications such as cooling, water desalination, gas separation and drying. It has some advantages from the environmental point of view however it still have some drawbacks that refrains its commercial spread. One of these drawbacks is its low relative performance in terms of low cooling capacity (in cooling applications) or low water production (in desalination applications). Trials to solve this problem have been conducted in different ways such as increasing the adsorption capacity of the used adsorbents either physically or chemically getting new composite materials. i.e. Aristov [1] presented a new family of the adsorbents "salt inside a porous host matrix". A new metal-organic framework of MIL-101 was synthesized and presented as an adsorbent by Zhengqiu RUI et al. [2]. The water adsorption isotherms were obtained and reached as high as 0.95 kg/kg. Chan et al. [3], synthesized MWCNT embedded zeolite (13X/CaCl2) with different MWCNT mass ratios. The operational range synthesized zeolite was found to be 0.5 kg/kg.
Ye et al. [4], investigated the adsorption characteristics of Activated carbon fiber cloth/CaCl2 as a composite material with water vapour using impregnation method. The maximum adsorption capacity for the this materials had been found to be as high as 0.5 g/g
In this research, an improvement on the adsorption capacity of Syloid has been studied by impregnating it in ionic liquid solutions.

Discussion and Results

1-ethyl-3-methylimidazolium methanesulfonate has been used as an ionic liquid to impregnate the Syloid. The impregnation process has been held by making a solution of the ionic liquid in water at different concentrations ranging from 10% to 50%. The Syloid sample

has been left inside the solution for 24 hours then it has been dried up to 120ºC for another 24 hour.

Fig.1 shows the isotherms of water vapour adsorption/desorption onto impregnated Syloid at different ionic liquid concentrations at 25ºC. The figure indicates that the ionic liquid has a significant effect on the adsorption capacity of the Syloid where the higher ionic liquid concentration the higher adsorption capacity we get. In addition, the shape if the adsotion isotherm has been changed from type I adsorption for the normal Syloid to type III for the impregnated Syloid.

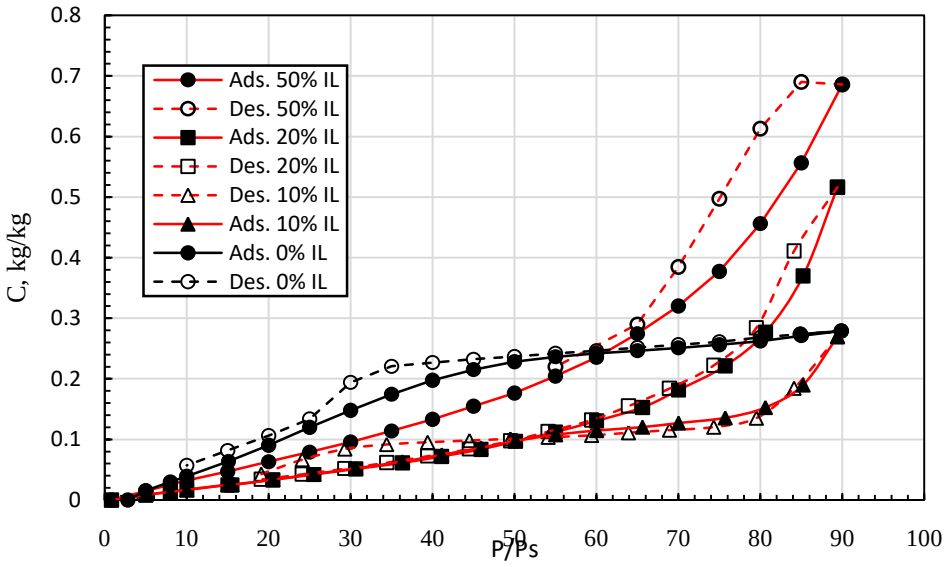

Fig. 1. Adsorption isotherms of water in Syloid at different ionic liquid concentrations.

Summary/Conclusions

There is a great improvement for the adsorption capacity of water vapour on the Syloid by impregnating it in the ionic liquid. The maximum adsorption capacity at 25ºC has been increased from 0.3 kg/kg to 0.7 kg/kg.

Acknowledgements

This research is supported by EPSRC within the "Micro-scale energy storage for super-efficient wet appliances" project EP/P010954/1.

References:

[1] Aristov, Y.I., G Restuccia, G Cacciola, V. N. Parmon, "A family of new working materials for solid sorption air conditioning systems", Applied Thermal Engineering, 2002,

[2] Zhengqiu, R.U.I., Quanguo, L.I., Qun, C.U.I., WANG, H., CHEN, H., YAO, H., "Adsorption Refrigeration Performance of Shaped MIL-101-Water Working Pair", Chinese Journal of Chemical Engineering, 2014.

[3] Chan, K.C., Christopher, Chao, Y.H., Wu, C.L.,"Measurement of properties and performance prediction of the new MWCNT-embedded zeolite 13X/CaCl2 composite adsorbents", International Journal of Heat and Mass Transfer, 2015.

[4] Ye, H., Yuan, Z., Li, S., Zhang, L.,"Activated carbon fiber cloth and CaCl2 composite sorbents for a water vapor sorption cooling system", Applied Thermal Engineering 2014.

Heat rejection stage of an adsorption heat storage cycle: The useful heat and sorption dynamics

V. Palomba[1*], A. Sapienza[1] and Y.Aristov[2,3]

[1]CNR ITAE Institute for Advanced Energy Technologies, Salita S.Lucia sopra Contesse 5, 98126 Messina, Italy
[2]Boreskov Institute of Catalysis, Lavrentiev Av. 5, Novosibirsk, Russia
[3]Novosibirsk State University, Pirogova Str. 2, Novosibirsk, Russia
[*]Corresponding author: valeria.palomba@itae.cnr.it

Abstract

In this work, a performance of the adsorption stage of a seasonal heat storage cycle was experimentally investigated under realistic boundary conditions. The tests were performed by a lab scale testing bench. The studied adsorber is based on a compact aluminium heat exchanger of a flat tube type. Three water sorbents were tested: two commercial materials (microporous silica Siogel and AQSOA FAM Z02) and a composite SWS-1L ($CaCl_2$ in mesoporous silica).

Keywords: Adsorption thermal storage, Pressure driven cycle, Sorption dynamics

Introduction

Among the various available technologies, adsorption heat storage (AHS) is gaining attention, due to the high storage density available and the possibility to store heat for a theoretically infinite time without heat losses [1]. Nonetheless, there are still some open issues, such as the poor heat and mass transfer, which leads to bulky systems. In order to overcome such barriers, the study of adsorption dynamics is necessary.
Accordingly, the focus of this work is the detailed study of the adsorption stage of an AHS cycle to get information about the sorption dynamics under the real operating conditions for seasonal heat storage and about the useful heat obtainable from different sorbents.

The adsorption heat storage cycle

A typical AHS cycle consists of two stages, namely, the heat storage (desorption) (1-2-3 in Fig. 1a) and heat rejection (adsorption, 3-4-4'-1). It differs significantly from the common chilling cycle with two isosters and two isobars (1-2-3-4'). At point 3, the adsorbent is dry and heat is stored. Then, the adsorbent is cooled down to the ambient temperature T4. The stored heat can be got back on demand, e.g. during autumn or winter time, by connecting the adsorber to the evaporator. The adsorption process is initiated by the pressure jump from the initial pressure P4 over the adsorbent at T4 to the final pressure P1 maintained by the evaporator at the ambient temperature. This stage is isobaric and non-isothermal, because of the adsorption heat release that causes an increase in the adsorbent temperature. It reaches the maximum at point 4'. At longer time, the adsorbent temperature reduces down to T1 which is still suitable for heating. After that the heat rejection process was stopped. Thus, the heat rejection stage presents a kind of pressure-driven adsorption process which has been poorly studied so far, because the majority of processes in adsorptive chillers and heat pumps are temperature-driven [2].

Experimental

The experimental activity was carried out at CNR-ITAE by the lab-scale adsorption bench described in [3]. Three sorbents were tested: a microporous silica gel (Siogel - Oker Chemie), the Mitsubishi AQSOA FAM Z02 and the composite SWS-1L ($CaCl_2$ in mesoporous silica gel). All the sorbents were in shape of grains with the size ranging between 0.30 and 0.710 mm. The loose grains were embedded in a commercial aluminium heat exchanger of a flat-tube type, as shown in Fig. 1b. Various operating conditions were tested, corresponding to the wide range of

ambient conditions of different climates. In particular, the initial adsorption temperature T4 was considered in the range 10 to 30°C, together with the evaporation temperatures in the range 5-30°C. The effect of the flow rate of a heat transfer fluid (water) at the adsorber inlet was also evaluated.

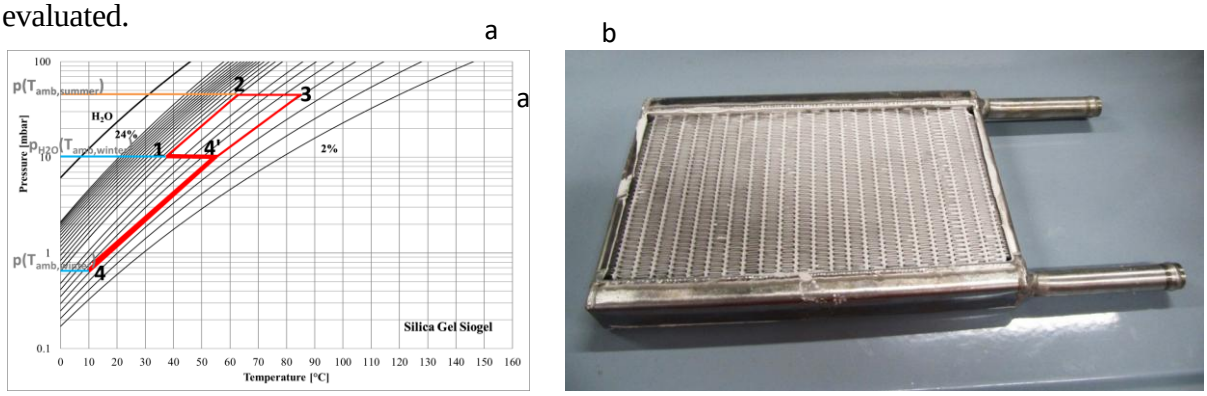

Fig. 1. a: the P-T diagram for a typical AHS cycle (red lines). The blue and orange lines indicate the ambient conditions in summer and winter. b: view of the tested heat exchanger.

Results

In Fig. 2b it is possible to notice that a maximum temperature lift ΔT of 9°C was measured at the adsorber outlet with an exponential decay following the maximum. Peak power of 800 W was measured, with a progressive reduction to 400 W when the ΔT reduces below 4°C. Under those conditions, the useful heat reached 250 kJ/kg_{ads}. No useful heat can be generated with the Siogel at T_{ev} < 10°C. Much larger heat can be stored and released by using AQSOA FAM Z02 and SWS-1L because they sorb much larger mass of water. These sorbents can produce the useful heat even at T_{ev} as low as 5°C and below, due to their stronger affinity to water vapour as compared with the silica gel. They can be recommended for colder climatic zones.

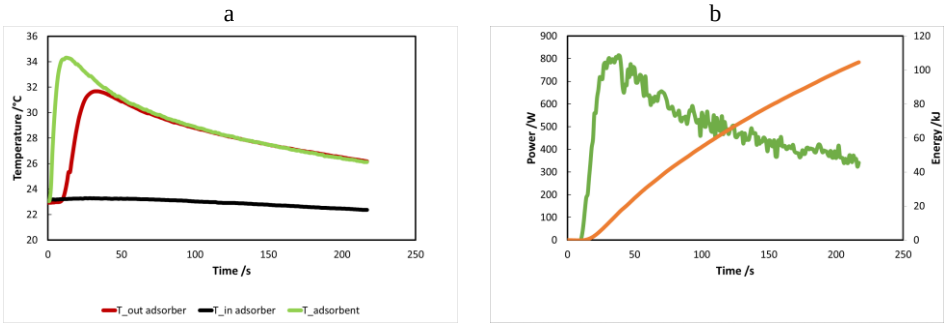

Fig. 2. a: temperature evolution of the adsorbent and the heat transfer fluid. b: power delivered and useful energy. Testing conditions: T_{ads} = 20°C, T_{ev} = 15°C, heat carrier flow rate 1.2 LPM.

References

[1] Cabeza L.F., Sole A., Barreneche C., Review on sorption materials and technologies for heat pumps and thermal energy storage, Renewable Energy 2017 doi: 10.1016/j.renene.2016.09.059

[2] Aristov, Yu.I., Adsorptive transformation/storage of heat: temperature-driven vs. pressure -driven cycles, Abstract of this Conference.

[3] Sapienza A., Santamaria S., Frazzica A., Freni A.. Influence of the management strategy and operating conditions on the performance of an adsorption chiller. Energy 2011doi: 10.1016/j.energy.2011.07.020.

Adsorptive transformation/storage of heat: temperature-driven vs. pressure-driven cycles

Yu.I. Aristov[1, 2]

[1]Boreskov Institute of Catalysis, Ac. Lavrentiev av. 5, Novosibirsk 630090, Russia

[2]Novosibirsk State University, Pirogova st. 2, Novosibirsk 630090, Russia

[*]Corresponding author: aristov@catalysis.ru

Abstract

Adsorption heat transformation/storage (AHTS) is an environmentally benign and energy saving technology for effective utilization of low-temperature heat from various sources (renewable heat, thermal wastes, geothermal heat, etc). Two types of the AHTS cycles were suggested, which essentially differ by the way of adsorbent regeneration: either adsorbent heating (***temperature-driven*** cycles), or reducing the adsorptive pressure over adsorbent (***pressure-driven*** cycles). In this work, these cycles are analyzed and compared from both thermodynamic and dynamic points of view. Appropriate recommendations are made.

Keywords: Adsorption cooling/heating/storage, Adsorbent regeneration, Cycle dynamics

Introduction

The adsorption heat transformation/storage (AHTS) is an emerging technology gaining more and more attention. A simplest AHTS unit exchanges heat between three thermostats at high (T_H), middle (T_M) and low (T_L) temperatures and transforms heat at three modes: (1) cooling, (2) heating, and (3) upgrading the temperature potential. Two types of the suggested AHTS cycles essentially differ by the way of adsorbent regeneration: (i) adsorbent heating up to the temperature sufficient for the adsorbate removal (***temperature driven***, TD cycles, Fig. 1a), (ii) reducing the adsorptive pressure over the adsorbent (***pressure driven***, PD cycles, Fig. 1b).

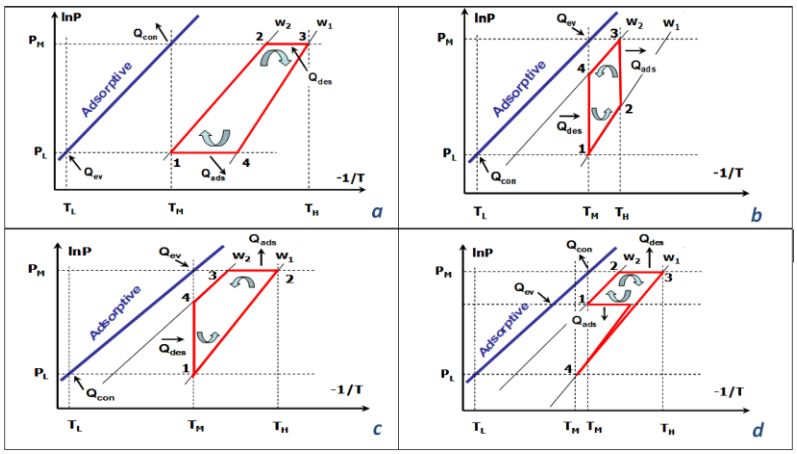

Fig. 1. P-T diagrams of various 3T AHTS cycles: a – TD cycle, b – PD cycle, c – combined TD/PD cycle, and d – heat storage cycle.

TD cycles are very common and widely used to realize cooling and heating modes [1]. PD cycles are much less spread and suggested mainly for the temperature upgrading and heat storage modes [1,2]. In this work, we generally considered TD cycles as the most prevalent. PD cycles were studied by taking as example a new “Heat from Cold” cycle (HeCol) recently

suggested for upgrading the ambient heat [4]. Combined TD/PD cycles (Fig. 1c) and heat storage cycles (Fig. 1c, [5]), which have both TD and PD stages, are also considered.

Results and Discussion

Comparative analysis of the energy and entropy balances for TD and PD cycles revealed an important difference between them. For TD cycles, a quite large entropy is generated during desorption and adsorption stages due to the thermal coupling of the adsorber and external heat source/sink. Quite the contrary, for PD cycles, these stages are isothermal with a zero thermal coupling that can lead to the higher second law efficiency as compared with TD cycles. For both cycles, this efficiency can reach the Carnot efficiency, if the weak and rich isosters coincide, i.e. for a mono-variant equilibrium.

Although the adsorptive is exchanged between the same weak and rich isosters, the TD and PD dynamics can be different [6,7]. Indeed, at the beginning of ad-/desorption stages, the driving force for TD cycles is the temperature drop/jump and the limiting process is heat transfer, whereas for PD cycles the driving force is the pressure jump/drop and the limiting process is mass transfer.

Summary/Conclusions

Both ***temperature- and pressure-driven*** adsorptive cycles for heat transformation/storage allow an efficient heat conversion process to be realized. For both cycles, there are threshold conditions (e.g. a minimal desorption temperature or pressure) to be necessarily fulfilled in order the cycle can be realized. The PD cycles can ensure the higher second law efficiency due to smaller (or zero) temperature coupling of the adsorber and external heat source/sink. The cycle dynamics can be fast enough in both cases, although the adsorption driving forces may significantly differ. In the short run, more attention should be paid to studying PD cycles for heat amplification as well as combined TD/PD and heat storage cycles.

Acknowledgement. This work is supported by the Russian Science Foundation (grant 16-19-10259).

References:

[1] Li, T., Wang, R. Z., Li, H., Progress in the development of solid-gas sorption refrigeration thermodynamic cycle driven by low-grade thermal energy, Progress in Energy Combustion Science, 2013, doi: 10.1016/j.pecs.2013.09.002.

[2] Chandra, I., Patwardhan, V. S., Theoretical studies on adsorption heat transformer using zeolite-water vapour pair, Heat Recovery Systems and CHP, 1998, doi: 10.1016/0890-4332 (90)90203-V.

[3] Aristov, Yu., Adsorptive transformation of ambient heat: a new cycle, Appl. Therm. Eng. 2017, doi: 10.1016/j.applthermaleng.2017.06.051.

[4] Tokarev, M.M., Grekova, A.D., Gordeeva, L.G., Aristov, Yu.I., A new cycle "Heat from Cold" for upgrading the ambient heat: the testing a lab-scale prototype with the composite sorbent CaClBr/silica, Applied Energy, 2018, doi: 10.1016/j.apenergy.2017.11.015.

[5] Palomba, V., A. Sapienza, A., Aristov, Yu.I., Heat rejection stage of an adsorption heat storage cycle: the useful heat and sorption dynamics, Abstract HPC2018.

[6] Aristov, Yu.I., Experimental and numerical study of adsorptive chiller dynamics: a loose grains configuration, Applied Therm. Eng., 2013, doi: 10.1016/j.applthermaleng.2013.04.051.

[7] Aristov, Yu., Adsorptive transformation and storage of renewable heat: review of current trends in adsorption dynamics, Renewable Energy, 2017, doi: 10.1016/j.renene.2016.06.055.

Database of Sorption Materials Equilibrium Properties

Zhiyao Yang[1,2], Kyle R. Gluesenkamp[2*], and Andrea Frazzica[3]

[1]Lyle School of Civil Engineering, Purdue University
550 W Stadium Ave
West Lafayette, IN 47907 USA

[2]Oak Ridge National Laboratory
1 Bethel Valley Rd
Oak Ridge TN 37831 USA

[3]Istituto di Tecnologie Avanzate per l'Energia "Nicola Giordano"
Consiglio Nazionale delle Ricerche
Salita Santa Lucia Sopra Contesse, 5
Messina, Italy

[*]Corresponding author: gluesenkampk@ornl.gov

Abstract

A wide review of available equilibrium vapor pressure data was conducted for sorption working pairs (liquid absorption and solid adsorption). The data were programmed into a publicly available database library called SorpPropLib for standalone use, or use with the open source program SorpSim. Four commonly used functional forms for solid adsorbents were included, as well as 12 common functional forms for liquid absorbents, and numerous custom equations that have been proposed for specific working pairs in the literature. Altogether, the database currently includes 285 functional correlations describing 194 working pairs. It has also been assembled in a way that will facilitate future expansion.

Keywords: Sorption, VLE, isotherms, PTX, materials properties, database

Introduction/Background

One task for the IEA Annex 43 includes the compilation of a database of materials properties. Numerous literature reviews have been conducted in the past such as Tamainot-Telto et al. (2009). These have generally focused on a particular material, or a particular application, and none has been comprehensive. Considering that new sorbents and sorbent composites are being constantly generated, there is a need for a framework that can grow as properties of new materials are defined. The SorpPropLib framework presented in this work aims to meet this objective.

Discussion and Results

Table 1 shows a summary of the working pairs that are included in this work.

Table 1: Summary of refrigerants and number of working pairs

Refrigerant Category	**Refrigerant**	**# of sorbents included**	***Refrigerant Category***	**Refrigerant**	**# of sorbents included**
Inorganic	Water	28	*Fluorocarbons*	R12	3
	Ammonia	26		R13B1	1
	CO_2	12		R22	4
Hydrocarbon	Propane	4		R23	1
	Propylene	6		R32	13
	Isobutane	3		R115	1
	1-butane	1		R124	1
	Ethane	1		R125	12
	Hexane	1		R134a	24
	Benzene	5		R143a	8
	Toluene	1		R152a	5
	Cyclohexane	4		R507A	2
	Cyclohexene	1		R125/R143a	1
	Acetone	4		R1234ze(E)	2
Alcohol	Ethanol	8		R1234yf	1
	Methanol	2		R134a/R227ca	1
	2-propanol	2		R22/R142b	1
Other	TFE	3			
	THF	1			

Summary/Conclusions

Compilation of a wide range of equilibrium vapor pressure properties for various sorbent working pairs was assembled. The results were coded into a database called SorpPropLib that can be readily accessed and extended.

References:

[1] Tamainot-Telto, Z., et al., Carbon–ammonia pairs for adsorption refrigeration applications: ice making, air conditioning and heat pumping. International Journal of Refrigeration, 2009. 32(6): p. 1212-1229.Faghri, A., *Heat Pipe Science and Technology*, Taylor and Francis, 1995.

Overview and step forward on SAPO-34 based zeolite coatings for adsorption heat pumps

L. Calabrese[1,3*], L. Bonaccorsi[2], A. Freni[3], P. Bruzzaniti[1], E. Proverbio[1]

[1]Department of Engineering, University of Messina, Contrada di Dio Sant'Agata, 98166 Messina, Italy
[2]Department of Civil Engineering, Energy, Environment and Materials, University Mediterranea of Reggio Calabria, Salita Melissari, 89124 Reggio Calabria, Italy
[3]CNR-ICCOM, Via G. Moruzzi 1, I-56124 Pisa, Italy

*Corresponding author: lcalabrese@unime.it

Abstract

In this work, at first, an overview on SAPO-34 zeolite coating for adsorption heat pumps was presented. Afterwards, we present new adsorbent composite coatings on aluminum support, which were prepared by dip-coating method starting from a water suspension of SAPO-34 zeolite and an organic-inorganic binder. Adhesive and mechanical properties were evaluated by pull-off test confirming the good interaction between metal substrate, filler and matrix. Adsorption equilibrium of water vapor on the adsorbent coating were studied in the range T= 30–150°C and pH_2O=11 mbar. It was found that the organic-inorganic binder does not affect the water adsorption capacity and adsorption kinetics of the original SAPO-34 zeolite.

Keywords: SAPO-34, zeolite, coating, direct synthesis, composites

Introduction/Overview

Some research activities on adsorption heat pumps development are focused on the optimization of the integration between heat exchanger and adsorbent material, to create the so called adsorber. Two different approaches are currently evaluated: embedding of granular adsorbent inside an efficient heat exchanger [1] or coating the heat exchanger with the adsorbent material
Granular zeolite adsorbent inside the heat exchanger induces a low vapour transfer resistance and low manufacturing costs. However, a significant limit that avoid its use in high efficiency systems is the very low heat transfer due to a punctual contact between the grains and the surface of heat exchanger [2]. In this concern, coated exchanger choice is related mainly to its good heat exchange efficiency at the coating/metal interface and to the cycle times reduction. The most promising coating methods are in-situ zeolite growth [3] [4] and binder-based coating processes [5] [6]. Direct accretion of zeolite crystals on the metal surface allows very good adhesion. However, multiple depositions are required to reach an acceptable zeolitic layer thickness (<0.1 mm). The binder-based coating method is an alternate way to deposit a thin layer of adsorbent on the heat exchanger surface. On the contrary, the binder-based coating method offers the possibility to vary coating thickness in the range 0.1–1 mm by, e.g., controlling the viscosity of the liquid suspension and the dipping velocity. Full scale dip-coated adsorbers were experimentally tested in [7], showing promising results in terms of reduced adsorption cycle time and elevated specific power.
Nevertheless, still some issues are present. The coating is usually characterised by poor mechanical strength that favours easy loss of zeolite particles from the supports upon repeated temperature swings, due to the difference in their thermal expansion coefficients. A drawback of this route is the low zeolite amount in the adsorber, due to the limited coating thickness, that induces low adsorbent density (typically 150-300 g/dm^3).

Step Forward: Discussion and Results

To overcome the previous issues, a new formulation based on a mixture of polysiloxane with proper catalyst was employed to form a flexible and micro-porous composite coating. During the raw components mixing, the SAPO-34 powder (2 μm crystal dimension) was dispersed at

different percentages (from 60 wt.% up to 90 wt.%). The pull off test evidenced a good adhesion of the coating to the substrate with optimal adhesion strength for composite coating with 80% of filler. Furthermore, the adsorption performances on coating (90 wt.% zeolite amount) and pure adsorbent powder, carried out by DVS instrument, are reported in figure 1, evidencing that the binder does not hinder the water vapour diffusion and zeolite efficiency is maintained.

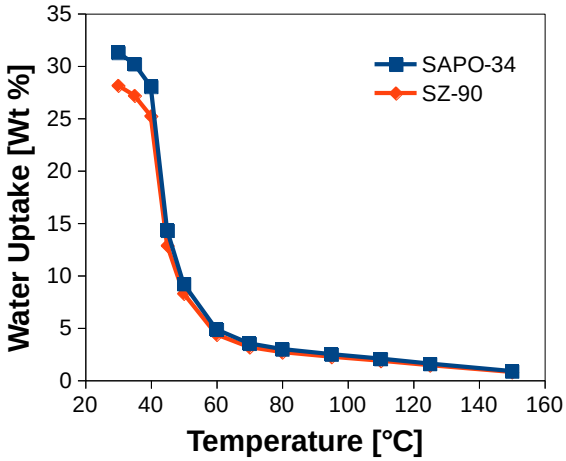

Figure 1: Water adsorption isobars at 11 mbar for 90% zeolite coating (SZ-90) and pure zeolite powder (SAPO-34)

Summary/Conclusions

The advantages related to the use of coating technologies are:
- possibility of easily coat complex heat exchanger geometries with an adsorbent layer, maintaining a uniform thickness,
- tuneable coating thickness changing the formulation parameters, typically between 0.1-0.5 mm,
-reduction of heat and mass transfer resistances, thanks to the good contact between adsorbent layer and heat exchanger surface and to the low adsorbent thickness
The new composite coating characterised by hybrid polymer binder evidenced promising results as potential alternative of conventional adsorbent materials and coatings.

References:

[1] I. S. Girnik and Y. I. Aristov, “Making adsorptive chillers more fast and efficient: The effect of bi-dispersed adsorbent bed,” *Appl. Therm. Eng.*, 106, 254–256, 2016.
[2] Y. I. Aristov, “Challenging offers of material science for adsorption heat transformation: A review,” in *Appl. Therm. Eng.*, 50, 2, 1610–1618, 2013.
[3] L. Bonaccorsi, L. Calabrese, A. Freni, E. Proverbio, and G. Restuccia, “Zeolites direct synthesis on heat exchangers for adsorption heat pumps,” *Appl. Therm. Eng.*, 50, 2, 1590–1595, 2013.
[4] J. Bauer, R. Herrmann, W. Mittelbach, and W. Schwieger, “Zeolite/aluminum composite adsorbents for application in adsorption refrigeration,” *Int. J. Energy Res.*, 33, 13, 1233–1249, 2009.
[5] A. Freni, L. Bonaccorsi, L. Calabrese, A. Caprì, A. Frazzica, and A. Sapienza, “SAPO-34 coated adsorbent heat exchanger for adsorption chillers,” *Appl. Therm. Eng.*, 82, 1–7, 2015.
[6] A. Freni, A. Frazzica, B. Dawoud, S. Chmielewski, L. Calabrese, and L. Bonaccorsi, “Adsorbent coatings for heat pumping applications: Verification of hydrothermal and mechanical stabilities,” *Appl. Therm. Eng.*, 50, 2, 1658–1663, 2013.
[7] B. Dawoud, “Water vapor adsorption kinetics on small and full scale zeolite coated adsorbers; A comparison,” *Appl. Therm. Eng.*, 50, 2, 1645–1651, 2013

Effects of storage period on the performance of salt composite sorption thermal energy storage

M. Rouhani, W. Huttema, C. McCague, M. Khajehpour and M. Bahrami*

Laboratory for Alternative Energy Conversion (LAEC), School of Mechatronic Systems Engineering, Simon Fraser University, 250-13450 102 Avenue, Surrey, BC, Canada, V3T 0A3
*Corresponding author: mbahrami@sfu.ca

Abstract

Effects of storage duration, high-conductivity additives and non-condensable gases on the storage performance of salt composite sorption thermal energy storage are experimentally investigated. We observed that sorption hot storage is more suitable for short-term storage, since there is a 58% decrease in energy storage density (ESD) from 1.03 (no storage-time) to 0.43 $MJ \cdot kg^{-1}$ (seasonal applications). The hot storage ESD is almost the same for silica gel-$CaCl_2$ and silica gel-$CaCl_2$-graphite flake (1.04 $MJ \cdot kg^{-1}$), while the averaged discharge power of the composite with graphite flake is higher. A 25% decrease in the ESD of seasonal cold storage is observed, compared to the cyclic operation, when 1.7 kPa pressure build-up in condenser occurred. This indicates the importance of occasional degassing for long-term applications.

Keywords: sorption thermal energy storage, residual gas, storage period, salt composites

Introduction/Background

Thermal energy storage (TES) is needed for the efficient use of intermittent renewables. Among TES systems, sorption thermal energy storage (sorp-TES) shows great potential for short- and long-term storage, because of high energy storage density (ESD) and negligible heat loss [1]. However, Schreiber et al. [2] showed that long-term storage dramatically decreased the ESD of a Zeolite-based hot storage sorp-TES. Composite sorbents, salts in porous matrix, provide the highest ESD [3], although salt composites are corrosive to most heat exchanger materials and corrosion reactions release non-condensable gasses, causing pressure build-up in the sorber bed and evaporator/condenser. Glaznev et al. [4] showed that presence of even small amount of residual gas can dramatically decrease the adsorption rate and the cooling power. In this study, the effect of storage duration, from no storage to few minute-storage and seasonal application, is examined using a custom-built low-temperature driven sorp-TES with silica gel-$CaCl_2$ and silica gel-$CaCl_2$-graphite flake. Effects of residual gas build-up inside the sorber bed on ESD, for both cold and hot storage, are investigated. Moreover, the effects of adding high-conductive additives, graphite flake, to the salt composite on the ESD and discharge power are studied.

Experimental study

The closed sorption prototype, which consisted of: i) two sorber beds, fin-tube heat exchanger; ii) a condenser, shell-and-tube heat exchanger; and iii) an evaporator, custom-built capillary-assisted low-pressure evaporator, is shown in Figure 29a. One of the sorber beds was filled with 1.302 kg silica gel-$CaCl_2$ (SG-CC: 55 wt% B150 silica gel, 30 wt% $CaCl_2$ and 15 wt% PVA), while the other one was filled with 1.513 kg silica gel-$CaCl_2$-graphite flake (SG-CC-G: 42 wt% B150 silica gel, 23 wt% $CaCl_2$, 20 wt% graphite flakes and 15 wt% PVA). Each bed was examined separately. Prior to the experiments, the entire sorption system was evacuated at 90 °C for several hours to remove the residual gas. During the charging process, adsorber bed was heated by an external water loop and the desorbed water vapour was transferred to the condenser through a one-way valve. Any non-condensable gas in the sorber bed also flowed to the condenser. In the storage process, the sorber bed was isolated from the evaporator and condenser. To study the effect of storage duration on the performance, the sorp-TES was discharged in cyclic mode (no storage time) and after various storage durations. In cyclic operation (considered as baseline test), periodically a quick degassing (few seconds) was done between the half-cycles, to maintain a constant condenser pressure. For other storage durations, the degassing was not performed to study the effect of the presence of residual gases on the storage performance. For seasonal application, the system was turned off and reached the ambient temperature, which took 1-2 days for this system. In the discharging process, the valve between the evaporator and the sorber bed was opened and water vapour went to the sorber bed, at lower pressure than the evaporator. For cold storage, the cooling energy

provided by evaporator and for hot storage the heat (adsorption and sensible) produced in sorber bed were used.

Discussion and Results

Figure 29b shows the ESD and discharge power of the SG-CC and SG-CC-G sorber beds, for cold and hot storage. As shown in Figure 29b, ESD of cold storage of SG-CC bed is higher than SG-CC-G bed (0.57 compared to 0.39 $MJ \cdot kg^{-1}$), due to the more active sorbent and more evaporation in the evaporator. ESD of hot storage for SG-CC-G (thermal conductivity of 0.231± 0.006 $W \cdot m^{-1} \cdot K^{-1}$) and SG-CC (thermal conductivity of 0.098±0.002 $W \cdot m^{-1} \cdot K^{-1}$) are almost the same (1.04 $MJ \cdot kg^{-1}$). Similar to the cold storage ESD, the discharge power for cold storage is also higher for the SG-CC bed compared to SG-CC-G one, although the discharge power for hot storage is higher for the bed with graphite flake (720 W) compared to the bed without graphite flake (635 W), because of high thermal diffusivity of graphite flake, which speed up the discharging process and make it more suitable for fast-heat delivery applications. Figure 29c shows the effect of storage duration on the cold and hot storage ESD. Cold ESD slightly decreases from the cyclic mode to a few minutes of storage and seasonal application. Sorp-TES systems are known for having no cold energy loss [5] and this drop in the cold ESD is due to the pressure build-up inside the condenser, as a result of released non-condensable gases by the corrosion reactions in the salt composite sorber bed. This residual gases add to the mass transfer resistance inside the sorber bed and, other than using corrosion-resistant materials and corrosion-protection layer, as stated in ref. [6], occasional degassing is necessary for long-term use of a closed sorption system, due to the residual gas and leakage. As shown in Figure 29c, the pressure difference between the sorber bed and the condenser is decreased during the time, falling by 38 Pa from the cyclic mode to seasonal mode, which causes a 25% decrease in the cold ESD. A significant decrease is observed in hot ESD from the cyclic operation mode (1.03 $MJ \cdot kg^{-1}$) to seasonal application (0.43 $MJ \cdot kg^{-1}$), due to the (non-condensable gas) pressure increase in condenser and sensible heat loss in the sorber bed. The latter highlighted that, for hot storage, the sorp-TES systems are suitable for short-term storage rather than seasonal applications, where a part of the input sensible heat can be discharged as well.

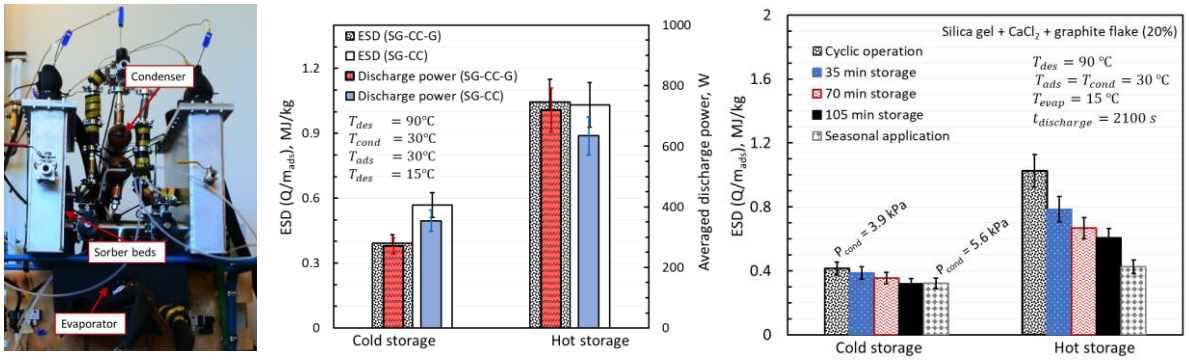

(a) (b) (c)

Figure 29. (a) Front-view of the sorption thermal energy storage prototype, (b) effect of high-conductive additives on ESD and discharge power and (c) effects of storage duration and residual gas on ESD.

References:

[1] L. F. Cabeza, *Advances in Thermal Energy Storage Systems : Methods and Applications*. Woodhead Publishing, 2014.

[2] H. Schreiber, F. Lanzerath, C. Reinert, C. Grüntgens, and A. Bardow, "Heat lost or stored : Experimental analysis of adsorption thermal energy storage," *Appl. Therm. Eng.*, vol. 106, pp. 981–991, 2016.

[3] Y. I. Aristov, "Current progress in adsorption technologies for low-energy buildings," *Futur. Cities Environ.*, vol. 1, no. 1, p. 10, 2015.

[4] I. Glaznev, D. Ovoshchnikov, and Y. I. Aristov, "Effect of residual gas on water adsorption dynamics under typical conditions of an adsorption chiller," *Heat Transf. Eng.*, vol. 31, no. 11, pp. 924–930, 2010.

[5] X.-R. Zhang and I. Dincer, *Energy Solutions to Combat Global Warming*. 2017.

[6] A. Sapienza, A. Frazzica, A. Freni, and Y. Aristov, "Dramatic effect of residual gas on dynamics of isobaric adsorption stage of an adsorptive chiller," *Appl. Therm. Eng.*, vol. 96, pp. 385–390, 2016.

Experimental investigation of a novel absorption heat pump with organic working pairs

P. Chatzitakis[1*], B. Dawoud[2], J. Safarov[3] and F. Opferkuch[1]

[1]Technische Hochschule Nuernberg Georg Simon Ohm, Nuremberg Campus of Technology,
Fuerther Str. 246b, 90429 Nuernberg, Germany
[2]Ostbayerische Technische Hochschule Regensburg, Laboratory of Sorption Processes,
Faculty of Mechanical Engineering, Galgenberg Str. 30, 93053 Regensburg, Germany
[3]University of Rostock, Institute of Technical Thermodynamics,
Albert-Einstein-Str. 2, 18059, Rostock, Germany
*Corresponding author: paris.chatzitakis@th-nuernberg.de

Abstract

As part of a systematic approach towards the search for alternative absorption heat pump (AHP) working pairs that could potentially provide comparable performance to conventional ones, a previous work performed a detailed theoretical cycle analysis and simulation that revealed concrete correlations between key working fluid thermophysical properties and AHP performance indicators [1]. Following this work, targeted combinations of two organic refrigerants, 2,2,2-trifluoroethanol (TFE) and 2,2,3,3,3-pentafluoropropanol (5FP) and two organic absorbents, 1,3-dimethyl-2-2imidazolidinone (DMI) and 2-pyrrolidone (PYR) were tested in a prototype 5 kW AHP, based on the highly compact plate heat exchanger design, which has been introduced in [2]. The purpose of this effort was to validate the findings of the previous work, through correlations based on experimental measurements and at the same time to test the performance of the new AHP system design. The working pair combinations were also subjected to vapor liquid equilibrium (VLE) measurements, in order to determine solution activity coefficients and to regress the parameters for NRTL-VLE models and improve the accuracy of the simulation models. The experimental performance results agree well with the simulations and show to be consistent with the conclusions derived from the previous theoretical work.

Keywords: absorption heat pump, coefficient of performance, organic working pairs, specific solution circulation

Introduction/Background

Alternative absorption heat pump working pairs have already been extensively reviewed by many researchers with main focus on absorbent replacements, water in the case of ammonia, and LiBr in the case of water. They have worked on pinpointing the fundamental working pair criteria that influence thermodynamic efficiency in order to facilitate the identification of alternative working pairs. A smaller part of the studies concerns refrigerant replacement with organic substances like alcohols, amines and hydrocarbons. Nevertheless, despite all efforts there is still no recognized alternative working pair with the potential to exceed the impact of the two conventional pairs [3].
The lack of success of these partially qualitative screening processes signified the need for an alternative quantitative approach. Our previous work focused towards improving the quantitative understanding of the multitude of parameters that influence the performance of absorption heat pumps/chillers by developing correlations between the coefficient of performance (COP) and the specific solution circulation (SSC), and readily available basic substance properties, like molecular mass and critical point properties. The current work aims to validate those findings with experimental property and heat pump performance measurements amongst 4 candidate working pairs, as an initial comparison. More specifically, two refrigerants, TFE and 5FP, and two absorbents, DMI and PYR, each with similar chemical structure but significant differences in key properties, like molecular weight, vaporization enthalpy and vapor pressure.

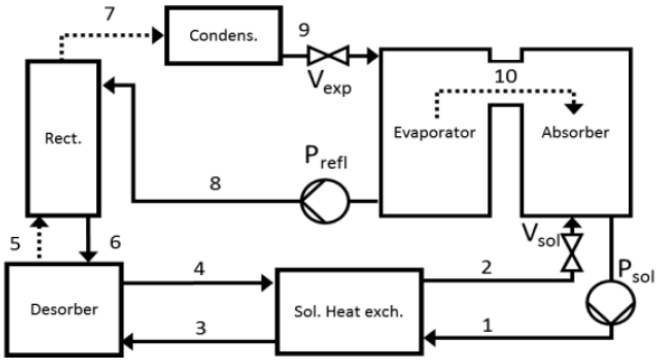

Fig. 1: Absorption heat pump cycle diagram

Results and Discussion

The working pair VLE vapor pressures were measured using two high precision static method apparatuses at the University of Rostock [4]. The activity coefficients were regressed and modelled using the NRTL method and they were used within the simulation models developed in the previous work. The actual system performance was determined following the VDI 4650-2 standard [5] on an AHP-prototype having a rated heated power of 5kW. Fig. 1 illustrates the schematic of the AHP prototype. Some of the obtained results are presented in Fig. 2.

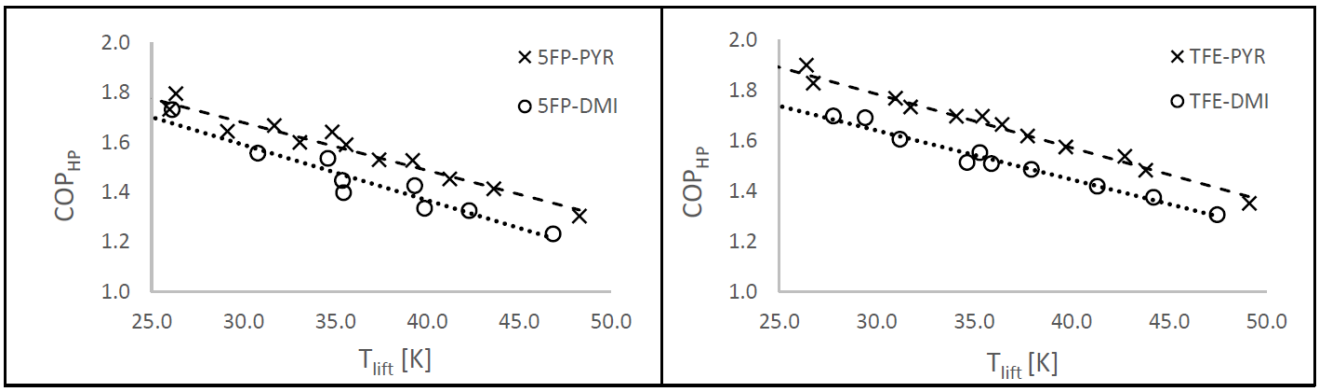

Fig. 2: COP comparisons of the 4 fluid combinations

Summary/Conclusions

The experimental AHP performance measurements seem to agree well with the new simulations. Even though PYR exhibits higher activity coefficients with the two refrigerants as DMI, the combination of lower molecular weight and relative volatility overcompensates and results in higher COPs and lower SSCs. In general the results provide a good validity to the conclusions of the previous theoretical work.

References:

[1] Chatzitakis, P., Dawoud, B., "An alternative approach towards absorption heat pump working pair screening", Renewable Energy, 2017 doi.org/10.1016/j.renene.2016.08.014.
[2] Ishikawa, M., Kayanuma, H., Isshiki, N., "Absorption heat pump using new organic working fluids", Proceedings of the International Sorption Heat Pump Conference, 1999.
[3] Herold, K.E., Radermacher, R., Klein, S.A., *Absorption Chillers and Heat Pumps*, 2nd Ed., CRC Press, 2016.
[4] Safarov, J., Kul, I., Talibov, M.A., Shahverdiyev, A., Hassel, E. Vapor pressures and activity coefficients of methanol in binary mixtures with 1-Hexyl-3-methylimidazolium bis(trifluoromethylsulfonyl)imide, Journal of Chemical and Engineering Data 2015, 60 (6), 1648–1663.
[5] VDI 4650 Blatt 2, Beuth Verlag GmbH, 10772, Berlin, Januar 2013, Kurzverfahren zur Berechnung der Jahresnutzungsgrads von Sorptionswärmepumpenanlagen; Gas-Wärmepumpen zur Raumheizung und Warmwasserbereitung.

Silica Gel microfibres by electrospinning for adsorption heat pumps.

A. Freni[1], L. Calabrese[2], A. Malara[3], P. Frontera[3] and L. Bonaccorsi[3*]

[1]Affiliation and full institutional address (10-pt. Times New Roman)

[2]Dipartimento di Ingegneria, Università di Messina, C.da Di Dio, I-98166 Messina

[3]DICEAM, Università Mediterranea, Loc. Feo di Vito, I-89060 Reggio Cal.

[*]Corresponding author: lucio.bonaccorsi@unirc.it

Abstract

Silica gel is one of the most used porous material in commercial water adsorption heat pumps and chillers for the inexpensive cost and large market availability. In most applications silica gel is used as granules, with limitation in heat transfer and material hydrothermal stability. A new hybrid material is presented obtained by the electrospinning of silica gel/polymeric microfibres. The microfibres mat shows high surface area, high permeability and improved thermal stability. Measurements of the water adsorption properties show that the original porosity of the material is largely preserved.

Keywords: Water adsorption, Silica gel, Heat pumps, Microfibres.

Introduction/Background

Silica gel is one of the most used porous material in adsorption heat pumps and chillers for its low cost and large availability on the market [1,2]. Competing as adsorbent with more performing materials like zeolites, silica gel is particularly appropriate in all adsorption applications where a low regeneration temperature is available. Compared to crystalline zeolites, silica gel has an amorphous structure and lower hydrothermal stability, lower adsorption enthalpy, lower maximum water capacity. However, the possibility to use silica gel in large quantities at reduced costs in adsorption heat pumps and chillers compensates for the worst performances and make this material the preferred choice in commercial equipment. Silica gel is available in a wide variety of granules and powders and generally directly used as filler in the free space among the fins of a heat exchanger. This simple configuration, however, shows important limitations and while for zeolite adsorbers several improved solutions have been proposed during the years, for example by synthesizing the material directly on the heat exchanger surfaces or by the realization of advanced zeolite coatings [3], a similar development for silica gel applications has not been carried out. In this study, we propose an innovative material for adsorption applications made of hybrid microfibers of silica gel obtained by the electrospinning technique. The prepared electrospun fibres have been characterized by TGA/DSC, SEM-EDX and measurements of water adsorption properties in a vacuum microbalance.

Discussion and Results

Silica gel powders are added to a polymeric solution of polyacrylonitrile (PAN) and dimethylformamide (DMF) and then electrospun. Each prepared solution was loaded in 5 cc syringe fitted with 1 mm steel needle, the flow rate was 0.5 mL/h and the applied voltage 15kV. The amount of powder with respect to the polymer solution was optimized to 25-30% w/w to obtain an optimal spinnability. The electrospinning process generated a mat which looks like a compact multilayer where silica gel particles are embedded in a polymeric net of microfibres that keep the whole granules interconnected (Figure 1).

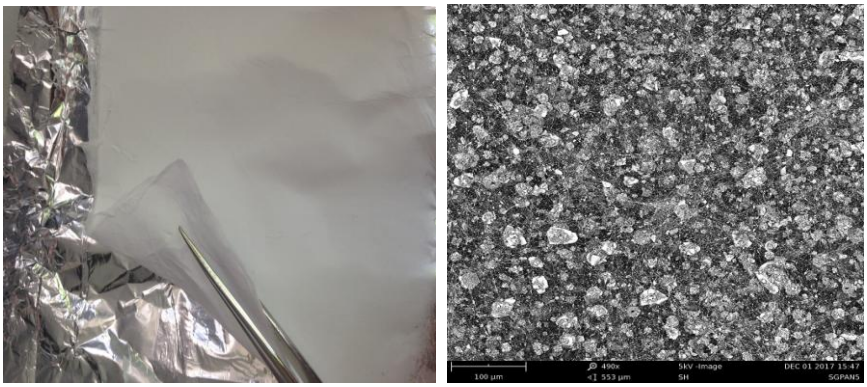

Figure 1. Macroscopic and SEM images of a silica gel mat.

In Figure 2 is shown a comparison between TGA curves of pure silica gel powder and silica gel microfibres where is evident that the mass loss of the electrospun fibres is due to water desorption, showing that the polymeric phase does not occlude the silica porosity.

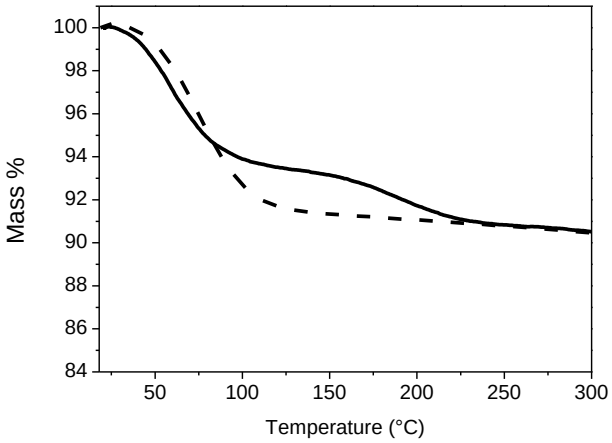

Figure 2. TGA of silica gel powder (dashed line) and silica gel microfibres (solid line).

Summary/Conclusions

The electrospinning process had no negative effects on the adsorbent material capability of water adsorption/desorption. Having structured the silica gel powder in a microfibres mat showed significant advantages such as blocking the loose particles in a multilayer with high surface area per weight and mechanical resistance, improved thermal stability and usability. The electrospinning process is versatile and easily scalable.

References:

[1] Demir, H., Mobedi, M., Ülkü, S., "A review on adsorption heat pump: Problems and solutions", Renewable and Sustainable Energy Reviews, 2008, 12, 2381, doi:10.1016/j.rser.2007.06.005

[2] Meunier, F., "Adsorption heat powered heat pumps", Applied Thermal Engineering, 2013, 61, 830, doi: 10.1016/j.applthermaleng.2013.04.050

[3] Freni, A., Dawoud, B., Bonaccorsi, L., Chmielewski, S., Frazzica, A., Calabrese L., Restuccia, G., *Characterization of Zeolite-Based Coatings for Adsorption Heat Pumps,* SpringerBriefs in Applied Sciences and Technology, Springer 2015,

Air-channel composite desiccant for northern climate humidity recovery ventilation system

E. Cerrah[1], C. McCague[1], M. Bahrami[1*]

[1]Laboratory for Alternative Energy Conversion, School of Mechatronic Systems Engineering, Simon Fraser University, Surrey, British Columbia, Canada

[*]Corresponding author: mbahrami@sfu.ca

Abstract

A $CaCl_2$ sorbent in mesoporous silica gel consolidated with poly (vinyl alcohol) binder was prepared and tested for dehumidification (exhale mode) and air humidification (inhale mode) for building ventilation in northern climates. The performance was evaluated in terms of degree of de/humidification, and pressure drop. Degree of humidification, which is one of the key features of the system, is about 0.8 out of 1 in cyclic adsorption desorption tests with the pressure drop of 50 Pa for 14.4 m^3/h air flow. The performance is comparable with the values presented in literature for a similar system with about 3 times higher weight [1,2].

Keywords: Desiccant, heat and mass transfer, ventilation, humidity swing adsorption

Introduction

At low ambient temperatures, e.g.-15 to -30°C, the moisture content in the air is low, 1-2 g/kg. Therefore, the fresh air drawn into buildings must be heated and humidified. Aristov et al. [1] presented a cyclic adsorption/desorption and heat storage system driven by the humidity ratio difference between indoor and outdoor air with 70-90% moisture recovery and 60-96% heat recovery. The system is comprised of a sorbent bed that stores and recovers humidity and a heat storage bed to store both adsorption heat and the sensible heat from the temperature difference between the indoor and outdoor conditions. The only cost of the system is the fan power.

In order to choose a suitable sorbent material for this application, an experimental study was performed for silica gel, Al_2O_3 and $Al_2O_3/CaCl_2$ with different pellet sizes [2]. The degree of humidification, (β), is calculated by the ratio of water released from the sorbent to the total amount of water leaving the system during the inhale period. β ranged between 0.79 to 0.98, depending on the sorbent type and air flow rate [2]. The highest β was achieved with small pellet $Al_2O_3/CaCl_2$, e.g. β =0.96 for an air flow of 14.6 m^3/h, however this had the highest pressure drop, ~90 Pa. The efficiency of the moisture recovery bed can be improved by reducing the pressure drop and increasing the water uptake.

In order to improve the efficiency of this system we are proposing a novel consolidated silica gel-$CaCl_2$ composite design. The adsorption performance is improved by the high uptake properties of the silica gel-CaCl2 and the pressure drop is reduced by designing the composite to include air channels. A similar composite with air channels was previously tested by Chen et al. [3] in a desiccant – air conditioning system.

Discussion and Results

A test bed, shown in Fig. 1a, was loaded with seven consolidated sorbent pieces, ~1 kg in total. Each piece was prepared with small size (0.25-0.5 mm) silica gel pellets, 27% $CaCl_2$ bound by PVA and had 5 mm diameter air channels formed by glass rods. Room air (22-27°C, 40-45%RH) passed through the bed during sorption and the following desorption process was performed by flowing dry air (23-25°C, 4-6%RH) with 14.4 m^3/h flow rate from the other end of the test-bed. Sorption and desorption processes were performed with 5-minute half cycles until cycle-to-cycle performance was consistent, typically after six cycles.

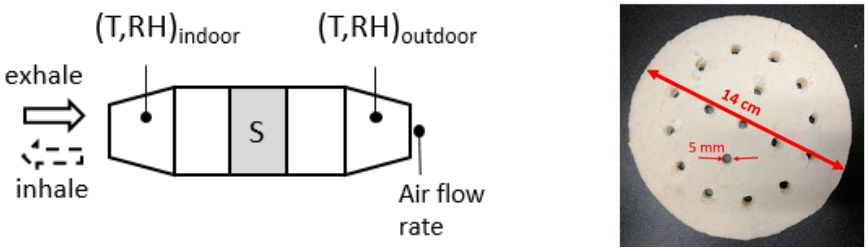

(a) (b)

Fig. 1 (a) Sorbents placed in a testbed where dry air is passed during exhale and room air is drawn in inhale period, (b) consolidated sorbent piece with 17 air channels

The humidity ratio at the indoor and outdoor ends of the test bed, was calculated from the temperature and RH measurements and is shown in Fig. 2. With the air flow rate set to 14.4 m^3/h for both the inhale and exhale periods, $\Delta\omega$ between indoor and outdoor is in the range of 3-6 g/kg. The sorbent ad/desorbed about 8 g of water in 5 minutes. β was about 0.8, which is comparable to reported sorbent performance from previous studies [1,2], which were in the range of 0.87-0.96 for a similar air flow rate. Humidification degree was 0.96 with about 90 Pa pressure drop for ~3 kg of $CaCl_2$ Alumina sorbent (IK-011-1) at similar flow rate [2]. It indicates about 6 g of water uptake per 10 min half cycle. It can be concluded that composite silica gel-$CaCl_2$ sorbent with air channels could be a good candidate for humidity recovery ventilation systems as it has high water uptake capacity (8 g in about 5 minutes) and lower pressure drop ~50 Pa. Further tests should be performed for different flow rates. β

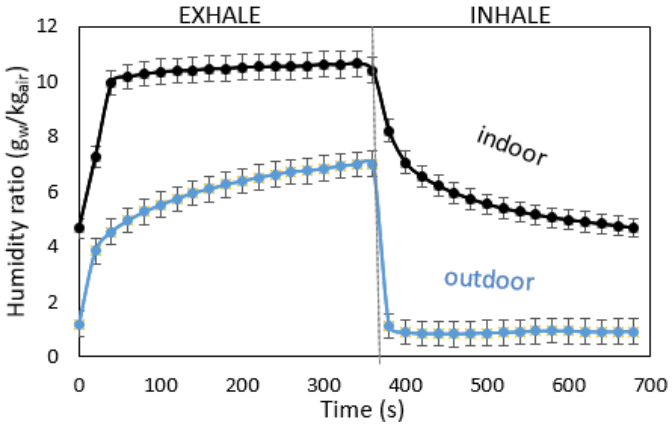

Fig. 2 Humidity ratio at the indoor and outdoor ends of the testbed during exhale and inhale

Summary/Conclusions

A composite silica gel-$CaCl_2$ sorbent with air channels has been prepared and tested for a humidity recovery ventilation system. A humidification degree of 0.8 was achieved for 14.4 m^3/h air flow rate, which is a similar performance and higher water uptake compared with other sorbents presented in literature for this application [2]. Further experiments will be done to evaluate the performance for different flow rates.

References:

[1] Aristov, Y. I., Mezentsev I. V., Mukhin V. A., "A new approach to regenerating heat and moisture in ventilation systems." Energy and Buildings, 2008.

[2] Aristov, Y. I., Mezentsev I. V., Mukhin V. A., "Investigation of the moisture exchange in a stationary adsorbent layer through which air is passed." Journal of Engineering Physics and Thermophysics, 2005.

[3] Chen, C. H., Hsu, C. Y., Chen, C. C., Chen, S. L., “Silica gel polymer composite desiccants for air conditioning systems.” Energy and Buildings.

Influence of the fluid dynamics on an air-cooled fixed-bed adsorber with connected water evaporator

M. Jäger[1*], K. Hurtig[2], R. Kühn[1] and J. Römer[2]

[1]Dipl.-Ing., [2]M.-Sc., Researcher at Department of Mechanical and Systems Engineering, TU Berlin, Marchstr. 18, 10587 Berlin, Germany

[*]Corresponding author: mike.jaeger@tu-berlin.de

Abstract

In this publication two different levels of detail for a simulation model for fixed-bed adsorbers connected to an evaporator are introduced. Both approaches are compared to each other on basis of various design parameters. The considered adsorber is a cuboid chamber filled with spheres of silica gel to be used with water as refrigerant that is provided by an evaporator. The coupling of adsorber and evaporator induces increased computing time.

The first approach with the highest level of detail includes the thermal and fluidic bed dynamics by characterising every transport process: the heat transfer within the bed, the mass transfer inside the adsorbent, the mass transfer in the gaps of the fixed-bed and the momentum transfer of the adsorptive. The second approach does not include the fluid dynamics of the adsorptive in the gaps of the fixed-bed. The two approaches are compared concerning specific cooling power (SCP) and efficiency (COP). The mass and momentum transfer equations of the adsorptive influences the results most at the beginning of the adsorption process and its influence decreases with proceeded adsorption time. However, neglecting the fluid dynamics will lead to a noticeable offset on the specific cooling power.

Keywords: adsorber fluid dynamics, dynamic simulation, adsorption, air-cooled adsorber

Introduction/Background

Until 2030 the world-wide demand of energy will increase by 60% [1]. Adsorption cooling could be a promising alternative to conventional cooling methods by using waste heat, i.e. from district heating grids in summer [1]. According to cost-efficiency it is appropriate to use air-cooled fixed-bed adsorbers, thus expenses for an additional cooler and piping are saved. To achieve high energy efficiency, it is beneficial to describe the processes in an adsorber mathematically to improve geometry or operating parameters.

In this publication two different levels of detail for a simulation model are examined. The high level of detail includes the fluid dynamics of the adsorptive, water vapor, whereas the other approach is neglecting it. The objective is to find out in which cases it is appropriate to skip considering the mass and momentum transfer of the adsorptive in a fixed-bed adsorber. To save calculation time, which is the crucial factor for wide range optimization, it is essential to make simplifications and to evaluate their influence on the result.

There are some publications considering fluid dynamics in an adsorber itself, but without coupling it to an evaporator [2] [3]. In this simulation model the evaporator is connected to the adsorber mathematically by the boundary condition that the water evaporating in the evaporator must be adsorbed by the adsorber instantly. Due to this assumption the differential equations for the fluid dynamics of the adsorptive cannot be solved directly and therefore iteration is necessary. This coupling is crucial to simulate the evaporator as a transient operating component, which is rarely found in literature, and is the basis for simulating the complete adsorption/desorption cycle later on coupled with condenser, desorber and throttle.

Figure 1 shows the symmetric physical model of the cuboid fixed-bed adsorber. The working pair is spheres of silica gel as adsorbent and water as refrigerant and adsorptive.

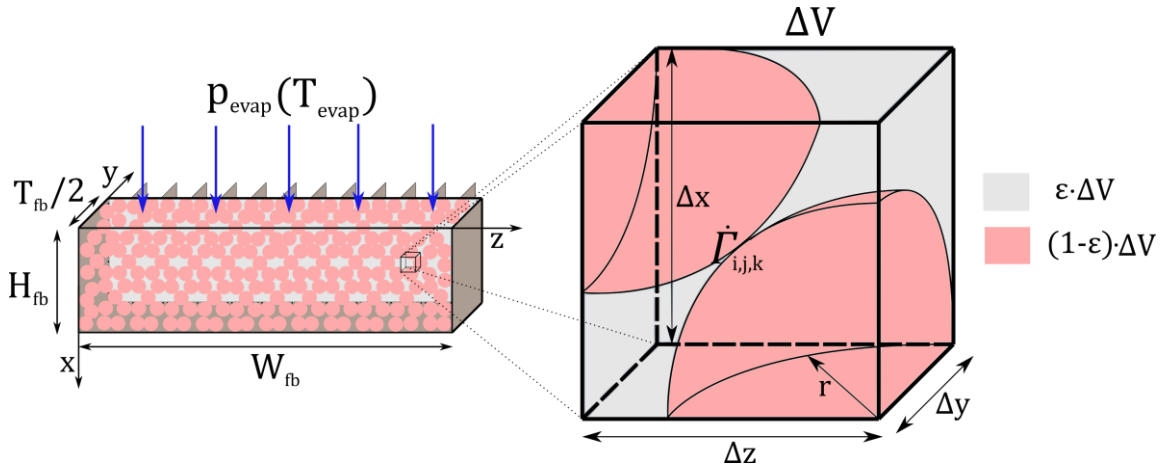

Fig. 30*: Sectional view of the fixed-bed adsorber and subdivision in discrete volumes ΔV*

The height, width and thickness of the adsorber are the parameters H_{fb}, W_{fb} and T_{fb}. At the inlet on top of the chamber the adsorptive has the inlet pressure p_{evap}, resulting from the assumed boiling temperature T_{evap} in the evaporator. There is a significant pressure drop caused by adsorption and friction in flow direction (x-axis). To solve the governing mass, energy and momentum equations by the method of finite differences the model is subdivided in discrete volumes ΔV in which a specific adsorption mass flow $\dot{\Gamma}_{i,j,k}$ is generated. Thereby produced heat conducts through the fixed-bed to the wall equipped with fins $W_y = (x = [0, H_{fb}], y = T_{fb}/2, z = [0, W_{fb}])$, where it is transferred to the ambient air.

Discussion and Results

It is shown that the fluid dynamics of the adsorptive in the fixed-bed influences the results significantly especially at the beginning of the adsorption process. By neglecting the mass and momentum transfer equations the, otherwise very long calculation time, can be reduced drastically. The deviation of specific cooling power and efficiency between both levels of detail is decreasing with increasing adsorption time and decreasing flow length of the adsorptive.

Summary/Conclusions

Air-cooled fixed-bed adsorbers as considered in this publication have to be operated with comparatively long adsorption cycle times in order to reach acceptable efficiency. The results show that fluid dynamics must not be neglected to identify geometry and operating parameters for an efficient fixed-bed adsorber.

References

[1] Rouhani, M., Sharafian, A., Cheppudira, P., Mehr, S. M. N., Dhillon, A., Huttema, W., Bahrami, M., *Performance enhancement of an adsorption cooling system with AQSOA FAM-Z02 and low-finned tube evaporator*, IMPRES Conference, Sicily, 2016.

[2] Kwapinski, W., Salem, K., Mewes, D., Tsotsas, E., *Thermal and flow effects during adsorption in conventional, diluted and annular packed beds*, Chem. Eng. Sc. 65, pp. 4250-4260, 2010.

[3] Otten, W., Kast, W., *Der Durchbruch in Adsorptions-Festbetten: Methoden der Berechnung und Einfluß der Verfahrensparameter*, Chem. Ing. Tech. 59, pp. 1-12, 1987.

Experimental proof of concept for a water/LiBr single stage absorption heat conversion system as a house connection station

S. Hunt1*, S. Petersen1, F. Ziegler1and C. Hennrich1

[1]Technische Universität Berlin, Institute of Energy Engineering, KT2, Marchstr. 18, 10587 Berlin, Germany

[*]Corresponding author: sarah.hunt@tu-berlin.de

Abstract

An installation of a single stage LiBr/Water absorption chiller was modified to enable heating mode operation to replace the house connection station with the aim to lower the district heating return temperature and thus increase local grid capacity. The concept is explained and preliminary operation results are presented.

Keywords: Absorption heat converter, house connection station, district heat return temperature

Introduction/Background

At Technische Universität Berlin, a new generation of single stage LiBr/water absorption chillers with a nominal cooling capacity of 50 kW (Bee) and 160 kW (Bumble Bee) has been developed. In 16 installations 25 absorption chillers are currently monitored within an extensive field test (Feldtest Absorptionskälte für Kraft-Wärme-Kälte-Kopplung-Systeme, FAkS, funded by BMWi as project FKZ 03ET1171a-d).

One of the systems, can be operated in heating mode as well as in cooling mode. Unlike in conventional heat pumps, the heat input into the evaporator of the heat conversion system is not drawn from the environment, but is derived from the district heating return line. The reject heat from the absorber and condenser of absorption heat pump is transferred to the building as useful heat This enables an increase in temperature glide and the temperature in the district heating return line is decreased below the building return temperature, therefore reducing the district heat volume flow rate needed at the site. This in turn enables for a larger heating capacity to be installed in the grid in the area. Lower return temperatures at the power plant are also expected to increase the electrical capacity of the CHP plant. The reject heat An additional heat exchanger (HE) between the district heating supply after the desorber and the heating circuit water at the exit of the absorber and condenser of the heat converter can be used to reach higher temperatures for the building supply temperature and to further reduce the temperature of the district heating supply line.

The system discussed, has been operated in cooling mode several years. In September of 2017 the adaptations of the system to enable operation in heat converter mode were first completed.

Discussion and Results

Figure 1 shows the flow chart of the installation. Assuming a coefficient of performance (COP_{AC}, heat flow rate of evaporator to heat flow rate of desorber) of 70% and a heat exchanger effectiveness ε of 93%. Table 1 shows the expected temperatures and local grid capacity increase.

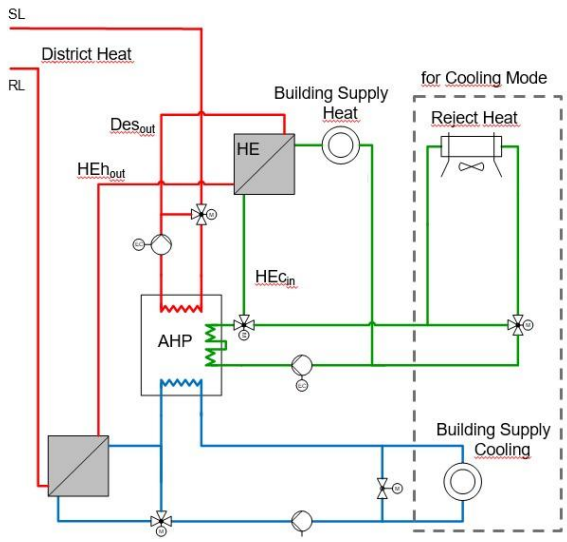

Figure 1: Flow chart of installation

Table 1: Temperatures and grid capacity increase for different load conditions
COP_{AC}=0.7, ε=0.93

Load		**20%**	**50%**	**100%**
Building Supply Heat Supply Line (BSH-SL)	[°C]	50	55	65
Building Supply Heat Return Line (BSH-RL)	[°C]	40	42	45
District Heat Supply Line (DH_SL)	[°C]	85	110	135
House Connection Station (HCS)				
District Heat Return Line (DH-RL)	[°C]	43	47	51
Absorption Heat Pump (AHP)				
Desorber Outlet (Des_out)	[°C]	60	65	75
District Heat Return Line (DH-RL)	[°C]	42.5	33.5	33
Absorption Heat Pump (AHP) + Heat Exchanger HE				
Desorber Outlet (Des_out)	[°C]	60	65	75
Heat Exchanger Hot Stream Outlet (HEh_out)	[°C]	48.8	54.2	63.9
District Heat Return Line (DH-RL)	[°C]	31.3	22.7	21.9
Heat Exchanger Cold Stream Inlet (HEc_in)	[°C]	47.9	53.4	63.0
Increase of local grid capacity				
AHP	[%]	1%	21%	21%
AHP+HE	[%]	28%	39%	35%

Results for one week in November 2017 from initial operation of the AHP and HE1 are shown in Figure 2.

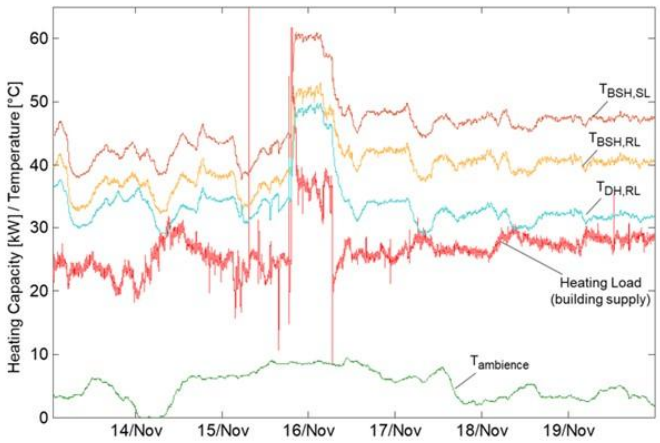

Figure 2: Experimental results

Even though the heat exchanger between the district heat and the external evaporator circuit was operated in parallel flow instead of the intended counter flow, Figure 2 shows a district heating return temperature ($T_{DH,RL}$) which was up to 12 K below the building return temperature ($T_{BSH,RL}$). This demonstrates the ability of the system to reach its intended goal. The temperature predicted for this case in Table 1 was already reached - the change of the installation of the heat exchanger to counter current operation and operation including heat exchanger HE should allow for even lower district heating return temperatures. Results of entire heating season 2017/2018 will be presented.

Summary/Conclusions

The installation showed that it possible to operate an absorption chiller in absorption heating mode, enabling a district heating return temperature below the building return temperature while increasing local grid capacity.

Temperature- vs. Pressure-Initiated Cycles for Upgrading Low Temperature Heat: Dynamic Comparison

I. Girnik[1,2*] and Yu. Aristov[1,2]

[1]Boreskov Institute of Catalysis, Lavrentiev ave., 5, Novosibirsk, 630090, Russia
[2]Novosibirsk State University, Pirogova str., 2, Novosibirsk, 630090, Russia
*Corresponding author: girnik@catalysis.ru

Abstract

This work is addressed to the study of methanol ad-/desorption dynamics under various conditions of a novel "Heat from Cold" cycle, and, first of all, to a comparison of the cycles driven by pressure drop and temperature jump between the same cycle isosters.

Keywords: Adsorptive heat transformation, activated carbon, methanol, driving force.

Introduction/Background

Adsorption heat transformation (AHT) is attracting increasing attention because of its ability of effective conversion/storage of waste and renewable heat. Recently, a novel AHT cycle "Heat from Cold" (or HeCol) has been suggested for amplification of the temperature poten-tial of the ambient heat in cold countries [1]. The common 3T HeCol cycle (1-2-3-4) consists of two isosters (1-2), (3-4) and two isotherms (2-3), (4-1) (Fig. 1) and operates between three thermostats at low T_L, middle T_M, and high T_H temperatures. An adsorbent is regenerated at constant temperature T_M by the adsorptive pressure drop from P_4 to P_1 (isotherm 4-1). This cycle differs from a classical 3T heat amplification cycle (1-2*-3-4*) in which the adsorbate is exchanged between the same isosters, however, along isobars (4*-1) and (2*-3). In particu-lar, the adsorbent is regenerated due to the temperature jump from T_{4*} and T_M at constant pressure P_L (Fig. 1). In this work, a dynamic comparison of the isothermal and isobaric re-generation is performed.

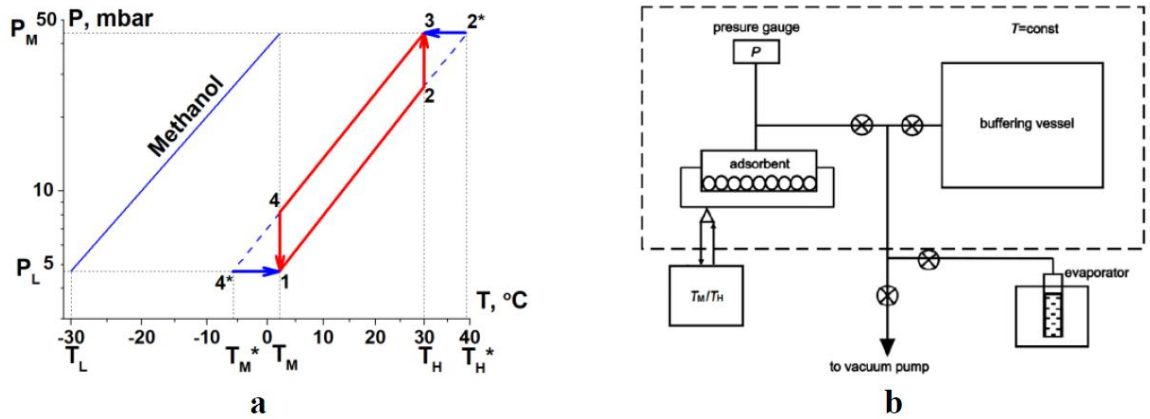

Fig. 1. a - P-T diagram of the studied 3T HeCol cycle with isothermal (4-1 and 2-3) and iso-baric (4*-1 and 2*-3) stages; b – schematics of the kinetic set-up.

Discussion and Results

The "activated carbon ACM-35.4 - methanol" working pair was investigated. The three temperatures which define the cycle for this pair were fixed at T_L = -30oC, T_M = 2oC, and T_H = 30oC (Fig. 1) that are typical for "HeCol" cycles [1]. The specific mass Δq of methanol exchanged in this cycle was 0.08 g/(g-carbon). The boundary conditions for the regeneration stages were as follows: (4-1) - T_M = 2oC, P_4 = 8.2 mbar and P_L = 4.7 mbar; (4*-1) - P_L = 4.7 mbar, T_M* = -6^{o}C and T_M = 2^{o}C. The dynamics was measured for a monolayer of carbon grains of 2.2-2.5 mm size in a custom-built kinetic setup described elsewhere [2].

All the obtained release curves can be well approximated by the exponential function Δq = (0.08 g/g) (1-$e^{-t/\tau}$) with a single characteristic time τ (Fig. 2a) equal to 104 ± 6 s. This time allows upper limits of the specific rate of methanol desorption 0.7·g/(kg s) and the specific power supply W = 0.9 kW/kg to be estimated. The power is used to evaluate the heat transfer coefficient between the carbon grain and the metal support α = 97 ± 10 W/(m2 K).
Another important finding is that the kinetic curves for both isothermal and isobaric desorption are almost identical (Fig. 2a). Hence, the regeneration dynamics is invariant with respect to the regeneration path, either isothermal (4-1) or isobaric (4*-1). The same trend is found for the adsorption dynamics via isobaric (2*-3) and isothermal (2-3) paths. Both uptake curves are exponential with τ = 78 ± 4 s (Fig. 2b) (W = 1.2 kW/kg) that is faster than the desorption run. If assume that τ ~ exp[-E_{act}/(RT)], the apparent activation energy E_{act} is estimated as 7 kJ/mol.

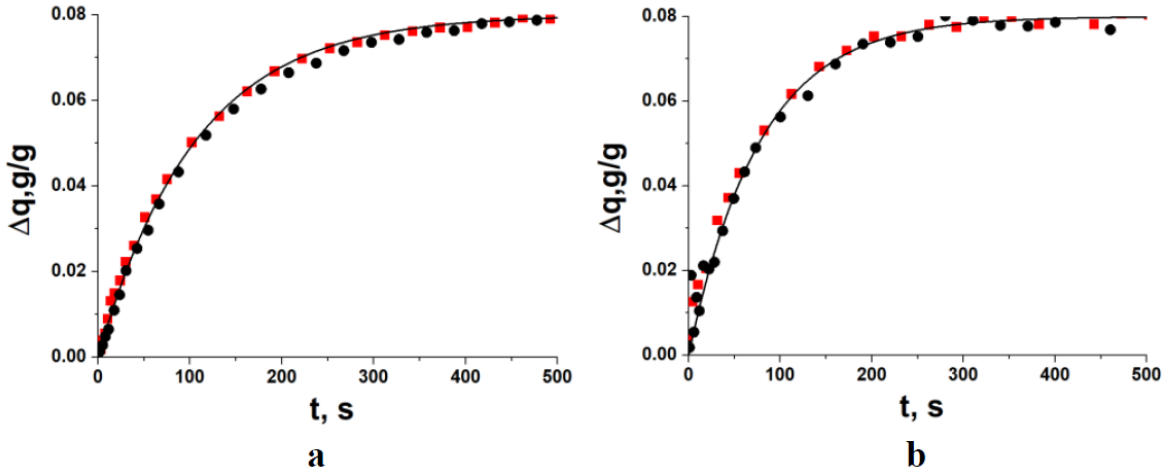

Fig. 2. Methanol release (a) and uptake (b) curves as a function of time: isothermal (●) and isobaric (■) paths. Solid lines – exponential approximation.

The revealed invariance of ad-/desorption dynamics is unexpected because isothermal and isobaric processes are initiated by quite different driving forces, namely, the pressure drop or the temperature jump, respectively. However, heat and mass transfer processes are strongly coupled so that after a short transient period a steady state regime is established in the adsorbent, which seems to be similar, regardless the initial driving force applied.

Summary/Conclusions

The dynamics of methanol ad-/desorption for two heat amplification cycles driven by either pressure drop or temperature jump between the rich and weak cycle isosters is found to be identical. The dynamics can be described by exponential release/uptake curves with the characteristic time 104 and 78 s which corresponds to the specific power 0.9 and 1.2 kW/kg reasonable for practical realization of the HeCol cycle.

References:

[1] Aristov, Yu. I., Adsorptive transformation of ambient heat: a new cycle, Applied Thermal Engineering, 2017. doi:10.1016/j.applthermaleng.2017.06.051
[2] Gordeeva, L., Aristov, Yu., Dynamic study of methanol adsorption on activated carbon ACM-35.4 for enhancing the specific cooling power of adsorptive chillers, 2014. doi:10.1016/j.apenergy.2013.11.073

This work was supported by the Russian Science Foundation (grant 16-19-10259).

Adsorption heat transformation: applicability for various climatic regions of the Russian Federation

A.D. Grekova[1,2*], L.G. Gordeeva[1,2] and Yu.I Aristov[1,2]

[1]Boreskov Institute of Catalysis, Ac. Lavrentiev av. 5, Novosibirsk 630090, Russia
[2]Novosibirsk State University, Pirogova st. 2, Novosibirsk 630090, Russia
[*]Corresponding author: grekova@catalysis.ru

Abstract

In this work, the applicability of the emerging technology of adsorption heat transformation (AHT) in the Russian Federation (RF) was analyzed. We considered various AHT applications (heat storage, heating, cooling, amplification of the temperature potential) for different climatic zones of the RF. Proper AHT applications are selected for each zone. Adsorption equilibrium data for various "adsorbent – adsorbate" working pairs are collected from the literature and analyzed to select the pairs most suitable for the particular application/zone.

Keywords: Adsorption heat transformation, water, methanol, adsorption potential, database.

Introduction/Background

Significant progress has been achieved in AHT over the past decades. This emerging technology can be used for various applications, such as heat storage, cooling, heating, amplification of the temperature potential, and their combinations. The choice of application is dictated first of all by particular climatic zone where the AHT unit is used and the heat sources available. In this work, the climatic conditions of various RF regions (Table 1, Fig. 1) are analyzed and the proper AHT applications are selected for each zone. Specific requirements to an adsorbent optimal for the selected zone and application are considered. Finally, real adsorbents which are the most suitable for the particular application/zone are selected by screening literature data on adsorption properties of numerous classical and innovative materials (silicas, zeolites, MOFs, composites salt/matrix, MeAPOs, etc.). The latter analysis is based on the use of the adsorption potential $\Delta F = RT\ln[P_0(T)/P]$ as a universal measure of both "adsorptive – adsorbent" affinity and cycle boundary conditions.

Table 1. The types of climate in the RF and typical temperatures in winter and summer.

	Type of climate	January, ºC	July, ºC
1	arctic	-24 -30	+2 -5
2	subarctic	-22 -24	+4 +12
3	moderate climate	↓	↓
3A	moderately continental	-4 -20	+12 +24
3B	continental	-15 -25	+15 +26
3C	abruptly continental	-25 -45	+16 +20
3D	monsoon	-15 -30	+10 +20
4	subtropical	+2 +8	+22 +30

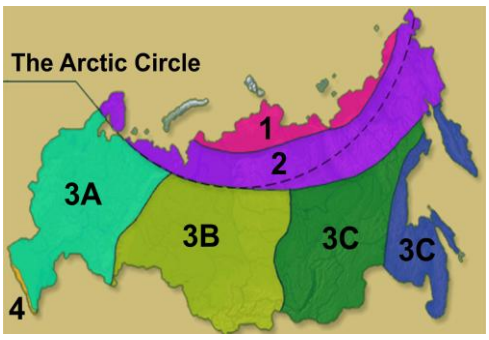

Figure 1. Climatic zones of the RF [1].

Discussion and Results

The climate in the RF is quite cold (Table 1), therefore the most demanded AHT applications are heating, seasonal heat storage [2], and amplification of the temperature potential of heat, including the ambient heat [3]. The first two modes can be realized during winter time only if there is a low

temperature (10-20°C) heat source available to drive evaporation process, e.g. underground water, heat wastes from industry and/or housing, etc.

Another opportunity is to use highly efficient solar collectors that can provide heat at 10-20 °C even at cold climate of zones 1-3. The heating/storage modes are more realistic in zone 3A during autumn and spring. Their realization needs adsorbents which ensure a large temperature lift (at least, 20-30 °C). More studies on adsorptive heat storage are needed, especially on the dynamics of heat rejection [4]. For heat generation during winter time the most practical AHT application for the RF climate is a new "Heat from Cold" cycle recently suggested for upgrading temperature potential of the ambient heat [3].

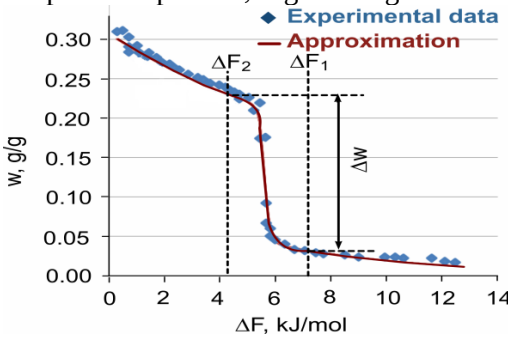

Figure 2. Experimental data and approximation for the working pair AlPO-18 - water.

During summer time there is a certain need for adsorptive air conditioning in the Southern Russia. This is the only possible application of water as adsorptive, whereas methanol and ammonia must be used in winter time. Requirements to adsorbents adapted to various RF climatic zones are formulated and discussed. The working conditions are calculated in terms of the boundary adsorption potential ΔF. We have collected the equilibrium adsorption data for a large number of "adsorbent – adsorptive" working pairs presented in the literature. These data are plotted in the coordinates "sorption w – adsorption potential ΔF" and approximated by analytical equations. For example, the adsorption equilibrium of the pair "AlPO-18 – water" is well fitted by the function (Fig. 2):

$$w = (A\cdot\Delta F+B)/(1+\exp(-k_1\cdot(\Delta F-C_1))) + L/(1+\exp(-k_2\cdot(\Delta F-C_2))) \qquad (1)$$

where A, B, C_1, C_2, L, k_1, k_2 are fitting parameters. That contributes to an equilibrium adsorption database for a wide range of working pairs. It is used to select the suitable pairs for typical AHT cycles, namely cooling, heating and heat storage for several climatic zones of the RF. For example, for seasonal heat storage cycle (T_c = 20ºC, T_e = 10ºC, T_a = 35 ºC and T_r = 85ºC) realizing in the third zone (3A region) the composite LiCl/vermiculite is the most promising.

Summary/Conclusions

The paper considers the possibility of realizing the AHT technology (heating, cooling, heat storage, and temperature amplification) in the climatic conditions of the RF. For each zone the most promising applications are identified. For a wide range of conventional and innovative sorbents (activated carbons, silica gels, alumina, MeAPOs, MOFs, "Salt in porous matrix" composites, etc) the characteristic sorption curves "sorption vs. ΔF" have been plotted and approximated by analytic equations. That contributes to the equilibrium adsorption database, which is used for the selection of suitable working pairs for specific application/climatic zone.

Acknowledgments

The work was supported by the Russian Science Foundation (project № 17-79-10103).

References:

[1] The map http://meteoinfo.ru/climate
[2] A.D. Grekova, L.G. Gordeeva, Yu.I. Aristov, Composite "LiCl/vermiculite" as advanced water sorbent for thermal energy storage, Appl. Therm. Engn., 2017, v. 124, pp. 1401-1408. https://doi.org/10.1016/j.applthermaleng.2017.06.122
[3] Yu.I. Aristov, Adsorptive transformation of ambient heat: a new cycle, Appl. Therm. Engn., 2017, v. 124, pp. 521-524. doi: 10.1016/j. applthermaleng.2017.06. 051.
[4] V. Palomba, A. Sapienza, Yu.I. Aristov, Heat rejection stage of an adsorption heat storage cycle: the useful heat and sorption dynamics, Abstract HPC2018.

Design of a Gas-Fired Carbon-Ammonia Adsorption Heat Pump

A. M. Rivero Pacho*, S. J. Metcalf, R. E. Critoph, H. Ahmed

The University of Warwick, School of Engineering, Library Road, Coventry, CV4 7AL, UK
*Corresponding author: A.Rivero-Pacho@warwick.ac.uk

Abstract

This paper presents the design and manufacturing of a novel carbon-ammonia adsorption generator for application to an air source domestic gas fired heat pump and also shows preliminary testing results of the complete heat pump system. This laminated generator has the characteristic of delivering high heating power at a high efficiency but having an inexpensive manufacturing cost. The machine which is currently under construction has a predicted power output of between 5 and 10 kW at a COP of 1.40 to 1.35 for low temperature radiators for domestic applications.

Keywords: heat pump, carbon, ammonia, domestic heating

Introduction/Background

The University of Warwick is currently developing a carbon-ammonia adsorption cycle gas fired heat pump with a target Gas Utilisation Efficiency (GUE, the ratio of heat output to gas input) of 1.25 using air source, but at a much reduced size and capital cost compared to alternative machines on the market (<4 times).
Previous research focused on the development of micro-tube adsorption generators (Critoph and Metcalf [1]). Whilst these achieved high power density and efficiency, they proved difficult and costly to manufacture. This work describes the design and construction of a carbon-aluminium laminate adsorption generator, which has both low thermal mass and high power density whilst being cost effective to manufacture.

Discussion and Results

Figure 1 shows the carbon-aluminium laminate used in the construction of the adsorption generators. The carbon is a monolithic type as described in Tamainot-Telto [2]. The laminate is made by compression in a die before pyrolysis in a furnace to bind the carbon into a monolithic layer between the aluminium fins.

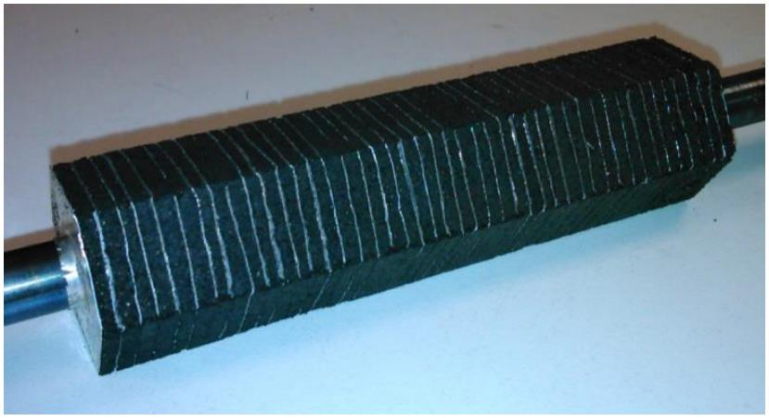

Figure 1: Carbon-aluminium laminate adsorption generator.

The performance of these laminate heat exchangers has been verified by performing a large temperature jump experiment on a 100 mm test section and comparing it to a transient model developed in MATLAB. Figure 2 shows the comparison between the large temperature jump experiment and the model

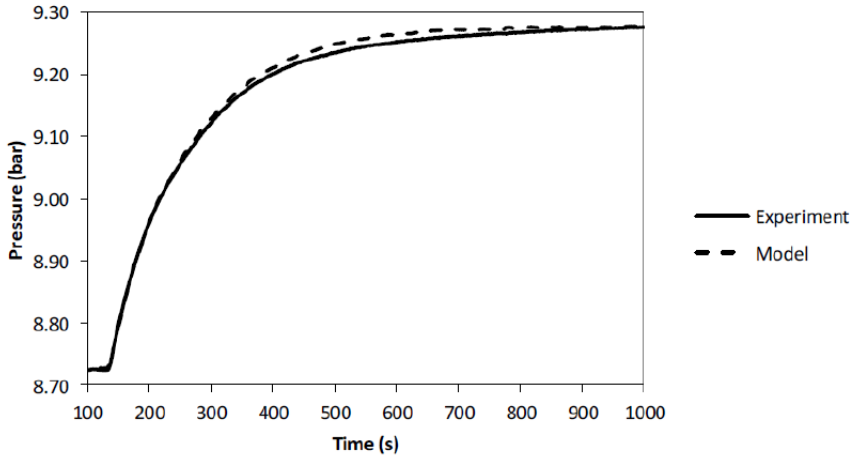

Figure 2: Comparison between large temperature jump experiment and computational model.

Several laminates will be assembled into two sorption generators, each with a volume of approximately 3 litres.

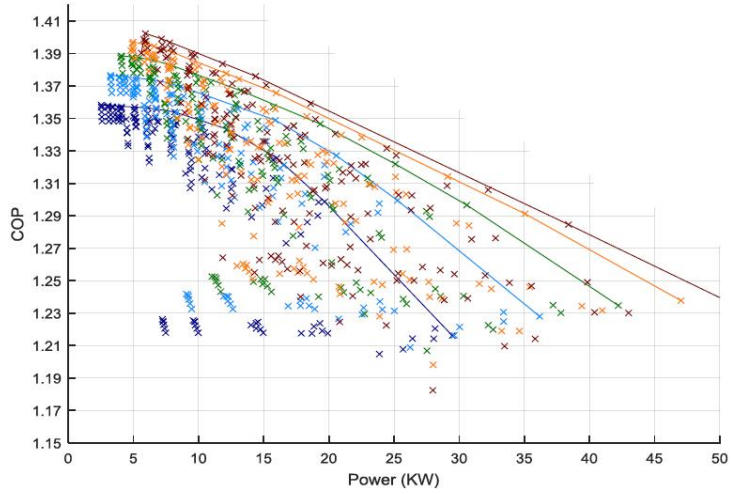

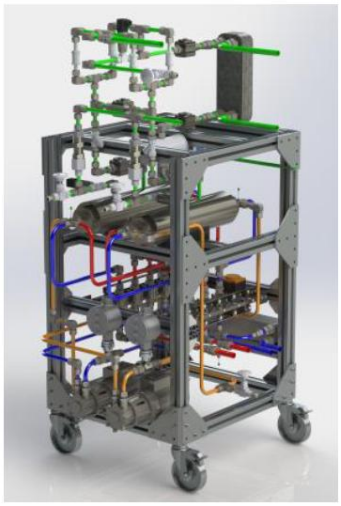

Figure 3: Predicted performance map of machine & 3D Model of machine under construction

The cycle will operate with both heat and mass recovery. Figure 3 shows the performance envelope for the system predicted by the computational model for a delivery temperature of 50°C and an evaporating temperature of 5°C.

Summary/Conclusions

The design of a novel carbon-aluminium laminate adsorption generator is presented for application to a domestic gas fired heat pump. The machine which is currently under construction has a predicted power output of between 5 and 10 kW at a COP of 1.40 to 1.35.

Nomenclature

COP Coefficient of Performance GUE Gas Utilisation Efficiency

References

[1] Critoph, R.E., Metcalf, S.J., “Progress in the development of a carbon-ammonia adsorption gas-fired domestic heat pump”, Int. Sorption Heat Pump Conf. 2011 proc., pp. 849-854.
[2] Tamainot-Telto, Z., Critoph, R.E., “Monolithic carbon for sorption refrigeration and heat pump applications”, App. Thermal Eng. 21, pp. 37-52, 2001.

High temperature heat and water recovery in steam injected gas turbines using an open absorption heat pump

Annelies Vandersickel*, Wolf G. Wedel, Hartmut Spliethoff

[1]Institute for Energy Systems, Technical University Munich,
Boltzmannstr. 15, 85748 Garching b. München, Germany
*Corresponding author: annelies.vandersickel@tum.de

Abstract

The advantages of reinjecting steam from the heat recovery steam generator (HRSG) in the preceding gas turbine are increased power and electrical efficiency at low specific cost and a high operating flexibility. The discharge of the injected steam to the ambient has however two major drawbacks: (1) a relevant water consumption and (2) a large thermal loss related to the latent heat of steam. An open absorption heat pump cycle (HT-CBT) downstream of the HRSG can solve both problems, as it allows to recover the steam from the flue gas and use its condensation heat at elevated temperature. This paper presents a concept to efficiently integrate both technologies and assesses the potential of the absorption system for a steam injected gas turbine (STIG). Over a wide range of steam injection rates, the power output of the plant can be varied without the associated energetic penalty achieving improvements in the fuel efficiency of up to 26%.

Keywords: open absorption heat pump; steam injected gas turbine; cogeneration; flue gas condensation

Introduction/Background

In steam injected steam turbines (STIG), Steam generated in the HRSG can be either used for district/process heating or injected in the gas turbine to increase its power output. This allows to vary the power-to-heat ratio over a wide range, allowing the plant to respond rapidly to fluctuations in the heat or electricity demand. Economic advantages of the STIG result from (1) the larger number of operating hours, as the plant can run with high steam injection rates when heat demand is low and (2) a reduction of the peak power and the associated cost when electricity demand is high.

The discharge of the injected steam into the ambient, has two major drawbacks: (1) a high water consumption and (2) a low fuel efficiency. Heat recovery through flue gas condensation addresses both disadvantages. Condensing the water vapour and using its latent heat increases the fuel efficiency, whereas reinjecting the condensate into the power cycle significantly reduces the cycle's water consumption. Due to the low dew point temperatures of the flue gas, ranging between 45 and 70°C, a flue gas condensing heat exchanger can only be used if a low temperature heat sink is available. This is seldom the case in district heating and industrial applications. Open absorption heat pump cycles, as proposed by Bergmann et al. (e.g. in [1]), allow to exploit the condensation energy contained in the flue gas at significantly higher temperature levels.

This "High temperature Condensation Boiler Technology" (HT-CBT) has been realized in several pilot plants e.g. a diesel engine cogeneration [2] and gas-fired heating plant [1] resulting in a fuel efficiency increase of about 10%. The high humidity of the flue gas in a STIG motivates to integrate the HT-CBT. Up till now, however, no analysis on how to integrate both technologies has been made, nor have the achievable heat and power augmentation and water recovery been assessed. This analysis is performed in the current paper, based on detailed process simulations validated with data from the Cheng cycle

installed at the Technical University in Munich [3] as well design data from the HT-CBT plant in Berlin Buch [1].

Discussion and Results

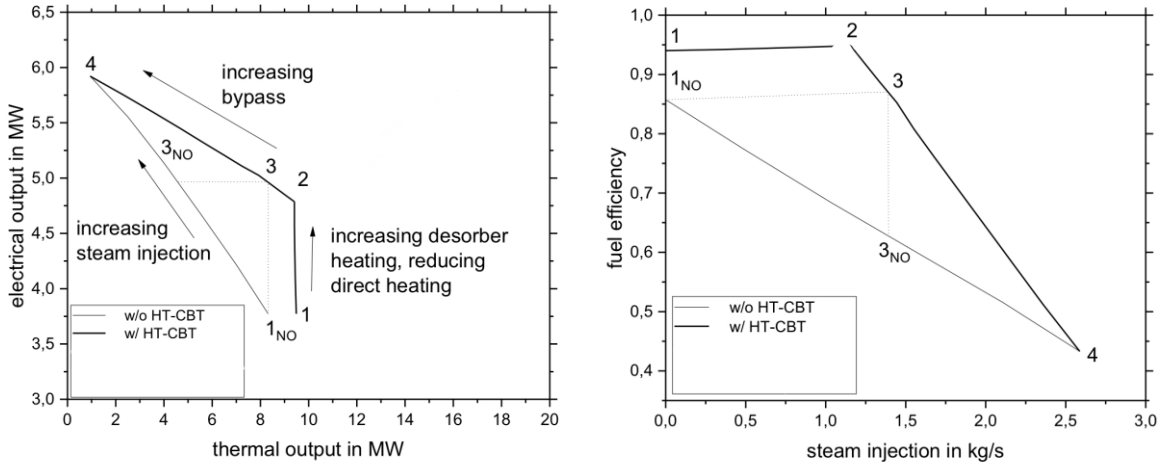

Figure 1: Performance of the Cheng Cycle with and without the HT-CBT integrated for steam injection rates varying from zero (1) till 2.6 kg/s (4) and a network return temperature of 60 C

For a heating network return temperature of 60°C, a maximum increase in fuel efficiency of 26% can be achieved for an intermediate steam injection rate of 1.36 kg/s. For higher steam injection rates, the heat recovery is restricted by the availability of desorber heating from the HRSG, such that the benefit of the HT-CBT and hence the fuel efficiency drops significantly. For lower steam injection rates, the fuel efficiency however remains nearly constant at 95%, allowing to vary power output without the associated energetic penalty. Except for steam injection rates above 2.16 kg/s full water recovery eliminates the high water usage of the Cheng Cycle, making it a suited technology for cogeneration also in dry areas.
In contrast to previous applications, the HT-CBT can here not only be used to increase the heat output but also to increase the power output for a given heat demand with a maximum of 33% (from 1no to 3) with only limited impact on fuel efficiency, improving economic viability.

Summary/Conclusions

For higher heating network temperature (60C) significant improvements in fuel efficiency and water usage can be achieved through the integration of the HT-CBT in a steam injected gas turbine, in particular for plants designed to operate with low to moderate steam injection rates.

References:

[1] M. Pokojski, A. Heuer, T. Bergmann und U. Tamm-Woydt, *„Hochtemperatur-Brennwertnutzung in Dampfkesselanlage: Heizkraftwerk Buch,“* Euroheat & Power 36

[2] M. Ruch, U. Tamm-Woydt, G. Wartig und J. Furmanek-Battke, „*Vierte Hochtemperatur-Brennwertnutzung an einem BHKW realisiert,“* Euroheat & Power 34, 2005

[3] D. Hein und K. Kwanka, *Cheng Cycle cogeneration for a significantly varying demand of heat and power,* Proceedings of the Symposium on Energy Engineering in the 21st Century (SEE2000) Vol. 4, New York, Begell House, 2000

Methanol and its Sorption Heat Pump and Refrigeration Potential

S. Hinmers*, R.E. Critoph

School of Engineering, University of Warwick, Coventry CV4 7AL, United Kingdom

*Corresponding author: s.hinmers@warwick.ac.uk

Abstract

Methanol is a favourable process fluid in sorption technology due to its small molecular weight, hydrogen bonding properties and by having a high latent heat. This poster aims to shed a light on the most relevant research performed, particularly the most recent innovations. The purpose is to pave way for analytic and experimental work that will review the potential of methanol in various sorption systems. Methanol is practical, relatively safe and could be employed in consumer products. How do we enhance the technology to give attractive efficiencies and make it commercially viable? Research into methanol as a sorbate for heat pumping and refrigeration has largely focussed on Methanol/Activated Carbon systems, utilising physical adsorption. There has also been significant interest in the performance of Methanol/$CaCl_2$ in chemical adsorption systems. Furthermore, methanol has featured in absorption systems with various liquid solvents acting as a sorbent, including Lithium Bromide and similar derivatives (sometimes in combination).

Keywords: Heat Pump, Refrigeration, Methanol, Sorption, Thermal Energy, Absorption, Adsorption

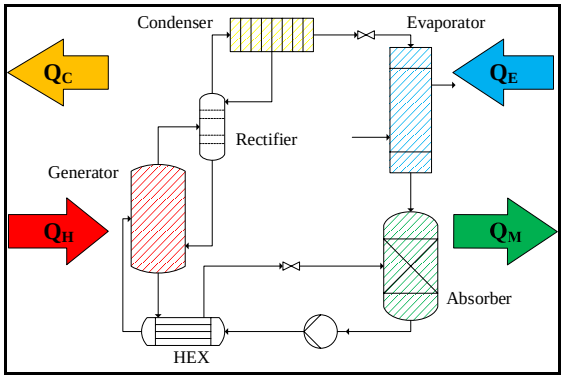

Figure 31 Example Absorption System

Background

Much of this research highlights the advantage of methanol as a working fluid for all kinds of sorption systems. It is particularly effective in refrigeration; this is due to the low freezing point of methanol at 175.59K and its ability to evaporate below 0˚C [1]. This enables cooling that is effective for ice making and air conditioning. Solid-Vapour cycles have focussed most of all on the working pair of methanol and activated carbon, this is likely due its polarity and high adsorption capacity [2]. Such a system is relatively benign and the low vaporisation temperature means the system operates below ambient pressure. This increases safety as an

ingress of air will occur before any methanol may leak [3]. These systems have relatively low coefficients of performance (COP). Adding mass or heat recovery increases the complexity of systems but increases the COP and Cooling capacity. Chemical adsorption offers the prospect of greater concentration changes, but can suffer agglomeration problems. Composite systems aim to address this with the salt embedded within a framework. There are still unanswered questions, including the potential of mass recovery and other lessons learnt in previous work that may enhance such salt systems [4].

Comparatively less work has been done into absorption systems utilising methanol, a typical example being illustrated in *Figure 31*; such systems don't necessarily require a rectifying column. These liquid-vapour systems in theory should be more attractive, because of their continuous operation, but incorporate more complex process equipment such as rectifiers [2]. Work on absorption systems using methanol include the use of complex organic solvents [5] and ionic liquids [6]and could form the basis of practical systems. The use of Metal organic-frameworks is the one of the latest topics of research utilising methanol to produce highly efficient heat pumps within adsorption systems [7].

Conclusion

There is a clear necessity to explore how effective methanol is as a process fluid or refrigerant. An overview of methanol within sorption technologies, will enable one to understand the properties that are favourable for sorption thermal technologies. By identifying gaps in knowledge, future work can be done focussing on the increased performance of methanol systems which already show great potential.

References:

[1] H. G. Carlson and E. H. Westrum Jr., "Methanol: Heat Capacity, Enthalpies of Transition and Melting, and Thermodynamic Properties 5-300K," The Journal of Chemical Physics, vol. 54, no. 1464, pp. 1464-1471, 1971.

[2] P. O. Offenhartz, T. V. Rye, R. E. Malsberger and D. Schwartz, "Methanol-Based Heat Pump for Solar Heating, Cooling and Storage, Phase III," Department of Energy and Environment, New York, 1981.

[3] M. Pons and J. J. Guilleminot, "Design of an Experimental Solar Powered, Solid-Adsorption Ice Maker," Journal of Solar Energy Engineering, vol. 108, pp. 332-337, 1986.

[4] Z. S. Lu and R. Z. Wang, "Study of the new composite adsorbent of salt LiCl/silica gel- methanol used in an innovative adsorption cooling machine driven by low temperature heat source," Renewable Energy , no. 63, pp. 445-451, 2014.

[5] S. C. Kaushik, S. Chandra and S. M. B. Gadhi, "Thermodynamic Feasibility of Double Effect Generation Absorption System Using Water-Salt and Alcohol-Salt Mixtures as Working Fluids," Heat Recovery Systems, vol. 5, no. 1, pp. 19-26, 1985.

[6] S. Iyoki, K. Tanaka and T. Uemura, "Theoretical performance analysis of absorption refrigerating machine, absorption heat pump and absorption heat transformer using alcohol as working medium," International Journal of Refrigeration, vol. 17, no. 3, pp. 180-190, 1994.

[7] F. Jeremias, D. Frölich, C. Janiak and S. K. Henninger, "Water and methanol adsorption on MOFs for cycling heat transformation processes," New Journal of Chemistry, vol. 38, no. 1846, pp. 1846-1852, 2014.

Optimal design and control of a low-temperature geothermally-fed parallel CHP plant

Sarah Van Erdeweghe[1,3*], Johan Van Bael[2,3], Ben Laenen[2] and William D'haeseleer[1,3]

[1] University of Leuven (KU Leuven), Applied Mechanics and Energy Conversion Section, Celestijnenlaan 300 – box 2421, B-3001 Leuven, Belgium
[2] Flemish Institute for Technological Research (VITO), Boeretang 200, B-2400 Mol, Belgium
[3] EnergyVille, Thor Park, Poort Genk 8310, B-3600 Genk, Belgium
[*]Corresponding author: sarah.vanerdeweghe@kuleuven.be

Abstract

In this work, we propose a two-step methodology for the design and off-design optimization of a low-temperature (130°C) geothermally-fed combined heat-and-power (CHP) plant. We investigate electricity production via Organic Rankine Cycle (ORC) and heat delivery to a high-temperature district heating (DH) system (~90°C/60°C) in Mol (Belgium) in 2016. In the first step, we optimize the design of the heat exchangers and air-cooled condenser, assuming fixed values for the environment temperature, heat demand and supply and return temperatures of the DH system – for all of them, the average values are used. When comparing the parallel CHP with a pure electrical power plant for the same conditions, the CHP plant is economically feasible (NPV_{CHP} = 1.72$MEUR_{2016}$) whereas the pure power plant is not ($NPV_{power\ plant}$ = -4.60$MEUR_{2016}$). However, we found that an off-design analysis is of the utmost importance. Therefore, we use hourly data for the heat demand, supply and return temperatures and for the weather data. The off-design optimization results show that the CHP plant cannot satisfy the entire heat demand of the DH system and back-up boilers are needed. This also means that the CHP is not optimally designed – the design for the average DH system heat demand is not justified – and this results in a negative NPV_{CHP} = -3.67$MEUR_{2016}$.

Keywords: CHP, Design optimization, District heating, Low-grade geothermal energy, Off-design optimization, ORC, Thermoeconomics

Introduction/Background

Many studies have been performed regarding low-temperature geothermally-fueled power plants, e.g., [1]–[3]. Research topics include the optimization of the power plant design, the impact of the geothermal source conditions on the plant performance, economic feasibility, etc. However, low-temperature geothermal power plants in non-volcanic regions (like NW Europe) are mostly not economically competitive without some kind of feed-in tariff. Therefore, one way to increase the economic attractiveness of a deep-geothermal plant in these regions is by providing other valuable products next to electricity. In this work, we consider a combined-heat-and-power (CHP) plant, and we will feed a district heating (DH) system with geothermal heat in addition to electricity production via an Organic Rankine Cycle (ORC).Some studies have already been performed on CHP plants connected to DH systems, e.g., [3]–[6]. They show that, in most cases, higher profits can be achieved with the CHP plant compared with electricity production only. However these studies have been done for medium to high source temperatures (185°C geothermal, biomass, thermal solar). In this work we will investigate the economic feasibility of a low-temperature (130°C) geothermal CHP plant, coupled to a DH system (~90°C/60°C). The main improvements with respect to the existing literature are the use of hourly weather data instead of fixed or monthly-averaged values, the use of hourly data of a real DH system and the NPV as the optimization objective.

Discussion and Results

In the first step, we optimize the CHP plant design towards maximal NPV for the average heat demand (2760kWth) and the average environment temperature. In the second step, we perform an off-design optimization during a typical year. Figure 32 shows the load duration curve of the DH system heat demand $\dot{Q}_{DH}$ and the corresponding environment temperature T_{env} . The electrical power $\dot{P}_{net}$ and thermal power $\dot{Q}_{CHP}$ of the CHP are results of the off-design optimization. Two conclusions can be made based on Figure 32. First, for high heat demands, the CHP is not able to satisfy the heat demand of the DH system ($\dot{Q}_{CHP} < \dot{Q}_{DH}$) so back-up boilers are needed. And second, the CHP was designed for the average heat demand of the DH system (2760kWth). However, the real thermal power which can be delivered by the CHP is lower. As a consequence, the ORC can produce the design electrical power output (2455kWe) only a few hours a year. So both incomes from selling heat and electricity are lower than we considered in the design step. Therefore, very likely, it is better to design the CHP plant not for the average heat demand of the district heating system but for a higher heat demand.

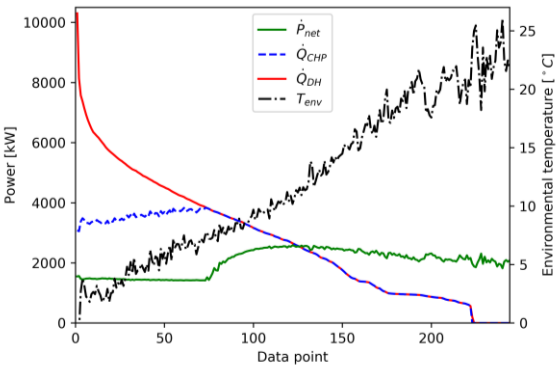

Figure 32: Load duration curve of the DH system heat demand (red) and corresponding environment temperature (black dash-dotted), thermal (blue dashed) and electrical (green) power output of the CHP.

Summary/Conclusions

In this work, we propose a two-step optimization methodology for the design and control of a binary geothermal CHP plant, coupled to a district heating system. Our results show that it is important to take real hourly data for the DH system and the environment conditions into account. Furthermore, we conclude that the economic feasibility of the CHP plant might be better than for a pure electrical power plant for the same low-temperature geothermal source – on the condition that the CHP plant is properly designed (based on a well-considered parameter assumption for the nominal heat demand of the CHP in the design step).

References

[1] D. Walraven, B. Laenen, and W. D'haeseleer, "Economic system optimization of air-cooled organic Rankine cycles powered by low-temperature geothermal heat sources," *Energy*, vol. 80, pp. 104–113, 2015.

[2] D. Budisulistyo, C. S. Wong, and S. Krumdieck, "Lifetime design strategy for binary geothermal plants considering degradation of geothermal resource productivity," *Energy Convers. Manag.*, vol. 132, pp. 1–13, Jan. 2017.

[3] M. Usman, M. Imran, Y. Yang, D. H. Lee, and B.-S. Park, "Thermo-economic comparison of air-cooled and cooling tower based Organic Rankine Cycle (ORC) with R245fa and R1233zde as candidate working fluids for different geographical climate conditions," *Energy*, vol. 123, pp. 353–366, Mar. 2017.

[4] E. Martelli, F. Capra, and S. Consonni, "Numerical optimization of Combined Heat and Power Organic Rankine Cycles – Part A: Design optimization," *Energy*, vol. 90, pp. 310–328, Oct. 2015.

[5] F. Capra and E. Martelli, "Numerical optimization of combined heat and power Organic Rankine Cycles – Part B: Simultaneous design & part-load optimization," *Energy*, vol. 90, pp. 329–343, 2015.

[6] F. Marty, S. Serra, S. Sochard, and J.-M. Reneaume, "Economic optimization of a combined heat and power plant: heat vs electricity," *Energy Procedia*, vol. 116, pp. 138–151, Jun. 2017.

A Study on Optimum Discharge Pressure of Transcritical CO_2 Heat Pump System under Different Ambient Temperatures and Compressor Frequencies

Xiang Qin, Xinli Wei, Dongwei Zhang* and Xiangrui Meng

Research Center on the Technology and Equipments for Energy Saving in Thermal Energy System of MOE, School of Chemical Engineering and Energy, Zhengzhou University, Henan, 450001, China
*Corresponding author: zhangdw@zzu.edu.cn

Abstract

In order to study on how the evaporation temperature, discharge pressure and compressor performance will influence the transcritical CO_2 heat pump cycle, an experimental system for a transcritical CO_2 air source heat pump with internal heat exchanger was established. Under the ambient temperature of 15℃ and 30℃, we made the discharge pressure varied from 70bar to 120bar, and changed the compressor frequency from 20Hz to 40Hz. The test results show that under different ambient temperatures and compressor frequencies, the variation trend of the COP of the system, heating capacity and outlet water temperature are almost same. However, as the ambient temperature increases, the COP decreases, the heating capacity does not change, and the outlet water temperature increases. With the increase of compressor frequency, the COP of the system decreases, the heating capacity and outlet water temperatures increase. Finally, two non-generalized correlations are obtained by combining the experimental data. One is the highest outlet temperature under different ambient temperatures and compressor frequencies, the other is the optimum outlet pressure under different ambient temperatures and compressor frequencies. The error range is within ± 5%.

Keywords: Transcritical cycle, Carbon dioxide, Compressor frequency.

Introduction

As a natural refrigerant, CO_2 has been widely used in ships, theaters and other refrigeration systems since the end of the 19th century. However, due to the appearance of artificial refrigerants, CO_2 gradually fades out of the refrigeration system. Nowadays, with the destruction of artificial refrigerants to our environment, the natural refrigerants once again return to the stage. Compared with traditional refrigerants, CO_2 has many advantages, such as non-flammable, non-toxic, and cost-friendly. At the end of the 20th century, Lorentzen proposed the transcritical CO_2 circulation systems for automotive air conditioning and other applications [1]. The critical temperature of CO_2 is only 31.1℃, which is similar to the ambient temperature, so it is beneficial to the direct conversion of CO_2 at both subcritical and supercritical levels [2]. And there is no phase change in the exothermic process of CO_2, the temperature slip of the refrigerant and the increase of the water temperature can better match and produce hot water with higher temperature. Compared to the evaporator in the traditional system, it is called gas cooler [3].

Results and discussion

COP and the Maximum COP

After the demarcation point, the temperature of the gas cooler outlet rapidly decreased, the discharge pressure increased, and the enthalpy value of the gas cooler outlet rapidly

increased. The change in enthalpy slows down. This trend is the main reason for the large COP. (That is theoretical COP without the friction loss and the machine loss)

Heating and outlet water temperatures

The non-generalized correlation of the highest water outlet temperature corresponding to the compressor frequency at different ambient temperatures was fitted by experimental data.

$$T_{\mathrm{w,corr}} = 16.51 + 0.737T_{\mathrm{amb}} + 1.549f_{\mathrm{com}} \quad (1)$$

Optimal discharge pressure

We take the changes of compressor frequency and ambient temperature into consideration, and fit it into a non-generalized correlation of optimal discharge pressure, see Eq. 2. its relevance applies of ambient temperatures is from 15℃ to 30℃ while the compressor frequencies is from 20Hz to 50Hz.

$$P_{\mathrm{opt,corr}} = (0.034 + 0.00013T_{\mathrm{amb}})f_{\mathrm{com}}^2 - 1.493f_{\mathrm{com}} + 0.473T_{\mathrm{amb}} + 87.18$$

$$(0℃ < T_{\mathrm{amb}} \leq 30℃, 20\mathrm{Hz} \leq f_{\mathrm{com}} \leq 50\mathrm{Hz}) \quad (2)$$

Conclusion

Under different ambient temperatures and compressor frequencies, there will be peaks in the system COP as the discharge pressure rises. Analytical experimental results show that the cause of the peak is the rapid drop in the enthalpy of the outlet gas cooler. The temperature of the CO_2 outlet of the gas cooler decreased slowly at first, then it decreased rapidly, finally it maintained a constant trend. Since the isotherm above the critical point is almost horizontal and the temperature of the CO_2 outlet of the gas cooler falls slowly, it is almost same as the isotherm trend, which leads to a rapid drop of the of the CO_2 gas cooler enthalpy. This rapid decline makes COP reaches its peak. After that, the temperature of the CO_2 outlet of the gas cooler decreased rapidly, and change of the enthalpy of the CO_2 gas cooler outlet slowed down. Finally, because the inlet water temperature is fixed, the CO_2 outlet temperature of the gas cooler will be the same as the water inlet temperature. This result in the stable enthalpy of the CO_2 gas cooler outlet. This is also the main reason for the higher COP in this experiment.

According to the change of the compressor frequency and the ambient temperature, we obtained a correlation about the highest outlet temperature, which can provide guidance for the selection of compressor frequency under different water temperature requirements.

We also obtained a correlation about the optimal discharge pressure. We selected the discharge pressure corresponding to the maximum COP as the optimal discharge pressure, and obtained a correlation about the optimal discharge pressure based on the changes of the ambient temperature and the compressor frequency.

References

[1] Lorentzen G, Pettersen J., A new efficient and environmentally benign system for car air-conditioning, International Journal of Refrigeration, 1993.

[2] Fartaj A, Ting S K, Yang W W., Second law analysis of the transcritical CO2, refrigeration cycle, Energy Conversion & Management, 2004.

[3] Ma Y, Liu Z, Tian H., A review of transcritical carbon dioxide heat pump and refrigeration cycles, Energy, 2013.

Numerical analysis for dehydration and hydration of calcium hydroxide and calcium oxide in a packed bed reactor

S. Funayama[1*], M. Zamengo[2], H. Takasu[3], K. Fujioka[4], and Y. Kato[5]

[1]Graduate Major in Nuclear Engineering, Tokyo Institute of Technology, 2-12-1-N1-22, Ookayama, Meguro-ku, Tokyo 152-8550, Japan
[2]Department of Materials Science and Engineering, Tokyo Institute of Technology, 2-12-1-S8-29, Ookayama, Meguro-ku, Tokyo 152-8550, Japan
[3]Department of Nuclear Engineering, Tokyo Institute of Technology, 2-12-1-N1-22, Ookayama, Meguro-ku, Tokyo 152-8550, Japan
[4]Functional Fluids Ltd., 5th Fl., Chiyoda Bldg. Annex, 1-4-5, Utsubohonmachi, Nishi-Ku, Osaka 550-0004, Japan
[5]Laboratory for Advanced Nuclear Energy, Institute of Innovative Research, Tokyo Institute of Technology, 2-12-1-N1-22, Ookayama, Meguro-ku, Tokyo 152-8550, Japan
[*]Corresponding author: funayama.s.aa@m.titech.ac.jp

Abstract

This study focuses on the TCES using Ca(OH)2/CaO/H2O reaction system. The operating temperature of the system is around 400 to 600°C and the reaction used in the system is expressed as follows:

$$Ca(OH)_2\,(s) \rightleftharpoons CaO\,(s) + H_2O\,(g) \qquad \Delta H^\circ = 104\ \text{kJ mol}^{-1} \qquad (1)$$

The forward reaction is called dehydration. This is endothermic reaction which is applied to the heat storage mode of the system. On the other hand, the backward reaction is hydration. This is exothermic reaction which is used for the heat output mode of the system.
In this study, a numerical model of a cylindrical reactor was established. At first, the model was evaluated by the experimental data using Ca(OH)2 pellets. Secondly, the effects of thermal conductivity on the reaction conversion rate, bed temperature, heat storage/output rate and density was investigated numerically.

Packed bed experiment and numerical analysis method

The experimental data was obtained from the experiment using 59.6 g of Ca(OH)2 pellets with a packed bed reactor. Thermal conductivity of the bed of the Ca(OH)2 pellets measured by a thermal conductivity meter (QTM-500, Kyoto Electoronics) was 0.18 W m-1 K-1.
In the present study, reaction rate equations of dehydration and hydration coupled with heat conduction equation were solved at numerical grids by the finite volume method [1-2]. Numerical calculation was conducted by open source CFD tool, OpenFOAM®.

Results and Discussion

Fig. 1 shows numerical and experimental results of temperature at the center of the reactor and the reaction conversion during dehydration. The calculated conversion was in agreement with the experimental data. Temperature curves imply that high thermal conductivity increases plateau temperature during dehydration. Distributions of temperature and conversion during dehydration are given in **Fig. 2**. It appears that high conductivity facilitates conversion due to enhancement of transfer of heat supplied from the heater placed around the reactor.

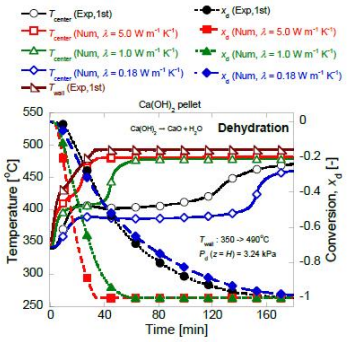

Fig. 1 Comparison of temperature and conversion during dehydration.

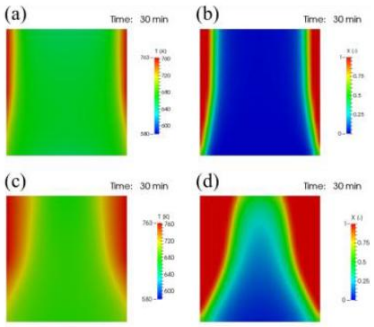

Fig. 2 Distribution of temperature (left) and conversion (right) during dehydration. (a),(b): $\lambda = 0.18$ W m^{-1} K^{-1}; (c),(d): $\lambda = 1.0$ W m^{-1} K^{-1}

In this study, to focus on effects of thermal conductivity of the bed, vapour flow in the bed was neglected. However, a numerical model for practical reactors requires the effects of the flow of water vapour. Therefore, mass transfer equations e.g. the Brinkman Forcheimer equations will be taken into consideration using parallel computing to reduce the computer demands in future work.

Conclusions

A numerical model of dehydration and hydration reaction in a packed bed reactor was developed. The increment of reaction rate due to higher thermal conductivity was demonstrated and it was also found numerically that the plateau temperature during dehydration seems to increase due to high thermal conductivity of the bed. The results would be beneficial for development of composite materials for TCES in the future work.

References:

[1] Schaube F, Koch L, Wörner A, Müller-Steinhagen H, *Thermochimica Acta*, 538, 2012.
[2] M. Zamengo, J. Ryu, Y. Kato, *ISIJ Int.*, 55(2), 2015.

Development of a low-cost, electricity-generating Rankine cycle, alcohol-fuelled cooking stove for rural communities

Wigdan Kisha[1*], Paul H.Riley[2] and David Hann[3]

[1, 3] Faculty of Engineering, University of Nottingham, UK
[2]School of Mathematics, Computer Science & Engineering, City University of London, UK
Corresponding author: *Email address: wigdan.kisha@nottingham.ac.uk

Abstract

The article describes a novel design of a helical tube flash boiler that uses a 2kW nominal methylated spirit burner to heat an approximately 2.5m long coil of copper pipe fed by a nominal 8 bar electrically operated solenoid water pump. The final embodiment is for superheated steam to be converted to electricity and the waste exit heat from the generator used either for cooking or for ethanol production. The performance of the flash boiler has been evaluated experimentally based on the well-known "Direct-Method"; by measuring both the flow of the fuel and the steam. It found that the pressure inside the pipe can reach up to 7.4 bar and the temperature of the steam released by the flashing process can reach 255 ℃ utilising a low-cost water pump.

Keywords: Flash boiler, Spirit burner, copper coil, electrical generator

Background

During the last decades, numerous advanced thermodynamic cycles and variations/ combinations of technologies have been developed for low-grade waste heat recovery [1]. A flash boilers is one that is widely used to recover energy from combustion gasses. In a flash boiler, the heating surface is a single or a series of tubes into which the feed water pumped against the developed pressure. The heat source is usually a petrol, oil or gas flame directed against the tube. The tube is often coiled and housed in a thin lightweight case of metal, frequently stainless steel and the flame is directed through the centre of the coil. The development of high-pressure steam is very rapid, hence the term flash steam [2].

System Configuration

As shown on **Figure 1**, the system consists of a 10 mm diameter single copper coil in a multi-layer spiral horizontal configuration. A methylated alcohol burner is placed at the bottom of the system to heat up the pipe. The feed water flows inside the tubes after being pumped from a water tank through a 10 mm diameter plastic pipe utilizing a diaphragm high-pressure pump while the hot gases from combustion of alcohol flow around the outside of the pipe. The steam is taken out from the system near the roof via the steam take-off pipe before being directed (in the experimental case) to a cooking pot. In the final embodiment, a generator would convert the superheated steam to electricity and the exhaust heat used for cooking.

Figure 1: Flash boiler experimental test rig

Results and discussion

The thermal performance of a flash boiler stove was investigated and measured in terms of combustion input power, thermal output power, specific fuel consumption, fuel ratio and efficiency. There are three phases of heating in the pipe as follows: Exit combustion gases heat the water inlet from ambient (21°C) to boiling point (100°C), Water is boiled in the horizontal section of the pipe where two-phase flow occurs, and the last phase is that steam is superheated in the last section of the pipe by the hot combustion gasses from the burner. **Figure 2** illustrates the performance of the system when 1.3 kg of alcohol was introduced at the start of the test to fire the boiler. Pressure in the copper pipe can reach up to 740 kPa while the maximum temperature of the steam near the nozzle reached 255°C.

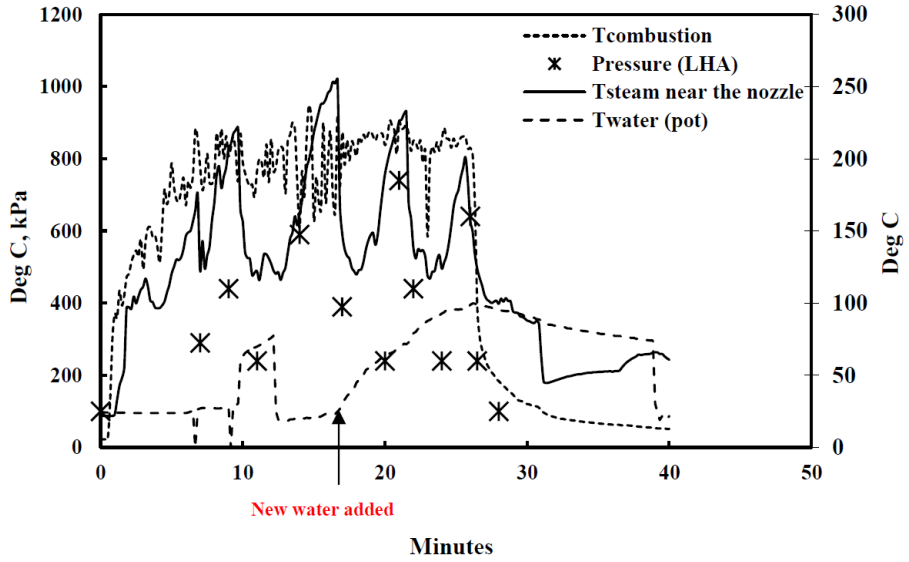

Figure 2: Performance of the flash boiler during the test

Summary

This paper describes design and development of a copper pipe flash boiler. Direct method is used for the boiler calculation of boiler efficiency. The heat supplied to the boiler from the burning of alcohol and the heat absorbed by the water in the boiler at a given period of time is calculated. The results show that the maximum steam exit temperature is 255°C and the boiler efficiency reached 47% at 2kW heat input from burning of alcohol. Further experimental tests need to be carried out utilizing for example, a tesla turbine as an expander and evaluate the overall performance of the cycle.

References:

[1] Tartakovsky, L., et al., *Simulation of wankel engine performance using commercial software for piston engines*. 2012, SAE Technical Paper.
[2] Ganapathy, V., *Industrial boilers and heat recovery steam generators: design, applications, and calculations*. 2002: CRC Press.

A Micro-Turbine-Generator-Construction-Kit (MTG-c-kit) for Small-Scale Waste Heat Recovery ORC-Plants

A. P. Weiß*[1], T. Popp[1], G. Zinn[2], M. Preißinger[3,4] and D. Brüggemann[4]

[1] Competence Center for Combined Heat and Power Systems, University of Applied Sciences Amberg-Weiden, Kaiser-Wilhelm-Ring 23, 92224 Amberg, Germany

[2] DEPRAG GMBH u. CO, Carl-Schulz-Platz 1, 92224 Amberg, Germany

[3] illwerke vkw Professorship for Energy Efficiency, Energy Research Center, Vorarlberg University of Applied Sciences, 6850 Dornbirn, Austria

[4] Chair of Engineering Thermodynamics and Transport Processes, Center of Energy Technology, University of Bayreuth, Universitätsstraße 30, 95447 Bayreuth, Germany

*Corresponding author: a.weiss@oth-aw.de

Abstract

Experimentally determined efficiency characteristics of two micro turbines are discussed in this paper. One turbine (15 kW) is working with cyclopentane, the other turbine (12 kW) expands hexamethyldisiloxane (MM). The two turbines are designed and built in accordance to the concept of a micro-turbine-generator-construction-kit (MTG-c-kit) for small scale organic Rankine cycle (ORC) waste heat recovery. The motivation for this MTG-c-kit and its architecture will be briefly introduced. Both single stage impulse turbines show a high design point total-to-static isentropic efficiency: the 15 kW cyclopentane turbine achieves 65.0 %, the 12 kW hexamehylidisiloxane turbine achieves even 73.4 %. Furthermore, the discussed off-design characteristics of the turbines prove that their operating behavior is very advantageous for small waste heat recovery plants: the turbine efficiency keeps a high level over a wide range of pressure ratio and rotational speed.

Keywords: Organic Rankine Cycle (ORC)**,** turbine, experimental, waste heat recovery.

Introduction/Background

Due to the various possible applications in waste heat recovery business it is not appropriate to design and build some standard machines to stock. In fact, it is necessary to develop a very flexible micro-turbine-generator-construction-kit (MTG-c-kit) by means of which a customized turbine generator can be designed, built quickly and cost efficiently for any required power output, any working fluid and any boundary conditions out of a wide range. The tested micro turbines are built in accordance to the design principles of the addressed MTG-c-kit. Figure 1 displays its principal architecture.

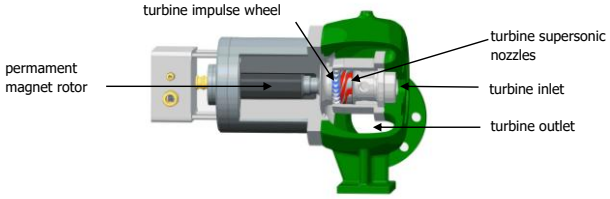

Fig. 1: Architecture of the micro-turbine-generator-construction-kit (MTG-c-kit) [1]

Two ORC research plants with direct evaporation were designed and built at the Center of Energy Technology at the University of Bayreuth for developing and testing the MTG-c-kit. Both plants were heated by a propane gas burner. The first plant used cyclopentane as working fluid because it was designed to investigate waste heat recovery from a 250 kW internal combustion engine with a rather low exhaust gas temperature of about 300 degree Celsius. The second plant worked with hexamethyldisiloxane (MM) for higher exhaust gas temperatures of about 500 degree Celsius.

Results and Discussion

The efficiency characteristics of both turbines as a function of rotational speed and pressure ratio are shown and discussed in the full paper. Here, the total-to-static isentropic efficiencies as function of total-to-static pressure ratio are depicted in Fig. 2. The corrected rotational speed n_{corr} normalized by its design point value serves as parameter. The design pressure ratio of PR = 13.6 could not be achieved for the 15 kW cyclopentane turbine. The power of the propane gas burner which heated the ORC research plant was not sufficient to evaporate the required mass flow rate. The highest measured efficiency of 65.0 % occurs at design speed and the highest measured pressure ratio (PR = 12.8).

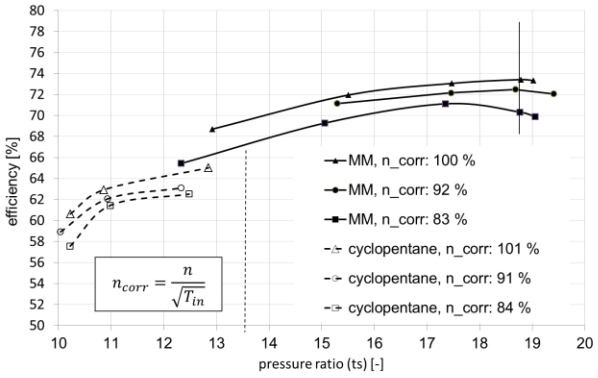

Fig. 2: Total-to-static isentropic efficiency as function of pressure ratio; dashed lines: 15 kW cyclopentane turbine, solid lines 12 kW MM turbine

Due to the problems with the propane burner in the first ORC plant, the design power output of the MM turbine in the second plant was reduced to 12 kW. Maximum efficiency of 73.4 % occurs at design rotational speed and design pressure ratio (PR = 18.8) in the case of the MM turbine. It is significantly higher because the MM turbine works with full admission, the cyclopentane turbine with about 55% partial admission. In particular, the characteristics are rather flat for the MM turbine i.e. it reacts rather insensitively on deviation from design pressure ratio.

Summary/Conclusions

The experimentally determined turbine characteristics of two representatives of the MTG-c-kit confirm the practicality of its approach. Furthermore, the achieved high expansion efficiencies prove that micro turbines are competitive as expander in small ORC plants below 100 kW_{el}. Their operating behavior is very advantageous for those small waste heat recovery plants: the turbine efficiency keeps a high level over a wide range of pressure ratio and rotational speed.

References:

[1] Weiß A. P., “Volumetric Expander Versus Turbine – Which is the better Choice for Small ORC Plants?”, 3rd International Seminar on ORC Systems, October 12-14, Brussels, Belgium 2015

Real-time operational optimization of a complex DHC plant

L. Urbanucci[1*], D. Testi[1] and J. C. Bruno[2]

[1]DESTEC (Department of Energy, Systems, Territory and Constructions Engineering), University of Pisa, Largo L. Lazzarino, 56122 Pisa, Italy

[2]Department of Mechanical Engineering, University Rovira i Virgili, Avda. Països Catalans 26, Tarragona 43007, Spain

[*]Corresponding author: luca.urbanucci@ing.unipi.it

Abstract

The combined production of electricity, heat and cold by a polygeneration system connected to a district heating and cooling network can provide high energy utilization efficiency. The inherent complexity of simultaneous production of different services and the high variability in the energy demand make CCHP systems performance highly dependent on the operational strategy. In this paper, an operational optimization method based on the moving average of real-time measurements of energy demands and ambient conditions is proposed. Real energy demand data from a DHC close to Barcelona, Spain, are used to test the method. A complex polygeneration system is considered, consisting of an internal combustion engine, a double-effect absorption chiller, an electric chiller, a boiler, and a cooling tower. A detailed modelling of the system is provided, considering partial load behaviour of the components and ambient condition effects. Results of the optimal management are discussed and compared to traditional operational strategies.

Keywords: CCHP, DHC, real-time optimization, operational optimization, partial load

Background and objectives

Combined Cooling, Heating and Power (CCHP) systems are proven to be a reliable, competitive and very efficient alternative to separate production. CCHP is a common configuration for decentralized systems where the end users are close to the energy generation point, so that these systems can be connected to a District Heating and Cooling (DHC) network. Nevertheless, the energy, environmental and economic performance of CCHP systems are strongly influenced by system synthesis, equipment selection and capacity and operational strategy.

Different optimization techniques have been adopted over the years to identify the optimal design of polygeneration systems. Some works have specifically focused on the optimal exploitation of the CCHP potential in existing plants. Moreover, several methods based on both demand forecast and real-time information have been proposed, in order to implement optimal operational strategies in actual polygeneration systems. Advanced control algorithms for real-time operations of CCHP systems have become a subject of great interest. Uncertainties in energy demand forecast, non-linear part-load performances, multiple time-varying loads and various economical features make optimal management of a polygeneration plant a very challenging task.

The main purpose of this work is to define an operational optimization method based on the moving average of real-time measurements of energy demands and ambient conditions.

Real energy demand data from a polygeneration plant close to Barcelona (Spain) [1] are used to test the method. Such data consist of hot water demand (at 90 °C) and chilled water demand (at 5 °C) and are available on a minute by minute basis for 166 consecutive days (from May 1, 2013 to October 13, 2013).

The energy system under investigation comprises an internal combustion engine, a double-effect absorption chiller, an electric chiller, a boiler, and a cooling tower. An extensive modelling of the equipment is provided, to perform a realistic and detailed simulation of the energy system. The proposed method is tested and compared to traditional operational strategies.

Discussion and Results

Several widths of the sliding window adopted for the moving average of the measured demand data have been tested in order to find the optimal width. Fig. 1 shows the difference between the cost obtained under the proposed real-time optimization management and the ideal cost with perfect forecast of the energy demand, for different sliding window widths.

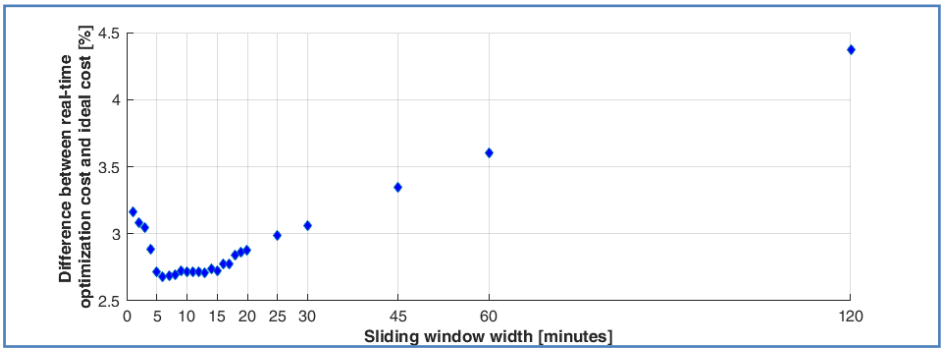

Fig. 33. *Real-time optimization cost vs. ideal cost for different sliding window widths*

Fig. 2 shows the operating cost of several operational strategies of the plant. Traditional strategies turned out to be significantly suboptimal compared to the real-time optimization management.

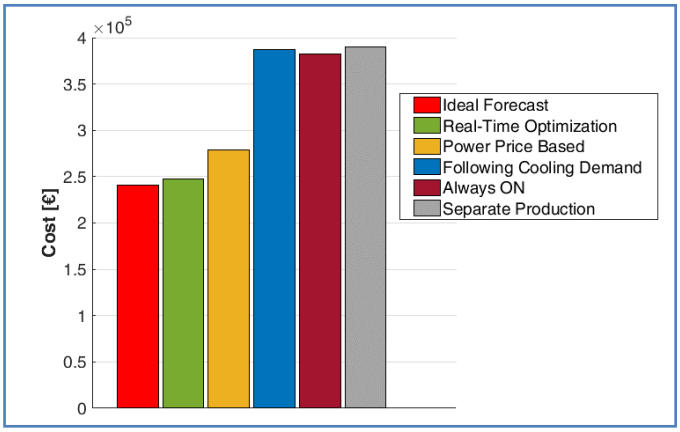

Fig. 2. *Operating cost of different operational strategies*

Conclusions

An original operational optimization method based on the moving average of real-time measurements of energy demand and ambient conditions has been proposed and tested on real energy demand data. The best performances are achieved for a width of the sliding window ranging from 5 to 15 minutes. The proposed method has been compared to traditional operational strategies and its effectiveness has been revealed. The operating cost achieved is less than 3% higher than the ideal cost obtainable with perfect forecast.

References

[1] Conte, B., Bruno, J. C., Coronas, A., "*Optimal cooling load sharing strategies for different types of absorption chillers in trigeneration plants*", Energies, 9, 573 (Open access), 2016.

Thermodynamic analysis of S-CO_2 cycle for coal-fired plant

Yawen Zheng[1], Jinliang Xu[1*], Lei Lei[1]

[1] Beijing Key Laboratory of Multiphase Flow and Heat for Low Grade Energy Utilization, North China Electric Power University, Beijing, 102206, P.R. China

[*]Corresponding author: Dr Jinliang Xu, email: xjl@ncepu.edu.cn

Abstract

A new S-CO_2(supercritical carbon dioxide) Brayton cycle is analysed in this paper. Coal-fired boiler is used as a heatsource in the cycle. Optimization of maximum temperature, minimum temperature, intercooling pressure to maximum thermal efficiency is implemented. Comparison of intercooling and non-intercooling is also carried out. Convective heat transfer and radiative heat transfer is distinguished in boiler. Results show that there exists a best intercooling pressure, and it's closed to the inlet pressure of LP(low pressure) compressor. The pinch point shifts to inside of the LTP(low temperature recuperator) compare to the non-intercooling case. Invited intercooling can improve thermal efficiency almost 2%, but the exergy efficiency nearly stay the same. The extraction rate of CO_2 to boiler makes no difference to both thermal efficiency and exergy efficiency. When the minimum temperature approaches to critical temperature of CO_2, the thermal efficiency is higher, but exergy efficiency shows a parabolic trend with the minimum temperature.

Keywords: S-CO_2 cycle, thermodynamic , parameter optimization, coal-fired

Introduction/Background

S-CO_2 cycle has received large attention in recent years. It is first proposed in 1948s[1] and integrated with nuclear power[2]. The investigation in nuclear and solar power has been deeply conducted. However, S-CO_2 cycle integrates with coal-fired plant is only a few researches reported[3, 4]. This paper is aimed at combining S-CO_2 cycle with boiler and analysing the performance of the cycle.

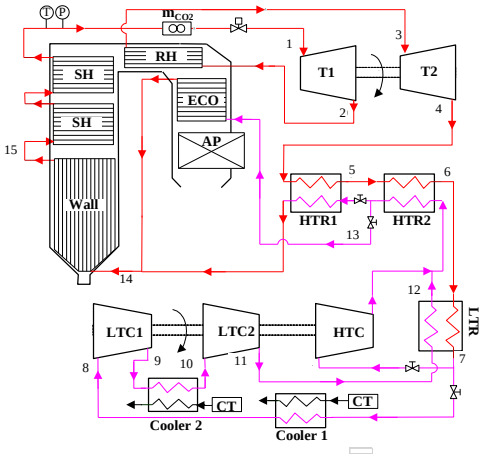

Figure 1. The diagram of S-CO_2 cycle integrates with boiler.

Discussion and Results

As is shown in the Fig 2, the thermal efficiency is first increasing with intercooling pressure and then going down. It is because that the heat release to the environment reaches a minimum value, while the heat absorbs from boiler keep constant. However, the exergy efficiency keep falling

with intercooling pressure, mainly due to the exergy destructions in HTR(high temperature recuperator) gets higher with intercooling pressure increase.

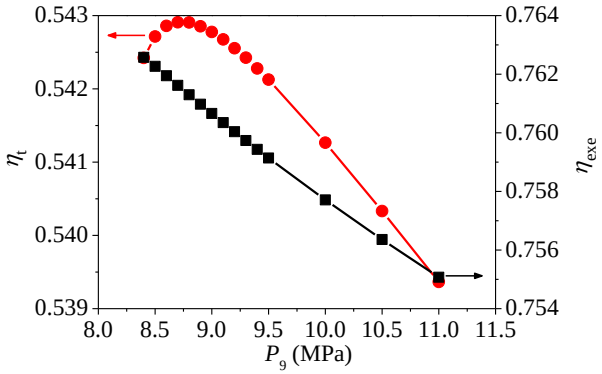

Figure 2. The influence of intercooling pressure on thermal efficiency and exergy efficiency

Introduce intercooling can improve the thermal efficiency almost 2%, but when the minimum temperature approaches to the critical temperature of CO_2, the enhancement of thermal efficiency decrease. For intercooling, it reduces output work of compressor thus to get a higher net work. Less heat is released to environment and more heat is recuperated inside the cycle. Therefore, it is benefit to the performance of the cycle. The reason why does increase maximum temperature can raise the thermal efficiency is similar to intercooling. Compare to non-intercooling, the exergy efficiency nearly unchanged, that's because the total exergy destructions almost keep constant.

Thermal efficiency goes down when the minimum temperature increase. The high inlet temperature of CO_2 in precooler will cause more heat release to environment, reduce the heat load through recuperation, at the same time, increase consuming work leads to less net work. However, the exergy efficiency gets a different trend compare to thermal efficiency. It shows a parabolic curve with the change of minimum temperature. That's because there exists a balance of exergy destruction in each component.

Summary/Conclusions

This paper discusses a new S-CO_2 Brayton cycle integrated with boiler and used a simplified method to analyse the performance of the cycle. Parameters analysis are carried out. Maximum temperature, minimum temperature and intercooling pressure are studied in this paper. The influence of intercooling is also discussed. Introducing intercooling will make the pinch point shifts to inside of the LTR, at the same time, enhance the thermal efficiency. But when the minimum temperature approaches to critical temperature of CO_2, the enhancement will decrease. The study investigates the cycle both from first law and second law of thermodynamics. Increase maximum temperature or decrease minimum temperature will both enhance the thermal efficiency.

References:

[1] Sulzer, G., Verfahren zur Erzeugung von Arbeit aus Warme, Swiss Patent, 269599(1950).

[2] Dostal,V., Driscoll, M.J., Hejzlar, P., "A supercritical carbon dioxide cycle for next generation nuclear reactors", *Massachusetts Institute of Technology*, Department of Nuclear Engineering, 2004.

[3] Mecheri, M., Moullec,Y. L., "Supercritical CO_2 Brayton cycles for coal-fired power plants", Energy, 2016, doi: 10.1016/j.energy.2016.02.111

[4] Yang, Y., Bai, W., Wang, Y., Zhang, Y., Li, H., Yao, M., Wang, H., "Coupled simulation of the combustion and fluid heating of a 300MW supercritical CO_2 boiler", Applied Thermal Engineering, 2017, doi: 10.1016/j.applthermaleng.2016.11.043

Pumped Thermal Energy Storage (PTES) as Smart Sector-Coupling Technology for Heat and Electricity

W.-D. Steinmann[1], H. Jockenhöfer[1] and D. Bauer[1*]

[1]German Aerospace Center (DLR), Institute of Engineering Thermodynamics, Pfaffenwaldring 38, 70569 Stuttgart

[*]Corresponding author: dan.bauer@dlr.de

Abstract

PTES systems are considered as an alternative concept for large scale storage of electricity. In contrast to other concepts like pumped hydro or compressed air energy storage, PTES does not demand specific geological requirements. CHEST (Compressed Heat Energy Storage) is a PTES variant based on Rankine cycles using either water or organic media as the working fluid in a combination of steam processes. The presentation will give an overview of the different options for the implementation of PTES systems based on the CHEST concept. For these CHEST variants, characteristic values like roundtrip efficiency and storage density will be given and the required components will be described. The focus will be on the technological possibility of using PTES as a sector-coupling technology for heat and electricity through low temperature heat integration. In addition, new findings of an in-depth numerical simulation of a fully heat-integrated, subcritical PTES using butene as the working fluid are presented. Detailed results regarding exergy losses during heat transfer, efficiencies of machinery and parasitic energy consumption are shown. The conducted numerical simulation includes pressure losses and pinch points, allowing for a more in-depth understanding and for a pre-optimization of the hydraulic design.

Keywords: thermo-mechanical energy storage, bulk energy storage, PTES, CHEST.

Introduction/Background

The availability of systems for site-independent, cycle-stable and cheap storage of electrical energy at a power plant scale is considered as a necessary condition for a successful implementation of the energy system transformation to renewable energies. Today's existing technologies cannot meet the increasing requirements. DLR's specialists in process system engineering, electrochemical energy technology and thermal process technology from different institutes have joined forces since January 2017 in order to develop tomorrow's electricity storage technologies: Power-to-X-to-Power storage.
In doing so, they pursue the three main technologies with high future potential:

- Power-to-Heat-to-Power storage
- Adiabatic compressed air energy storage
- Power-to-Gas-to-Power storage

Besides developing key components and innovative system concepts, DLR's specialists deal with technology assessment and market models.

Discussion and Results

Pumped Thermal Energy Storage (PTES) is a form of Power-to-Heat-to-Power storage [1]. PTES can be implemented by various combinations of storage systems, working fluids, compressors and expanders. CHEST (Compressed Heat Energy Storage) [2] is a PTES variant based on Rankine cycles using either water or organic media as the working fluid in a combination of steam processes, see Fig.1. During charging, the temperature of saturated

steam is increased by compression. The thermal energy storage system is then charged by desuperheating, condensation and subcooling of the compressed steam. During discharging, a thermal cycle similar to a conventional Rankine cycle is used to convert the heat delivered by the thermal energy storage system into electricity.

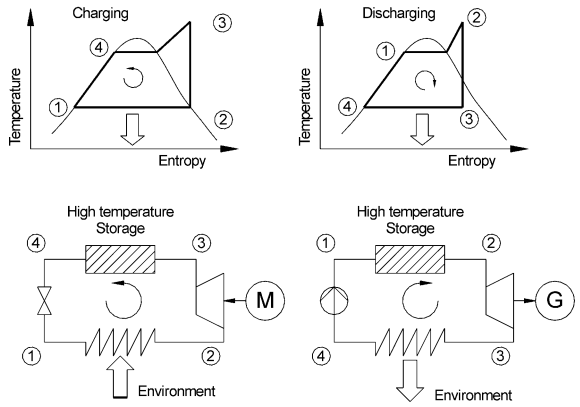

Fig.1: Schematic of the CHEST concept used for storage of electrical energy

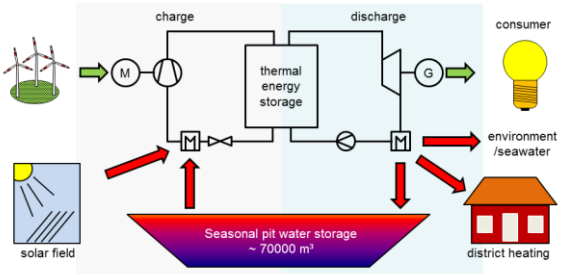

Fig.2: CHEST system as an energy management tool for electricity and heat in smart district heating

CHEST is considered as a promising option for the implementation of PTES since many components are already available. Besides using the concept primarily for the delivery of electrical energy, there is also the possibility for providing both electrical energy and heat during discharge. Additionally, low temperature heat from external sources can be integrated during the charging process. These options make CHEST a versatile energy management tool for balancing supply and demand of heat, cold and electricity, see Fig.2. Water is the preferred working fluid for systems in the multi-MW range, mainly applied for the delivery of electrical energy. Organic working fluids are intended for systems with a lower capacity, which deliver both heat and electricity during discharging [3]. An in-depth numerical simulation of a fully heat-integrated, subcritical PTES using butene as the working fluid shows that such systems are additionally able to convert low-temperature heat, e.g. waste heat below 100°C, efficiently into electricity.

Summary/Conclusions

PTES systems could be a key element for a successful implementation of the energy system transformation to renewable energies. Especially systems based on Rankine cycles might play an important future role, as they allow for an efficient sector coupling of heat and electricity in both directions, leading to a very smart technology for renewable energy management, storage and dispatchable supply.

References:

[1] Steinmann, W.-D., *Thermo-mechanical concepts for bulk energy storage*. Renew Sustain Energy Rev 2016.

[2] Steinmann, W.-D., *The CHEST (Compressed Heat Energy STorage) concept for facility scale thermo mechanical energy storage*. Energy 2014;69:543–52.

[3] Jockenhöfer, H., Steinmann ,W.-D., Bauer, D., *Detailed numerical investigation of a Pumped Thermal Energy Storage with low temperature heat integration*. Submitted to Energy

A theoretical approach to identify optimal replacement fluids for existing vapour compression refrigeration systems and heat pumps

D. Roskosch[1*], V. Venzik[1] and B. Atakan[1]

[1] University of Duisburg-Essen, Thermodynamics, Lotharstr. 1, 47057 Duisburg, Germany

[*]Corresponding author: dennis.roskosch@uni-due.de

Abstract

The nowadays used working fluids for vapour compression refrigeration systems and heat pumps partly have a high global warming potential and will have to be replaced. This holds for systems in operation but also to a large number of existing cycle designs. Therefore, it would be very helpful if alternative working fluids for a given plant could be found which do not require a redesign of the system and which, in best case, also are more efficient. Although it seems possible to achieve this goal with modern process simulation tools, it remains unclear how detailed a concrete plant design must be modelled to obtain a reliable ranking of working fluids, useful for selection. In order to investigate this question a vapour compression heat pump test rig is simulated by thermodynamic models with different levels of complexity. The model results are compared among each other and to measured values for various different fluids. It turns out that simple cycle calculations lead to incorrect results regarding the efficiency and thus are not sufficient to find replacement fluids for existing plants. The implementation of a compressor model significantly improves the simulation and leads finally to reliable fluid rankings. However, the information whether the heat exchangers are of sufficient size and whether the fluid is suited at all for a given task can only be obtained by means of the most complex model which includes extensive models for the heat exchangers.

Keywords: refrigerants, retrofit, process simulation, replacement fluids.

Introduction/Background

Induced by agreements of the United Nations and regulations of the European Union, fluid selection for thermodynamic cycles like refrigeration cycles or heat pump cycles has come back into focus. Various publication were published in recent years aiming to find fluids with a low global warming potential in order to replace the established hydrofluorocarbons (HFC). These investigations can generally be divided into theoretical and experimental approaches. The theoretical approaches commonly start with the process and compare different working fluids by means of mostly simple process simulations (e.g. [1]). The experimental work often evaluates the performance of different new fluids in a single test rig and compares the results, in part with common refrigerants (e.g. [2]). Such studies may be beneficial for new plants, where the fluid selection is part of the design process, but are not very helpful if a replacement fluid for a given existing system is to be found. The comparison of different fluids in a single test rig, and by means of simulations, leads to interesting findings but does not clarify how a fluid would actually perform in a different plant. Therefore, this work focuses on the development and comparison of different theoretical approaches to evaluate suitable replacement fluids for existing plants.

Discussion and Results

Figure 34 shows the coefficient of performance (COP) of various fluids from three different simulation levels and the measured values in a test rig. For each steady-state-scenario, the

evaluated COPs are given relative to the COP of R134a, which was assumed to be the fluid to be replaced. The first simulation level, a simple refrigeration cycle calculation with constant isentropic efficiency and fluid properties from REFPROP, leads only to marginal differences for the considered fluids and it results in large deviations when compared to the measurements. Implementing a model for the fluid dependent isentropic efficiency for the compressor [3] and a pinch-model for the heat exchangers (sim-2) improves the results significantly. The tendency of COP variation for the different fluids normalized to the value for R134a are generally reflected satisfactorily, however the COP of isobutane is overpredicted.

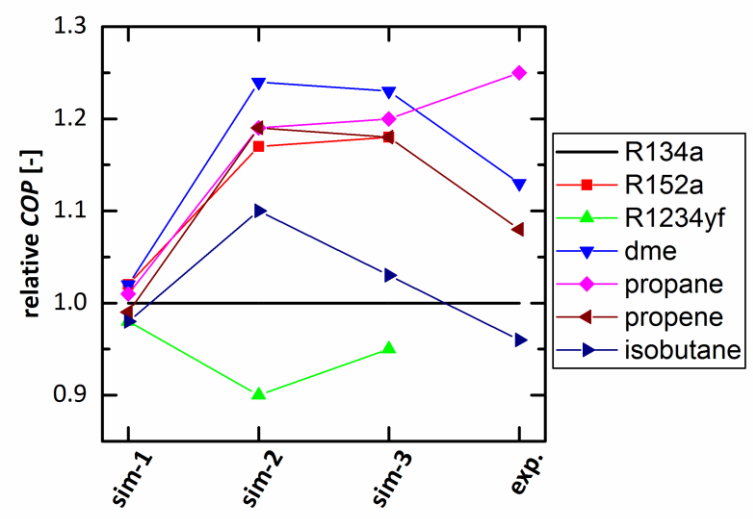

Figure 34: COPs of different fluids relative to the COP of R134a from three simulation levels and experimental results.

The third simulation level includes differential models for the heat exchangers, including correlations for the heat transfer coefficients, improving the COP results further. Besides the COPs, also the resulting fluid dependent heat fluxes are evaluated being another important process value. Finally, heat pumps have to guarantee a given heat flow rate. It turned out that the predictions of sim-3 modelling is also superior with respect to the heat flux predictions.

Summary/Conclusions

The present work shows that cycle modelling with constant compressor efficiency, as often applied in the literature, is not an appropriate tool to identify promising replacement fluids for existing plants or existing designs. Implementing a compressor model and a simple model for the heat exchangers already lead to reliable estimates, at least for trends. More complex models for the heat exchangers further improve the results, especially for the heat flux predictions but increase the computational effort largely.

References

[1] Dalkilic A.S, Wongwises S., A performance comparison of vapour-compression refrigeration system using various alternative refrigerants, International Communications in Heat and Mass Transfer(9) 2010;37, 1340–9.

[2] Sánchez D., Cabello R., Llopis R., Arauzo I., Catalán-Gil J., Torrella E., Energy performance evaluation of R1234yf, R1234ze(E), R600a, R290 and R152a as low-GWP R134a alternatives, International Journal of Refrigeration 2017;74, 269–82.

[3] Roskosch D., Venzik V., Atakan B., Thermodynamic model for reciprocating compressors with the focus on fluid dependent efficiencies, International Journal of Refrigeration 2017;84, 104–16.

Experimental Results of a 1 kW Heat Transformation Demonstrator based on a Gas-Solid Reaction

J. Stengler[1*], E. Fischer[1], J. Weiss[1] and M. Linder[1]

[1]German Aerospace Center (DLR), Institute of Engineering Thermodynamics,
Pfaffenwaldring 38-40, 70569 Stuttgart, Germany

[*]Corresponding author: jana.stengler@dlr.de

Abstract

Heat transformation based on reversible chemical reactions has gained significant interest due to the high achievable output temperatures. These chemical heat pumps use a reversible gas-solid reaction in which the back and forward reaction take place at different temperatures: by running the discharge reaction at a higher temperature than the loading reaction, the released heat is thermally upgraded. In this work, we report on the experimental investigation of a salt hydrate with regard to its use for heat transformation in the temperature range from 180 °C to 300 °C on a 1 kW scale. The reaction temperature is set by adjusting the pressure of the gaseous reactant, water vapor, in a range from 1 kPa up to 0.6 MPa. In our prior experimental studies, we found the properties of the solid bulk phase to be subject to considerable changes due to the chemical reaction: amongst others, the particle size distribution shifts, resulting in agglomeration and altered bulk permeability. In order to better understand how this affects the thermal performance of a thermochemical reactor, we combine our experimental work with a modelling approach. Our current work includes the development of a reactor concept that allows handling gas-solid reactions at high specific thermal powers as well as an easy scale-up for industrial applications.

Keywords: Heat Transformation, Thermochemical Reaction, Chemical Heat Pump, Thermal Upgrade, Gas-Solid Reaction

Introduction

Heat transformation processes are discussed in the context of industrial waste heat utilization. The basic concept of heat transformation requires three temperature levels and two pressure stages (see Fig. 1a). In our work, we developed a different approach to achieve thermal upgrade at a higher temperature range. As depicted in Fig. 1b, it requires four temperature stages: the two upper ones are related to the later application process; the two lower ones are used for thermal compression of the gaseous reactant. The lowest temperature level is needed for vapor removal from the reaction chamber (condensation at ambient temperature) in order for the reaction to reach complete turnover. Hence, the endothermic loading process takes place at a low pressure and temperature, respectively. This way, low value process heat is sufficient to charge the thermochemical reactor. During the exothermic discharging process, evaporation is driven by low temperature waste heat. Its temperature defines the vapor pressure and thus the maximum thermal upgrade of the released high value process heat.

With this approach, we are able to re-use low temperature waste heat from industrial processes as driving source for a high temperature heat pump. Depending on the chosen gas-solid working pair, the operating temperature of the heat pump process can be adapted to a specific application.

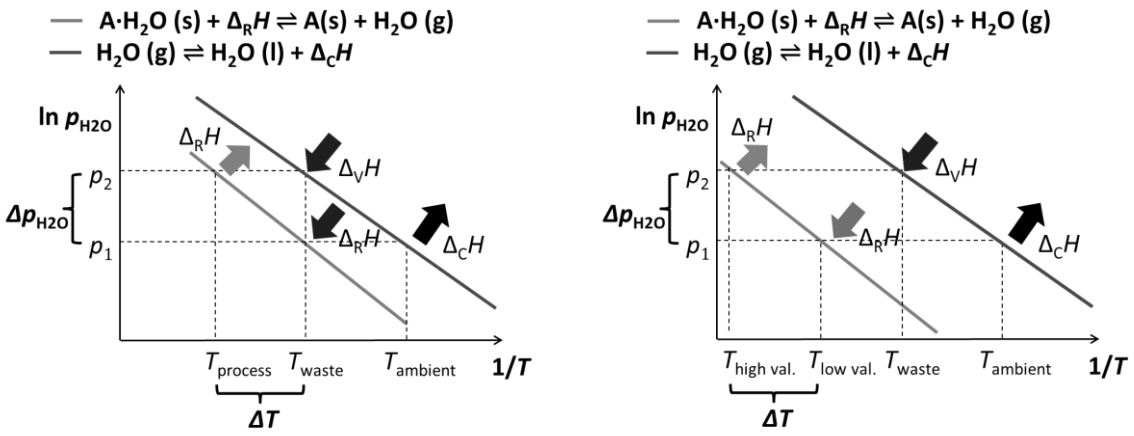

(a) (b)

Fig. 1: Van't Hoff diagrams of generic gas-solid reactions combined with the vapor-liquid equilibrium of the gaseous reactant. Depending on the chosen gas-solid working pair, two modes of operation are possible:
(a) thermal upgrade of low temperature waste heat, and
(b) thermal upgrade of high temperature process heat driven by low temperature waste heat (operation concept of this work).

Results and Discussion

In a previous study, we identified strontium bromide ($SrBr_2$) as a suitable candidate for thermochemical heat transformation [1]. Its exothermic reaction from the anhydrous phase to the monohydrate takes place at around 240 °C when water vapor is supplied at a pressure of 0.1 MPa. By performing experiments in a very simple generic reactor geometry, we observed agglomeration effects that occurred in the bulk already after 11 dehydration/re-hydration cycles [2]. To better understand how this affects the thermal performance of a thermochemical reactor, we included the relevant physical processes during the chemical reaction into a model based on FEM (finite element method). Based on our experimental experience and the results of our simulation studies, we developed a reactor setup that allows for high specific thermal powers, and that is easily scalable to larger applications.

Summary

We present first experimental results from our new test facility that allows for heat transformation with thermal powers of roughly 1 kW per kg of reactive material and output temperatures up to 300 °C, which is far beyond the working range of conventional heat pumps.

References

[1] Richter, M., Habermann, E.-M., Siebecke, E., Linder, M., "A systematic screening of salt hydrates as materials for a thermochemical heat transformer", Thermochimica Acta, 2017, doi:10.1016/j.tca.2017.06.011
[2] Stengler, J., Ascher, T., Linder, M., "High temperature thermochemical heat transformation based on $SrBr_2$", 12th IEA Heat Pump Conference 2017, May 14.-18.2017, Rotterdam, Netherlands.

A study on optimizing of pure working fluids in Organic Rankine Cycle (ORC) for different low grade heat recovery

Rong He[1], Xinling Ma[1,2] and Xinli Wei[1,2*]

[1] School of Chemical Engineering and Energy, Zhengzhou University, Zhengzhou 450001, Henan, China

[2] Research Centre on the Technology and Equipments for Energy Saving in Thermal Energy System, Ministry of Education, Zhengzhou 450001, Henan, China

*258366880@qq.com

Abstract

Organic Rankine cycle (ORC) is proved to be reliable technology that can efficiently convert these low to medium-grade heat sources into useful power [1-3]. This paper research the optimum working conditions by the 12 different working fluids. Among the group of pure working fluids in this study for different low grade heat recovery, at the temperature of 100℃, 120℃, 140℃, 160℃, the ORC make the maximum net-working respectively by R-115, R-227ea, R-236fa, R-236ea, R-114, R-245fa and R-601a. The maximum thermal and exergetic efficiency are R-245ca, R-600, R-236fa, R-114, respectively. The optimum evaporation temperature is about 0.8 to 0.85 times the heat source temperature, and the optimum evaporation temperature is 0.65 times the heat source temperature for the working medium with a critical temperature greater than the heat source.

Keywords: organic Rankine cycle, working fluids, performance optimization, net-working, thermal/exergetic efficiency.

Discussion and Results

Table 1. Optimization results of ORCs operating with pure working fluids.

H(℃)	Fluid	W(kW)	η_t (%)	η_{ex} (%)
100	R-227ea	255.926	7.80	22.09
120	R-227ea	532.13	10.46	29.62
140	R-C318	733.73	11.68	33.09
160	R-236ea	1076.07	14.51	41.09

H(℃)	Fluid	W(kW)	η_t (%)	η_{ex} (%)
100	R-245ca	222.171	7.80	22.09
120	R-600	378.97	10.46	29.62
140	R-236fa	704.93	11.68	33.09
160	R-114	973.95	14.51	41.09

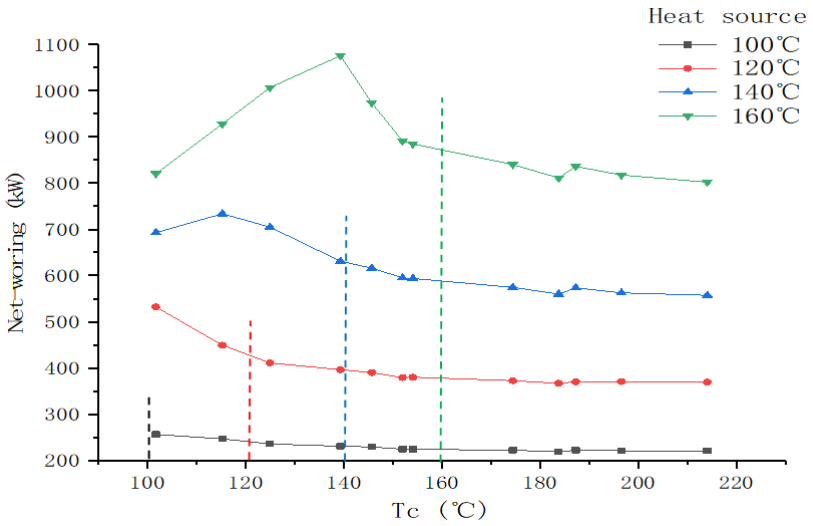

Figure 1. The trend of the net-working with the different working fluids

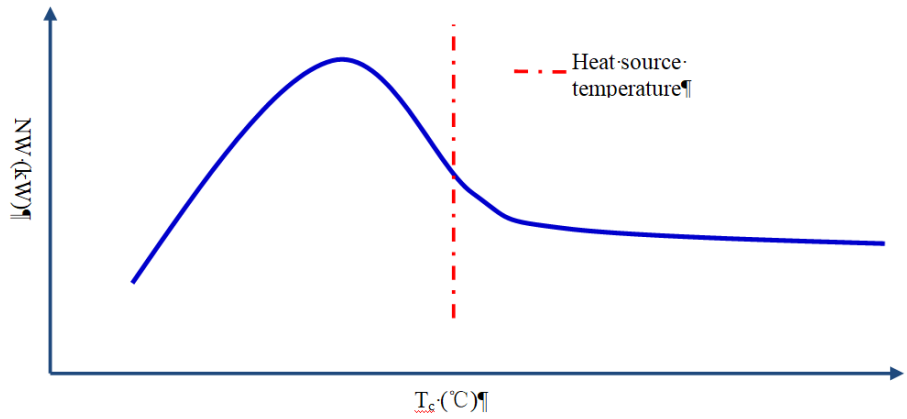

Figure 2. The trend of net output power with critical temperature of working fluids

Table 1 shows the optimization results with the method in this paper. The maximum net-working at 100℃, 120 ℃, 140 ℃, 160 ℃ respectively is 225.93kW (R-227ea), 532.13 kW (R-227ea), 737.73 kW (R-C318), 1076.07 kW (R-236ea). The maximum thermal and exergetic efficiency are always the same fluid, but different from the refrigerants with maximum power. It is R-245ca (η_t =8.59 η_{ex} =24.34), R-600(η_t =10.52 η_{ex} =29.81), R-236fa (η_t =12.89 η_{ex} =36.53), R-114 (η_t =14.72 η_{ex} =41.71), respectively.

From figure 1, we can divide the refrigerants into 3 groups: (1) Group 1: The critical temperature of refrigerants is greater than the heat source. With the increase of critical temperature, the net power decreases, but the change is not significant, and the R-601a always do the better than the R-123. (2) Group 2: The critical temperature of refrigerants are far less than the heat source temperature. With the increase of critical temperature, the net power increases rapidly until the critical temperature of refrigerants approaches the heat source temperature. (3) Group 3: The critical temperature of refrigerants are closed to and less than the heat source temperature.

The working fluid which critical temperature is 80%~85% of the heat source temperature always makes the maximum net-working. When critical temperature of working fluid is greater than the heat source, the evaporation temperature of the maximum net-working is about 65% of the heat source.

When the critical temperature of fluid is smaller than the heat source, the maximum net-working increases to a peak value as the mass-flow increases, and then sharp decline. It's like two linear equations crossing.

When the heat source temperature is constant, the maximum net output power first increases to a peak at 0.8 times HT and then decreases with the increase of critical temperature of working fluid, finally tends to be stationary.

In the future, we hope to verify our simulation through real devices and research on mixed refrigerants and transcritical conditions, and get the general equation between critical temperature and maximum net output power, such as the curve of figure 3.

References:

[1] Sylvain, Q., Martijn, B., Sebastien D., *Techno-economic survey of Organic Rankine Cycle (ORC) systems*. Renewable and Sustainable Energy Reviews, 2013.

[2] Satanphol, K., Pridasawas, W., Suphanit, B., *A study on optimal composition of zeotropic working fluid in an Organic Rankine Cycle (ORC) for low grade heat recovery*, Energy, 2017.

[3] Kiyarash, R., Saad, M., Raya K., *Review of organic Rankine cycle for small-scale applications.* Energy Conversion and Management, 207.

Numerical analysis of a heat pump based on combined thermodynamic cycles using ASPEN plus software

Mohammed Ridha Jawad Al-Tameemi[1], and Zhibin[1*]

[1]School of Engineering, University of Glasgow, Glasgow, G12 8QQ, Scotland

[*]Corresponding author: Zhibin.Yu@glasgow.ac.uk

Abstract

This paper proposes and analyses a gas fueled heat pump system that integrates a gas burner, an Organic Rankine Cycle (ORC) power generator, and an air-sourced heat pump (ASHP). The heat produced by the gas burner is used to drive an ORC power system to produce mechanical power that is directly used to drive a vapour compression cycle heat pump to produce heat using air as heat source. The heat rejected by ORC power system and contained in the flue gases is recovered for heating. A commercially available software ASPEN plus is used to model and analyse the proposed heat pump system. It is designed for domestic hot water application, so the cold tap water can be heated to 65 ^{o}C or more. Steady state evaluation and sensitivity analysis have been carried out on the integrated system. The results show that the proposed heating system can potentially achieve a significantly higher fuel-to-heat efficiency than other competing heating technologies, and can potentially be frost-free.
Keywords: Heat pump cycle, Organic Rankine cycle, Combined thermodynamic cycles.

Introduction

In the UK, approximately 50% of energy is consumed for heating applications, which accounts for nearly one third of the carbon emissions [1]. Gas boilers are the most common appliances for providing domestic hot water and central heating. There are some alternative heating technologies, including heat pumps (HPs), electrical resistive heaters, and micro-CHP (combined heat and power) systems, etc. However, these devices utilise electricity, mostly generated from fossil fuel, with resultant high wasted energy during power generation and transportation [2]. In the foreseeable future, gas will still be the main primary energy source for domestic heating in the UK. So far, only limited efforts have been made to investigate systems that integrate heat pumps with power generation cycles. This paper proposes and analyses a novel gas fueled heat pump system that integrates an ORC power generator, an air-sourced HP, and gas burner as shown in Figure (1).

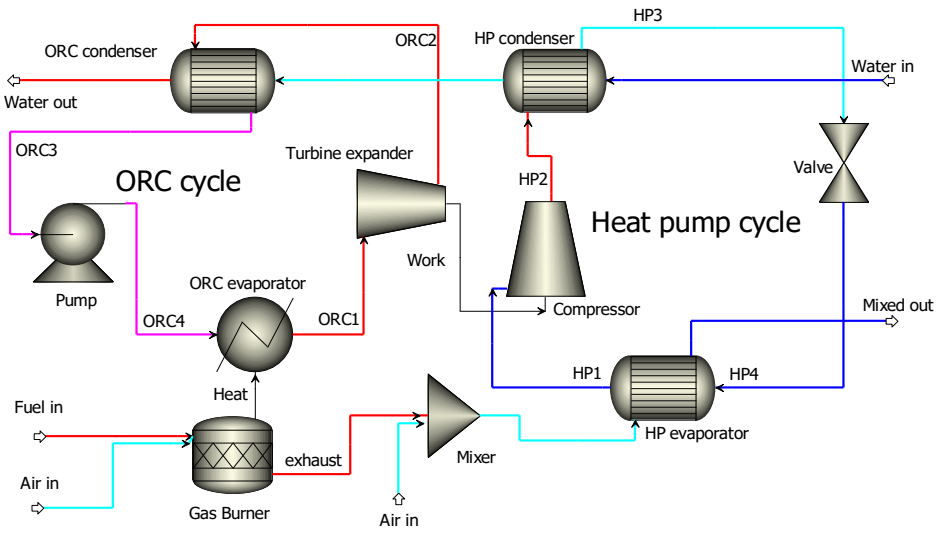

Figure 1 Combined cycle configuration

Discussion and Results

The proposed system simulated by ASPEN plus software. In addition, a MATLAB code linked with REFPROP software is used to obtain the TS diagrams for HP and ORC cycles (Figure 2).

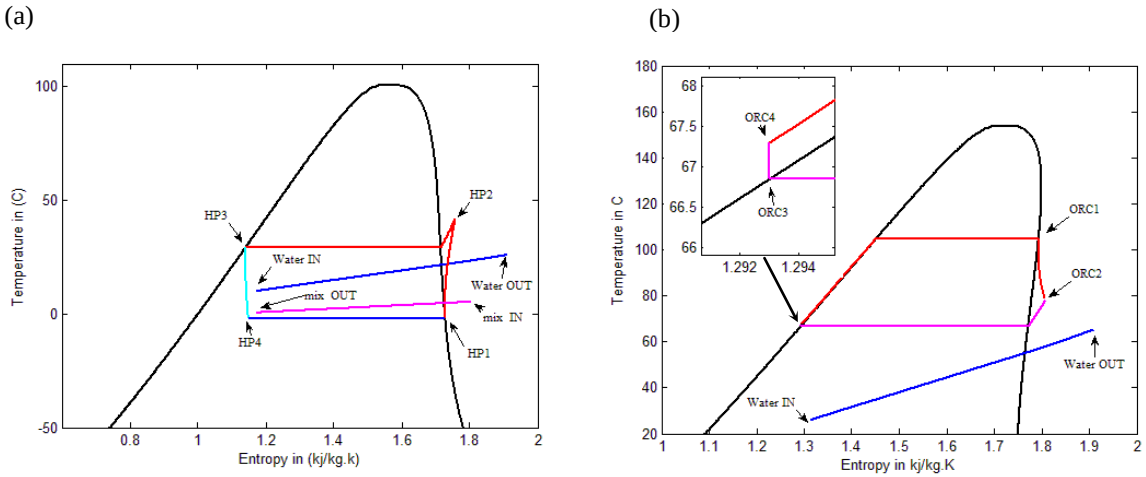

Figure 2. (a) TS diagram for HP cycle (R134a as working fluid); (b) TS diagram for ORC cycle (R245fa as working fluid)

Some of the simulation results of the proposed system are presented in Table 1.

Table 1 Combined cycle's results

	Heat pump cycle	ORC cycle
Condenser heat duty, kW	5.825	14.189
Water temperature leaving the cycle	26	65
Evaporator heat duty, kW	4.884	15.068
Temperature of gas mixture exiting the evaporator of the heat pump, ^{o}C	1.2	-
Power produced by the expander of ORC , kW	-	0.941
Power input to the compressor of HP, kW	0.941	-
Coefficient of performance	6.18	5.83%
Overall fuel-to-heat efficiency Combined cycle	117.88%	

Conclusions

Thermal analysis has been carried out for the combine system taking the advantages of CHP and heat pump technologies. The results show that although the outlet water temperature reaches 90 ^{o}C, however, the system achieved maximum efficiency at 65 ^{o}C. The advantages of the proposed system include: 1) High COP for heat pump; 2) The heat rejection by the power cycle can be utilized; 3) the heat contained in the flue gases can also be recovered. The results show that the proposed heat pump system can achieve a significantly higher fuel-to-heat efficiency in this preliminary design. Furthermore, its function for preventing frost formation in the evaporator of HP has also been demonstrated.

References:

[1] UK Government. The UK Low Carbon Transition Plan.
[2] Collings P., Al-Tameemi M., Yu Z., *A Combined Organic Rankine Cycle-Heat Pump System for Domestic Hot Water Applications*, 12th International Conference on Heat Transfer, Fluid Mechanics and Thermodynamics, Malaga, Spain, 11 - 13 Jul 2016.

Latent heat storage for direct integration in the refrigerant cycle of an air conditioning system

T. Korth[1*], F. Loistl[1], A. Storch[1], R. Schex[2], A. Krönauer[2] and C. Schweigler[1]

[1]Munich University of Applied Sciences, Lothstraße 34, 80335 Munich, Germany

[2]Bavarian Center for Applied Energy Research, Walther-Meißner-Straße 6, 85748 Garching, Germany

[*]timo.korth@hm.edu

Abstract

Theoretical and experimental investigations on latent heat storages (LHS) using paraffin as the phase change material with direct heat exchange with an evaporating or condensing refrigerant flow are presented. The focus is on the use of the LHS operated as a cold store serving as a "subcooler" for the refrigerant flow leaving the condenser of a vapour compression cycle. The results of the calculation models underline the feasibility and predict an increase of the cycle's refrigeration capacity during unloading of the LHS by about 25%.

Keywords: Latent heat storage, Phase change material, Air-Conditioning, VRF-System

Introduction/Background

The increased use of renewable energy sources leads to a growing demand for storage systems facilitating an efficient and consistent use of these energies. In the field of heating and cooling applications huge potential is seen in latent heat storages (LHS). The new approach which is presented in this paper comprises loading and unloading of the LHS by means of direct heat exchange with the refrigerant. The concept shall be applied for a Variable-Refrigerant-Flow heating and cooling system (VRF-System) which is driven by the electricity output of a PV generator. In VRF systems which directly act on the supply air flow no secondary heat carrier is available for integration of a heat or cold storage. Thus, a thermal storage in direct contact to the refrigerant cycle offers a straightforward solution with minimal technical complexity.

To study the storage under real conditions a pilot plant will be built. As preparation, laboratory experiments shall bring profound knowledge about the thermal performance of the thermal storage. Apart from other options, in the current development the heat storage serves as subcooler for the condensed refrigerant leaving the condenser of the refrigerant cycle. Aiming at efficient operation of the heat storage, heat conduction across the phase change material (PCM) in the storage is increased by addition of graphite powder or fins for the enhancement of the outer surface of the heat exchanger [1], [2].

Methodology

Integration of the latent heat storage acting as subcooler in the refrigerant cycle is shown in Figure 35 (left) together with the resulting enhancement of the evaporator capacity which can be read from the log(p)h-diagram for the refrigerant R410a (right). In loading mode the storage is connected in parallel to the evaporator and the cycle (solid line in Figure 1) operates with regular subcooling of the refrigerant at the condenser outlet (state points 1 to 6). During this loading phase the refrigerant evaporates in the LHS and heat is extracted from the storage. The dotted line marks the unloading process with subcooling of the liquid refrigerant by heat transfer to the LHS at the condenser outlet (state point 1' to 6'). Consequently, due to the reduced vapour quality of the refrigerant at the evaporator inlet an increased enthalpy change of the refrigerant in the evaporator is accomplished. As a result the refrigeration capacity increases, with unchanged operation of the compressor. A laboratory test rig which

has been built to investigate different operation modes of latent heat storages in a refrigerant cycle is used for analyzing the performance of the LHS acting in subcooler mode [3].

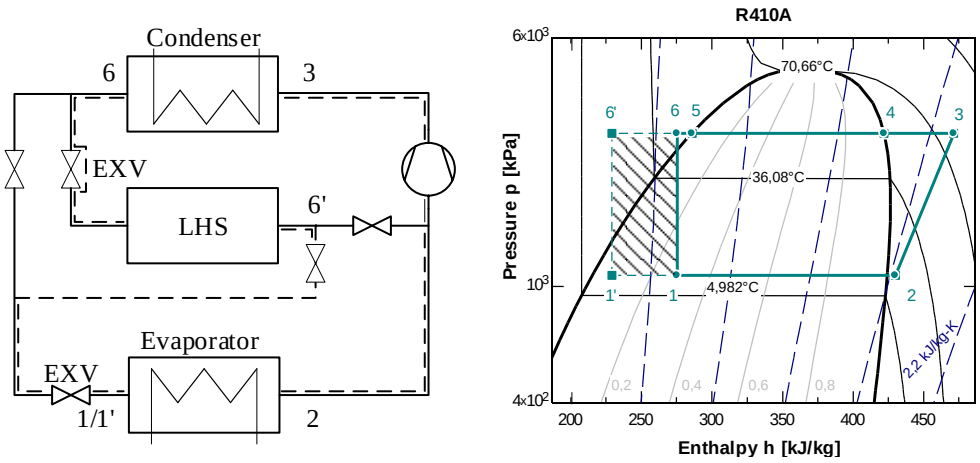

Figure 35: Integration of the latent heat storage in the refrigerant cycle (left) and enhancement of refrigeration capacity during unloading of the storage log(p)h-diagram (right).

Calculation Model and Results

The calculation model for the system has been implemented, using the Engineering Equation Solver (EES) Software. The time-dependent heat transfer characteristic of the LHS is calculated with regard to the varying heat resistance of the PCM. The assumption for this approach is an ideal radial melting of the solidified PCM volume around the refrigerant tubes passing through the volume of the LHS. Figure 36 shows the relative increase of the cooling capacity $Q_{boost}/Q_{nominal}$ in dependence on the degree of subcooling $\Delta T_{subcooling}$. The cycle modeling predicts at the given condition a capacity gain up to 30% of the cooling capacity.

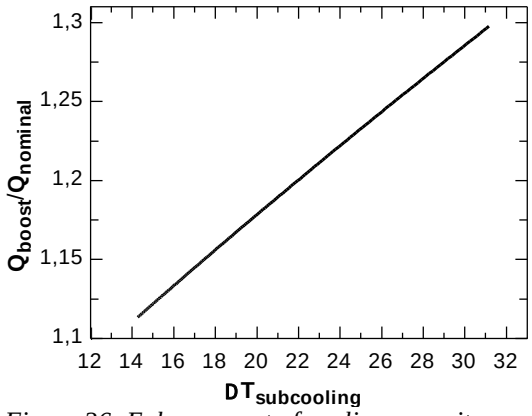

Figure 36: Enhancement of cooling capacity during unloading of the storage.

Conclusions

To take advantage of the characteristics of a latent heat storage, the LHS can be implemented in an air-conditioning system in order to subcool the refrigerant after the condenser. A gain of refrigeration capacity of about 1% per Kelvin subcooling of the refrigerant is obtained. Thus for typical operating conditions a maximum gain of capacity of about 25 % can be achieved. To state the change of the overall efficiency of the system a whole cycle with loading and unloading of the storage has to be taken into account. Based on experimental data the theoretical prediction for the cycle performance shall be verified. In addition, the dynamic behavior will be used for validation of the thermal modeling of the LHS.

References:

[1] Mehling, Harald; Cabeza, Luisa F., Heat and cold storage with PCM – An up to date introduction into basics and applications, Springer Verlag, Heidelberg, 2008

[2] Hauer, A., Hiebler, S., Reuß, M., Wärmespeicher, 5., vollständig überarbeitete Auflage, Fraunhofer IRB Verlag, Karlsruhe, 2013

[3] Loistl, F., Korth, T., Schweigler, C., Einsatz von Latentwärmespeichern in Klimageräten, DKV-Tagung, Kassel, 2016

Detailed exergetic analysis of a packed bed thermal energy storage unit in combination with an Organic Rankine Cycle

A. König-Haagen* and D. Brüggemann

Chair of Engineering Thermodynamics and Transport Processes (LTTT), Center of Energy Technology (ZET), University of Bayreuth, Universitätsstraße 30, 95447 Bayreuth, Germany

*Corresponding author: andreas.koenig-haagen@uni-bayreuth.de, lttt@uni-bayreuth.de

Abstract

Thermal energy storage (TES) can reduce or overcome the issues that appear when an Organic Rankine Cycle (ORC) is adopted to a fluctuating heat source. However, detailed exergetic studies about the optimisation potential and the influence of the TES on the overall system are still missing for this application and TES in systems in general. Therefore, in this work a detailed exergetic evaluation is numerically performed for a packed bed TES in combination with an ORC. For the chosen boundary conditions, the overall pressure drop and the heat resistance from the heat transfer fluid (HTF) to the particle have the most influence on the overall exergetic efficiency. By optimizing the parameters of the storage unit, the overall exergetic efficiency can be increased from 36 % to 43 %.

Keywords: packed bed thermal energy storage, Organic Rankine Cycle, exergetic analysis

Introduction/Background

In the future energy supply thermal energy storage (TES) can play a key role. One promising application for TES is the combination with an Organic Rankine Cycle (ORC) for the utilization of fluctuating waste heat. Here, the TES allows to downsize the ORC and to run it less in off-design. For evaluation and optimization of such a system, exergetic analysis are well suited. However, in most previous studies the TES was simplified very strongly e.g. Manfrida et al. [1] and hence no detailed analysis of the TES nor the overall system was possible.

Figure 37: Storage modules of the combined TES and ORC facility at the University of Bayreuth

Therefore, within this work a detailed numerical model – validated with results of a demonstrator located at the University of Bayreuth (UBT), see Figure 1 – is adopted for the storage unit to study the combination of TES and ORC. The model is set up in MATLAB Simulink and the ORC is implemented based on characteristics deduced from the results of Preißinger [2]. A comprehensive exergetic analysis is performed which takes into account the optimisation limits of the TES and its influence on the overall system. For this purpose the storage and the periphery is idealized to identify the effect of different physical aspects on the exergetic efficiencies. The physical aspects which were studied are: heat losses to the ambient from the storage and the periphery, pressure drop within the storage and the periphery, heat resistance from the heat transfer fluid (HTF) to the particles and heat conduction in flow direction within the packed bed. The influence of each physical aspects y is calculated by

	$y = \frac{\varepsilon^{ideal}}{\varepsilon^{real}}$	(1)

with ε^{real} the exergetic efficiency of the real process and ε^{ideal} the exergetic efficiency of the idealized process, whereat y can be determined for a single component up to the entire system.

Discussion and Results

A TES with 4.7 t of sand (this corresponds to one module of the storage system developed by enolcon GmbH and set up at the UBT, see Figure 1) with a diameter of 2 mm is considered in combination with an ORC working with toluene [1]. Air is used as HTF for the vertical flow TES with six parallel sections. Each section has a size of about 1.1 m x 1.1 m x 0.4 m in depth, height and length, respectively. For a charging temperature of 600 °C and a standard volume flow of 2/3 m³/s exergetic efficiencies of about 36 % for the overall system and more than 80 % for the TES where achieved in the numerical simulations with the TES as it is. The overall pressure drop and the heat resistance from the HTF to the particles have the highest influence on the exergetic efficiency of the system. The influence of the physical aspects is outlined in Figure 2.

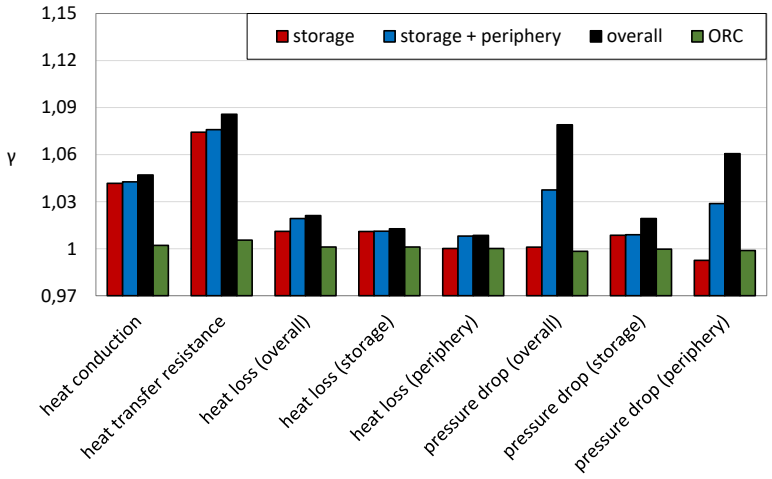

Figure 38: Influence of physical aspects on the exergetic efficiencies of different components and the overall system

After an optimization performed with a downhill simplex method [3] combined with a branch-and-bound algorithm the influence of the physical aspects gets much more even. The achievable exergetic efficiencies are more than 90 % for the TES and about 43 % for the overall system.

Summary/Conclusions

A detailed exergetic analysis of a TES in combination with an ORC is performed. Within this scope validated numerical models are applied and the influence of several physical aspects on the exergetic efficiencies of the TES and the complete system are analysed. The entire pressure drop and the heat resistance from the HTF to the particles have the highest influence on the overall exergetic efficiency. By means of an optimization this efficiency increased from 36 % to 43 %.

References:

[1] Manfrida, G. et al. *Modelling and simulation of phase change material latent heat storages applied to a solar-powered Organic Rankine Cycle*. Applied Energy 2016;179:378–88.

[2] Preißinger, M. *Thermoökonomische Bewertung des Organic Rankine Cycles bei der Stromerzeugung aus industrieller Abwärme*. Dissertation Univ. Bayreuth, Logos Verlag Berlin GmbH, 2014.

[3] Nelder, J. A., Mead, R. A. *Simplex Method for Function Minimization*. Comput J 1965;7:308–13.

Novel High Temperature Steam Transfer Pipes

M. J. Tierney[1], M. Pavier[1]

[1]Department of Mechanical Engineering, University of Bristol, UK, BS8 1TR.

[2]Affiliation and full institutional address

[*]Corresponding author: mike.tierney@bristol.ac.uk

Abstract

Cycle analysis has been applied to simple versions of supercritical steam plant with novel steam transfer pipes. The impact of this innovation on cycle efficiency was acceptably small.

Keywords: A-USC cycles, cycle analysis, thermal coatings

Introduction/Background

We have proposed that Advanced Ultra Super Critical (A-USC) power plant might incorporate internally coated and externally cooled pipe sections (Figure 1). This would cool the pipes below a limit enabling more readily available steel alloys to replace part of the 32% nickel content in metals in proposed plant [1]. An illustrative example concerns a straightforward regenerative cycle with superheat (Figure 2) with a thermally coated zone (TCZ) cooled with feedwater. At any axial location (z) along the TCZ the hottest pipe-wall temperature ($T_w(z)$) is related to thermal resistances R_1 and R_2 by

$$\dot{Q}_r(z) = \frac{T_{steam} - T_w(z)}{R_1} = \frac{T_w(z) - T_{coolant}}{R_2} \quad ; \quad T_w(z) < T_{limit}$$

where R_1 acts between the bulk supercritical steam and pipe-inner-surface, and R_2 acts between the pipe-inner-surface and the bulk coolant.

Discussion and Results

For co-current cooling, R_2 and coolant flow rate were adjusted so that $T_2 = T_{limit}$ at all axial locations; a range of temperature limits had little effect on the cycle efficiency (Table 1 (a)). For counter-current cooling, the coolant flow rate was adjusted to give $T_w(0) = T_{limit}$ at z=0. Reducing coating thickness from 5-mm to 1-mm similarly had minimal impact on cycle efficiency (Table 1(b)). Co-current cooling gave a slightly higher efficiency.(Compare the 44.75% in part (a) against the 44.67% in part (b)). For more complex plant (please see the full paper) reductions in cycle efficiency were less than the small gains of 1% in moving from single to double reheat cycles [2], and far less than the 15% gain in moving from conventional cycles to A-USC [1].

Summary/Conclusions

Reductions in cycle efficiencies owing to TCZs might well be justified by acceptably lower temperatures and use of more sustainably available materials of construction.

References

[1] Marion, J., Drenik, O., Frappart, C., Kluger, F., Sell, M., Skea, A., Vanstonee, R., Walker, P. Advanced ultra-supercritical steam power plants, Proc IEA Clean Coal Centre W'shop

[2] K. M. Retzlaff, W. A. Ruegger, Steam turbines for ultrasupercritical power plants, POWER-GEN, Vol. 98, 1996, pp. 9–11.

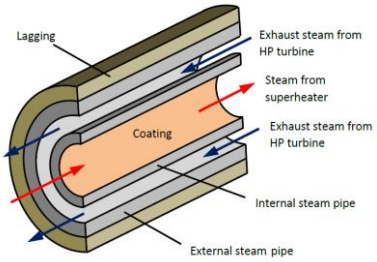

Figure 1 Proposed arrangement of cooled steam pipe

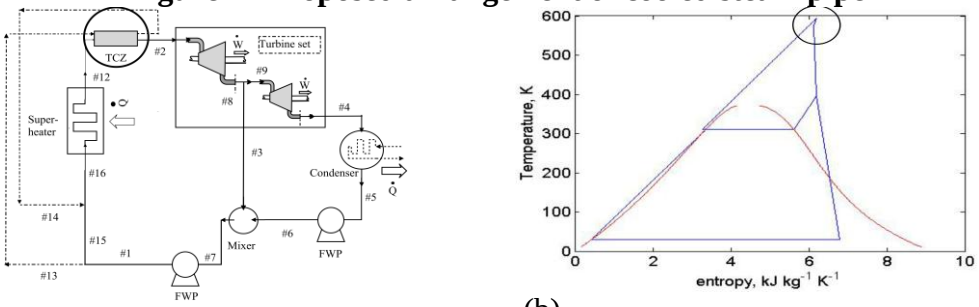

(a) (b)

Figure 2: regenerative cycle with thermally coated zone (a) plant (b) TS diagram. Thermal resistance R_1= 0:0221K kW^{-1} (a only), turbine isentropic efficiency = 90 %,T_5 = 29.0°C (condenser), T_{12} = 593.8°C (superheater)

Table 1: Impact of limiting temperature (co-current) or coating thickness (counter-current) on cycle efficiency. Parameters are λ_{tcz} = 1.2 W m^{-1} K^{-1}, T_{12} = 593.8°C

T_{limit} , °C	Cycle efficiency, %	Coolant flow rate, fraction of m_1	T_2 °C	w_{tcz}, m
No cooling	44.83	-	593.8	0.005
(a) Co-current cooling				
590	44.82	0.72%	593.3	0.005
550	44.75	9.72%	588.1	0.005
500	44.66	26.32%	581.6	0.005
450	44.57	54.91%	575.1	0.005
425	44.52	78.64%	571.9	0.005
(b) Counter-current cooling				
550	44.67	3.088%	582.2	**0.005**
550	44.60	5.012%	577.6	**0.003**
550	44.39	43.9 %	562.9	**0.001**

Technical and thermodynamic evaluation of hybrid binary cycles with geothermal energy and biomass

D. Toselli*, F. Heberle and D. Brüggemann

Chair of Engineering Thermodynamics and Transport Processes (LTTT),
Center of Energy Technology (ZET), University of Bayreuth
Universitätsstraße 30, 95447 Bayreuth, Germany

*Corresponding author: davide.toselli@uni-bayreuth.de

Abstract

Combining two different renewable sources available in Bavaria could represent a valuable choice in order to produce green and flexible power. In this study, hybrid binary cycles are investigated exploiting both geothermal energy and biomass. For this purpose, different power plant layouts are analysed and several off-design working conditions are considered. Biomass is firstly defined as a biogas waste heat recovery providing an increase of about 250 kW on the geothermal cycle, which produces alone 4.35 MW. Higher power rates are obtained while adopting an additional storage system and exploiting solid biomass, increasing both the nominal power (5 MW) and the power granularity (1 MW) in order to comply with the German Energy Market requirements.

Keywords: Geothermal, Biogas Waste Heat Recovery, Flexible Power Generation, Minute Reserve

Introduction/Background

Flexible power generation is an everyday more and more diffused challenge that increasingly affects the German power grid due to higher shares of renewable resources. Enhancing renewable and flexible power generation is one of the most important topics in the Energiewende agenda. The geothermal power plant in Oberhaching is taken as a case study since it represents the typical Bavarian geothermal reservoir (130 °C as brine temperature), with a gross power output equal to 4.3 MW_{el}. The major objective of this study is to investigate the possibility to design a binary hybrid geothermal power plant and to integrate it into the German Energy Market, taking as secondary available resource exhaust gases coming from a biogas engine (GE Jenbacher JMS 620 GS-B.L) with an available thermal power equal to 1365 kW_{th}.

Discussion and Results

Three main concepts are defined in order to exploit the available exhaust gases: increasing the geothermal fluid temperature (A) (see Figure 2), superheating the working fluid (B) and adopting an additional evaporator where the working fluid is heated only by exhaust gases (C) [1]. Simulations have been performed with Aspen Plus 8.8, according to stationary and quasi-stationary conditions. After a brief comparison, R600a is chosen as optimal working fluid. First simulations demonstrated that the additional thermal power allows reaching an increase of electric power of approximately 250 kW, depending on the followed layout. Next to a valuable comparison of the three on-design concepts, off-design conditions are also investigated [2], regarding both the unavailability of exhaust gases and the yearly ambient temperature variations [3]. Since the available extra thermal power does not result as enough in order to comply with the Minute Reserve requirements, additional solutions are investigated. In this context, applying a storage system and, furthermore, increasing the extra

thermal power seem to be feasible concepts. With regard to the latter, the secondary resource is redefined as exhaust gases from a solid biomass power plant, according to the typical German boundary conditions [1]. The two purposed solutions allow separately reaching the two main requirements asked by the Minute Reserve: a nominal power equal to 5 MW and 1 MW as power granularity. While the previously assumed models are defined as on-design when exhaust gases are available, also a different configuration is investigated as off-design, when exhaust gases are available. In the end, a feed-in tariffs analysis is performed in order to generally evaluate the advantages of adopting a binary hybrid power plant. According to the assumed hypothesis, it is demonstrated that a unique hybrid power plant instead of two separated ones can lead to a reduction in cost of maintenance while increasing the revenues nett values.

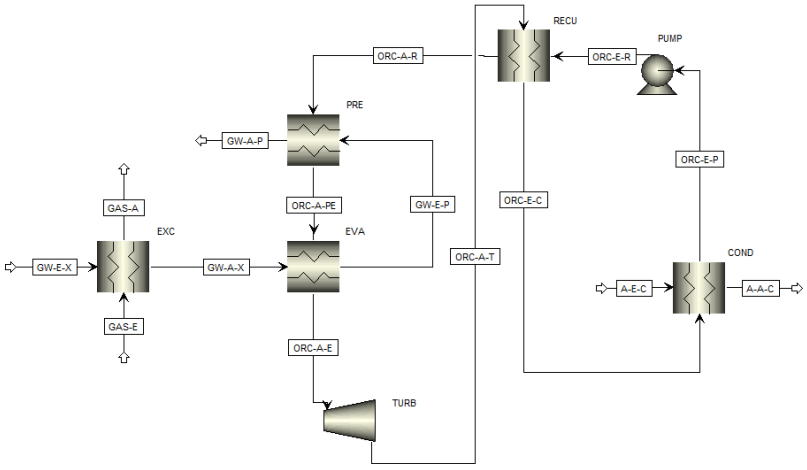

Figure 2: Hybrid binary cycles layout according to Concept A. Biogas exhaust gases are exploited in order to increase the geothermal wellhead temperature.

Table 1: Main results regarding Concept A and Concept B in on-design (when geothermal and biogas exhaust gases are exploited)

Concept	Turbine Power as on-design [kW]	Evaporating Pressure [bar]	Condensing Pressure [bar]	Working fluid mass flow [kg/s]
A	4594	14.8	3.95	109.9
B	4500	14.6	3.96	106.1

Summary/Conclusion

This work aims to provide a valuable and extended overview regarding the possibility to realize a hybrid binary power plant which exploits geothermal energy and waste heat recovery from gaseous biomass. Nowadays, no similar examples to what is presented in this work already exist in Germany, even if hybrid solutions may provide more flexibility in the energy market and can contribute to develop renewable power production.

References

[1] Macchi, E., Astolfi, M., Organic Rankine Cycle (ORC) Power Systems - Technologies and Applications, Woodhead Publishing, 2015.

[2] Ghasemi, H., Hybrid solar-geothermal power generation: optimal retrofitting, in Applied Energy, Elsevier, 2014, pp. 158-170.

[3] Toffolo, A., Lazzaretto, A., Manente, G., Paci, M., An Organic Rankine Cycle off-design model for the search of the optimal control strategy, in Proceedings of ECOS , Perugia, Italy, 2012.

Experimental Analysis of a Regenerative Organic Rankine Cycle using Zeotropic Working Fluid Blends

Peter Collings[1], Andrew McKeown[1] and Zhibin Yu[1*]

University of Glasgow, University Avenue, Glasgow G12 8QQ, UK

[*]Corresponding author: zhibin.yu@glasgow.ac.uk

Abstract

In order to reduce harmful carbon dioxide emissions, as well as increase, affordability and security of energy supply, it is vital that we either increase the efficiency of current power generation processes, of make use of the large amount of low-temperature thermal energy contained in low-temperature heat sources. The Organic Rankine Cycle (ORC) has been identified as the most promising technology for exploiting the lower temperature range of these heat sources, which exist at less than 200°C. There is a lack of published literature on experimental analysis of ORCs, and most of this focuses on pure working fluids and non-regenerative cycles. The motivation for this paper is to address the gap in the literature by constructing a small-scale regenerative ORC test rig capable of being charged with a mixture of the working fluids r245fa and r134a, and comparing the obtained results with numerical predictions. The key findings were that the cycle efficiency increased with the implementation of the regenerative cycle, although the increased flow resistance from the additional heat exchanger did decrease the mass flow rate of the working fluid. Adding a secondary component to the working fluid with a higher vapour pressure increased the temperature glide, however, it also increased the condenser pressure of the cycle, reducing the overall efficiency compared to the pure working fluid, while also reducing the efficiency of the heat transfer process. The maximum net efficiency of the cycle was 6.4% with a heat source temperature of 95°C and a working fluid composed of pure R245fa.

Keywords: Organic Rankine Cycle, Zeotropic, Regenerative, Experimental

Introduction/Background

Table 2: Representative comparison of experimental Organic Rankine Cycles reported in the literature

Author	Working Fluid	Regen	Heat Source	Expander	Power	Efficiency
Peris et al [1]	R245fa	Yes	165°C	Scroll	7.5 kW	8.8%
Wang et al [2]	R245fa	No	115°C	Piston	1.73kW	4.2%
Pu et al [3]	Pure R245fa/ Pure HFE7100	No	100°C	Turbine	1.98kW	4.01%
Quoilin et al [4]	R123	No	165°C	Scroll	1.8kW	9.9%
Navarro-Esbrí et al [5]	HFO-1336mzz-Z	Yes	160°C	Scroll	1.1kW	8.3%
Jung et al [6]	R245fa/ 365mfc	No	160°C	Scroll	0.47kW	3.1%
Abadi et al [7]	R245fa/R134a	No	120°C	Scroll	1.4kW	7%

Table 2 presents a brief comparison of pre-existing experimental research on the Organic Rankine Cycle. From this information it can be seen that previous research has focused mainly on non-regenerative cycles and pure working fluids. There does not appear to be any previous experimental research comparing the effects of regenerative and non-regenerative cycles in the same system, zeotropic working fluids have been investigated there were no studies investigating the effect of progressively changing the working fluid composition on a single system. A MATLAB model was developed using REFPROP 9.1 [8], and was used to design a system capable of investigating the effects of these two key parameters. Using the data from this model a 1kW experimental rig was built and tested in both regenerative and non-regenerative configurations across a range of working fluid compositions, heat source

temperatures, pressure ratios to provide an experimental characterisation of how a real system reacts to variation in these parameters, compared to theoretical predictions.

Discussion and Results

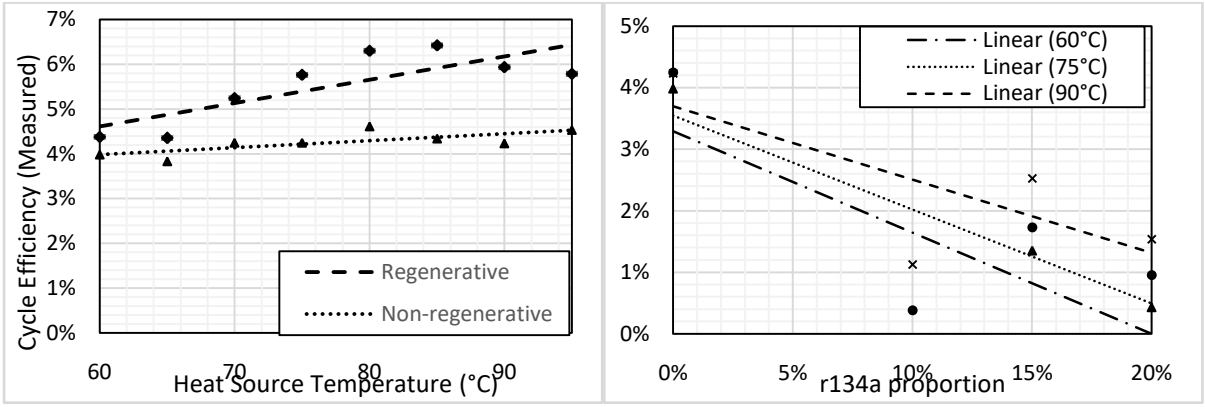

Figure 39: Variation in Cycle Efficiency with the implementation of the regenerator (left) and with varying working fluid composition (right)

The main results of this experimental analysis are shown in Figure 39. It can be seen that the addition of a regenerator to the cycle increases the cycle efficiency noticeable, with an increasing effect at higher heat source temperatures. It can also be seen that increasing the proportion of the lower-boiling-point component r134a in the working fluid reduces the cycle efficiency, an effect thought to be due to the decreased cycle pressure ratio that this causes.

Summary/Conclusions

A 1kW experimental ORC rig has been designed and built, and used to analyse the effects of working fluid composition, cycle configuration, heat source temperature and pressure ratio on the efficiency of the cycle. It was found that adding a regenerator and increasing the heat source temperature and pressure ratio both increased the efficiency of the cycle, but that adding a secondary working fluid component with a higher vapour pressure reduced the pressure ratio and therefore the power output and cycle efficiency.

References:

[1] B. Peris, J. Navarro-Esbrí, F. Molés, J. P. Martí and A. Mota-Babiloni, "Experimental Characterisation of an Organic Rankine Cycle (ORC) for micro-scale CHP applications," *Applied Thermal Engineering*, vol. 79, pp. 1-8, March 2015.

[2] X. Wang, L. Zhao, J. Wang, W. Zhang, X. Zhao and W. Wu, "Performance Evaluation of a Low-Temperature Solar Organic Rankine Cycle System utilising R245fa," *Solar Energy*, 2009.

[3] W. Pu, C. Yue, D. Han, W. He, X. Liu, Q. Zhang and Y. Chen, "Experimental Study on Organic Rankine Cycle for Low Grade Thermal Energy Recovery," *Applied Thermal Engineering*, vol. 94, pp. 221-227, February 2016.

[4] S. Quoilin, V. Lemort and J. Lebrun, "Experimental Study and Modeling of an Organic Rankine Cycle using Scroll Expander," *Applied Energy*, vol. 87, no. 4, pp. 1260-1268, April 2010.

[5] J. Navarro-Esbri, F. Molés, B. Peris, A. Mota-Babiloni and K. Kontomaris, "Experimental Study of an Organic Rankine Cycle with HFO-1336mzz-Z as a low global-warming potential working fluid for micro-scale low temperature applications," *Energy*, vol. 133, pp. 79-89, August 2017.

[6] H.-C. Jung, L. Taylor and S. Krumdieck, "An Experimental and Modelling Study o a 1kW Organic Rankine Cycle Unit with Mixture Working Fluid," *Energy*, vol. 81, pp. 601-614, March 2015.

[7] G. B. Abadi, E. Yun and K. C. Kim, "Experimental Study of a 1kW Organic Rankine Cycle with a Zeotropic Mixture of R245fa/R134a," *Energy*, vol. 93, no. 2, pp. 2363-2373, December 2015.

[8] E. Lemmon, M. Huber and M. McLinden, " NIST Standard Reference Database 23: Reference Fluid Thermodynamic and Transport Properties-REFPROP, Version 9.1," Gaithersburg, 2013.

Experimental Results from R245fa Ejector Chiller

J. Mahmoudian[1], A. Milazzo[1*], I. Murmanskii[2], A. Rocchetti[1]

[1]DIEF - Department of Industrial Engineering – University of Florence – via di S.Marta, 3 – 50139 Firenze (ITALY)

[2] Ural Power Engineering Institute, Ural Federal University, Ekaterinburg, Russia

[*]Corresponding author: adriano.milazzo@unifi.it

Abstract

Ejector chillers need a significant performance increase in order to be competitive with other heat-powered refrigeration systems. DIEF is continuing its experimental activity on a 40 kWf prototype, which features a modified CRMC design of the ejector. The working fluid, R245fa, has favourable thermodynamic properties (e.g. dry expansion and moderate pressure at generator) and allows sub-zero temperatures at evaporator. This paper reports some experimental results and shows that our prototype chiller is able to reach relatively low evaporation temperatures, even if the performance is obviously lowered with respect to the design condition.

Keywords: Ejector chiller, CRMC, R245fa, Experimental.

Background

R245fa was tested as a working fluid for an ejector chiller in 2006 by Eames et al. [1]. This fluid has a vapour density at 5°C which, when compared to steam, is 586 times bigger and hence should reduce the physical size of the system. Moreover, the saturated vapour curve of R245fa has a positive slope and hence an isentropic expansion starting from the generator outlet conditions does not enter the wet-vapour region. Finally, the saturation pressure at generator for R245fa ranges from 8 to 20 bar (at 80 and 120°C respectively), while a more common refrigerant like R134a would need 26 bar at 80°C and would reach the critical point at 101°C with a pressure above 40 bars. A lower pressure at the generator greatly simplifies the selection and operation of the feed pump.

The ejector described in ref. [1] was a CRMC design, i.e. the flow sections were calculated by imposing a constant rate of deceleration along the mixer/diffuser. The experimental results showed that for saturation temperatures of 110°C at generator and 10°C at evaporator the COP could be as high as 0.47, with a critical condenser temperature of 32.5°C. Raising the generator temperature at 120°C, the COP was decreased to 0.31, but the critical condenser temperature was 37.5°C.

A modified version of the CRMC profile, featuring a conical exit, was used in our prototype. A complete description of the ejector, as well as some experimental and numerical results, were presented in ref. [2]. Saturation temperature was 90°C at generator and 10°C at evaporator, yielding a COP of 0.55 and a critical condenser temperature around 29.5°C. When the saturation temperature at the evaporator was lowered at 5°C, the COP was 0.41 and the critical condenser temperature was 28°C. By comparison with numerical results, the importance of a smooth internal surface was demonstrated, chiefly in terms of critical condenser temperature.

Meanwhile, the problem of high GWP affecting R245fa was addressed in ref. [3]. According to thermodynamic simulations, the best candidates for replacing this fluid were water and R1233zd. Obviously, the first option would require a complete re-design of the ejector and would be suitable for relatively high generator and evaporator temperatures. On the other

hand, R1233zd should basically guarantee a drop-in replacement and could be an interesting option for lower temperature applications. Therefore, it was decided to continue the experimental activity on the existing prototype at low evaporation temperature.

Discussion and Results

An example of experimental result is shown in Fig. 1. In order to guarantee a stable operation and a reasonable critical condenser temperature at low evaporator temperature, the generator temperature was raised at 95°C. This produces a lowering of the COP with respect to the results presented in ref. [2]. On the other hand, at evaporator temperature $T_{E\text{-}sat}$ = 5°C, the critical condenser temperature is now 30.5°C. The efficiency at $T_{E\text{-}sat}$ = -5°C is obviously very low, but this working condition is far from the design point and hence represents a limit operation mode.

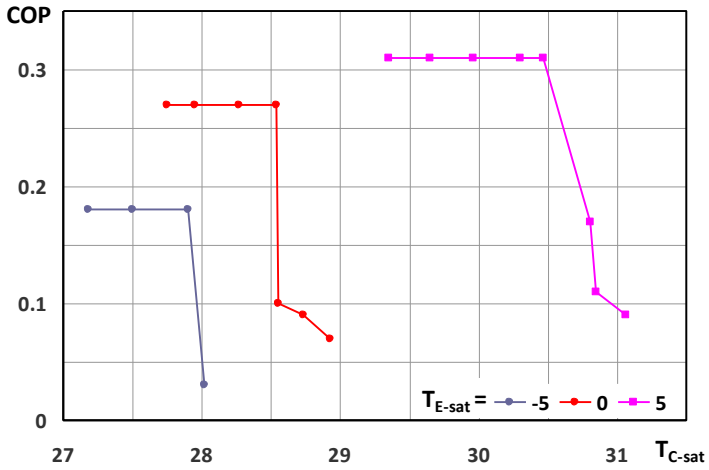

Fig. 1 – COP as a function of saturation temperature at the condenser

Summary/Conclusions

The CRMC ejector chiller working with R245fa has proved to be effective even at relatively low evaporation temperatures. If specifically designed, an ejector featuring the same criteria and structure could be suitable for new applications. The experimental activity will continue on the same prototype as soon as the replacement fluid R1233zd will be available. Hopefully this activity will prove the feasibility of a robust and low-cost heat powered refrigeration system, featuring a low-GWP refrigerant and operating below 0°C with a moderate temperature heat input.

References:

[1] Eames, I.W., Ablwaifa, A.E., Petrenko V., "Results of an experimental study of an advanced jet-pump refrigerator operating with R245fa", Applied Thermal Engineering, 2007, doi.org/10.1016/j.applthermaleng.2006.12.009

[2] Mazzelli F., Milazzo A., "Performance analysis of a supersonic ejector cycle working with R245fa", International Journal of Refrigeration, 2015, doi.org/10.1016/j.ijrefrig.2014.09.020

[3] Milazzo, A., Rocchetti, A., "Modelling of ejector chillers with steam and other working fluids", International Journal of Refrigeration, 2015, doi.org/10.1016/j.ijrefrig.2015.05.015

Adapting the $MgO-CO_2$ working pair for thermochemical energy storage by doping with salts

A. I. Shkatulov[1,2*], T. Yu. Kardash[1,2] and Yu. I. Aristov[1,2]

[1]Boreskov Institute of Catalysis, Ac. Lavrentiev av. 5, Novosibirsk 630090, Russia

[2]Novosibirsk State University, Pirogova st. 2, Novosibirsk 630090, Russia

[*]Corresponding author: shkatulov@catalysis.ru

Abstract

Thermochemical energy storage (TES) is a promising technology which provides durable storage and high storage density. In this work, the $MgO-CO_2$ working pair was adapted for TES by the oxide modification with a salt. A brief screening of various salts showed that a lithium acetate (LiOAc) additive considerably promotes the MgO carbonation. The kinetics of the process was studied at T = 280°C-340°C and P(CO_2) = 1-10 bar. Decomposition of LiOAc/$MgCO_3$ was studied by differential scanning calorimetry. The transitions of MgO to $MgCO_3$ and backwards were studied by X-ray diffraction analysis *in situ*.

Keywords: Thermochemical energy storage, Magnesiun oxide/carbonate, Modification

Introduction

Search for novel materials for efficient TES at medium temperatures (200-400°C) is important since this technology is promising for utilizing waste heat from some industrial processes. One of the materials proposed for TES is $MgCO_3$ which is able to store/release heat due to the reversible reaction $MgCO_3 = MgO + CO_2$ with the high enthalpy (96 kJ/mol). To the best of our knowledge, this reaction was firstly proposed for TES by Wentworth [1] and has been attracting little attention since then due to the very low reactivity of MgO towards carbonation, i.e. the poor process reversibility [2]. A promising approach to enhance the reactivity of oxides is a doping with a salt. Previously, this approach was shown to be fruitful for dehydration of $Mg(OH)_2$ [3] and $Ca(OH)_2$ [4]. For instance, in the case of the working pair $CaO-H_2O$, the dehydration temperature was decreased and the rehydration rate was increased. Doping with mixed nitrates was shown to promote carbonation of MgO [5]. However, no assessment of the salt-promoted $MgO-CO_2$ system for TES was reported. In this work, we made a brief screening of salt additives to MgO aiming at finding single salts that increase the oxide reactivity towards carbonation. The carbonation kinetics under the conditions that might be relevant for TES/heat pumping was studied.

Results and Discussion

Pure MgO cannot be carbonated at T = 300°C and P(CO_2) = 10 bar due to kinetic impediments (Fig. 1a). The same is true for MgO with additives of Li_2CO_3 and KNO_3 (for all the mixtures Salt/MgO, the salt content was 10 mol. %). The mixtures with Na_2CO_3, K_2CO_3, and KOAc (Ac = CH_3CO) can be carbonated, however, the conversion after 60 minutes α_{60} does not exceed 0.1 and the released heat Q_{60} is less than 200 J/g-MgO. Additives of $NaNO_3$ and LiOAc considerably increase the conversion and the released heat which can exceed 1400 J/g-MgO in the case of lithium acetate. Therefore, this additive was chosen for further study.

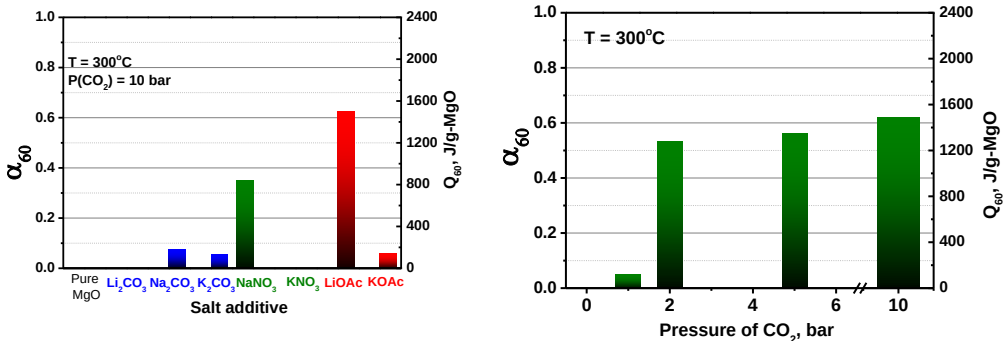

a b

Fig. 1. The parameters α_{60} and Q_{60} for the Salt/MgO (a) and LiOAc/MgO mixture at various CO_2 pressures (b).

One can see that the CO_2 pressure affects α_{60} only slightly within a pressure range of 2-10 bar, however, the conversion dramatically drops at $P(CO_2)$ = 1 bar (Fig. 1b). Therefore, kinetic studies at various temperatures were carried out at $P(CO_2)$ = 2 bar.

Kinetic curves at T = 280°C and 300°C almost coincide with each other, however, the final conversion in the former case is slightly higher as the system is further from the equilibrium (Fig. 2). At T = 340°C no carbonation is observed. The carbonation heat exceeds 1200 J/g-MgO at T = 280°-300°C which may be promising for TES. The average specific heating power at 60 min is 0.33 W/g-MgO.

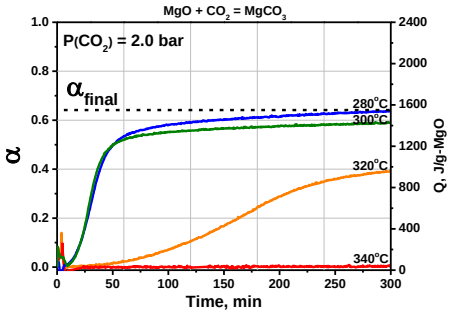

Fig. 2. Carbonation kinetics of LiOAc/MgO at various temperatures and $P(CO_2)$ = 2 bar.

The DSC studies show that the carbonated material (α_{final} ~ 0.6) starts to decompose in the inert atmosphere at T ~ 380°C, therefore, the heat can be stored at this temperature.

The XRD studies *in situ* show that the phase LiOAc disappears upon heating at 120°C. It is in accordance with the mechanism involving a reaction pathway through a molten phase. The $MgCO_3$ phase emerges at 300°C upon supplying CO_2 and can be transformed back to MgO upon heating in the helium atmosphere.

Summary

Carbonation of MgO was promoted by the salt additives with the aim to adapt the MgO-CO_2 working pair for TES at middle temperatures. The screening of the single salts showed that $NaNO_3$ and LiOAc considerably increase the carbonation conversion. The specific heat released at T = 300°C and $P(CO_2)$ = 2 bar exceeds 1200 J/g-MgO which is promising for TES. The possibility to decompose the carbonated material at T > 380°C was shown. The XRD studies *in situ* confirmed the transitions of MgO to $MgCO_3$ and backwards.

References:

[1] Wentworth, W., Chen, E., Solar Energy, 1976, doi:10.1016/0038-092X(76)90019-0
[2] Gregg, S. J., Ramsay, J. D., Journal of the Chemical Society A, 1970, doi:10.1039/J19700002784
[3] Shkatulov, A. I., Aristov, Yu. I., Energy, 2015 doi: 10.1016/j.energy.2015.04.004
[4] Shkatulov, A. I., Aristov, Yu. I., RSC Advances, 2017, doi:10.1039/c7ra06639b
[5] Harada, T., Simeon, F., Hamad, E., Hatton, T. A., Chemistry of Materials, 2015, doi: 10.1021/cm503295g

Effect of the apex gap size on the performance of a small scale Wankel expander

G. Tozer[1*], R. Al-Dadah[1], S. Mahmoud[1]

[1] Mechanical Engineering Department
The University of Birmingham
Edgbaston
Birmingham
B15 2TT
United Kingdom
[*]Corresponding author: gxt357@bham.ac.uk

Abstract

In this paper, a computational fluid dynamics (CFD) model was developed to investigate the effect of different apex gap sizes on the performance of a small-scale (50-100W) Wankel Expander without apex seals. Such a Wankel expander without seals offers the advantages of ease of manufacturing, lower cost and reduced friction and wear. However, without the seals leakage increases across the apexes leading to reduction in power output. Therefore, this study investigated the effect of apex gap size on the power output of such a Wankel expander. Preliminary results showed that at a low rotational speed of 1200 rpm, the power output was reduced from 93.6W for the case with apex seals to 79.5W and 52.7W when the gap size is 0.1mm and 0.25mm respectively.

Keywords: Wankel expander, computational fluid dynamics, Liquid air energy storage

Introduction/Background

Liquid air energy storage (LAES) is a method of storing energy in which air is liquefied using work and later reheated and expander to retrieve the work. Two key components in LAES cycles are compressors and expanders. The Wankel engine has seen substantial development as a combustion engine. However, it is only recently that some efforts have been directed at using it as a compression or expansion device. Advantages of the Wankel combustion engine include smoother and quieter running along with a larger power to weight ratio when compared to 4-stroke piston engines. The Major disadvantage of the Wankel combustion engine is the fact that it utilises apex seals which requires oil lubrication that normally injected into the combustion chamber leading to burned oil and poor emissions.

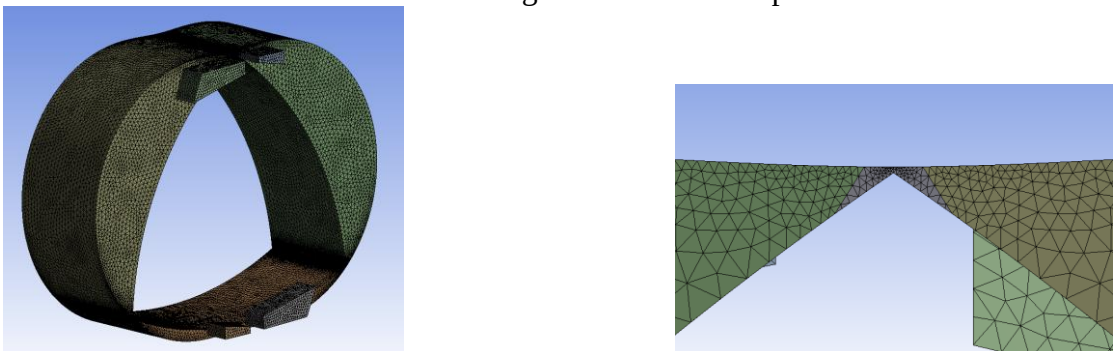

(a) (b)

Figure 1 – (a) Wankel expander used in simulations (b) Mesh at apex gap

If the Wankel geometry is used as a compressor [1, 2] or expander [3, 4] then this oil lubricant will mix with the working fluid and needs to be pumped in and separated after exhaust leading to further cost and complexity.

Garside [1] has previously investigated the performance of a Wankel compressor with no apex seals, with the theory that the oil flooded air would allow for sealing at the apexes. However, this concept still employs oil lubrication, which has the disadvantages mentioned previously. Garside [1] also states that an apex gap size of 0.05mm ± 0.04 is feasible to manufacture. There is therefore a need to develop a Wankel device without apex seals and without oil lubrication in the working fluid and then to investigate the effect of the gap size between the rotor apexes and the housing. Figure 1 shows the geometry of the Wankel expander and the meshing used in the CFD modelling. In this paper the Wankel expander's performance is simulated with apex gap sizes of 0.1mm and 0.25mm.

Discussion and Results

Figure 2 shows the Wankel expander power output at apex gaps of 0.1mm and 0.25mm compared to the no gap case, representing the case with apex seals. This case was simulated at 1200rpm, inlet pressure of 2bar and no oil lubricant in the working fluid (air). The power was reduced by 15.0% with gaps of 0.1mm and by 43.6% with gaps of 0.25mm. Such results highlights the potential of developing a seal-less Wankel geometry.

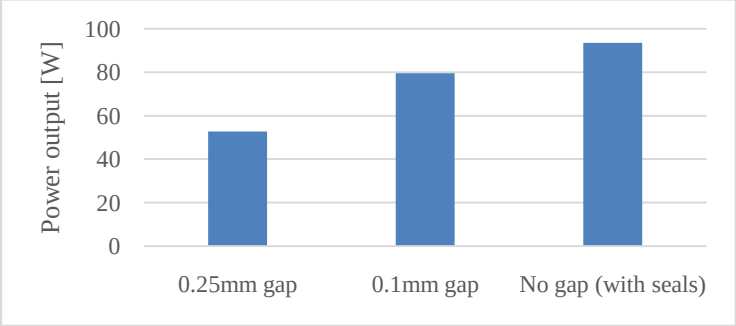

Figure 2 – Power output of the expander with different apex gap sizes

Summary/Conclusions

Despite the advantages of Wankel devices, they suffer from friction loss due to the usage of apex seals power loss from oil lubricant systems. The development of seal-less Wankel geometry that does not need lubricant oil will be a major progression in this field. Advanced CFD techniques were used to simulate a small scale Wankel expander with gaps of 0.1mm and 0.25mm and results of power output were compared to the case with seal at 1200rpm and 2bars inlet pressure. Results showed that a gap of 0.1mm offers only 15% loss in the power output which is acceptable when considering the advantages of reduced complexity due to no use of an oil system and apex seals.

References:

1. Garside, D.W., *A new Wankel-type compressor and vacuum pump.* IOP Conference Series: Materials Science and Engineering, 2017. **232**.
2. Zhang, D.-l., Y.-t. Wu, J.-f. Wang, C.-x. Du, X. Chen, R. Ma, and C.-f. Ma, *Theoretical Study of Seal Spring in a Wankel Compressor*, in *23rd International Compressor Engineering Conference at Purdue*. 2016.
3. Antonelli, M., M. Francesconi, A. Baccioli, and G. Caposciutti, *Experimental Results of a Wankel-type Expander Fuelled by Compressed Air and Saturated Steam.* Energy Procedia, 2017. **105**: p. 2929-2934.
4. Sadiq, G.A., G. Tozer, R. Al-Dadah, and S. Mahmoud, *CFD simulations of compressed air two stage rotary Wankel expander – Parametric analysis.* Energy Conversion and Management, 2017. **142**: p. 42-52.

Water Mixtures as Working Fluids in Organic Rankine Cycles

P. Bombarda[1*], G. Di Marcoberardino[1], C. Invernizzi[2], P. Iora[2] and G. Manzolini[1]

[1]Politecnico di Milano, Energy Department, via Raffaele Lambruschini, 4. 20156 Milano

[2]University of Brescia, Department of Mechanical and Industrial Engineering, via Branze, 38. 25123 Brescia

[*]Corresponding author: paola.bombardaolimi.it email address

Abstract

The adoption of a near-azeotropic mixtures as working fluid is here suggested. Two different mixtures are considered: both consist of water plus a substance completely soluble in water, and each one is aimed at a particular temperature range of application. The paper presents the evaluation of the thermodynamic properties of the mixture together with some experimental results for the thermal stability of the pure components. The ORC plant performance adopting the considered mixtures as working fluid is finally evaluated for two different case studies.

Keywords: ORC cycles, water mixtures, near-azeotropic mixtures, thermal stability.

Introduction/Background

It is well known that the choice of the right working fluid in an ORC is crucial. Usually pure working fluids are selected, mainly refrigerants, hydrocarbons, poly-siloxanes. As it is well known, water is not a suitable working fluid in Rankine cycles of (relatively) small power size or low temperature, but water is relatively inexpensive and safe. In this paper, we will investigate some thermodynamic characteristics of a couple of two-component, near-azeotropic mixtures, composed by water plus a substance completely soluble in water. The mixing with water (considered here as the solvent) basically reduces the flammability and the possible toxicity of the solute and substantially modifies the thermodynamic properties of the solvent itself. Mixtures of water for possible application in ORCs were investigated in the past [1,2,3,4]. There are many fluids totally miscible in water and forming near-azeotropes, for example, alcohols, acids, esters, etc. Here we will discuss mainly mixtures of water and alcohols (n-butanol, for heat recovery from low temperature geothermal sources, and 2,2,2-trifluoroethanol for higher temperature sources). The final aim is to find a mixture composition so that it allows a convenient turbine sizing and an almost dry expansion (vapour quality at the end of the expansion close to one).

Discussion and Results

The thermodynamic properties of the different working fluid mixtures and plant performance were evaluated by Aspen Plus v9.0. Experimental test for the thermal stability of 2,2,2-trifluoroethanol and n-butanol are in progress.

Firstly, the influence of the mixture composition on the thermodynamic properties is investigated, as shown in **Figure 1a**. This figure shows the saturation curve (or dew and bubble line for a mixture) in T-s plane, which depends on the σ parameter[1]. Pure component curves are also reported in the figure: the curve of water (σ = -10.38) exhibits a wide "bell" shape, while the curve of 2,2,2-trifluoroethanol (σ = -2.76) exhibits a narrow shape; the curves corresponding to mixtures of two different compositions show an intermediate behaviour. The mixture composition affects several thermodynamic properties: e.g. the critical temperature,

[1] Parameter of molecular complexity. It is correlated with the slope of the dew curve in the TS plane: $\sigma = (\frac{dS}{dT})\frac{T_{cr}}{R}$

the evaporation (and condensation) enthalpies, which vary considerably with the composition. Similar results may be obtained for other mixtures, for example water – n butanol mixture.

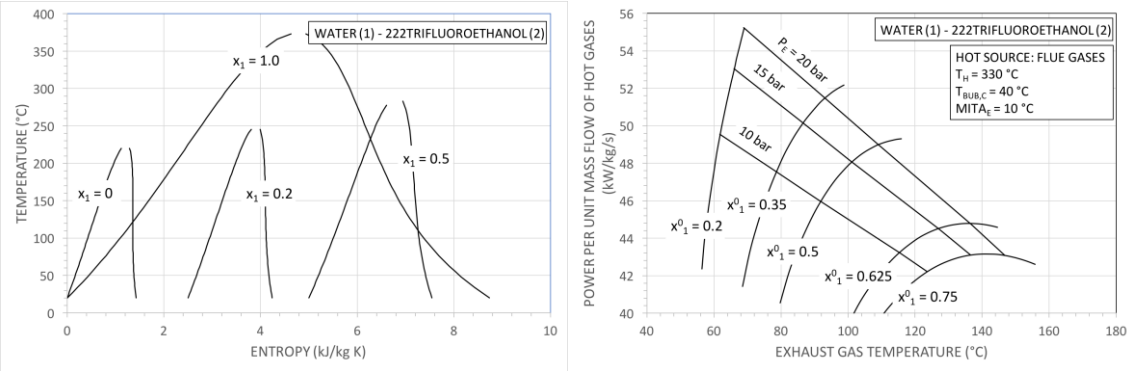

Figure 1 Binary mixtures of water/2,2,2-trifluoroethanol. (a) Dew and bubble lines in the T-s plan; (b) net power per unit mass flow of hot gases as a function of the exhausts temperature.

Afterwards, the performance of a high temperature, heat recovery application is evaluated. The heat source is assumed as constituted by exhaust flue gases at 330 °C, from a Diesel engine. Performance is evaluated for different molar fractions of mixture, assuming constant condensation temperature, constant minimum temperature difference in the primary heat exchanger, negligible pressure losses. **Figure 1b** shows the obtainable specific net power, with reference to water/2,2,2-trifluoroethanol mixtures: basically, the net power decreases with the increasing of the water molar fraction. For example, for a mixture with $x_1^0 = 0.5$, assuming an evaporation pressure of about 13 bar, which corresponds to an isentropic enthalpy drop of about 200 kJ/kg (reasonable for a single stage axial turbine), $\dot{W}$ results 48 kW per unit mass flow of hot gases, and the isentropic discharge vapour quality turns out to be about 0.9. On the other hand, with $x_1^0 = 1.0$ (pure water), even at the optimized evaporation pressure $P_E = 9\ bar$, the maximum power results 44 kW, with an isentropic discharge vapour quality of 0.8 and a turbine isentropic enthalpy drop of 716 kJ/kg (which could not be accomplished in a single stage turbine). As a second case study, the exploitation of geothermal source is considered, and, due to the lower temperature, a mixture of water and n-butanol is selected as working fluid.

Summary/Conclusions

The evaluation conducted for the plant performance shows that the adoption of a water-based mixture in ORCs may be convenient. The adoption of water-based mixtures, in fact, reduces the risk of flammability and toxicity of several potential working fluids, still maintaining the advantage of a convenient sizing of the turbine and a satisfying cooling of the heat source, which results in an adequate plant performance. Other mixtures could be also considered.

References:

[1] Rogdakis E.D., "Thermodynamic analysis, parametric study and optimum operation of the Kalina cycle", International Journal of Energy Research, Vol. 20, 359-370, 1966.

[2] Somekh G.S., "Water-Pyridine Azeotrope is an Excellent Rankine Cycle Fluid", Journal of Engineering for Power, 97(4), 583-588, 1975.

[3] Patel P., Doyle E.F., Raymond R. J., Sakhuja R., "Automotive Organic Rankine-Cycle Powerplant - Design and Performance Data", SAE Paper 740297, Automotive Engineering Congress. Detroit, Mich., February 25-March 1, 1974.

[4] Victor R. A., Kim Jin-Kuk, Smith R., "Composition optimization of working fluids for Organic Rankine Cycles and Kalina cycles", Energy, 2013, Vol. 55, 114-126.

Constant power production with an organic Rankine cycle from a fluctuating waste heat source by using thermal storage

K. Couvreur[1], J. Timmerman[1], W. Beyne[2], S. Gusev[1], M. De Paepe[2] W.D. Steinmann[3], and B. Vanslambrouck[1*]

[1]Department of Flow, Heat and Combustion Mechanics, Ghent University – UGent, Graaf Karel de Goedelaan 5, 8500 Kortrijk, Belgium

[2]Department of Flow, Heat and Combustion Mechanics, Ghent University – UGent, Sint-Pietersnieuwstraat 41, 9000 Gent, Belgium

[3]Institute of Technical Thermodynamics, German Aerospace Center (DLR), Pfaffenwaldring 38-40, 70569 Stuttgart, Germany

[*]Corresponding author: Bruno.Vanslambrouck@Ugent.be

Abstract

Waste heat to power (WHP) systems such as organic Rankine cycle (ORC) create enormous opportunities to increase the energy efficiency in energy intensive industries and reduce emissions. ORC is considered as a viable technology for converting low- and medium-temperature heat to electricity. However, thermal power fluctuations can negatively affect the operation of ORC. Intermediate thermal storage is able to mitigate these fluctuations and prevent ORC part-load operation. A pilot scale latent heat storage (LHS) system is connected to a 250 kW_e heater and 11 kW_e ORC and is used to demonstrate the advantage of a combined LHS ORC system.

Keywords: LHS, Waste heat recovery, Organic Rankine cycle, Thermal energy storage.

Introduction/Background

Waste heat to power (WHP) systems such as organic Rankine cycle (ORC) create enormous opportunities to increase the energy efficiency in energy intensive industries and reduce emissions [1]. The organic Rankine cycle (ORC) is considered as a viable technology for converting low- and medium-temperature heat to electricity [2, 3]. However, thermal power fluctuations are often present in waste heat sources.

These fluctuations negatively affect the operation of ORC systems, while ORC's are conventionally designed for a certain nominal heat load and can only operate well in a certain limited off-design range. A steady heat load close to the nominal load is thus preferable to operate an ORC. To optimize ORC use and maximize waste heat source utilization, intermediate thermal storage is required. By integrating thermal storage the nominal heat load and thus size of the ORC can be reduced, while allowing a better exploitation of peaks in the waste heat availability. In this way part of the thermal storage cost can be compensated by a smaller ORC.

Thermal energy storage (TES) can be classified as sensible, latent or thermochemical. In sensible heat systems (water buffers, concrete blocks, molten salts, etc.) heat is stored by raising the temperature of a storage medium and therefore the amount of heat that can be stored depends on the specific heat capacity of the storage medium. LHS using phase change materials (PCMs) allows to store more heat than sensible storage systems due to its higher energy density.

Moreover, during charging or discharging the mean temperature of a latent heat storage system stays on a nearly constant level, as long as part of the storage medium is still in the transition phase, which is not the case for sensible heat storage. As a consequence, LHS can provide a heat sink at nearly constant temperature for a waste heat stream, e.g. residual steam to be condensed. Analogously, LHS can provide a heat source at nearly constant temperature to heat up a cold process stream (e.g. to evaporate the ORC fluid).

Thermochemical storage systems are still in the research phase, but it can potentially store more energy than sensible or LHTES systems due to the heat of reaction [4].

According to the performance evaluation of an ORC unit integrated in a steel mill to recover waste heat from the fumes of an electric arc furnace (EAF) it is proven that thermal storage is capable of attenuating a highly fluctuating heat source to protect the ORC from oscillations [5]. In this case a steam accumulator was used while in our case a LHTES is evaluated.
A pilot scale system is installed at Ghent University Campus Kortrijk within the frame of the European CORNET ShortStore project. The system consists of a LHS, a 250 kW electric heater which can simulate a fluctuating waste heat source and an 11 kW_e ORC, interconnected via a thermal oil circuit (Figure 40). The characteristics of the PCM are listed in Table 1.

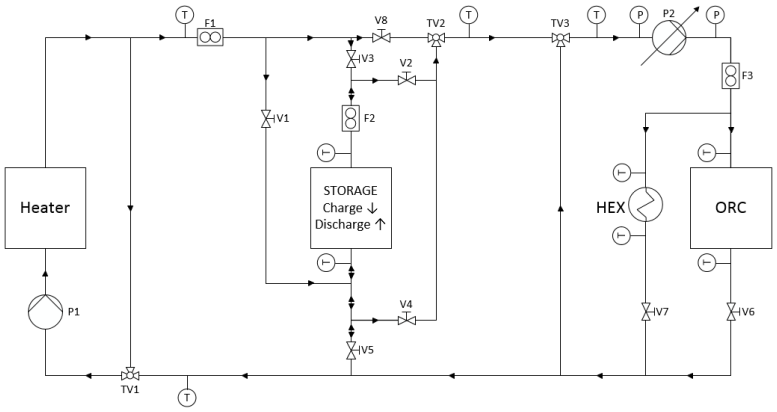

Figure 40. Schematic of the test set-up. Flow directions in the system are indicated by arrows. Globe valves are indicated by 'V', three way valves by 'TV', flowmeters by 'F', temperature measurements by 'T'.

The aim of this research is to develop a performant control procedure enabling stable ORC operation under fluctuating waste heat conditions. The heater and the ORC can be regarded as fluctuating process streams to be heated up or cooled down.
As a first step, the charging and discharging behaviour of the LHS is analysed at variable mass flow rates and temperatures of the incoming oil. An heat exchanger with the environment will act as a heat sink and the electric heater as a heat source. In a second step the capability of the LHS in flattening fluctuations in waste heat availability due to variations in mass flow rate or temperature are investigated. In a third step, the main aim of this research, a control procedure will be developed to enable stable ORC operation under fluctuating waste heat conditions by charging and discharging the LHS system.
The integration of a LHS between the waste heat source and the ORC will allow to decrease the nominal load and thus the investment cost of the ORC. Therefore, this research contributes to the further development of waste heat recovery technologies.

Table 3. PCM characteristics

Material	**Eutectic mixture $KNO_3/NaNO_3$**
Melting temperature	223°C
Volume	2 m^3
Thermal capacity	112 kWh (latent heat) 220 kWh in temperature range 180-250°C

References:

1. BCS, *Waste Heat Recovery: Technology and Opportunities in U.S. Industry*. 2008.
2. Tchanche, B.F., et al., *Low-grade heat conversion into power using organic Rankine cycles - A review of various applications.* Renewable & Sustainable Energy Reviews, 2011. **15**(8): p. 3963-3979.
3. Lecompte, S., et al., *Review of organic Rankine cycle (ORC) architectures for waste heat recovery.* Renewable & Sustainable Energy Reviews, 2015. **47**: p. 448-461.
4. Yu, N., R.Z. Wang, and L.W. Wang, *Sorption thermal storage for solar energy.* Progress in Energy and Combustion Science, 2013. **39**(5): p. 489-514.
5. Ramirez, M., et al., *Performance evaluation of an ORC unit integrated to a waste heat recovery system in a steel mill.* 4th International Seminar on Orc Power Systems, 2017. **129**: p. 535-542.

An Investigation of Nozzle Shape on the Performance of an Ejector

Mehdi Falsafioon[1*], Zine Aidoun[1]

[1]CanmetENERGY, Natural Resources Canada,
1615 boul. Lionel-Boulet, Varennes, Québec, Canada J3X 1S6
[*]Corresponding author: mehdi.falsafioon@canada.ca

Abstract

A wide range of industrial refrigeration systems are good candidates to benefit from the cooling and refrigeration potential of supersonic ejectors. These are thermally activated and can use waste heat recovery from industrial processes where it is abundantly generated and rejected to the environment. In other circumstances low cost heat from biomass or solar energy may also be used in order to produce a cooling effect. Ejector performance is however typically modest and needs to be maximized in order to take full advantage of the simplicity and low cost of the technology. The present work investigates the influence of geometrical changes of primary nozzle on the performance of ejectors. Since the experimental setup for different working conditions and different geometries are expensive and time consuming, the computational fluid dynamics has been applied for the study. This also provides a better visualization of the phenomena happening inside the ejector. The preliminary CFD results are validated with experimental data and are in good accordance in terms of entrainment and compression ratios.
Then, further CFD investigations were conducted in order to predict the most appropriate shape of primary nozzle to enhance the performance of an ejector. The simulations have been carried out with Air, CO_2 and R134a in a wide range of working conditions. The results show that the shape of primary nozzle plays a significant role on efficiency of an ejector.

Keywords: Ejector, Ejector Performance, Nozzle, Numerical Simulation, Refrigeration System.

Introduction/Background

Numerous experimental and numerical studies have been conducted to provide a better understanding of mixing and compression processes in ejectors. Among these studies, many have tried to improve the performance of ejectors by modifying the dimensions and/or the configuration of the internal components. One of the items that has a significant effect on the efficiency of an ejector is the shape of the primary nozzle. The importance of employing an optimized nozzle inside the ejector is both discussed on the basis of simulations and experimental studies. Matsuo et al. [1] did a study on nozzle shape and reported that the nozzle shape and the mixing area, between the nozzle exit and mixing chamber, has a significant effect on ejector performance. This study was also conducted by Fu et al. [2] who with the use of numerical simulation showed that a good design of nozzle structure can optimize the performance of an ejector. The experiments of Sag and Ersoy [3] also proves that an optimal nozzle can enhance the performance of an ejector by 8–13%. In all these studies the behaviour of motive flow is identified as one of the most important parameters that should be taken into account in an ejector design. Zhu and Jiang [4] studied the Mach wave lengths using Schlieren system and reported that ejector performance can be improved by reducing the first Mach wave length. A study on flow boundaries was also carried out by Addy [5]. Most recently, Chen et al. [6] investigated the Mach wave structure of the motive flow under off-design working conditions by both numerical and experimental methods. In their report, they have presented an extensive study of the flow regime inside an ejector using the method of characteristics. Despite the numerous studies addressed at ejector performance, there is still a lack of an accurate representation of the role of primary nozzle in ejector performance. In this work, we present a comprehensive study of ejector nozzle's shape following with recommendations for the design of this part of ejectors.

Discussion and Results

CFD simulation is used to determine the effect of the shape of primary nozzle on the performance of a conventional ejector. Because of the nature of ejectors, the conservation equations of continuity, momentum and energy are used in their compressible and steady state forms and non-linear sets of discretized equations are solved. The CFD code is first validated using in-house experimental results in different working conditions. Result show a good agreement between the CFD results and experimental data. At the next step, the developed CFD model was used to investigate the fluid flow inside an ejector with different nozzle shapes but with the same primary mass flow rate. Based on the results, the motive flow coming out of a nozzle can be divided into three main flow regimes: a) an over-expanded condition where the pressure of the motive flow is lower than suction pressure; b) an under-expanded condition where the pressure of the motive flow after the nozzle is higher than suction pressure; c) an ideally-expanded flow where the pressure of motive flow at the exit of the nozzle is the same as suction pressure. The impact of all three conditions on the performance of an ejector have been studied in this paper. The result show that the nozzle structure in the divergent part can change the flow structure and the Mach waves that have large impact on the performance of ejectors. Finally, a systematic way to design a nozzle based on different working conditions is proposed.

Summary/Conclusions

In this research, numerical study on motive flow inside an ejector is addressed. Results show that the functionality of an ejector is highly dependent on the working condition and the nozzle structure. In another word, the nozzle shape should be changed for different working conditions in order to get the best performance of an ejector.

References:

[1] K. Matsuo, K. Sasaguchi, Y. Kiyotoki, H. Mochizuki, *Investigation of supersonic air ejectors (Part 2, effects of throat-area-ratio on ejector performance)*, Bull. Jpn. Soc. Mech. Eng. 25 (210) (1982) 1898–1905.
[2] W.N. Fu, Y.X. Li, Z.L. Liu, H.Q. Wu, T.R. Wu, *Numerical study for the influences of primary nozzle on steam ejector performance*, Appl. Therm. Eng. 106 (2016)
1148–1156.
[3] N.B. Sag, H.K. Ersoy, *Experimental investigation on motive nozzle throat diameter for an ejector expansion refrigeration system*, Energy Convers. Manage. 124 (2016) 1–12.
[4] Y.H. Zhu, P.X. Jiang, *Experimental and numerical investigation of the effect of shock wave characteristics on the ejector performance*, Int. J. Refrig. 40 (2014) 31–42.
[5] A.L. Addy, *Effects of axisymmetric sonic nozzle geometry on Mach disk characteristics*, Am. Inst. Aeronaut. Astronaut. J. 19 (1) (1981) 121–122.
[6] Chen, Z., Dang, C., Hihara, E., 2017. *Investigations on driving flow expansion characteristics inside ejectors*, Int. J. Heat Mass Transf. 108, 490–500.

Salt hydrate-silicone foam composite for heat storage application

A. Frazzica[1], V. Palomba[1], V. Brancato[1], L. Calabrese[2], A.G. Fernández[3], M. Fullana[4], A. Solé[5], L. F. Cabeza[4]

[1]CNR - Istituto di Tecnologie Avanzate per l'Energia "Nicola Giordano", Via Salita S. Lucia sopra Contesse 5, 98126 Messina, Italy

[2]Department of Engineering, University of Messina, C.da di Dio 98166 Messina, Italy

[3]Energy Development Center, University of Antofagasta, Av. Universidad de Antofagasta 02800 Antofagasta, Chile

[4]GREiA Research Group, INSPIRES Research Centre, University of Lleida, Pere de Cabrera s/n, 25001 Lleida, Spain

[5]Department of Mechanical Engineering and Construction, Universitat Jaume I, Campus del Riu Sec s/n, 12071 Castelló de la Plana, Spain

[*]Corresponding author: andrea.frazzica@itae.cnr.it

Abstract

The present paper deals with the preliminary study carried out on innovative polymeric foams based on silicone and $MgSO_4 \cdot 7H_2O$, as a salt hydrate. Composites with variable quantity of embedded salt, from 40 wt.% up to 70 wt.%, were prepared, according to an established foaming procedure. A complete physicochemical characterization was carried out to investigate the main properties of the composite foams. The morphological characterization showed that the foam pores were homogenously distributed and well interconnected to each other. Thermo-gravimetric dehydration tests, under real operating conditions, demonstrated that the tested samples are able to efficiently exchange water.

Keywords: thermal energy storage (TES), polymeric foam, salt hydrate, composite

Introduction

The full exploitation of Renewable Energy Sources (RES) potential requires the presence of a thermal storage system, in order to decouple the availability of the heat source from the user's demands [1]. Different technologies for thermal energy storage (TES) exist, and, among them, thermochemical storage (TCS) represents a promising alternative [2]. Reversible reactions involving salts, such as hy/dehydration reactions, can be used for storing heat using thermochemical technology. To overcome the drawbacks due to the use of the pure salt hydrate [2], the dispersion of the salt in a porous matrix was proposed in the literature.

In such a context, the present work reports the development of composite materials for thermochemical storage based on magnesium sulphate heptahydrate ($MgSO_4 \cdot 7H_2O$), as salt hydrate and silicone foam, as matrix. The concept of embedding an active filler inside a polymeric foam was recently proposed for adsorption heat pump applications, where the silicone foam was holding zeolite powders, to obtain a sorbent composite with high porosity and adsorption capacity [3].

Result and discussion

A mixture of poly(methylhydrosiloxane) and a silanol terminated polydimethylsiloxane with proper catalyst was employed to form the polymeric foam. During the raw components mixing, the $MgSO_4 \cdot 7H_2O$ was dispersed in different percentages, afterwards the foaming process under controlled temperature was performed. In **Erro! Fonte de referência não encontrada.**, the obtained foam samples with salt content varying from 40 wt.% up to 70 wt.% are presented.

Foam morphology was evaluated by optical 3D digital microscope (Hirox HK-8700) and scanning electron microscope (FIB-SEM Zeiss Crossbeam 540), Figure 2a shows a detail of porosity and evidences the salt located inside the pore. The foam is characterized by an open

cell structure and a good interconnection among the pores is evidenced. This result assures an efficient water vapour diffusion inside the porous structure.

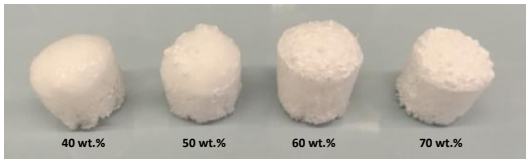

Figure 41: Prepared composite samples with different $MgSO_4 \cdot 7H_2O$ content.

(a)  (b) 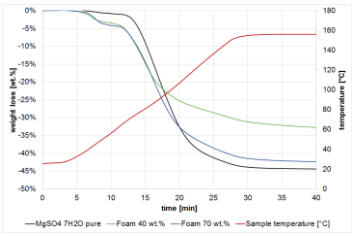

Figure 42: (a) 3D digital microscope picture of the porosity, (b) Thermo-gravimetric dehydration of $MgSO_4 \cdot 7H_2O$ sample as well as two composite foams, with 40 wt.% and 70 wt.%

In order to assess the ability of the synthetized composites foam-salt to properly react with water vapour, under typical working conditions, thermo-gravimetric dehydration tests were performed by means of modified Labsys Evo SETARAM apparatus. The results of the preliminary tests performed are reported in Figure 2b. In particular, the pure salt was tested as the reference, showing a mass loss of about 45% at 150°C, corresponding to about 6 water molecules released. Subsequently, composites with 40 wt.% and 70 wt.% salt were tested. Their weight loss is in line with the amount of salt inside the matrix, confirming the possibility to employ the developed composite material for TCS applications. FT-IR, SEM and thermogravimetric analyses are on-going to evaluate the nature of the interaction occurring between the silicone host matrix and the hydrate salt.

Conclusion

An innovative composite polymeric foam-salt hydrate (i.e. $MgSO_4 \cdot 7H_2O$) was synthetized, aiming at overcoming most of the common material problems related to thermochemical TES applications. The morphological characterization demonstrated that the samples are characterized by a homogenous porosity of the foam. The thermo-gravimetric analysis showed the capacity of the composite samples to efficiently exchange water, under real operating conditions.

Acknowledgements

The work partially funded by the Spanish government (ENE2015-64117-C5-1-R). The authors from UdL would like to thank the Catalan Government for the quality accreditation given to their research group (2014 SGR 123). GREA is certified agent TECNIO in the category of technology developers from the Government of Catalonia.

References

[1] D. Aydin, S. P. Casey, and S. Riffat, “The latest advancements on thermochemical heat storage systems”, Renewable and Sustainable Energy Reviews, 2015.
[2] H. Zhang, J. Baeyens, G. Cáceres, J. Degrève, and Y. Lv, “Thermal energy storage: Recent developments and practical aspects”, Progress in Energy and Combustion Science, 2016.
[3] L. Calabrese, L. Bonaccorsi, A. Freni, and E. Proverbio, “Synthesis of SAPO-34 zeolite filled macrocellular foams for adsorption heat pump applications: A preliminary study”, Applied Thermal Engineering, 2017

Model based assessment of working pairs for gas driven thermochemical heat pumps

E. Laurenz[1*], G. Füldner[1], J. Doell[1], C. Blackman[2,3], Lena Schnabel[1]

[1]Fraunhofer Institute for Solar Energy Systems ISE, Heidenhofstr. 2, 79110 Freiburg, Germany
[2]SaltX Technology, Västertorpsvägen 135, 12944 Hägersten, Sweden
[3]Dalarna University, Röda vägen 3, 78170 Borlänge Sweden
[*]Corresponding author: eric.laurenz@ise.fraunhofer.de

Abstract

The choice of a working pair for gas driven thermochemical heat pumps requires fast computation of estimates for efficiency (coefficient of performance, COP) and power (specific heating power, SHP) under different boundary conditions. A quasi-stationary cycle description with lumped parameters and linear driving force model with constant effective heat transfer coefficients is used. Further properties of the heating system are included as boundary conditions. This approach intrinsically takes into account the thermodynamic equilibrium data for different working pairs. Two working pairs $CaBr_2.xNH_3$ – NH_3 (sorption) and $MnCl_2.xNH_3$ – $PbCl_2.xNH_3$ (resorption) are compared. The overall performance is assessed according to EN 12309 as weighted averages for different boundary conditions. As a result the $CaBr_2$ sorption cycle shows significantly better performance compared to the $MnCl_2$ – $PbCl_2$ resorption cycle.

Keywords: thermochemical material, gas heat pump, performance indicators, modelling.

Introduction/Background

Gas driven thermochemical heat pumps are a promising option to reduce CO_2 emissions from the heating sector. For this technology a wide range of working pairs are under consideration. Examples of sorption cycles are salt hydrates – water, salt ammoniates – ammonia, and for resorption cycles combinations of two different salt ammoniates (or hydrates). These working pairs have been subject to different screenings and assessments mainly focused on energy storage density [1,2]. Earlier we presented a general assessment including the temperature levels resulting from thermodynamic equilibrium data [3].

The aim of the present study is to provide good enough estimates for efficiency (coefficient of performance, COP) and power (specific heating power, SHP) under realistic boundary conditions of building heating system. These estimates are required for the choice of working pairs and other basic design considerations. As an example, we compare the results for the two working pairs $CaBr_2.xNH_3$ – NH_3 (sorption) and $MnCl_2.xNH_3$ – $PbCl_2.xNH_3$ (resorption) which, in contrast to water based systems, are not prone to freezing of the working fluid at sub-zero temperatures.

The approach is a fast and efficient model based assessment using a quasi-stationary cycle description with lumped parameters and the NTU-ϵ method. A linear driving force (LDF) model with constant effective heat transfer coefficients is used to conveniently describe heat and mass transfer processes [4]. The driving forces result from thermodynamic equilibrium data of different working pairs [5] and set boundary conditions. In addition some simple realistic assumptions are taken for the gas burner and the building/heating system including different scenarios for climate conditions and the low temperature heat source. A realistic control strategy based on the ambient temperature and the heating curve is included in the model. As a result all temperature levels of the cycle vary with the boundary conditions and thermodynamic equilibrium requirements.

An overall performance indicator is created using a bin method according to EN12309. For the operation of any real appliance the boundary conditions would not be constant, but changing throughout the year. To account for this, the model is run at different operating points defined by ambient temperature. The different ambient temperatures lead to different demanded heating capacities, demanded outlet temperatures to heat sink and source inlet temperatures. From each simulation result, indicators like the gas utilization efficiency (GUE) can be calculated and aggregated with a weighted average to seasonal gas utilization efficiency (SGUE).

Discussion and Results

The results showed a distinct difference between the two working pairs under all different scenarios with a clear advantage for the resorption cycle in the chosen example. The method can be applied to other working couples providing a fast and efficient approach for screening.

The simulation results were verified by testing for a closed overall energy and mass balance. The implementation turned out to be very efficient with calculation times below 1 s for one set of boundary conditions although implemented in the high level programming language R.

Summary/Conclusions

The model presented in this study is a first step assessment under realistic boundary conditions. It shows how the working pair's thermodynamic equilibrium properties match the required temperature level from applications. More details require at least a simple dynamic model including heat capacities, evaporator/condenser dynamics and sorption dynamics. This includes a better understanding of the sorption kinetics and underlying heat and mass transfer processes in the salt with possible non-linearities and state dependencies.

References

[1] P. Touzain, Thermodynamic values of ammonia-salts reactions for chemical sorption heat pumps, in: Proc. Int. Sorption Heat Pump Conf, Munich, 1999, pp. 225–238.

[2] K.E. N'Tsoukpoe, T. Schmidt, H.U. Rammelberg, B.A. Watts, W.K.L. Ruck, A systematic multi-step screening of numerous salt hydrates for low temperature thermochemical energy storage, Applied Energy 124 (2014) 1–16.

[3] E. Laurenz, G. Füldner, L. Schnabel, Assessment of thermodynamic equilibrium properties of salt hydrates for heat transformation applications at different temperature levels, in: Proceedings of the Heat Powered Cycles Conference 2016, 2016.

[4] U. Wittstadt, G. Füldner, E. Laurenz, A. Warlo, A. Große, R. Herrmann, L. Schnabel, W. Mittelbach, A novel adsorption module with fiber heat exchangers: Performance analysis based on driving temperature differences, Renewable Energy 110 (2017) 154–161.

[5] J. Berthiaud, Procédé à sorption solide/gaz pour le transport de chaleur et de froid à longue distance. Dissertation, Perpignan, 2007.

The Obtention of an Ejector Cooling System's Performance Map Through Different Graphical Representations

Jorge I. Hernandez[1*], Roberto Best[1], Ruben Dorantes[2], Humberto Gonzalez[2], Raul Roman[3], Jacobo Galindo[1] and Pablo Aragon[1]

[1] Instituto de Energías Renovables, Universidad Nacional Autónoma de México
Priv. Xochicalco s/n, Col. Centro, CP 62589, Temixco, Morelos, México
[2] Universidad Autónoma Metropolitana Azcapotzalco, Av San Pablo Xalpa 180, Reynosa Tamaulipas, CP 02200, Ciudad de México, México
[3]Universidad Autónoma del Estado de Hidalgo, Campus Apan
Carretera Apan-Calpulalpan Km.8, Col.Chimalpa, C.P. 43920, Apan, Hidalgo, Mexico
[*]Corresponding author: jhg@ier.unam.mx

Abstract

Under the assumption that the performance map of an ejector's cooling system is a basic tool for its optimal operation, a methodology is proposed for its finding. It consists in keeping constant P_{GE} and P_{CO} while the secondary mass flow rate is varied. For the resulting P_{GE}, P_{CO} and P_{EV} values, a series of dimensionless plots are obtained in order to define the ejector's performance map, U-T_{CO} plot, corresponding to the ejector critical back pressure and should direct the optimal ejector cooling system operation at design and off design conditions.

Keywords: ejector cooling system; refrigeration; thermal cooling systems; ejector.

Introduction

For the ejector cooling system, its technical feasibility has been proved but a complete understanding of different graphical representations has not been given. Hernandez *et al* [1, 2] have presented an approach considering data from the literature.
In regard to the ejector cooling system's efficiency, the parameter employed for such end is its coefficient of performance, COP, given by

$$COP = U\frac{(h_2 - h_6)}{(h_1 - h_4)} \tag{1}$$

where $(h_2 - h_6)$ is the evaporator specific enthalpy difference producing the system cooling effect; $(h_1 - h_4)$ is the system specific enthalpy difference required to produce the cooling effect; and U is the ejector entrainment ratio, defined as

$$U = \frac{\dot{m}_2}{\dot{m}_1} \tag{2}$$

being $\dot{m}_1$ and $\dot{m}_2$ the mass flow rates for the ejector primary and secondary fluids. This parameter is also of relevance for the ejector performance.
Thermodynamically, the ejector cooling system is 3T and has the T_{GE}, T_{CO} and T_{EV} at saturation as its independent variables. Also, these temperatures define the system working pressures, which are also used as independent variables, and are the starting values when superheating and subcooling processes exist.
On the other hand, the expansion and compression processes are commonly defined by pressure ratios. In this regard, the driving pressure ratio, Γ, is defined as

$$\Gamma = \frac{P_{GE}}{P_{EV}} \tag{3}$$

where P_{GE} and P_{EV} are the generator and evaporator pressures. The compression ratio, r, is given as

$$r = \frac{P_{CO}}{P_{EV}} \tag{4}$$

being P_{CO} the condenser pressure. Finally, the expansion pressure ratio, ξ, is defined as

$$\xi = \frac{P_{GE}}{P_{CO}} \tag{5}$$

So, plots of U and COP should be obtained against the generation, condensation and evaporation pressure, as well as against r, ξ and Γ.
Accurate experimental data were obtained in the system shown in Fig. 1.

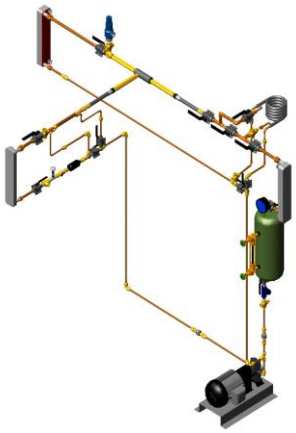

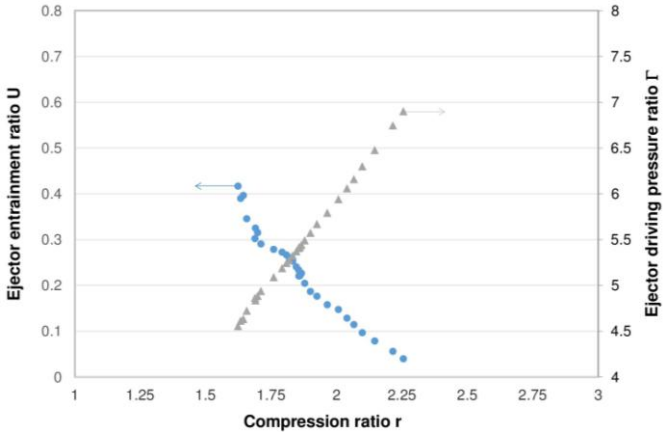

Fig. 1 Experimental rig configuration. **Fig. 2 Plot of U and Γ against r.**

Discussion and Results

The Figure 2 shows some experimental results in which P_{GE} and P_{CO} were kept constant; it is a plot of U and Γ against r. A group of similar data is analysed and represented in different plots.

Conclusions

Plots of U and COP should be obtained against the generation, condensation and evaporation pressure, as well as against r and Γ in order to find the ejector's cooling system's operation map directing its optimal operation.

References

[1] Hernandez Jorge I., Best Roberto, Roman Raul y Galindo Jacobo; *An advantageous representation of the critical behaviour of an ejector cooling system by dimensionless parameters*, Proceedings of the Heat Powered Cycles 2016, Paper No. HPC040, Nottingham, England, June 26-29, 2016.

[2] Hernandez J., Roman R., Best R. y Galindo J.; *Graphical representations of the behaviour of an ejector cooling system*, Proceedings of the International Conference on Polygeneration *2017*, Paper No. ICP51, Cuernavaca, Morelos, Mexico, May 24-26, 2017.

Thermodynamic and Thermoeconomic Assessment of a PVT-ORC Combined Heating and Power System for Swimming Pools

Kai Wang and Christos N. Markides*

Clean Energy Process (CEP) Laboratory, Department of Chemical Engineering, Imperial College London,
South Kensington Campus, London SW7 2AZ, UK
*Corresponding author: c.markides@imperial.ac.uk

Abstract

This paper studies the thermodynamic and thermoeconomic performance of a hybrid photovoltaic-thermal (PVT) system integrated with an organic Rankine cycle (ORC) system for covering the combined heating and power demands of swimming pools. Priority is given to meet the heating demand of the swimming pool in order to ensure a comfortable condition for swimmers in cold weather conditions, while excess thermal output from the PVT collector is converted into power by the ORC unit at warm weather conditions. The thermodynamic performance of this system and its dynamic response to environmental and occupant factors are analysed on the basis of a transient thermodynamic model. Various heat losses and gains are considered in accordance to meteorological conditions at specific locations. Optimization analyses are presented to identify the most suitable working fluid and integration configuration for the ORC unit under configurational and operational constrains. Finally, the thermoeconomic performance of the solar combined heating and power system are assessed and compared in terms of location, system configuration and operation strategy.

Keywords: PVT system, swimming pool, solar energy, organic Rankine cycle.

Introduction

Hybrid PVT collectors have been attracting interest in recent years due to their potentially improved electrical efficiency over single PV panels if operated suitably, and their ability to also provide a thermal energy output and the flexibility they have for further integration with other technologies, including for thermal energy storage. Many different hybrid PVT-based systems have been investigated for various purposes, such as PVT-water for domestic heating and power [1,2], PVT with low-temperature heat-driven thermodynamic cycles [3], etc.

Considering the potential of hybrid PVT systems for combined heating and power (CHP), the aim of this work is to assess the energetic and economic feasibility of hybrid PVT technology applied in swimming pool applications. Currently, almost all of the previous studies on solar swimming pool heating were focused on solar-thermal collector heating systems [4,5] or solar-assisted heat pump heating systems with conventional solar-thermal collectors [6,7]. Little work has been conducted on employing hybrid PVT collectors in solar-CHP (S-CHP) systems for meeting the heating and power demands of swimming pools. To the authors' knowledge, only one study has conducted the analyses of the PVT heating system for an existing indoor/outdoor swimming pool located in Naples, Italy [8]. In this study, results from transient simulations and sensitivity analyses performed with TRNSYS software showed that the system was not profitable without public funding policies and became convenient only in case of thermal feed-in tariffs (FITs) due to the high cost of PVT collectors. Since the solar irradiation and thermohygrometric conditions are highly geography dependent, the energetic and economic performance of PVT-based s-CHP systems may differ significantly at different configuration and operational strategies and locations, and requires further investigation.

This paper presents a solar-driven PVT-ORC S-CHP system for swimming pool facilities. The ORC unit converts the excessive thermal output of the PVT collector into electrical power when heating demand is low for the swimming pool, which helps to improve the overall efficiency. The

potential of the system at different locations will be assessed in terms of its thermodynamic and thermoeconomic performance.

System Configuration and Methodology

Figure 1 shows a simplified schematic of the proposed PVT-ORC S-CHP system for the swimming pool. A hot water thermal storage tank stores thermal energy produced from the PVT-water collectors. The system is designed to prioritise meeting the heat demand of the swimming pool, while the excess thermal output from the collectors is recovered and converted by the ORC unit for generating additional electrical power.

The PVT collector-field model, swimming pool model, ORC model and other component models are integrated in TRNSYS to form a dynamic system model. Important system design and operational parameters are optimized according to the variations of the solar input and of the heat demand. Optimal working fluids are considered, and an appropriate size of the ORC unit is selected in order to match the temperature and power levels of the PVT system. Key thermodynamic and thermoeconomic performance indicators of the hybrid system are then assessed and compared in terms of location, system configuration and operation strategy.

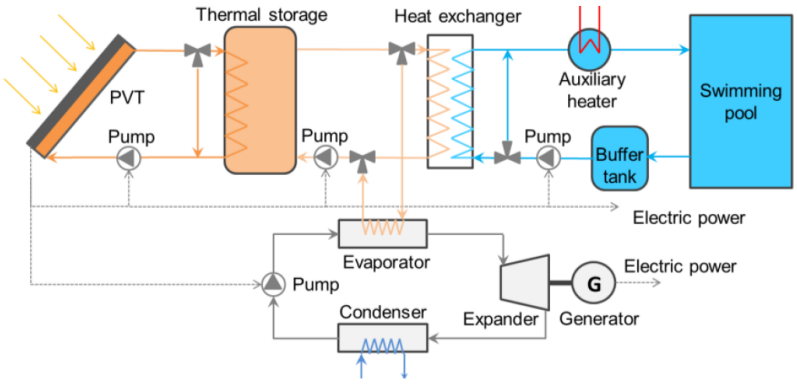

Figure 1. Simplified schematic of PVT-ORC S-CHP system for swimming pool application.

References:

[1] Ramos, A., Chatzopoulou, M. A., Guarracino, I., Freeman, J., Markides, C.N., "Hybrid photo-voltaic-thermal solar systems for combined heating, cooling and power provision in the urban environment", Energy Conversion and Management, 2017, doi:10.1016/j.enconman.2017.03.024

[2] Herrando, M., Markides, C. N., Hellgardt, K., "A UK-based assessment of hybrid PV and solar-thermal systems for domestic heating and power: System performance", Applied Energy, 2014, doi:10.1016/j.apenergy.2014.01.061

[3] Freeman, J., Hellgardt, K., Markides, C. N., "Working fluid selection and electrical performance optimisation of a domestic solar-ORC combined heat and power system for year-round operation in the UK", Applied Energy, 2017, 10.1016/j.apenergy.2016.04.041

[4] Singh, M., Tiwari, G. N., Yadav, Y. P., "Solar energy utilization for heating of indoor swimming pool", Energy Conversion and Management, 1989, doi:10.1016/0196-8904(89)90027-7

[5] Ruiz, E., Martinez, P. J., "Analysis of an open-air swimming pool solar heating system by using an experimentally validated TRNSYS model", Solar Energy, 2010, doi: 10.1016/j.solener.2009.10.015

[6] Tagliafico, L. A., Scarpa, F., Tagliafico, G., Valsuani, F., "An approach to energy saving assessment of solar assisted heat pumps for swimming pool water heating", Energy and Buildings, 2012, doi:10.1016/j.enbuild.2012.10.009

[7] Chow, T. T., Bai, Y., Fong, K. F., Lin Z., "Analysis of a solar assisted heat pump system for indoor swimming pool water and space heating", Applied Energy, 2012, doi: 10.1016/j.apenergy.2012.05.058

[8] Buonomano, A., De Luca, G., Figaj, R. D., Vanoli, L., "Dynamic simulation and thermo-economic analysis of a PhotoVoltaic/Thermal collector heating system for an indoor–outdoor swimming pool", Energy Conversion and Management, 2015, doi: 10.1016/j.enconman.2015.04.022

Application of Liquid-Air and Pumped-Thermal Electricity Storage Systems in Low-Carbon Electricity Systems

S. Georgiou[1], M. Aunedi[2], G. Strbac[2] and C. N. Markides[1,*]

[1]Clean Energy Processes (CEP) Laboratory, Department of Chemical Engineering, Imperial College London, London, UK

[2]Department of Electrical and Electronic Engineering, Imperial College London, London, UK

[*]Corresponding author: c.markides@imperial.ac.uk

Abstract

The competitiveness of any electricity storage technology is strongly affected by both technical and economic performance characteristics. An electricity storage system that is both efficient and economically competitive has the potential to deliver an optimal low-carbon electricity system, and also to increase the flexibility of the system, e.g. by reducing the cost of delivering and operating the system. It can support the cost-efficient integration of increasing penetration of intermittent renewable energy generation, while taking advantage of differences between peak and off-peak electricity prices as well as providing local and national services to network and system operators. The contribution and application potential of any technology in a power system will depend on its characteristics in combination with the requirements of the whole system. In this study, we present two newly proposed medium- to large-scale electricity storage systems currently under development, namely 'Liquid-Air Energy Storage' (LAES) and 'Pumped-Thermal Electricity Storage' (PTES). Thermodynamic models and costing methodologies for both systems are presented with the overriding objective of integrating the technologies' characteristics in a whole-electricity system assessment model. The aim is to assess the application feasibility, competitiveness and system value of LAES and PTES when integrating these technologies in the whole-systems model to provide a range of flexible system services.

Keywords: Liquid-Air Energy Storage, Pumped-Thermal Electricity Storage, Power system economics, Whole-system assessment.

Introduction/Background

Electricity storage systems are expected to facilitate the cost-effective integration of intermittent renewables and to enhance system flexibility. Electrical energy storage systems with different characteristics, such as power capacity, storage capacity, charge and discharge durations, can have markedly different purposes when connected to the grid. Consequently, the increase in diversity and flexibility of the system is desirable. Nevertheless, technologies with similar characteristics might act as competitors for their adoption and implementation by the grid and industry. Therefore, it is important to analyse and to determine both technical and economic specifications of a technology, but it is also vital to compare them against other technologies and to assess their potential within an electricity network. For emerging technologies with no or limited operational data available, this can be done based on detailed technology models.

Liquid-Air Energy Storage (LAES) is a technology being developed by Highview Power Storage [1]. It uses electricity to liquefy air that is stored in low-pressure storage vessels. When electricity is needed or when it makes financial sense to export, the liquid air is used in a power cycle to produce electricity [2]. Pumped-Thermal Electricity Storage (PTES) is also a newly proposed electricity storage system, but at a lower Technology Readiness Level (TRL) due to the lack of an operational pilot plant. PTES stores energy in the form of sensible heat in insulated storage tanks containing a storage medium [3]. It operates based on a reverse/forward Joule-Brayton cycle for charging/discharging, respectively [3,4]. A common costing methodology for the two systems

based on equipment module costing techniques was presented in Ref. [5], with the overriding aim of performing a preliminary economic feasibility assessment of the two technologies.

A whole-systems assessment approach to determine the system value of energy storage in low-carbon power systems was presented in Ref. [6]. It optimises investment for storage capacity, network capacity and new electricity generation as well as minimising system operation costs [6]. To the best of our knowledge, a study performing such an exercise specifically for LAES and PTES does not exist in literature. This work aims to explore this research gap.

Discussion and Results

In order to define and determine the technical and economic characteristic of LAES and PTES technology, thermodynamic and economic models are presented along with their integration in a whole-systems electricity network model. Based on a costing analysis presented in Ref. [5], which considers metrics such as power capital cost, levelised cost of storage and sell-to-buy ratios, the competitiveness of the two technologies against each other is assessed.

The results reveal the significant impact of the compression and expansion components on the capital cost of the two storage systems. LAES is found to have a lower power capital cost and a lower levelised cost of storage, while PTES appears to be more competitive when the operational energy costs dominate over the capital costs. In addition, the two technologies are found to differ in terms of their financially feasible sell-to-buy ratios, with LAES being better in this regard at lower electricity buying prices and PTES being better at higher electricity buying prices [5].

Differences in the specifications and economic aspects between LAES and PTES show the need for their testing in a network scale model to identify the conditions in which each technology is more valuable. Their competitiveness against alternative options, i.e. existing energy storage technologies, is also of interest for their potential of implementation.

Summary/Conclusions

LAES and PTES are two newly proposed medium- to large-scale electricity storage technologies. Their performance characteristics will strongly affect their applicability and overall value to the current and future low-carbon electricity system. These technologies have different strengths and weaknesses that need to be considered, and may therefore be applicable in different scenarios.

References:

[1] Highview Power Storage, “Liquid air energy storage 2016” – Available at: http://www.highview-power.com [accessed 15.2.2016].
[2] Centre for Low Carbon Futures, “Liquid air in the energy and transport systems: opportunities for industry and innovation in the UK”, York, UK: Centre for Low Carbon Futures; 2013 May, Report No. 021.
[3] White, A., Parks, G., Markides, C.N., “Thermodynamic analysis of pumped thermal electricity storage”, Applied Thermal Engineering, 2013, doi:10.1016/j.applthermaleng.2012.03.030
[4] McTigue, J. D., White, A. J., Markides, C. N., “Parametric studies and optimisation of pumped thermal electricity storage”, Applied Energy, 2015, doi:10.1016/j.apenergy.2014.08.039
[5] Georgiou, S., Mac Dowell, N., Shah, N., Markides, C. N., “Thermo-economic comparison of liquid-air and pumped-thermal electricity storage”, Proceedings of ECOS 2017 - the 30th international conference on efficiency, cost, optimization, simulation and environmental impact of energy systems 2-6 July 2017, San Diego, California, USA.
[6] Pudjianto, D., Aunedi, M., Djapic, P., Strbac, G., “Whole-system assessment of value of energy storage in low-carbon electricity systems”, IEEE Transactions on Smart Grid, 2014, doi:10.1109/TSG.2013.2282039

Pumped Heat Electricity Storage at Intermediate Temperatures: Basics and Limits

B. Atakan[1*] and D. Roskosch[1]

[1] University of Duisburg-Essen, Thermodynamics, Lotharstr. 1, 47057 Duisburg, Germany

[*]Corresponding author: Burak.Atakan@uni-due.de

Abstract

The rising share of renewable energy sources in power generation leads to the need of energy storage capacities. In this context, also some interest in thermal energy storages, especially in a concept called pumped heat electricity storage (PHES), arises. One possible design of such a PHES system at intermediate temperatures (300-500 K) consists of a compression heat pump, a thermal storage and an organic Rankine cycle (ORC). The present work analyses the general thermodynamic potential and limits of such a system by means of realistic simple Rankine cycles. The potential analysis starts with the optimal case of combining two reversible Rankine cycles with reversible heat transfer. Afterwards the cycles are transferred to Rankine cycles with irreversible heat transfer and the relation between power output of the discharging cycle and efficiency of the entire process is analysed. The considered working fluid is always a hypothetical one, which is optimized by an inverse engineering approach. It is shown that the total or roundtrip efficiencies are between 55 and 37% for a power output of 80% of the maximal value and decrease with increasing storage temperatures, in contrast to a Carnot cycle analysis. A further expansion of the investigation considers the influence of the isentropic efficiencies of the ORC expander and the HP compressor on the process efficiency. Here, a stronger sensitivity of the isentropic efficiency of the ORC expander on the roundtrip efficiency was found.

Keywords: pumped heat electricity storage, thermodynamic limits, inverse engineering, fluid optimization.

Introduction/Background

Most of the renewable energy sources like wind or solar radiation are not available continuously. This leads to fluctuations of the supplied power to the electricity grid, creating a need of large storage capacities within the grid. Several different technologies are discussed or already applied addressing this issue, which can be divided into two groups, chemical storages like common batteries or power to gas systems and non-chemical storages like pumped hydro storages or compressed air energy storages. A further storage technology recently discussed is the pumped heat electricity storage (PHES). The basic principle of such a PHES system is simple; in case of oversupply of energy to the grid, a thermodynamic cycle transfers heat from a low temperature heat source (e.g. the surrounding) to high temperature thermal energy by using electrical energy and charges the storage. If later, less electrical energy is generated than needed, a further thermodynamic cycle discharges the storage and converts thermal energy back to electrical energy again. There are a few possibilities in the design of a PHES system, one is combining a heat pump with an Organic Rankine Cycle (ORC). The thermodynamic limits with respect to the efficiency, as well as important variables of PHES systems, are nearly unknown so far and is addressed here systematically.

Discussion and Results

The present work focusses on the PHES designs with vapour compression heat pumps and ORCs and alternatively on combinations of electrical heaters and ORCs. It is analysed, which

roundtrip efficiencies are to be expected if real or nearly real cycles are considered and whether the results from Carnot cycles are transferable to real processes, at all. The advantage of analysing reversible comparison cycles is usually, that findings about important process parameters and influencing factors of the real process can be obtained by means of simple equations or correlations. For example, most of the innovations in power plant technology can be traced back to the Carnot cycle. However, it is not clear so far, if it is also true for PHES systems. Addressing this question, the step from reversible Carnot cycles to more realistic Rankine cycles considering typical boundary conditions is taken here. The roundtrip efficiency and the power output are analysed as a function of the storage temperature for different cases. The working fluid is defined by characteristic fluid parameters like e.g. the critical temperature and pressure; these are taken as continuous variables and optimized for every regarded storage temperature by an inverse engineering approach. This procedure ensures the calculation of the highest possible roundtrip efficiencies with respect to the boundary conditions, since the fluid is optimally adapted to the process. Components like pumps, expanders or compressors are initially assumed to be ideal, but subsequently, the influence of the isentropic efficiencies of the ORC expander and the HP compressor on the roundtrip efficiencies is investigated for a constant storage temperature.
First, the thermodynamic limit in process temperatures is analysed. Based on the Carnot cycles, the condensation and evaporation temperatures of the Rankine cycles are here always set to the storage temperature or the surrounding temperature, respectively (indicated as reversible Rankine cycle case). Indeed, this leads, based on the infinitely small temperature differences in the heat exchangers, to heat flow rates and power outputs close to zero, but usually promises the highest efficiencies.

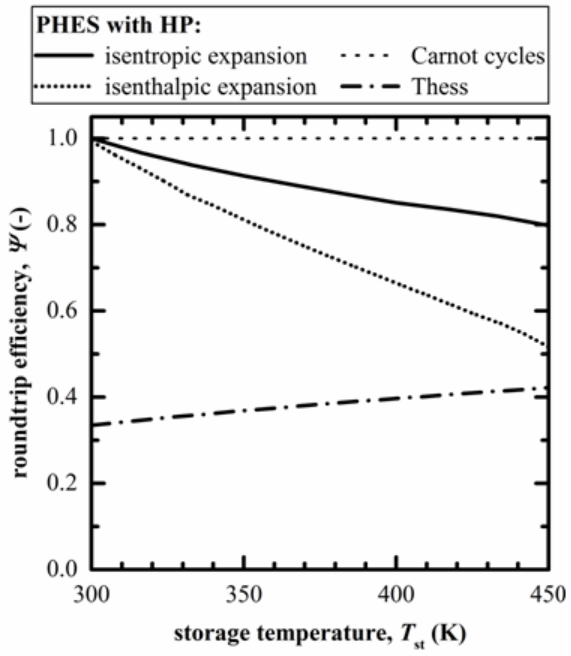

Fig. 2: Roundtrip efficiency as a function of storage temperature for the combination of two Carnot cycles and two reversible Rankine cycles.

shows the resulting roundtrip efficiencies for different process configurations as a function of the storage temperature; the solid line represents an isentropic expansion and the dotted line an isenthalpic expansion in the heat pump. In addition, the results of combining two full Carnot cycles (dotted line), that always leads to $\psi = 1$, and the results of {[1] (dotted dashed line) are also included. Regarding the results of [1], for the maximum power cycle, it gets

clear that the roundtrip efficiency increases with increasing storage temperature. Thus, the system becomes more efficient if the absolute spreading between the storage temperature and the surrounding temperature rises. However, the achieved roundtrip efficiencies are rather low for ideal cycles, At $T_{st} = T_{sur}$, the function is not defined, but a slightly higher storage temperature already leads to a roundtrip efficiency of 33.4 %, but, the power output is expected to be close to zero, then. The roundtrip efficiency for the highest considered storage temperature of T_{str} = 450 K is 42.1 % for the maximum power cycle. The results of the combination of two Rankine cycles lead to completely different results. For both cases (isentropic and isenthalpic expansion), the reached roundtrip efficiencies are significantly higher, but it is much more crucial that the lines, starting at $\psi \approx 1$ for T_{st} = 300 K, now decrease with increasing storage temperature.

Summary/Conclusions

It is concluded that Carnot cycles are of limited use to analyse PHES system. In this context two process steps were identified which lead to the difference. An analysis of the relation between power output and roundtrip efficiency, which was made as an example for a storage temperature of 400 K, emphasized that roundtrip efficiency and power output lead also for PHES systems to a Pareto frontier where values for the power output near to the maximum result in a strong decrease of the roundtrip efficiency.. It was shown that the roundtrip efficiency can be improved by in average 66 % while the power output is only decreased by 20 % based on the maximum power output. The reached roundtrip efficiencies are only between 56 % (T_{st} = 300 K) and 37 % (T_{st} = 430 K), although components like expander, compressor and pump were still assumed to be isentropic in this case. In this context, it was emphasized that the reached roundtrip efficiencies are even further reduced, if typical values for the isentropic efficiencies of HP compressor and ORC expander are assumed.

References

[1] Thess A. Thermodynamic efficiency of pumped heat electricity storage. Physical Review Letters 2013;111(11):110602.

Performance analysis of a novel polygeneration plant for LNG cold recovery

Antonio Atienza-Márquez*, Joan Carles Bruno, Alberto Coronas

Universitat Rovira i Virgili, CREVER, Mechanical Engineering Department,
Av. Països Catalans 26, 47003 Tarragona, Spain

*Corresponding author: antonio.atienza@urv.cat

Abstract

Because of its low temperature (around -162ºC) the regasification of Liquefied Natural Gas (LNG) has been proposed extensively for its use as heat sink in many power cycles. However, its application for the simultaneous production of power, refrigeration and cooling has remained relatively unexplored. In this paper are studied several configurations and optimized operation modes of a polygeneration plant to recover cooling from the regasification process of LNG in order to provide mechanical power and cooling at several temperatures using a District Cooling Network. The results show that the integrated recovery of power and cooling has a much higher efficiency than the simpler power recovery if a suitable cooling distribution network is designed to overcome the existing technical challenges.

Keywords: LNG, cold recovery, polygeneration of energy.

Introduction/Background

NG is one of the cleanest fuels of fossil origin and will keep play an important role in the next future. It is usually supplied by pipeline but, in some cases, it is provided as Liquefied Natural Gas (LNG). LNG has to be regasified before supplying it to the end-users. By now this process is usually done using seawater, so the cold is rejected to the ambient.

This could be a source of cold exergy. The recovery of waste heat and cold is one of the priorities mentioned in the Strategic Energy Technology (SET) Plan published in Nov. 2017 for Energy efficiency in industry [1]. The cold recovery of the LNG regasification process has been reviewed in the literature extensively for power production using the regasification heat as heat sink of a power generation cycle [2]. However, it could be more interesting to study the combined production of power and refrigeration [3] to replace refrigeration systems with its corresponding benefits in energy costs and environmental impact because it will be no longer necessary the use of GWP refrigerants for the users connected to this system.

The objective of this paper is to study several configurations and optimized operation modes of a polygeneration plant to recover cooling from the regasification process of LNG to provide mechanical power and cooling at several temperatures using a District Cooling Network.

Discussion and Results

Figure 1 shows the complete polygeneration system configuration. CO_2 is the heat transfer fluid selected as heat transfer fluid for the District Cooling system due to its good properties in terms of pumping energy required and others. To avoid freezing an initial Rankine Cycle (RC-1) is integrated in the system to recover cooling from the very lower initial temperature of the LNG. To finish the regasification process up to the ambient temperature it is possible to integrate also renewable energy, in this case a biomass driven Organic Rankine cycle. The system is

completed with additional power recovery in the CO_2 circuit and the direct expansion of the LNG down to the natural gas distribution pressure.

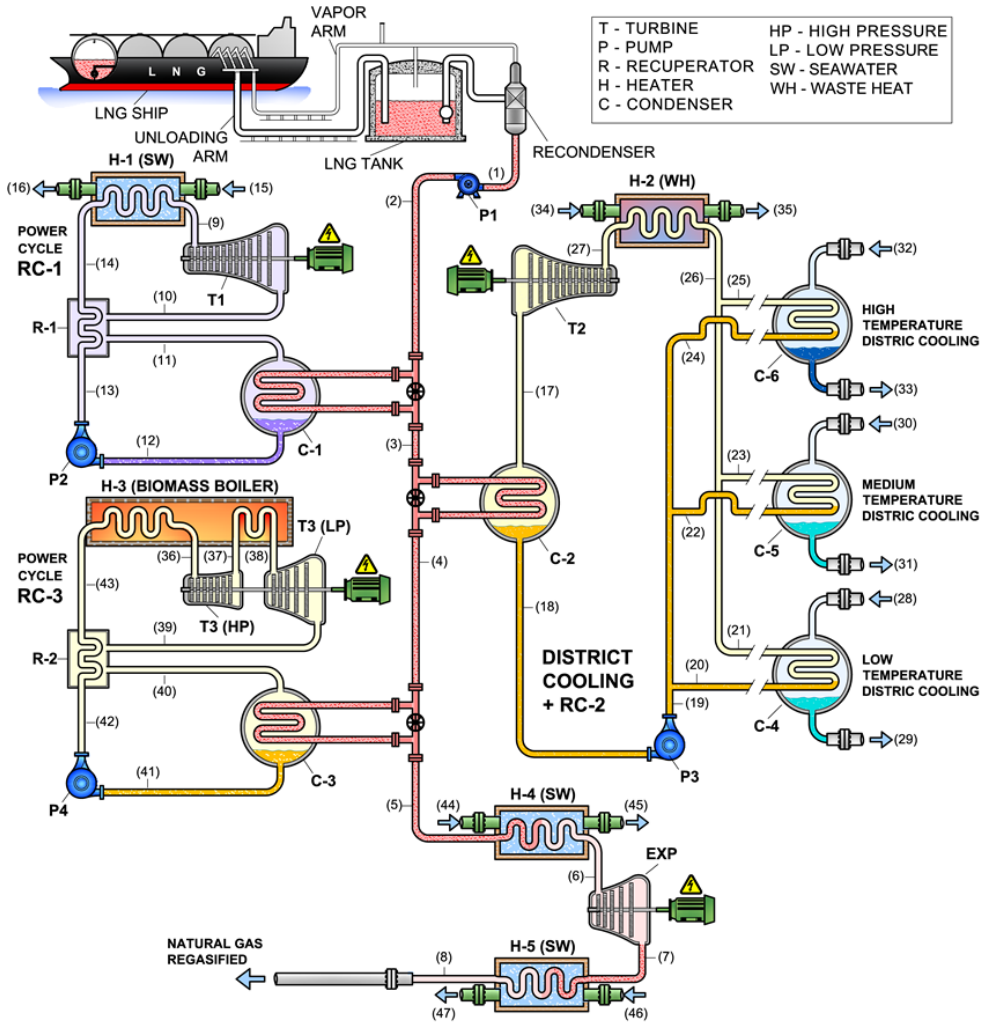

Figure 1. Scheme of the proposed polygeneration system.

Conclusions

The results show that the integrated recovery of power and cooling has a much higher efficiency than the simpler power recovery if a suitable cooling distribution network is designed to overcome the existing technical challenges such as freezing or pumping energy requirements of certain heat transfer fluids.

References:

[1] European Commission, *European Strategic Energy Technology Plan (SET-Plan)*, 2017. https://setis.ec.europa.eu/system/files/integrated_set-plan/issues_paper_action6_ee_industry_0.pdf, (Accessed 15 December 2017)

[2] B.B. Kanbur, L. Xiang, S. Dubey, F.H. Choo, F. Duan, *Cold utilization systems of LNG: A review*, Renewable and Sustainable Energy Reviews, 2017, doi:10.1016/j.rser.2017.05.161

[3] A. Atienza-Márquez, J.C. Bruno, A. Coronas, "Cold recovery from LNG-regasification for polygeneration applications", Applied Thermal Engineering, 2018, doi:10.1016/j.applthermaleng.2017.12.073

Small-scale Pumped Heat Electricity Storage for decentralised combined Heat and Power Generation

Annelies Vandersickel*, Amir Aboueldahabb, Hartmut Spliethoff

[1]Institute for Energy Systems, Technical University Munich,

Boltzmannstr. 15, 85748 Garching b. München, Germany

*Corresponding author: annelies.vandersickel@tum.de

Abstract

Decentralised rural electrification by means of renewable energy poses a challenge to electricity storage devices. Currently used lead-acid batteries have low lifetime and are a threat to human health and environment. Using environmentally friendly and long-lasting materials, Pumped Heat Energy Storage could offer a valuable alternative to these batteries. In this paper, a Pumped Heat Energy Storage is analysed with respect to its potential as a combined heat and power storage for the autarkic cogeneration of heat and power from renewable energy. The charging and discharging operation are modelled in Matlab for a kW-scale configuration using a two-stage heat pump for charging and pressurized water as the thermal energy storage. During discharge, the stored heat can either be reconverted to electricity using a subcritical organic Rankine cycle or immediately be used in various household applications. Finally, the economic feasibility of the Pumped Heat Energy Storage is compared to that of a lead-acid battery systems using cost function optimization for different scenarios.

Keywords: Pumped heat energy storage, rural electrification, water storage

Introduction/Background

More than 1.6 billion people worldwide do not have access to electricity and most of these people live in rural areas of the developing world. Renewable energies provide not only the most environmentally friendly but also the most cost-effective means of rural electrification. Besides economical and institutional obstacles, storing inherently intermittent renewable energy sources is a technical challenge which in practice is solved by the use of cheap and easily available lead-acid accumulators. Their limited cycling capability leads to replacement every 3-5 years and a lack of infrastructure complicates recycling, increasing human exposure to lead and causing severe health problems. In addition, improper disposal causes hydrofluoric acid leakage, which heavily pollutes the environment. Pumped Heat Electricity Storage (PHES) could be a valuable alternative to lead-acid batteries, providing electricity storage while using environmentally harmless materials and having a much longer lifetime.

All PHES concepts currently found in literature are intended for bulk scale electricity storage and cannot be applied for a decentralised application in the order of only a few kW, as required for rural electrification. There are first attempts to implement reversible heat pumping on a household level [1,2], focussing however on increased utilisation of the already existing heat pump instead of providing a system to store intermittent electrical energy. Objective of this paper is to extend the pumped heat storage concept for use as in a rural low cost environment and assess its performance as small scale combined heat and power system.

Discussion and Results

To assure cost effective system design, the PHES concept has been reduced to its simplest form, fixing several design criteria beforehand.

- No cold storage is installed, instead the environment is used as the low temperature heat reservoir
- Water is used as the storage medium for the high temperature heat reservoir, a two tank system with tanks at 80 and 115 C.
- Working fluids that would require sub-ambient or supercritical pressure levels to work under given operating conditions are not considered
- Only of the shelve components are considered

Direct utilization of power generated by PV and wind is always prioritized and charging/discharging of the PHES storage system only takes place, when there is a mismatch between power generated and electricity demand. During charging, a two stage air heat pump raises the water temperature from 80°C to 115°C. During discharge, the high temperature water is used to drive an ORC and generate electricity. To maximize the efficiency of the ORC, the heat source (high temperature water) is only partially exploited and the remainder is stored at a temperature of 95°C to be later used to cover heat demand. Heat demand is thus covered from the tank at 115 or 95°C.

The Matlab built-in genetic algorithm combined with a process model of the PHES, is used to size the PHES system, PV and wind turbine park, minimizing the invest costs of the entire energy supply and storage system for given electricity and heat demand profiles (time series).

Conclusions

For the system model designed based on off-the-shelve system components, the power-to-power roundtrip efficiency reaches an annual averaged value of only 5 to 12% and the system is not capable of competing with currently used lead-acid batteries. Possible improvements of compressor and expander isentropic efficiency as well as larger heat exchange areas could, however, enhance HP and ORC performance. A roundtrip efficiency of 26% would suffice to create a competitive storage system.

Special attention must be paid to limit thermal losses from the high temperature storage tanks. Although vacuum insulated tanks are used, yearly losses still amount to 1-2% of total heat provided by the heat pump and have a noticeable impact on total equivalent annual cost. The higher the heat-to-power ratio and the more wind based the generation becomes, the more beneficially the PHES becomes compared to the battery alternative.

References:

[1] Dumont O., Quoilin S., Lemort V., *Experimental investigation of a reversible heat pump/organic Rankine cycle unit designed to be coupled with a passive house to get a Net Zero Energy Building*. International Journal of Refrigeration 2015

[2] Schimpf S., Span R., *Techno-economic evaluation of a solar assisted combined heat pump-Organic Rankine Cycle system.* Energy Conversion and Management 2015

Experimental Investigation of the Effect of Magnetic Field on Vapour Absorption Rate of LiBr+H_2O Nanofluid

Shenyi Wu* and Camilo Rincon Ortiz

Fluids and Thermal Engineering Research Group
Faculty of Engineering

University of Nottingham, University Park, Nottingham, NG7 2RD, United Kingdom
* Shenyi.wu@nottingham.ac.uk

Abstract

This paper reports an experimental study on the vapour absorption process with an aqueous lithium bromide solution based nanofluid. It is a comparison study to investigate the effect of the nanofluid (base fluid + nanopowders) and the nanofluid under the influence of an external magnetic field. It is found that the vapour absorption rate increases using the nanofluid and applying the magnetic field to the nanofluid can further enhance the vapour absorption process. The vapour absorption rate is 1.53 and 1.67 times higher at the solution flow rates 3L min^{-1} and 3.5L min^{-1}, respectively. The enhancement correlates with the frequency of nanoparticles movement induced by the external magnetic field. The limited experimental results suggest that the high frequency of the nanoparticles' movement benefits the vapour absorption process.

Keywords: Nanofluid, heat and mass transfer, vapour absorption refrigeration, magnetic field

Introduction/Background

The use of absorption systems faces some barriers including the high initial cost, bulky volume and low COP - all of which are associated with the effectiveness of vapour absorption process in the system, which largely relies on heat and mass transfer in the process. Conventionally, the enhancement of heat and mass transfer is achieved from increasing the ratio of surface area to volume and/or use of surfactant agent to increase instability at the vapour-liquid interface. Use of nanofluid is a recently developed new approach to improve the effectiveness of the vapour absorption process. Kim *et al* reported their works on bubble absorber with binary nanofluid [1, 2]. With the addition of nanoparticles: Cu, CuO or Al_2O_3, to an NH_3-H_2O solution, they found that the NH_3-H_2O binary nanofluids demonstrated excellent absorption ability. The effective absorption ratio, defined as 'the ratio of the absorption rate by the nanofluid to the base fluid (without addition of nanoparticles)' was increased in all cases with the maximum effective absorption ratio of 3.21 when the nanofluid contained 18.7% ammonia and 0.10% of Cu nanoparticles [1]. Their work also found that the absorbers with nanofluids performed better than those without nanofluid as the absorption potential of the solution decreases. Kang et al [3] observed that carbon nanotubes at concentrations of 0.01 and 0.1% have a higher rate of mass transfer increase compared with Fe nanoparticles, concluding that CNT is the most optimal nanoparticles to be used in absorption systems. They measured the absorption rate in a H_2O/LiBr solution for a falling film absorber, the maximum mass transfer for CNT nanoparticles was 2.48 at 0.01 wt% while the maximum enhancement for Fe was 1.90 for 0.1 wt%.

This work, through experimental tests, investigated the effectiveness of this approach for vapour absorption of LiBr-H_2O to further explore this technology. It is focused on the influence of the external magnetic field on the vapour absorption process with nanofluid as the absorbent fluid by comparison of the test results. Table 1 shows the tests were carried out in this study.

Table 1 the tests completed in the investigation

	Base solution $LiBr+H_2O$ (25℃)		Base solution + nanoparticles $LiBr+H_2O+Fe_2O_3$ (25℃)	
	3.0 L min^{-1}	3.5 L min^{-1}	3.0 L min^{-1}	3.5 L min^{-1}
No Magnetic strip	√	√	√	√
Magnetic strip with no gap	N/A	N/A	√	√
Magnetic strip with 2cm gap	N/A	N/A	√	√
Magnetic strip with 3.5cm gap	N/A	N/A	√	√

Discussion and Results

It was found that applying the external magnetic field to the nanofluid absorbent could increase the absorption rate, which is shown in Figure 1.

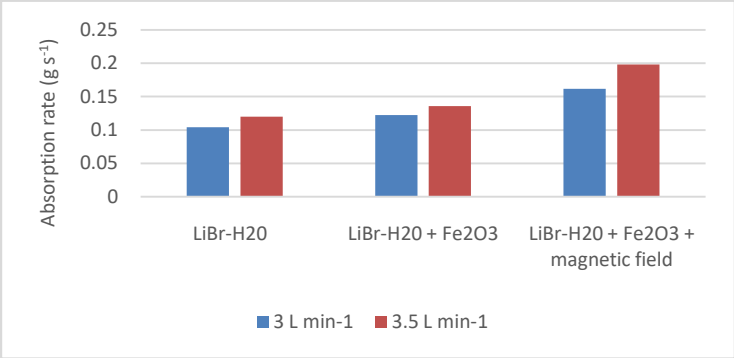

Figure 1 the results with/without additions of nanoparticles and magnetic field

The absorption rates are varied with the gap distance between the magnetic strips wounded on the absorption vessel. This analysis to this phenomenon shows that this may associate with the frequency of the nanoparticles' movement in the fluid. The results from this investigation suggest that the vapour absorption process benefits from a high frequency movement of nanoparticles.

Summary

This study show that the nanofluid can enhance the vapour absorption process, particularly, when the heat and mass transfer of the liquid phase dominates the whole process. The arrangement of the external magnetic field is appeared to be an influential factor which associates with the frequency of the nanoparticles' movement in the film flow. The vapour absorption rate increases with the frequency of the nanoparticles' movement between the wall and the surface of the liquid phase.

References

[1] Kim, J., Jung, J. Y., Kang, Y. T., The effect of nano-particles on the bubble absorption performance in a binary nanofluid, International Journal of Refrigeration, 29 (2006) 22-29

[2] Kim, J. K., Jung, J. Y. & Kang, Y. T., Absorption performance enhancement by nano-particles and chemical surfactants in binary nanofluids. International Journal of Refrigeration, 30 (2007) 50-57.

[3] Kang, H. J. Kim y K. I. Lee, Heat and mass transfer enhancement of binary nanofluids for H_2O/LiBr falling fill absorption process, International Journal of Refrigeration, 31 (2008) 850-856.

Thermal Performance of Nanofluids Applied to the Temperature Control of Electronic Components

Roger R. Riehl

National Institute for Space Research, INPE – DMC
Av dos Astronautas 1758, São José dos Campos, 12227-010 SP Brazil, E-mail: roger.riehl@inpe.br

Abstract

The subject of this article is related to the development of a thermal management solution for a surveillance equipment, which needs to dissipate high levels of heat loads using both active and passive thermal control devices. A thermal management system was designed to use both a single-phase forced circulation loop and heat pipes using copper oxide (CuO)-water nanofluid, designed to promote the thermal management of up to 50 kW of heat generated by several arrays of electronic components, being dissipated to the environment by a fan cooling system. The heat pipes collect the heat from electronic components that are far from the main single-phase forced circulation loop, rejecting the heat directly in its cold plates. Results show that with an addition of 20% by mass of CuO nanoparticles to the base fluid in the single-phase system, enhancements of 12% in the heat transfer coefficients were achieved but the increase in the pressure drop was around 32%. The use of nanofluid in the heat pipes resulted in a substantial decrease in the heat source temperature. Upon using nanofluids in heat pipes, the maturity of this technology is considerably high.

Keywords: thermal enhancement, electronics cooling, thermal control, pressure drop, nanofluids.

Introduction

The need for thermal management has increased over the last decade and the prediction is that a steeper increase is yet to come for the next years. Such an increase is related to more powerful electronics used for data processing in high-tech equipments used for satellites and defense/military. Several investigations related to nanofluids applications have been conducted with important contributions to many areas [1,2]. Considering current and future thermal management needs, the use of nanofluids is becoming inevitable. Nanofluids present to be an important approach to enhance the heat transfer capability of heat pipes and loop heat pipes systems, which has already been proven [3]. An important application for today's needs for heat dissipation is related to surveillance systems. As more compact and powerful equipments are necessary, higher heat fluxes need to be properly addressed. Focused on the need for designing a reliable and effective thermal management system that need to operate in hostile environments, with potential use of nanofluid.

Equipment Design and Operation

A specific design for a surveillance system has been conceived to operate in hostile environments where the ambient temperatures can range from +5 to +50 °C and humidity levels up to 95%. In this case, a single-phase thermal control loop has been designed to use a nanofluid, presenting a forced circulation using a pump to move the working fluid throughout the circuit to remove heat from the electronic components, rejecting this heat to the environment by a fan cooling system. For this thermal management system, a hybrid design has been applied where the heat generated by all PCBs are removed by open loop pulsating heat pipes, delivering the heat to the heat sinks allocated thorough the surveillance equipment (cold plates). The heat sinks are then connected to the single-phase thermal control loop that collects all the heat and dissipate it to the environment. The schematics of such arrangement is presented by Fig. 1a and the surveillance equipment where it is installed is shown by Fig. 1b, whilst Fig. 1c presents the hybrid setup where the pulsating heat pipe and the heat sink are connected. As the base fluid, water has been selected. The CuO nanoparticles present an average diameter of 29 nm and purity of 99.8%. The nanoparticles concentration (f) shall vary from 3.5% to 20% (by mass of the base fluid) to verify their effect on the overall thermal performance of the system.

Results and Discussion

Figures 2a and 2b present some results for the pressure drop and heat transfer coefficients, respectively, on a comparison between the use of pure water and the addition of copper nanoparticles at different concentrations (*f*), by mass percentage of the working fluid in the system. The results are related to each individual electronics module (composed of 3 PCBs), which dissipate a maximum of 50 W of heat, thus, based on the module's footprint and heat dissipation, the calculation for the heat transfer coefficient was performed. It is clear that as the nanoparticle concentration increases, the pressure drop also increases up to 32% for *f*=20% as more solid nanoparticles are present in the system

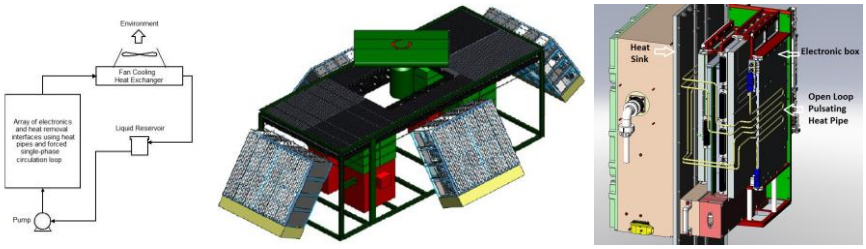

(a) (b) (c)

Figure 1: Schematics of the thermal control system arrangement.

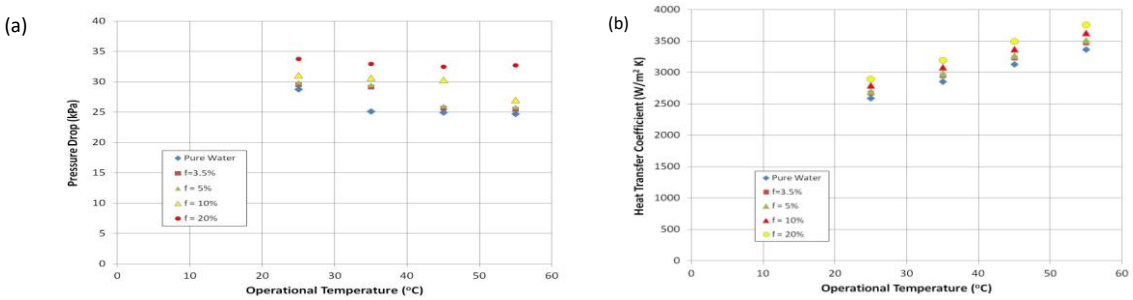

Figure 2: Results for (a) pressure drop and (b) heat transfer coefficient.

Conclusions

In general, the main conclusions that can be derived from this investigation are:

1. Higher heat transfer coefficients can be reached with the increase of the solid nanoparticles concentration, representing an enhancement of up to 12% for *f*=20% at 55 °C when compared with the operation with water;
2. The pressure drop also increases as the concentration of nanoparticles increases, which could compromise the pump operation;
3. The overall analysis indicates that the application of the nanofluid with higher concentrations can be used, as the major parameter for this analysis is the heat transfer coefficient, which is reducing the size of the thermal management system applied to control the temperature of the electronics components.

When considering that the thermal management system is operating at higher capacities, while keeping the working fluid's temperature differences between the fan cooling inlet and outlet within certain required parameters, the use of a nanofluid presents to be an important innovative approach for this project. This is directly resulting in more gains than loses for the overall thermal system analysis and should remain as the most indicated solution for this application.

References

1. E. Ebrahimnia-Bajestan, H. Niazmand, W. Dungthondsuk. S. Wongwises, Numerical investigation of effective parameters in convective heat transfer of nanofluids flowing under a laminar flow regime, *International Journal of Heat and Mass Transfer* 54 (2011) 4376-4388.
2. A. Ghadimi, R. Saidur, H.S.C. Metselaar, A review of nanofluid stability properties and characterization in stationary conditions, *International Journal of Heat and Mass Transfer* 54 (2011) 4051-4068.
3. R.R. Riehl, N. Santos, Water-copper nanofluid application in an open loop pulsating heat pipe, *Applied Thermal Engineering* 42 (2012) 6-10.

Two-Phase Pressure Drop Correlation During the Convective Condensation in Microchannel Flows

Roger R. Riehl

National Institute for Space Research, INPE – DMC
Av dos Astronautas 1758, São José dos Campos, 12227-010 SP Brazil, E-mail: roger.riehl@inpe.br

Abstract.

This paper presents the experimental results on two-phase pressure drop related to microchannel flows during convective condensation. Two pumping systems, one being on a capillary pumped loop (CPL) mode and the other being with a magnetic driven pump with variable flow rate, were used in the experimental apparatus to test microchannel condensers with methanol as the working fluid. Tests were conducted for two different saturation temperatures, for a range of heat dissipation rate from 20 to 350 W, four microchannel condensers and mass flow rates of up to 600 kg/m2 s. The results showed that the microchannel condensers presented high pressure drop (up to 63 kPa) for the mass flow rate applied, which is mainly related to the microchannels reduced geometry. The levels of pressure drop observed were also considered high, as only laminar flow was verified during the tests. A correlation for the two-phase multiplier was obtained to correlate the experimental data, which showed to predict 85 % of the experimental results within an error range of less than 35 % for both saturation temperatures tested. The obtained correlation presented very high sensibility when calculating the pressure drop along the microchannels, considering the geometric factors and heat transfer capabilities of such equipment, which was able to present a good correlation with the experimental data.

Keywords: convective condensation, microchannels, thermal control, pressure drop.

Introduction

The continuing miniaturization of electronic devices and systems has made area restrictions for the heat to be dissipated a significant problem. This issue becomes more important when considering that the device performance and reliability are known to increase when operating temperatures are kept below 80 ^{o}C. Investigations and applications using forced-air convection and pool boiling for electronics cooling have been performed, proving to be efficient on the thermal management, but limited heat dissipation rates and system integration are still a concern. Tuckermann and Pease [1] first proposed a cooling system for electronic devices using microchannel flows for forced single-phase liquid. This technology demonstrated to be promise for more compact arrangements of electronic devices and cooling systems in future electronic packaging. Based upon initial findings, a compact heat-sink microchannel was found to offer new degrees of freedom for system designs with considerable higher heat dissipation rates, but very significant high-pressure drop penalty. Focusing on such a problem, this paper presents an investigation to contribute to the understanding in two-phase pressure drop in microchannel flows. Four different microchannel heat exchangers were experimentally tested for condensing two-phase flow, in order to determine the mean pressure drop and to further develop a correlation. This procedure has the objective of helping future microchannel heat exchangers designs, to improve electronics and capillary pumping systems cooling.

Experimental Apparatus

To test the microchannel condensers, two pumping methods were used: the first was a capillary evaporator (Fig. 1a) and the second was a magnetic driven pump (Fig. 1b) in conjunction with a flow through evaporator. The capillary evaporator was used for testing at low flow rates along the condensation section, while the mechanic pump promoted higher flow rates. The condensers were designed considering that, as the channel size decreased the number of parallel channels increased. For the tests when higher flow rates had to be reached, a leak-free magnetic driven pump with speed control was used. This pump allowed controlling the flow rate up to a maximum of 3 l/min for a maximum pressure drop of 275 kPa. The details on the design for the loop used for testing the microchannel condensers are presented by Riehl (2000).

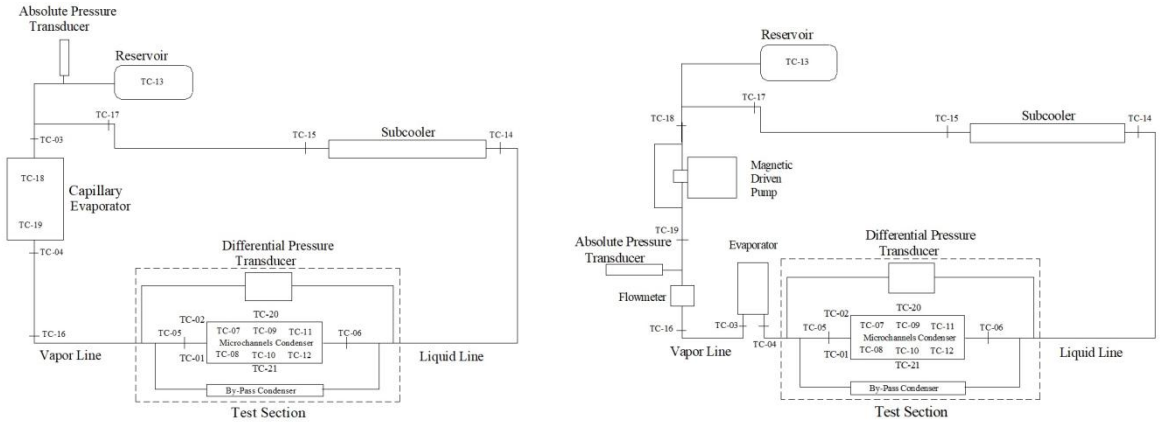

Figure 1. Experimental tests apparatuses.

Results and Discussions

In case of evaluating the single-phase pressure drop for the liquid, the two-phase multiplier would be represented as ϕ_l^2 and, for the vapor, ϕ_v^2. From the experimental results, an empirical relation for the two-phase multiplier for the liquid that showed better correlation is presented as:

$$\phi_l^2 = \left(1 + 10X^{0.188} + X^{2.0}\right)^{0.5}, \quad (1)$$

where X is the Martinelli Parameter defined as:

$$X^2 = \left(\frac{1-x}{x}\right)^{2-n}\left(\frac{\rho_v}{\rho_l}\right)\left(\frac{\mu_l}{\mu_v}\right)^n, \quad (2)$$

Equation (1) was compared against the experimental results for the pressure drop for both saturation temperatures and condensers. Figure 2 presents the comparisons for T_{sat}=45 and 55 ^oC.

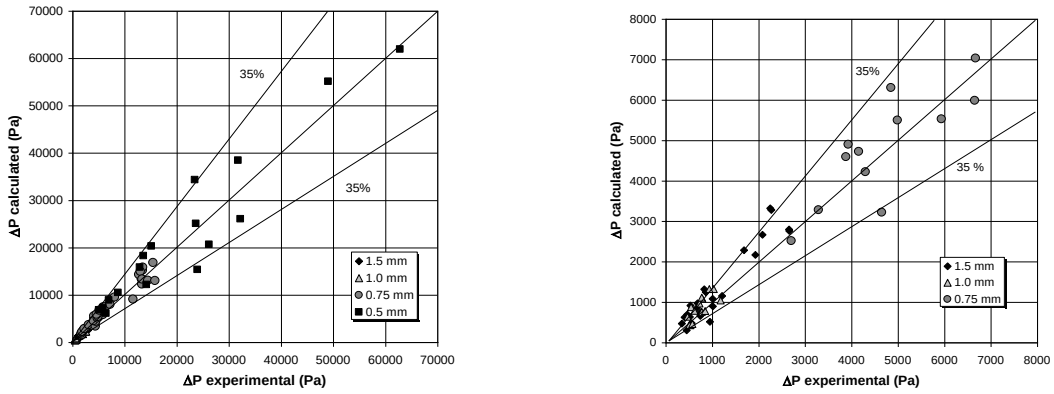

a) T_{sat} = 45 °C b) T_{sat} = 55 °C

Figure 2 – Comparison of the experimental results for pressure drop and Eq. (3).

Conclusions

A correlation to predict the pressure drop, using the two-phase multiplier from the Separated Flow Model, was derived. The two-phase multiplier correlation, represented by Eq. (3), provided good agreement with all experimental results for both saturation temperatures used, which correlated 85% of the experimental data within an error of +/- 35%.

References

[1] Tuckermann, D. B.; Pease, R. F. W., 1981, "High-Performance Heat Sinking for VLSI", IEEE Electron Device Letters, Vol. EDL-2, No.5, pp. 126-129.

Numerical Investigation of MOFs Adsorption Cooling System Using Microchannel Heat Exchangers

Majdi M. Saleh[1,2,3*], Raya AL-Dadah[1] and Saad Mahmoud[1]

[1]School of Mechanical Engineering, University of Birmingham, Birmingham B15 2TT, UK
[2]University of Benghazi, Mechanical Engineering Department, Libya
[3]University of Ajdabiya, Mechanical Engineering Department, Libya
[*]Corresponding author: email address: majdidwas@gmail.com

Abstract

Adsorption cooling systems have major challenges in terms of the large size and capital cost due to use of conventional heat exchangers for adsorber beds and the poor performance of the currently used adsorbent materials. This work numerically investigates the effect of tube diameter and CPO-27(Ni) adsorbent material thickness using micro-channels for adsorber beds on system performance in terms of mass and adsorption uptake. Results showed that increasing the adsorbent material thickness reduces the uptake while using a tube diameter of 1mm produces the highest adsorbent material to tube metal mass ratio of 6.91.

Keywords: COMSOL Multiphysics, adsorption cooling, CFD model, CPO-27(Ni)/Water, low-temperature refrigeration, micro-channel adsorber bed.

Introduction/Background

Adsorption refrigeration system has the advantages of being powered by solar and waste heat sources, using working fluids with no ozone depletion and low global warming potential and not having a corrosive effect on its components [1]. Metal- Organic Frameworks (MOFs) is a new class of adsorbent material with high surface area, volume and adsorption uptake which were investigated for many applications such as catalysis, gas storage and gas separation [2-4]. The water uptake of many MOF adsorbent materials is higher than that of silica gel at the same partial pressure [5]. Various adsorber bed configurations were investigated including finned tube bed adsorber [6], plate fin HEX, [6], flat tube heat exchanger with corrugated fins [6]. However, these adsorber beds suffer from being heavy, bulky and expensive. Therefore, this work investigates the performance of micro-channel adsorber bed using CPO-27(Ni) MOF material. CFD modelling is performed to investigate the effect of adsorbent layer thickness and the micro-channel diameter on the adsorber bed using CPO-27(Ni) water uptake and modelling results were compared to experimental measurement showing good agreement. Figure 1 illustrates the model set up consisting of a micro channel tube that is covered by a layer of CPO-27(Ni) and internal tube cooled by water flow. Various adsorbent material thickness ranging from 1 to 5mm and tube diameter ranging from 1 to 5mm were investigated. COMSOL Multiphysics software was used for modelling the adsorption process where Darcy equation was used to model the diffusion of water vapour into the adsorbent material.

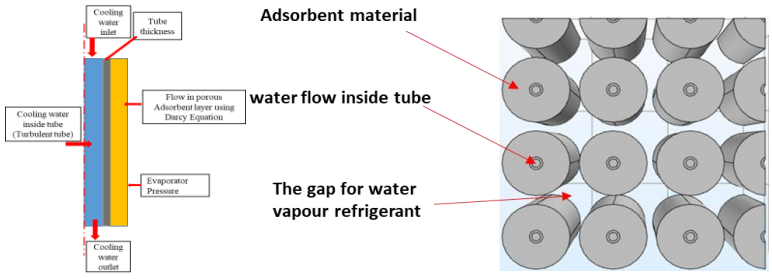

Figure 1. Schematic diagram of the micro-channel tube adsorber bed.

Discussion and Results

Table 1 shows the volume and weight of adsorbent material and the tube metal used in an adsorber bed with with 30mm × 30mm cross section area for different tube diameters 1,2,3,4 and 5mm. It can be seen that with tube diameter of 1mm, the ratio of adsorbent material to the tube metal is highest.

Table 1. Parameter study for different internal tube diameter with constant an adsorbent material thickness 3mm.

Internal tube diameter (mm)	Parameter	Volume (m^3)	Density (Kg/m^3)	Mass (g)	Adsorbent material to tube metal mass ratio
1	Adsorbent Material	5.072e-5	407	20.64	6.91
	Aluminium Tube	1.105e-6	2700	2.9835	
2	Adsorbent Material	4.838e-5	407	19.69	2.95
	Aluminium Tube	2.387e-6	2700	6.44	
3	Adsorbent Material	4.962e-5	407	20.19	2.19
	Aluminium Tube	3.405e-6	2700	9.19	
4	Adsorbent Material	4.567e-5	407	18.58	1.81
	Aluminium Tube	3.807e-6	2700	10.27	
5	Adsorbent Material	4.335e-5	407	17.64	2.05
	Aluminium Tube	3.184e-6	2700	8.59	

The model was utilized to investigate the impact of material thickness on the water uptake rate and the bed temperature during the adsorption process. Figure 2 shows the water uptake variation with time using different thicknesses ranging from 1mm to 5 mm. It can be seen that when the thickness increases, the water uptake decreases.

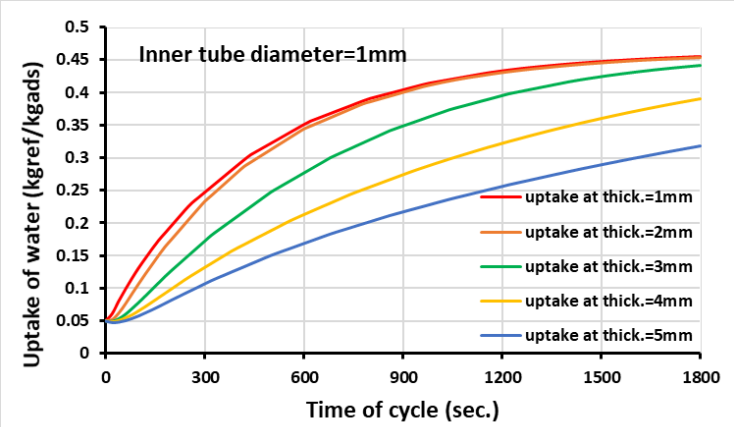

Figure 2. Variation the water uptake rate with time at different packing thicknesses.

Summary/Conclusions

- The developed model predictions are in good agreement with the experimental data for CPO-27(Ni)/water
- Comparison of the adsorbent mass and tube metal mass for various tube diameters showed that the maximum adsorbent to metal mass ratio is achieved for tube diameter of 1mm.
- Increasing the adsorbent material thickness results in reducing the water uptake.

References

[1] Rezk, Ahmed RM, and Raya K. Al-Dadah. "Physical and operating conditions effects on silica gel/water adsorption chiller performance." Applied Energy 89.1 (2012): 142-149.

[2] Elsayed, Eman, et al. "Aluminium fumarate and CPO-27 (Ni) MOFs: characterization and thermodynamic analysis for adsorption heat pump applications." Applied Thermal Engineering 99 (2016): 802-812.

[3] Rezk, Ahmed, et al. "Characterisation of metal organic frameworks for adsorption cooling." International journal of heat and mass transfer 55.25 (2012): 7366-7374.

[4] Saha, Dipendu, and Shuguang Deng. "Ammonia adsorption and its effects on framework stability of MOF-5 and MOF-177." Journal of colloid and interface science 348.2 (2010): 615-620.

[5] Henninger, Stefan K., Hesham A. Habib, and Christoph Janiak. "MOFs as adsorbents for low temperature heating and cooling applications." Journal of the American Chemical Society 131.8 (2009): 2776-2777.

[6] Sharafian, Amir, and Majid Bahrami. "Assessment of adsorber bed designs in waste-heat driven adsorption cooling systems for vehicle air conditioning and refrigeration." Renewable and Sustainable Energy Reviews 30 (2014): 440-451.

Natural graphite: Potential material for heat exchangers of waste heat recovery systems

N. Mohammadaliha, W. Huttema and M. Bahrami *

Laboratory for Alternative Energy Conversion (LAEC), School of Mechatronic Systems Engineering, Simon Fraser University, Surrey, British Columbia, Canada
*Corresponding author: mbahrami@sfu.ca

Abstract

Natural graphite sheets are promising candidates for the material of heat exchangers used in waste heat recovery systems for wet flue gasses due to their low density, low price, high thermal conductivity, and great corrosion resistance. To show the feasibility of using graphite as the material of heat exchangers working in corrosive environments, the performance of graphite as a condensation surface is investigated and compared to aluminium. It was observed that the condensation rate on a graphite surface is the same as an untreated aluminium surface, even though the graphite surface is more hydrophilic than the aluminium one.

Keywords: Wet flue gas, corrosion, waste heat, Graphite.

Introduction

Owing to the low thermal efficiency of industrial processes, more than half of the total energy input into the energy conversion systems is released to the environment in form of low-grade thermal energy or waste heat. Waste heat recovery from low-temperature flue gas streams is not only beneficial for compensating for the low energy efficiency of industrial units, but also helpful for decreasing fossil fuel consumption, controlling the release of harmful chemicals into the ambient, and addressing climate change and global warming. Using phase change heat exchangers results in much more efficient heat recovery systems due to the recovery of both sensible and latent heat in wet flue gas streams [1,2]. However, since the main source of wet flue gasses is burning fossil fuels, such as natural gas and coal, it raises the issue of corrosion in the heat exchangers because of water condensation on the heat exchanger surfaces and the formation of high-concentration sulfuric acid and other chemicals. Graphite is one of the best candidates for the material of heat exchangers used in waste heat recovery systems due to its great corrosion resistance properties, high thermal conductivity, and low density [3,4]. This study aims to compare condensation on graphite vs. aluminium surfaces.

Results and Discussion

The surface wettability is central to condensation efficiency, as it determines the condensation regime on the heat exchanger surface. Static contact angles of a droplet on a natural graphite sheet (Graphtech) and aluminium sheet (McMaster-Carr) were measured by OCA 15 Contact Angle Goniometer (DataPhysics Instruments, Germany) at five or more different locations on the samples. Filmwise condensation, in which a liquid film is formed on the surface, is the condensation regime on natural graphite surfaces due to its surface hydrophilicity (Fig 1c). The images captured from condensation surfaces by a digital microscope (AM7915MZTL, Dino-Lite) demonstrated that the surface tension of graphite is higher than aluminium, as the shape of droplet on the graphite surface is less spherical than the ones on the aluminium surface (Fig. 1a and 1b). While the hydrophilicity of graphite promoted droplet nucleation on the surface, it negatively affects the removal of condensate by gravity, and increases the thickness of condensate film compared to less hydrophilic surfaces.

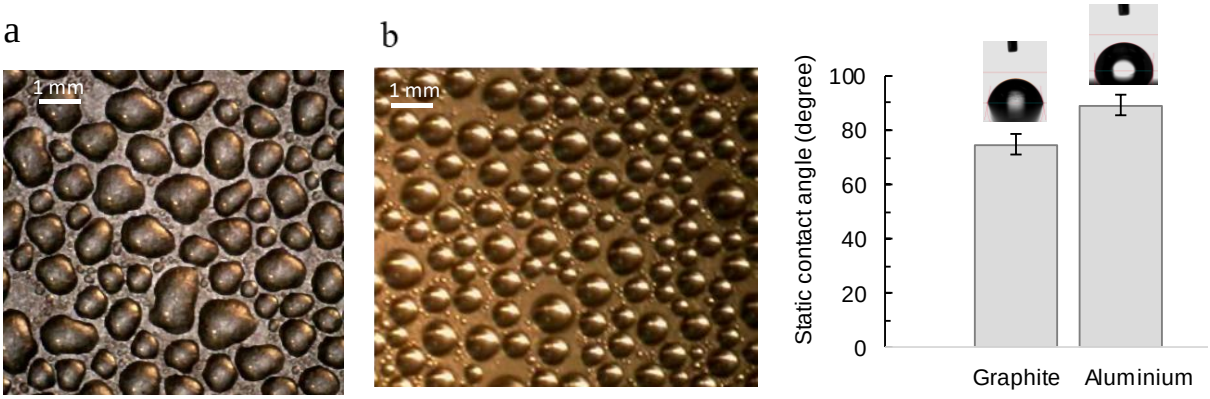

Fig 1. Shape of droplet forms on a) natural graphite sheet and b) aluminium surfaces during condensation; c) Contact angles of graphite and aluminium surfaces.

Several condensation tests were performed inside a standard environmental chamber (ESX-4CA Platinous, ESPEC) at two different ambient conditions, named as conditions: i) A (27˚C- 43 %RH); and ii) B (25˚C- 60 %RH). Using a cold plate, the surface temperature of the test samples was chilled and maintained at 8 ± 1˚ C for both conditions.

However, the results of the condensation tests at the two conditions (A and B) revealed that the trade-off between nucleation and removal of droplets leads to the same condensation rate on both graphite and aluminium surfaces. It can be concluded that increasing the contact angle of the surface doesn't necessarily increase the condensation performance of the surface. Moreover, the contact angle of the surface should be larger than a threshold to have dropwise condensation on the surface, which leads to an order of magnitude higher condensation heat flux compared to hydrophilic surfaces.

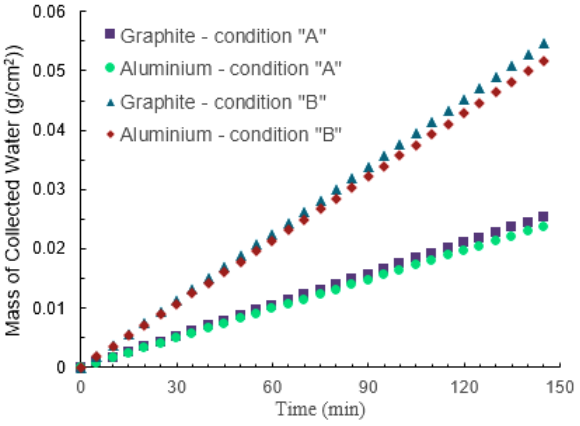

Fig 2. Mass of collected water on graphite and aluminium surfaces at two different ambient conditions : A: 27˚C - 43 % RH; B: 25˚C - 60 %RH.

Conclusion

Condensation on a natural graphite surface was compared to a conventional aluminium surface. It was found that the condensation regime on the graphite surface is filmwise, similar to an untreated aluminium surface. Although graphite is more hydrophilic than aluminium, the performance of graphite as a condensation surface is similar to aluminium. Impressive corrosion resistance properties, high thermal conductivity, and low density of natural graphite sheets make them an excellent candidate for the material of heat exchangers working in corrosive environment like the flue gas heat recovery.

References:

[1] Shi, X., Che, D., Agnew, B., & Gao, J., *An investigation of the performance of compact heat exchanger for latent heat recovery from exhaust flue gases*. International Journal of Heat and Mass Transfer, 2011.

[2] Terhan, M., & Comakli, K., *Design and economic analysis of a flue gas condenser to recover latent heat from exhaust flue gas.* Applied Thermal Engineering, 2016.

[3] Jia, L., Peng, X. F., Sun, J. D., & Chen, T. B. *An experimental study on vapour condensation of wet flue gas in a plastic heat exchanger*, Heat Transfer—Asian Research, 2001.

[4] Xiong, Y., et al., *Pilot-scale study on water and latent heat recovery from flue gas using fluorine plastic heat exchangers*, Journal of Cleaner Production, 2017.

Ultra-clean Biomass Gasification/Combustion Unit for Micro-CHP based on a Stirling Engine

M. Steiner, S. Beer [1*], D. Hummel [1]

[1] Ostbayerische Technische Hochschule Amberg-Weiden, Kaiser-Wilhelm-Ring 23

[2] Ostbayerische Technische Hochschule Amberg-Weiden

[*]Corresponding author: s.beer@oth-aw.de

Abstract

A biomass fired micro-scale CHP unit based on a 1 kW Stirling engine by Microgen engine corporation has been developed with a focus on overcoming the well known fouling and corrosion problems that occur at the heat exchanger of the Stirling engine. The objective is met by combining the principles of an updraft gasifier that comprises a fixed biomass fuel bed with a large height to diameter ratio and a low-emission combustion chamber using a swirl burner for the produced combustible gas. A low producer gas temperature of 60 to 80 °C at the outlet of the gasifier is the most significant parameter for the stability of the process. The working hypothesis of the project is: The lower the outlet temperature of the producer gas, the more of the chemical compounds produced in the hot oxidizing zone of the gasifier (e.g. oxides and salts of potassium, magnesium, calcium, sodium etc.) remain in the fuel bed and can be removed from the process via the ash. The feasibility of the concept was proven with wood chips made out of beech and spruce. The dust emissions in the flue gas were below 0.5 $mg/m^3_{n,dry}$. However, pelletized biomass seemed to be unsuitable for the process due to its tendency to swell in contact with tar and water condensate produced in the upper cold region of the gasifier. The problems could be overcome by a completely new gasifier design accounting for the volume increase of pelletized biomass caused by condensates. The new gasifier in combination with a low-emission combustion chamber can be used for micro-CHP units with Stirling engines as well as for ultra-low emission domestic heating systems.

Keywords: Gasification, Biomass, Stirling engine, Micro-CHP

Introduction/Background

For micro-CHP units using woody biomass and ranging from 1 to 10 kW electrical output, thermodynamic processes with external input of heat seem to be more suitable than internal combustion engines. The main advantages are the omission of a gas cleaning system and a continuous combustion process resulting in lower emissions. Conventional biomass combustion approaches that utilize flue gas in the heat exchanger of a Stirling engine lead to unsolvable problems with regards to fouling and corrosion on the heat exchanger surfaces. Fouling decreases the heat transfer rate dramatically and on longer terms corrosion caused by chemical compounds containing sulfur and chlorine can severely damage the engines. Therefore, the main goal of the newly developed process is to overcome these problems by using a two stage gasification/combustion unit instead of a conventional combustion unit. Updraft gasifiers for wood chips are well known for producing combustible gases with a high content of tar. If the gas is used in a combustion chamber designed according to the requirements for clean combustion, tar can be combusted completely. If the fuel bed in the gasifier is rather high in comparison to the diameter of the gasifier, the produced gas can be cooled and filtered in the fixed bed. Chemical compounds (e.g. oxides and salts of potassium etc.) will condensate in the fixed bed and will be transferred to the ash. To prove this working hypothesis, a micro-CHP test facility (updraft gasifier with ambient air as gasifying agent, combustion chamber,

Stirling engine, heat exchanger) was built in the laboratory and tests were carried out with different sorts of woody biomass like beech and spruce chips and spruce pellets. The amount of potassium was analyzed at different heights of the gasifier bed, in the dust of the flue gas, in the tar condensate and in the ash. During the test runs, the flue gas emissions (CO, NO_x, dust, VOC) were measured downstream the combustion chamber. Due to swelling problems of pelletized biomass in contact with the condensates of moisture and tar, a conventional updraft gasifier with cylindrical geometry tends to be clogged. [1-5] To overcome this problem, a new updraft gasifier geometry was designed to allow for a certain increase of the volume of the pellets without clogging.

Discussion and Results

The experimental data clearly confirms the working hypothesis: The flue gas emissions (normalized, dry at 13% O_2) were measured to be between 1-12 mg/m^3 for CO, 82-125 mg/m^3 for NO_x and below 0.5 mg/m^3 for dust. The amount of potassium compounds is very high in the ash of the gasifier and below the limit of detection in the dust of the flue gas. The surface of the heat exchanger of the Stirling engine remained clean and showed no signs of fouling during the test runs (ca. 100 hours). Further investigations are needed to understand the impact of the producer gas outlet temperature and the conditions in the gasifier on the composition, mixture and content of inorganic chemical compounds in the producer gas.

Summary/Conclusions

The newly developed process of a two stage gasifying/combustion unit shows a new way to overcome the traditional problems (fouling and corrosion on the surface of heat exchangers) related with biomass combustion. The process can be used for biomass fired CHP processes and also for heating systems with ultra-low emissions without needing any further flue gas cleaning devices to meet emission limits. The standard Microgen Stirling engine designed for gas fired domestic CHP systems proved to be very reliable.

References:

[1] Reil, S., Beer, S., Ultsch, C., Meiler, M., Hornung, A., *Thermochemical air-steam gasification of biomass and biomass chars in an updraft gasifier: Effect of air/steam ratio*. In: Integration of Sustainable Energy Conference iSEneC, 11-12.07.2016, Nürnberg

[2] Reil, S., Beer, S., Ultsch, C., Meiler, M., Hornung, A., *Thermochemical gasification of char from biomass with subsequent combustion for heat supply in endothermal biomass conversion processes.* 24th European Biomass Conference, 06.-09.06.2016, Amsterdam

[3] Beer, S., Pöcher, D., Kinzler, L., Hummel, D., Forschungsbericht 2016 der Ostbayerischen Technischen Hochschule Amberg-Weiden (S. 73-77) *„Entwicklung eines neuartigen Verfahrens zur Mikro-KWK mit biogenen Energieträgern“* , 03/2016, Amberg

[4] Reil, S., Beer, S., Karl, J.: *Experimental study on the impact of gasification conditions on process stability and tar yield in stratified downdraft gasifiers*, 4th International Symposium on Gasification and its Applications 03.09.2014, Vienna

[5] Beer, S., Reil, S., *Betriebserfahrungen bei kleinen Festbettvergasern*, OTTI Profi-Seminar „KWK mit Biomasse“, 07.-08.11 2013, Neumarkt